

SYNTHETIC, STRUCTURAL AND THEORETICAL STUDIES ON  
SUBSTITUTED ALLYL COMPLEXES AND THOSE OF RELATED  
4 $\pi$ -ELECTRON LIGANDS

by

Nicholas W. Murrall

Doctor of Philosophy

University of Edinburgh, 1984.



***To Evelyn Edith, never forgotten.***

## **ACKNOWLEDGEMENTS**

I am indebted to Dr. A.J. Welch for his supervision and guidance throughout this work. Thanks are also due to the other members of the crystallography laboratory and the inorganic section generally for the advice and suggestions which were readily given. I would also like to express my gratitude to the Department of Chemistry for funding and provision of laboratory facilities.

Last, but by no means least, special thanks are due to my friends for their support, particularly when the going got rough.

## ABBREVIATIONS

Ar	: Aryl Group
Bipy	: 2,2-Bipyridyl ( $C_{10}H_8N_2$ )
Bu <sup>t</sup>	: tert-Butyl Group
COD	: Cycloocta-1,5-diene ( $C_8H_{12}$ )
COOEt	: Ethoxycarbonyl group
Cp	: Cyclopentadienyl ( $\eta^5-C_5H_5$ )
Cp <sup>*</sup>	: Pentamethylcyclopentadienyl ( $\eta^5-C_5Me_5$ )
dppe	: Bis(diphenylphosphino)ethane ( $Ph_2P-CH_2-CH_2-PPh_2$ )
EWG	: Electron Withdrawing Group
EHMO	: Extended Huckel Molecular Orbital
Et	: Ethyl Group
L	: Electron Pair Donating Ligand
M	: Metal Atom
<u>M</u>	: Molecular Weight
M.O.	: Molecular Orbital
M.Pt.	: Melting Point
Nu	: Nucleophile
OAc	: Acetate Group
Ph	: Phenyl Group
Phen	: 1,10-Phenanthroline ( $C_{12}H_8N_2$ )
Py	: Pyridine ( $C_5H_5N$ )
R, R'	: Alkyl Groups
THF	: Tetrahydrofuran
TMEDA	: N,N,N',N'-tetramethylethylenediamine ( $Me_2N-CH_2-CH_2-NMe_2$ )
TMM	: Trimethylenemethane ( $C(CH_2)_3$ )

With reference to spectroscopic data:

n.m.r. : Nuclear Magnetic Resonance

I.R. : Infra-red

br : Broad

sh : shoulder

s : singlet

d : doublet

t : triplet

m : multiplet

$^nJ$  : coupling constant through n bonds

## DEFINITIONS

The isotropic thermal parameter ( U ) =

$$\exp(-8\pi^2 U (\sin^2 \theta / \lambda^2))$$

The anisotropic thermal parameter =

$$\exp[-2\pi^2 (U_{11} h^2 a^{*2} + U_{22} k^2 b^{*2} + U_{33} l^2 c^{*2} + 2U_{12} hka^* b^* + 2U_{13} hla^* c^* + 2U_{23} klb^* c^*)]$$

Agreement factors

$$R_{\text{merg}} = [\Sigma\{N_{\text{eq}} \Sigma(w(F_{(\text{mean})} - F_o)^2)\} / \Sigma\{(N_{\text{eq}} - 1) \Sigma(w(F_o)^2)\}]^{1/2}$$

$N_{\text{eq}}$  = Number of equivalent reflections

$$R = \Sigma(|F_o| - |F_c|) / \Sigma(F_o)$$

$$R_w = [\Sigma w(|F_o| - |F_c|)^2 / \Sigma w(F_o)^2]^{1/2}$$

$$S = [(\Sigma w(|F_o| - |F_c|)^2) / (N - N_p)]^{1/2}$$

## ABSTRACT

Chapter 1 summarises the use of  $\pi$ -allyl complexes in stereospecific organic syntheses. The factors governing the site and mechanism of nucleophilic attack are discussed. The origins of asymmetric allyl bonding in (allyl)MXY complexes and the necessary conditions for the study of such asymmetry, caused by asymmetrical substitution of the allyl ligand, are introduced, with reference to previously reported structures.

The routes for synthesising suitable asymmetrically substituted allyl-metal complexes are reviewed in Chapter 2, followed by a discussion of the spectroscopic properties of the complexes produced. Preliminary crystallographic investigations, to determine the suitability of the compounds for full 3-dimensional crystallographic studies, are also reported.

In Chapter 3 complete crystallographic studies of  $[(\eta^3-1-\text{Ph}-\text{C}_3\text{H}_4)\text{PdTMEDA}]\text{BF}_4$ ,  $(\eta^3-1-\text{Ph}-\text{C}_3\text{H}_4)\text{PdCp}$  and  $(\text{phen})\text{Mo}(\text{CO})_2(\text{NCS})(\eta^3-1-\text{Ph}-\text{C}_3\text{H}_4)$ , all of which contain the  $\eta^3-1$ -phenylallyl ligand are reported. This ligand binds to a metal centre such that the substituted peripheral allylic carbon atom is the further from the metal, even in the absence of steric congestion. The structure determination of  $[(\eta^3-1-\text{EtOOC}-\text{C}_3\text{H}_4)\text{PdTMEDA}]\text{BF}_4$ , on the other hand, reveals that the substituted carbon is the closer bound.

Chapter 4 assesses the electronic origins of this asymmetric bonding, as studied by EHMO calculations, and

predicts the manner of bonding in other substituted allyl complexes.

The structures of  $[\text{Cp}^*\text{Mo}(\text{CO})_2(\eta^4\text{-C}(\text{CH}_2)_3)]\text{BF}_4$ ,  $\text{CpMo}(\text{CO})_2(\eta^3\text{-2-Me-C}_3\text{H}_4)$  and  $\text{CpMo}(\text{Cl})_2(\eta^4\text{-C}_4\text{H}_6)$  are discussed in Chapter 5. A theoretical treatment of the bonding of the  $\text{C}_4\text{H}_6$  ligand to the metal fragment for the complexes  $[\text{CpMo}(\text{CO})_2(\eta^4\text{-C}(\text{CH}_2)_3)]^+$  and  $\text{CpMo}(\text{Cl})_2(\eta^4\text{-C}_4\text{H}_6)$ , again by EHMO calculations, is undertaken in Chapter 6.



## **CONTENTS**

DECLARATION	i
ACKNOWLEDGEMENTS	ii
LIST OF ABBREVIATIONS	iii
DEFINITIONS	v
ABSTRACT	vi
CHAPTER 1: INTRODUCTION	1
CHAPTER 2: SYNTHETIC, SPECTROSCOPIC AND PRELIMINARY CRYSTALLOGRAPHIC STUDIES	
2.1; Synthetic routes	16
2.2; Infra-red spectra	24
2.3; Assignment of $^1\text{H}$ n.m.r. spectra	25
2.4; High field $^1\text{H}$ n.m.r. studies	28
2.5; Preliminary crystallographic studies	36
2.6; Experimental	40
CHAPTER 3: STRUCTURAL STUDIES OF ALLYL COMPOUNDS	
3.1; Preamble	52
3.2; Pd-TMEDA	54
3.3; Pd-Cp	58
3.4; (Phen)Mo(CO) $_2$ (NCS)	61

3.5; The $\eta^3$ -1-phenylallyl ligand	64
3.6; The $\eta^3$ -1-ethoxycarbonyl ligand	71
3.7; Interligand steric interactions	73
3.8; Crystal packing	75
3.9; Experimental	77

#### CHAPTER 4: MOLECULAR ORBITAL STUDIES ON ALLYL COMPOUNDS

4.1; Preamble	82
4.2; Metal fragment orbitals	84
4.3; Allyl anion orbitals	88
4.4; Interaction of metal fragments with allyl <sup>-</sup>	89
4.5; Effects of substitution	93

#### CHAPTER 5: STRUCTURAL STUDIES ON CpMoL<sub>2</sub>-(ENE) SPECIES

5.1; Introduction	101
5.2; Solid state structure of [( $\eta^4$ -C(CH <sub>2</sub> ) <sub>3</sub> )Mo(CO) <sub>2</sub> ( $\eta^5$ -C <sub>5</sub> Me <sub>5</sub> )]BF <sub>4</sub> , TRIMET	105
5.3; Solid state structure of CpMo(CO) <sub>2</sub> ( $\eta^3$ -2-Me-C <sub>3</sub> H <sub>4</sub> ), CPMOME	111
5.4; Solid state structure of ( $\eta^4$ -C <sub>4</sub> H <sub>6</sub> )Mo(Cl) <sub>2</sub> ( $\eta^5$ -C <sub>5</sub> H <sub>5</sub> ), CPMOBUT	115
5.5; Experimental	119

CHAPTER 6: MOLECULAR ORBITAL STUDIES ON  $\text{CpMoL}_2-(\text{C}_4\text{H}_6)$   
SPECIES

6.1; Introduction	121
6.2; Metal fragment orbitals	123
6.3; Ligand orbitals	124
6.4; $\text{CpMo}(\text{CO})_2$ -TMM interaction	125
6.5; $\text{CpMo}(\text{Cl})_2$ -Butadiene interaction	130

APPENDIX 1: Thermal parameters for PHALPD, PDETAL,  
CPPHAL, MOPHAL

APPENDIX 2: Orbital contour plots for  $\text{MXL}_2\text{Y}_2$ ,  $\text{ML}_2\text{XY}$ ,  
MCp AND  $\text{ML}_2$  FRAGMENTS

APPENDIX 3: Thermal parameters for CPMOME, CPMOBUT and  
TRIMET

APPENDIX 4: Contour Plots for  $\text{CpMo}(\text{CO})_2^+$  and  $\text{CpMo}(\text{Cl})_2$   
fragments

APPENDIX 5: Reprints

APPENDIX 6: Courses attended

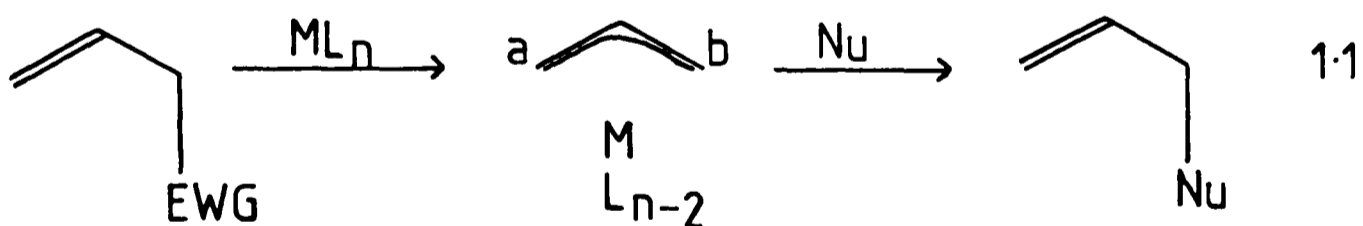
REFERENCES

## CHAPTER 1

### INTRODUCTION

A vast number of organometallic reagents or intermediates are currently employed in modern synthetic organic chemistry<sup>1</sup> due to an enhanced reactivity and/or greater stereochemical control, over normal synthetic methods, which can be achieved by their use. One specific example of their utility is in carbon-carbon bond forming reactions, often with stereochemical control, a fundamental step in the total synthesis of large organic molecules.

In this context  $\pi$ -allyl transition metal complexes have shown great potential and there is considerable current activity in this area<sup>2</sup>. Their ease of synthesis from a variety of alkenes makes them particularly attractive. Being electrophiles such species are subject to nucleophilic attack, addition taking place at one of the terminal carbon atoms, a or b, equation 1.1.



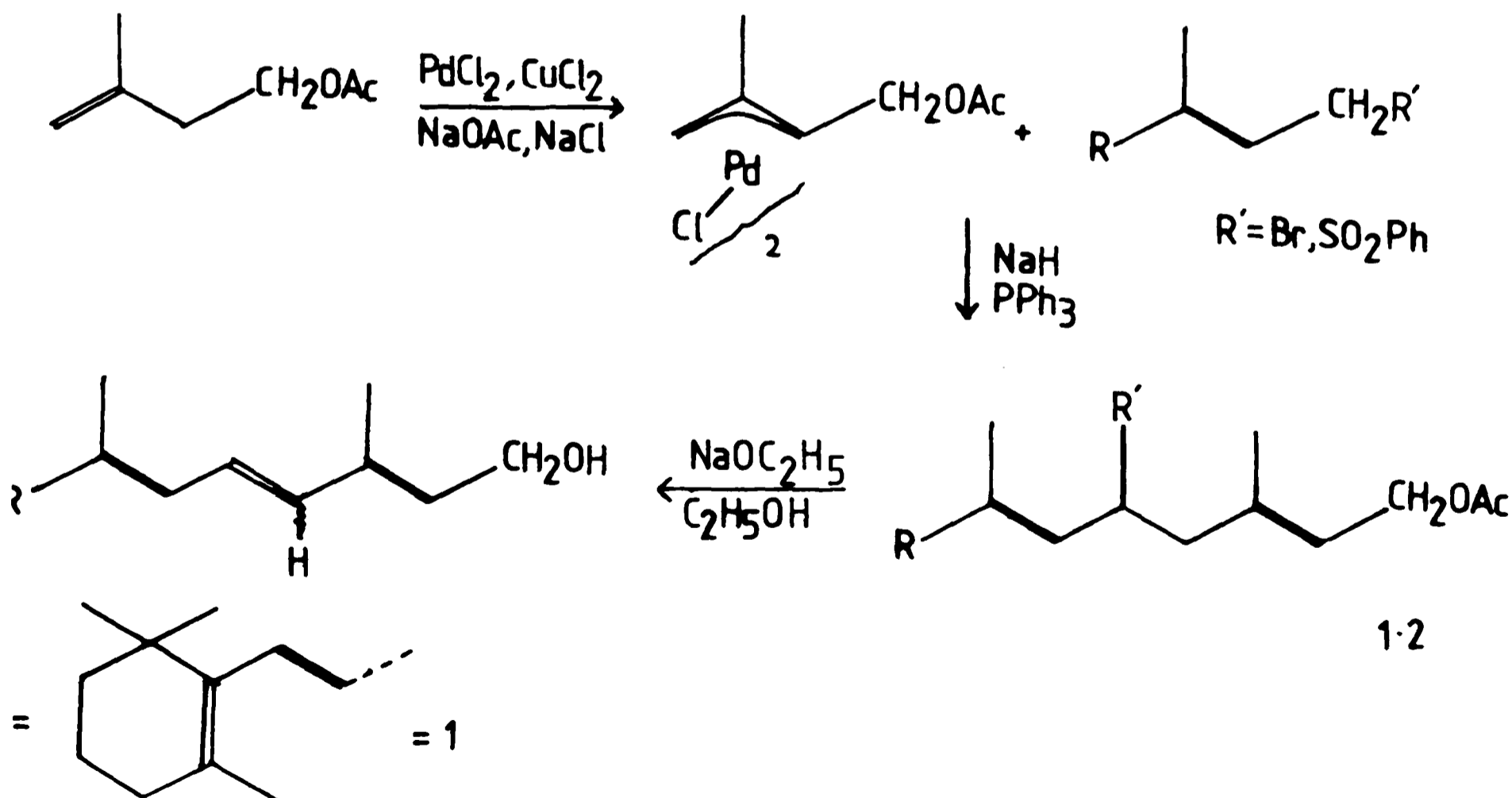
The most predominantly used metal centre is palladium<sup>3</sup> ( generating four-coordinate square planar complexes ) although other transition metals exhibit similar properties<sup>4</sup>.

The allyl complex may be preformed, or a catalytic amount ( ca. 5-10% ) of a metal substrate such as  $\text{Pd}(\text{PPh}_3)_4$

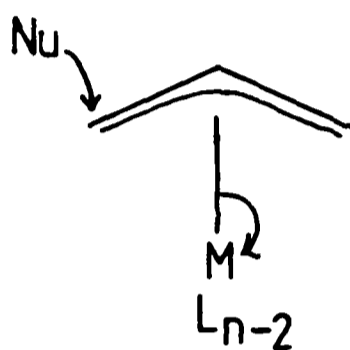
may be used in the reaction, in which case the  $\pi$ -allyl complex is formed *in situ*. In both cases, however, the stereochemistry of the product has been found to be dependant on:-

- (1) The nature of the nucleophile.
- (2) The substituents on the  $\pi$ -allyl function.
- (3) The nature of the ligands on the metal.
- (4) The metal substrate employed.

In most cases, however, due to the greater thermodynamic stability of 1-*syn* compared with 1-*anti* substituted allyls, it is generally the *E* isomer of the olefin that is formed, independant of the stereochemistry of the starting material. This fact is illustrated in the synthesis, by Manchand, Wong and Blout, of Vitamin A, 1, and derivatives<sup>5</sup>, equation 1.2

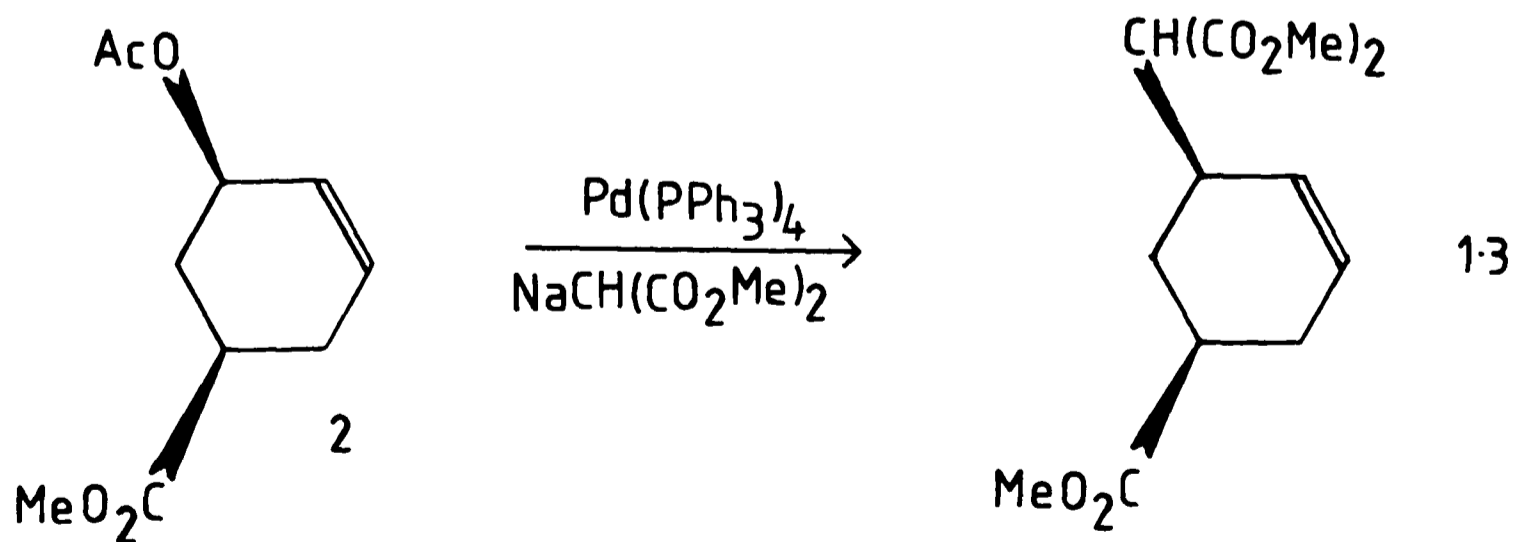


When different forms of nucleophile are used i.e. soft/stabilised or hard/non-stabilised, the mechanism of addition is different. Stabilised nucleophiles such as malonic esters<sup>6,7</sup> or  $\beta$ -keto sulphones<sup>5</sup>, attack the allyl directly, on the opposite face to the coordinated metal, at the least substituted allylic terminal carbon. The metal then becomes the leaving group, as in A.



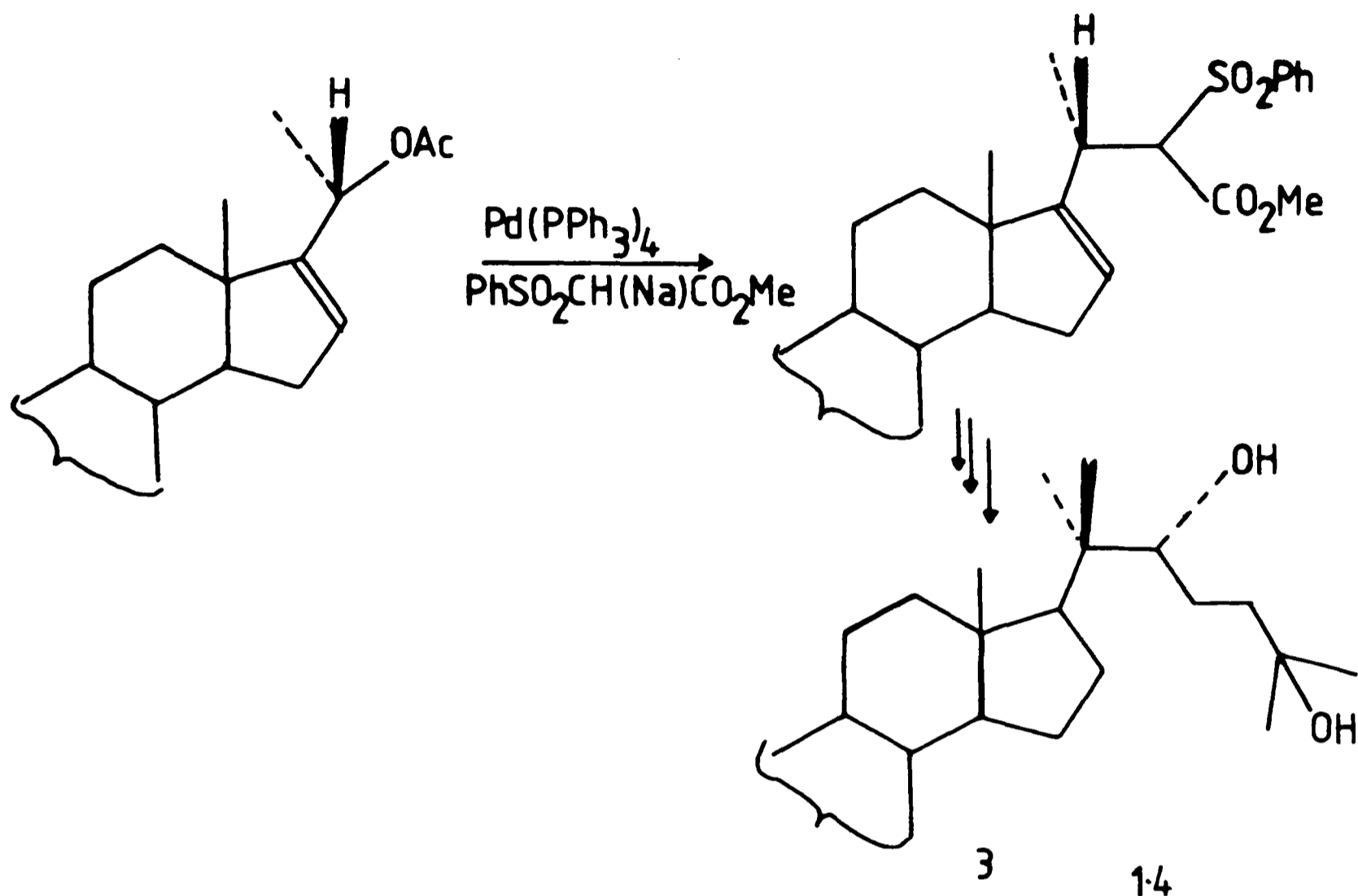
A

In a catalytic cycle this leads to a double inversion of configuration, once on formation of the  $\pi$ -allyl complex and again on nucleophilic attack, resulting in an overall retention of configuration<sup>6</sup>, equation 1.3.

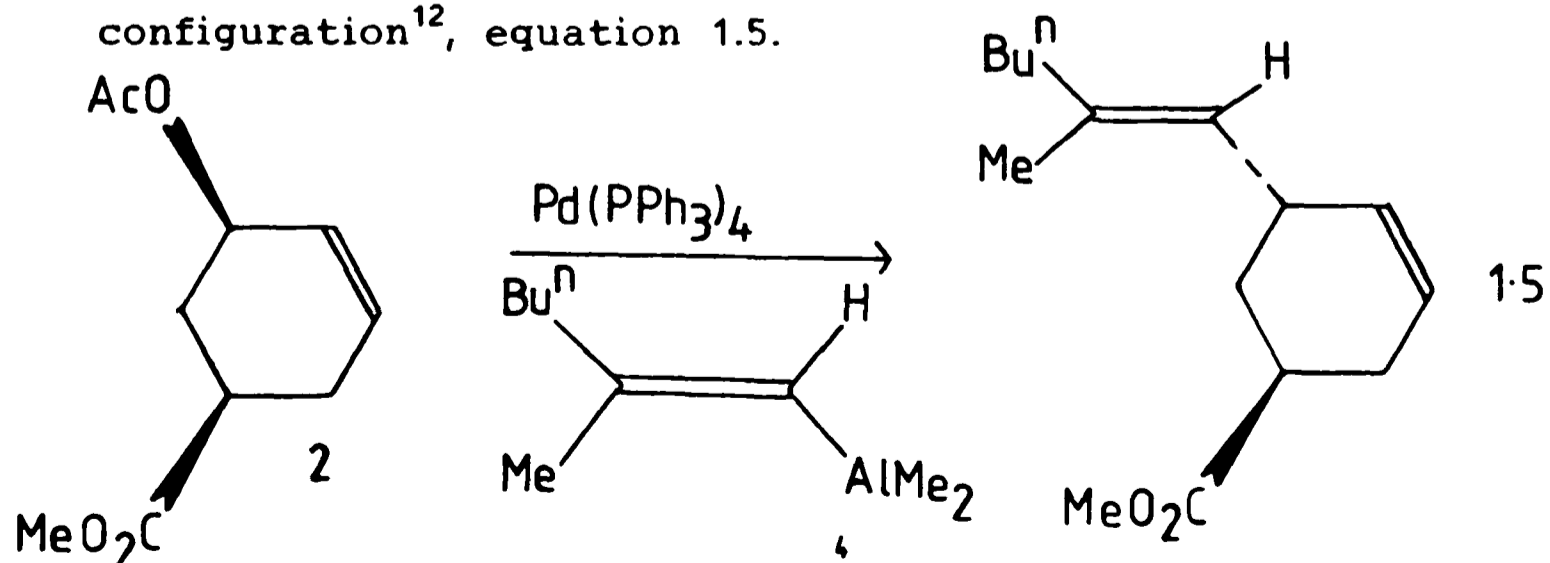


This fact has also been employed in the synthesis of

ecdysones ( insect moulting hormones ) and derivatives of cholesterol<sup>7</sup>, 3, equation 1.4.

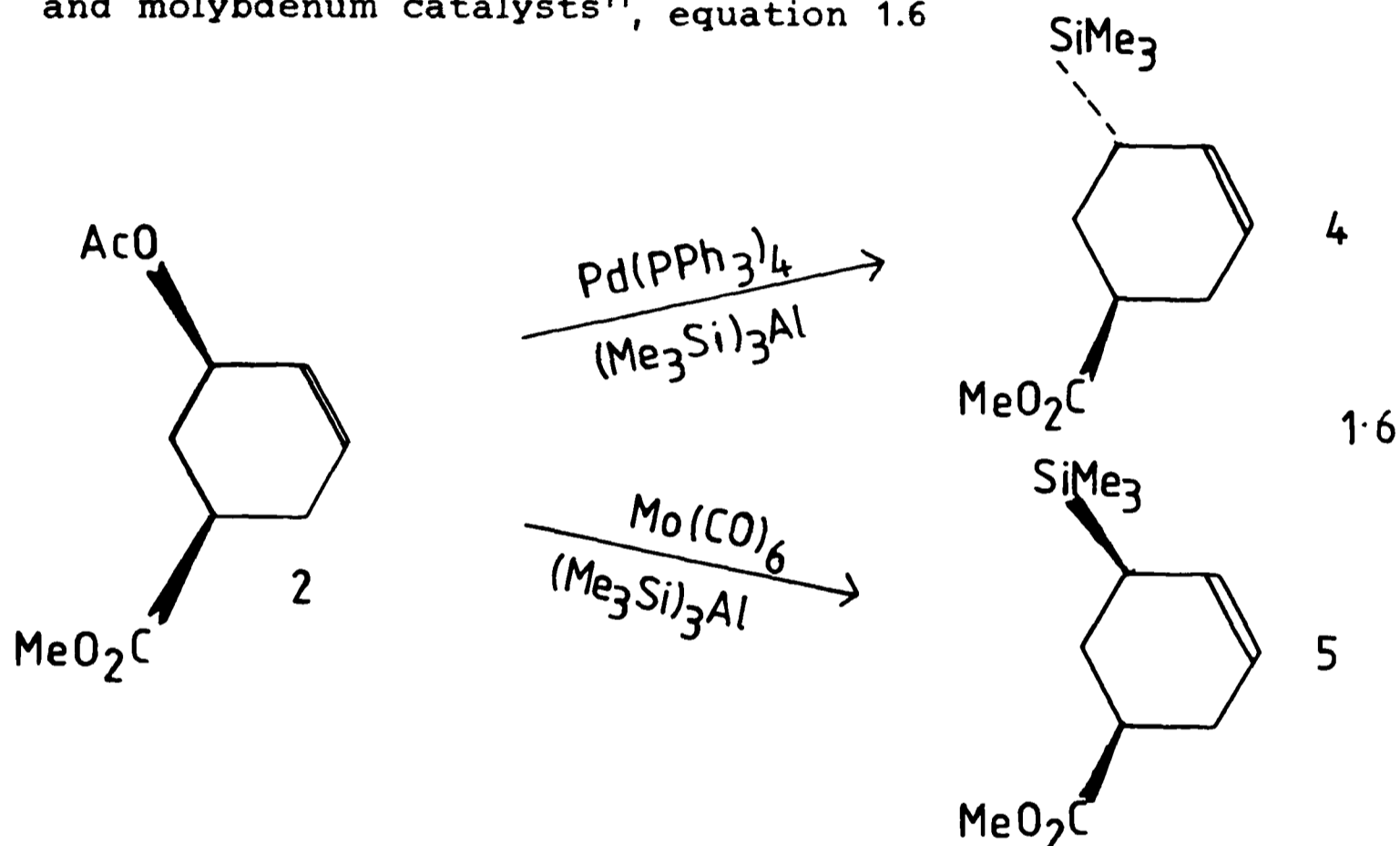


Non-stabilised nucleophiles, such as vinyl<sup>-8</sup>, aryl<sup>-9</sup>, methyl<sup>-10</sup> and trimethylsilyl<sup>-11</sup> organometallics, attack the metal first and then transfer to the allyl carbon. This leads to only one, and hence overall, inversion of the configuration<sup>12</sup>, equation 1.5.



Note that equations 1.3 and 1.5 both employ the same alkene, 2, yet the products have different stereochemistries due to the different nucleophile used.

A similar inversion/retention effect is observed when the metal substrate is changed. This is readily demonstrated by the silylation of the same cyclic alkene, 2, used in equations 1.3 and 1.5 in the presence of palladium and molybdenum catalysts<sup>11</sup>, equation 1.6

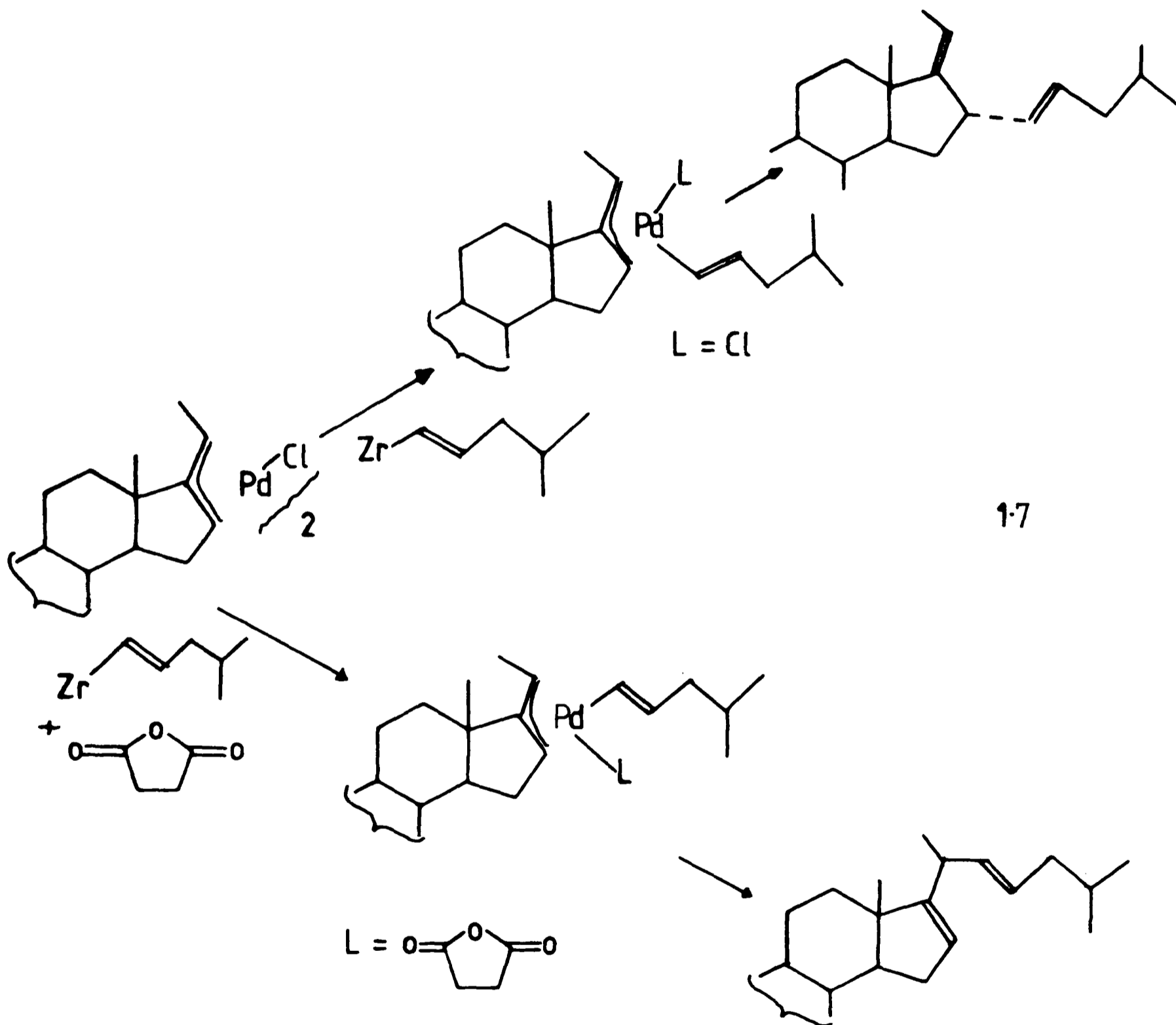


In the palladium catalysed reaction the nucleophile first attacks the metal and then the allylic carbon leading to inversion of configuration in product 4. However, with the molybdenum carbonyl catalyst, attack is directly on the allylic carbon despite the use of a hard nucleophile and this results in retention of configuration in the product, 5.

As already noted soft nucleophiles attack directly on the least hindered allylic terminal carbon. In the case of the hard nucleophiles it is the stereochemistry of the

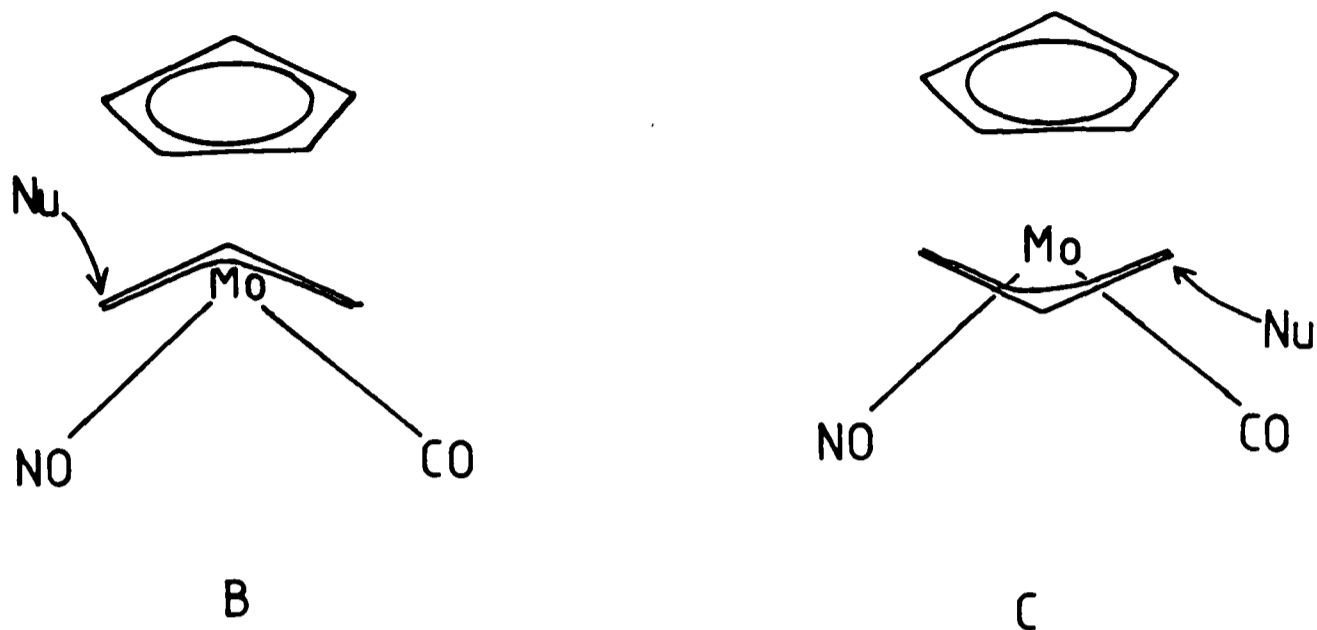


intermediate, formed by nucleophilic attack on the metal, which governs which allyl carbon undergoes substitution<sup>9</sup>. This stereochemistry can be altered by the use of different ligands on the metal, resulting in different products<sup>8,11</sup>, equation 1.7.



Ligand effects are also observed in nucleophilic addition to  $\text{CpMo}(\text{CO})_2(\eta^3\text{-C}_3\text{H}_5)^{13}$ , **6**. In the *exo* form of **6** addition takes place *cis* to the NO function, **B**, whilst addition is *trans* to NO

in the *endo* form, C.



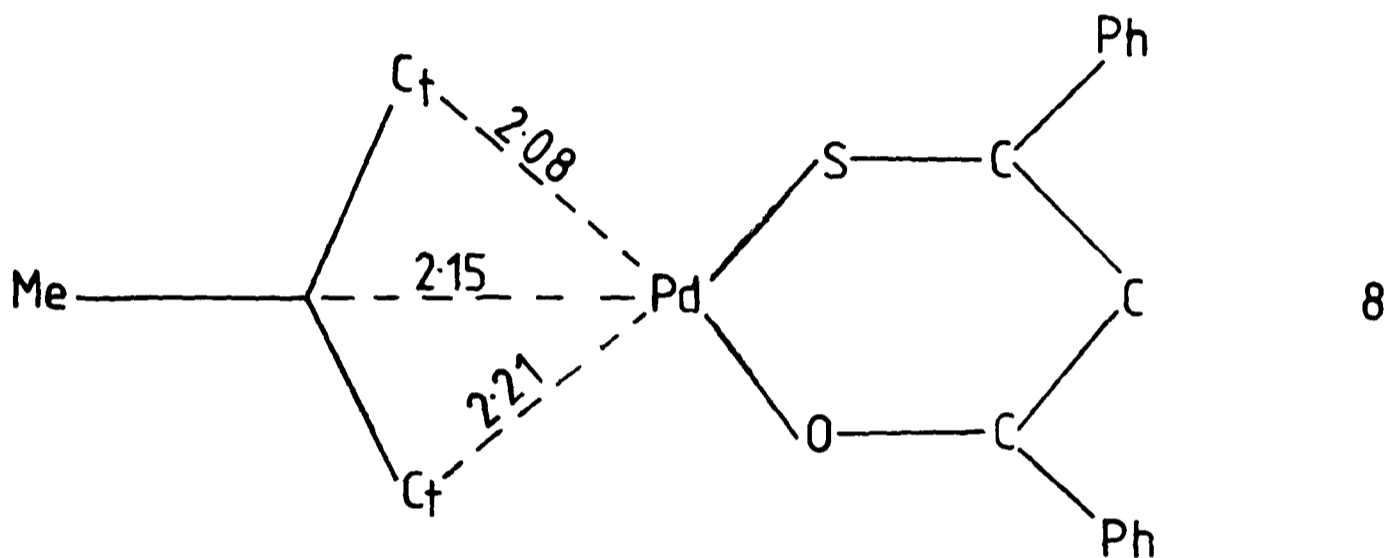
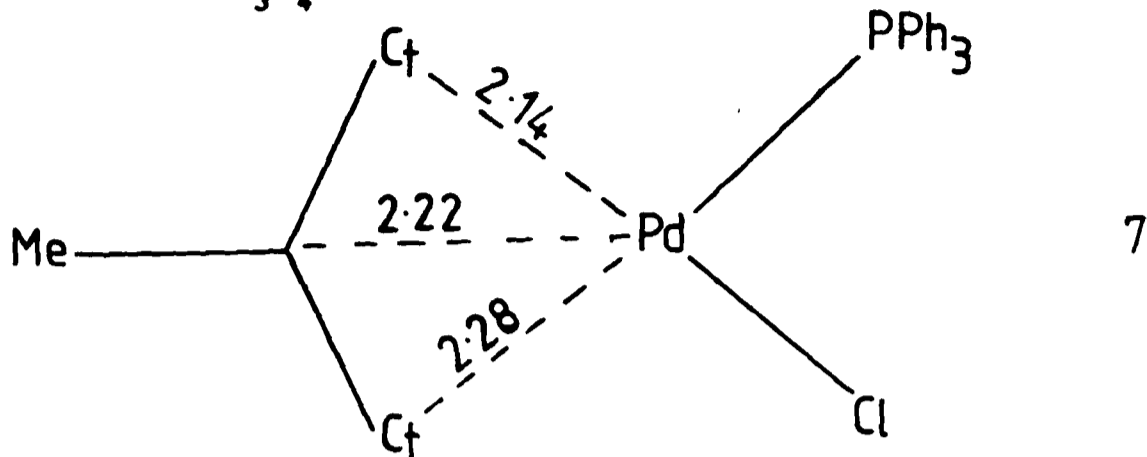
These differing regioselectivities are reproduced by the results of a theoretical study, which suggests that it is the orientation of the coordinated alkene that is generated which is the critical factor.

Thus the factors governing the regioselectivity of nucleophilic addition may be summarised<sup>15</sup> as:-

- (1) Steric considerations.
- (2) Charge distribution/stability of the  $\pi$ -allyl metal complex intermediate.
- (3) The stability of the alkene metal complex generated.

The effects of an asymmetric set of non-allyl ligands on the bonding of the allyl to a transition metal centre are well established and may be readily interpreted in electronic terms. In square-planar palladium complexes of the type (allyl)PdXY the differing *trans* influence of X and Y determines the direction of the asymmetry in the bonding of the allyl. Well known crystallographically studied examples

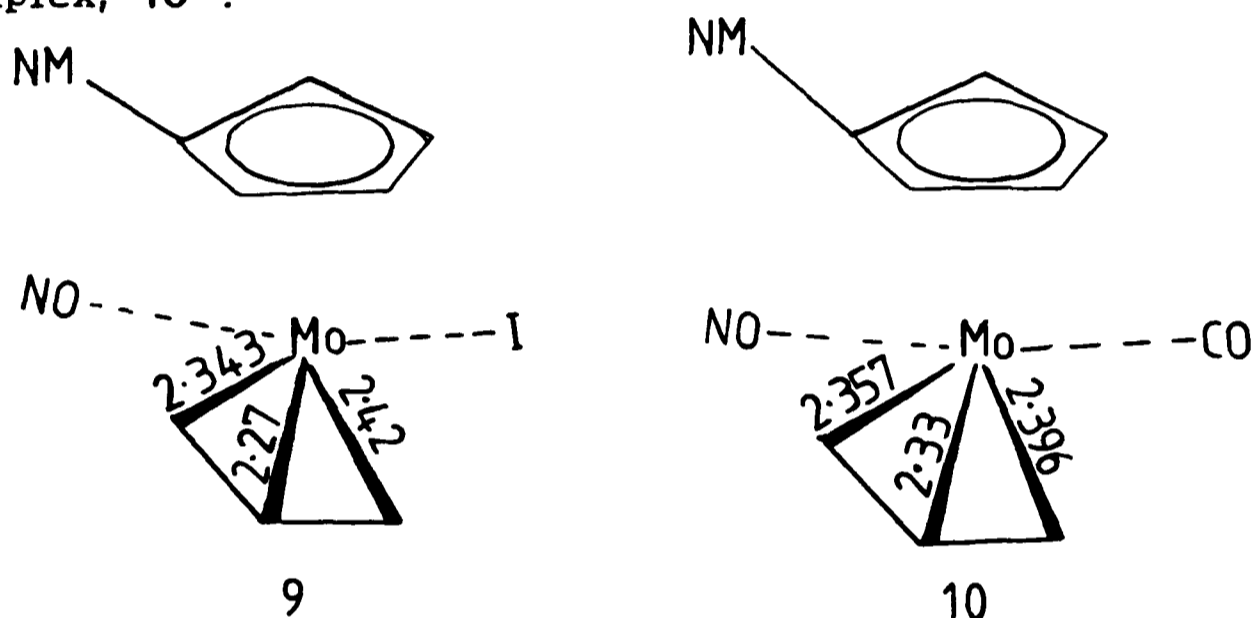
are  $(\eta^3\text{-2-Me-C}_3\text{H}_4)\text{Pd}(\text{PPh}_3)\text{Cl}$ <sup>16</sup>, 7, and  $(\eta^3\text{-2-Me-C}_3\text{H}_4)\text{Pd}(\text{SC}(\text{Ph})\text{C}(\text{H})\text{C}(\text{Ph})\text{O})$ <sup>17</sup>, 8.



In both cases the Pd-C<sub>t</sub> bond *trans* to the ligand with the greater  $\pi$ -acceptor character ( PPh<sub>3</sub> and S ) is longer than the other Pd-C<sub>t</sub> bond. This asymmetry is consistent with the expected *trans* influence of the ligands<sup>18</sup>. Furthermore, the conformation of alkyl, 1-*syn*, substituted (allyl)PdXY complexes is such that the substituted allyl carbon is *trans* to the ligand, X or Y, which is the better  $\pi$ -acceptor<sup>19</sup>. Here the rationale is that the labilised allyl carbon is stabilised by the inductive effect of the alkyl group<sup>20</sup>

Similar examples also exist in molybdenum and tungsten chemistry. CpMXY(allyl) complexes, and derivatives thereof, already mentioned with respect to the regiospecific

nucleophilic additions, have been structurally characterised<sup>21-24</sup>. In all cases the bonding of the allyl is severely distorted, the M-C<sub>t</sub> bond *trans* to the ligand ( X or Y = NO, CO or I ) with the greater  $\pi$ -acceptor character being the longer, as in 9. Consistent with this is the observation that the asymmetry of the allyl coordination is substantially reduced in the analogous nitrosyl-carbonyl complex, 10<sup>21</sup>.



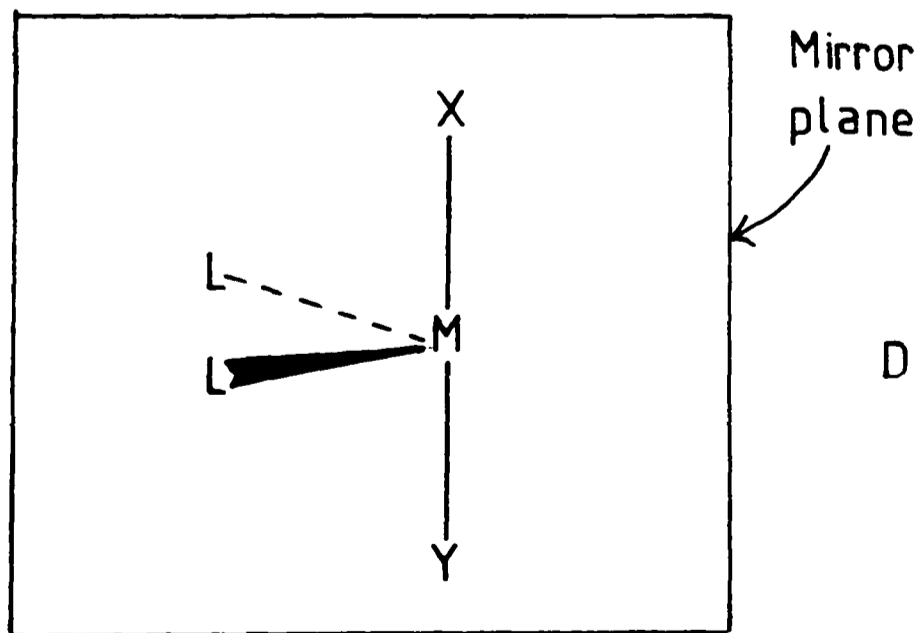
Moreover, the allyl ligand appears to have rotated, about the allyl-M vector, to bring the allyl C-C bond *trans* to the weaker  $\pi$ -acceptor parallel, or as near as possible, to the M-( $\pi$ -acceptor) bond.

Not only will the electronic properties of the other ligands on the metal affect the stability of the intermediates, formed in the nucleophilic additions, but any substituents on the allyl are also likely to be important. Schwartz has suggested that the electronic properties of the allyl termini may be different in an asymmetrically substituted ligand, and this could result in uneven bonding

to the metal<sup>8</sup>.

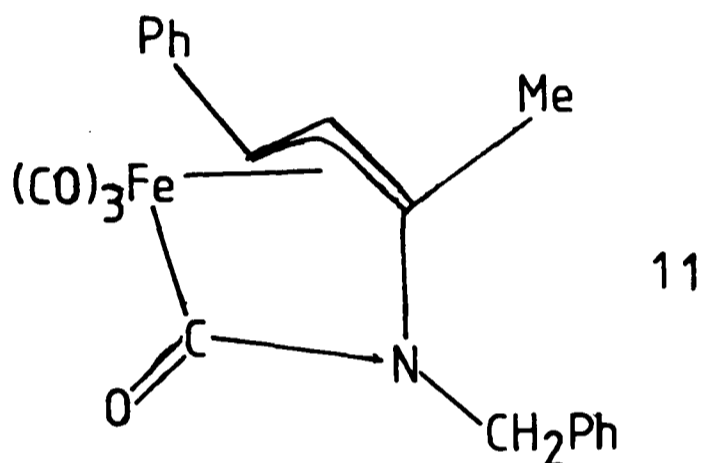
In order to observe and assess effects due to asymmetric allyl substitution it is necessary to study complexes which are otherwise symmetric. The metal fragment ( the metal plus non-allyl ligands ) must be of at least  $C_s$  symmetry and the allyl must be coordinated across the mirror plane which then bisects the C-C-C angle.

A suitable metal fragment would obviously be the  $ML_2$  moiety, in which  $L_2$  represents two identical monodentate ligands, such as phosphine or arsine, or a single bidentate ligand such as a diphosphine, diene or diamine whose substitution pattern is identical on both sides of the molecular mirror plane. The resulting allyl complex would be formally a four-coordinate one. Other suitable backbones would be the conical fragments  $M(CO)_3$ ,  $M(\text{arene})$  and  $MCp$ , generating a five-coordinate complex, a  $C_{2v}$   $ML_4$  fragment of the type  $ML_2XY$ , where X and Y are mutually *trans* ligands lying in the mirror plane, D, ( six-coordinate ), and the  $CpML_2$  fragment ( seven-coordinate ).



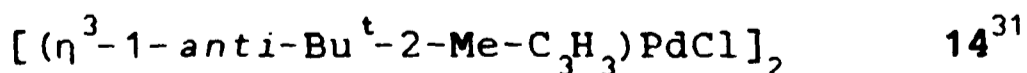
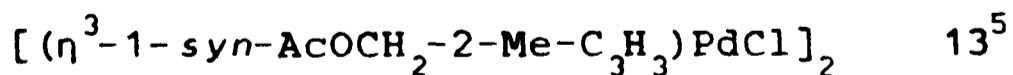
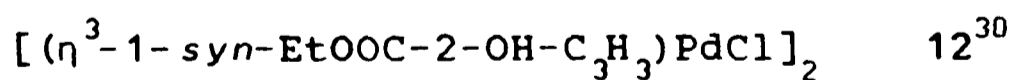
Furthermore, intramolecular interligand congestion should be avoided by the use of relatively compact ligands, with functions such as  $\eta^5\text{-C}_5\text{Me}_5$  ( $\text{Cp}^*$ ) probably proving too large.

Moreover, the allyl ligand must not be constrained by bonding, through its substituents, to the metal or other ligands either within the molecule by a cyclic system, or to a different one by hydrogen bonding. An example of the former occurs in  $(\text{CO})_3\text{FeC}(\text{O})\text{N}(\text{CH}_2\text{Ph})(\eta^3\text{-C}(\text{Me})\text{CHCHPh})^{25}$ , 11.

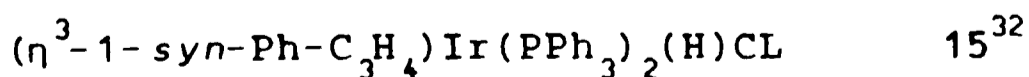


Altering the size of the chelate ring has been found to alter the degree of asymmetry in the allyl bonding<sup>26-29</sup>. Clearly, the allyl ligand must be "free".

Only five examples of free, asymmetrically substituted allyls coordinated to a symmetrical backbone have been characterised by three-dimensional crystallographic studies. They are:-



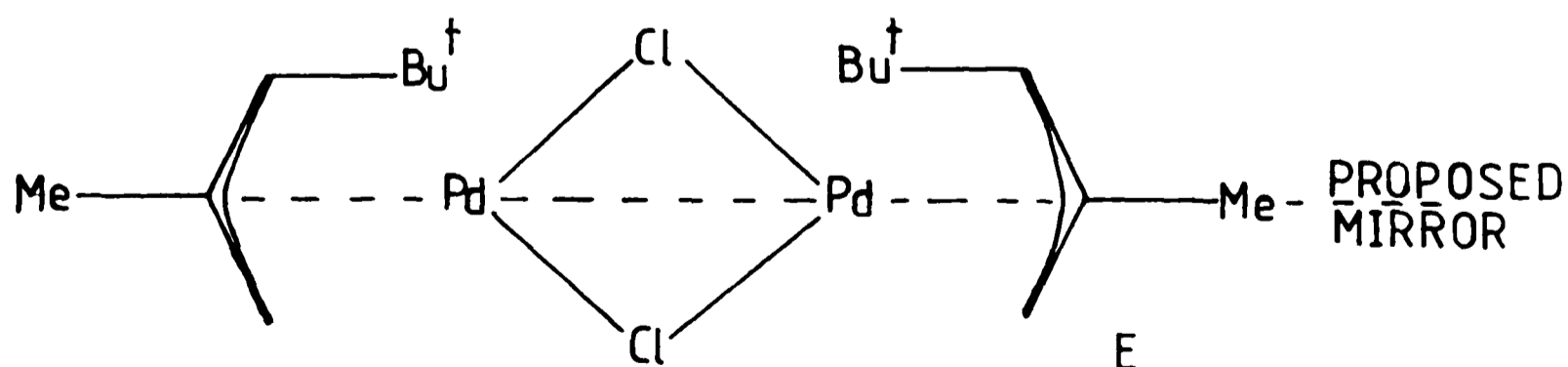
which are all four coordinate dimeric species,



a six-coordinate complex with a  $C_{2v} ML_2XY$  backbone,  
 and the seven-coordinate  $CpMoX_2(allyl)$  complex  
 $CpMo(1,2-C_6H_4S_2)(\eta^3-1-syn-Ph-3,3-Me_2-C_3H_2)$  16<sup>33</sup>.

The accuracy of the determination of 12 is very poor, the average palladium-carbon distance being  $2.11 \pm 0.05 \text{ \AA}$  with no significant difference between any of the three individual Pd-C lengths. There is also a network of hydrogen bonding between the hydroxyl group on one molecule and the carbonyl of another, related to the first by the centre of inversion (the space group is  $P\bar{1}$ ). Thus this determination is of little use in assessing the effect of the substitution.

Complex 14 is a rare example of a 1-*anti* substituted allyl complex; the conformation is *anti* because of the unfavourable steric interaction that would exist between the large  $Bu^t$  group and the methyl substituents in the *syn* form. However, doubt must be cast on the structure determination since De Boer *et al.* claim a mirror plane passes through the two palladium positions, bisecting the allyl groups, the  $Bu^t$  substituents being mutually *cis*, **E**.



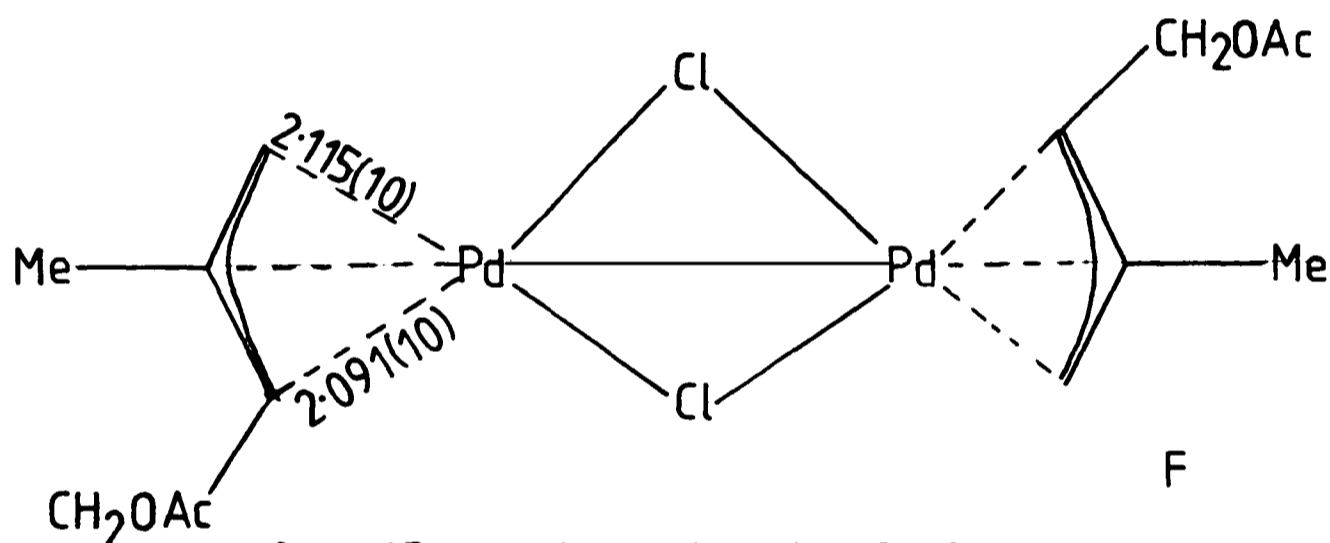
In the absence of disorder, which the authors do not

mention, these factors are clearly inconsistent.

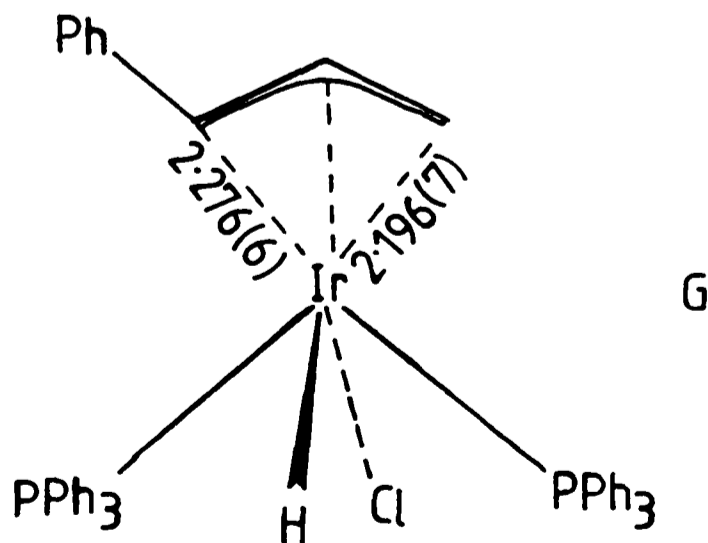
The allyl function in 16 is substituted on both termini, thus only the net result of the substituent effects will be observed, making analysis of the individual effects very complicated.

Eliminating complexes 12, 14 and 16 from our discussion leaves 13 and 15, the results for which are reliable and show some degree of asymmetry in allyl bonding.

In 13 the substituted allyl terminal carbon is closer to the metal than the unsubstituted one, although the result is not strictly significant, F.



Complex 15 on the other hand shows the reverse effect since the substituted allyl carbon atom is unequivocally further from the metal than the unsubstituted one, G.





Although this could be due to steric crowding between the phenyl rings on the allyl and those on the *cis* phosphorus no mention is made by the authors of any such contact. Moreover, the *trans* effect of the unevenly bound allyl group is observed in the iridium-phosphorus distances.

The differing directions of asymmetric bonding of the 1-*syn*-substituted allyl ligands of 13 and 15 may be understood *via* semi-empirical molecular orbital calculations carried out in this project as part of a general analysis of the problem; see Chapter 4.

The first section of this thesis ( Chapters 2-4 ) is involved with trying to further qualify the distortions in allyl bonding due to asymmetric substitution.

Specific, target, compounds have been synthesised and characterised spectroscopically ( Chapter 2 ). Full, three-dimensional, crystal structure determinations have been carried out, at low temperature, on suitable examples (Chapter 3 ) and finally, in order to probe the electronic reasons for the asymmetry, Extended Huckel Molecular Orbital ( EHMO ) calculations have been performed on idealised models of the structurally studied complexes.

The target compounds not only conform to the conditions outlined above, but, for ease and accuracy of the structure determinations, do not involve any strong Mo-K $\alpha$  X-ray absorbing elements such as the third row transition metals, Br or I. Furthermore, to simplify the molecular orbital calculations only mono-substituted allyls have been

studied.

The substituents employed are methyl-, phenyl- and ethoxycarbonyl-. Phenyl substitution was considered important since the one previously studied example, 15, showed marked asymmetry and, moreover, such complexes are relatively easily synthesised. The ethoxycarbonyl group has similar steric requirements to the phenyl group, although markedly different electronic properties and hence should be interesting for comparative purposes.

Both Ph and COOEt substitution could, in principle, alter both the  $\sigma$ - and  $\pi$ - type interactions between the allyl ligand and the transition metal. In contrast methyl substitution ought only to alter the  $\sigma$ -bonding capabilities.

The compounds studied range in coordination number from four to seven, if the allyl is considered as a bidentate ligand.

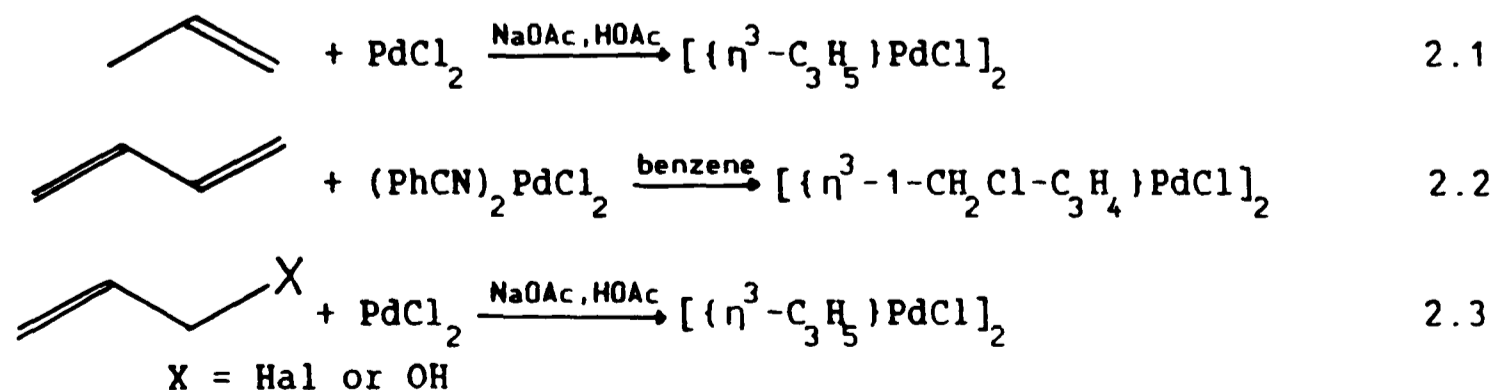
## CHAPTER 2

### SYNTHETIC, SPECTROSCOPIC AND PRELIMINARY CRYSTALLOGRAPHIC STUDIES.

#### 2.1 Synthetic routes:-

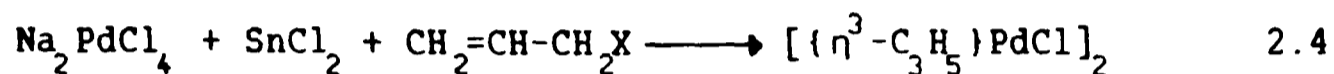
Although the first example of a  $\pi$ -allyl complex was synthesised in 1952<sup>34</sup>, the true nature of such species was not determined until 1961<sup>35</sup>, with the first crystallographic studies, on  $[\eta^3\text{-C}_3\text{H}_5\text{PdCl}]_2$  17, being published in 1965<sup>36</sup>. These chloro-bridged dimeric species are not only subject to nucleophilic attack, but also bridge cleavage reactions ( in which the allyl remains bound to the metal ) and allyl migrations ( in which it transfers to another metal ). There are several routes to the dimeric compounds, which makes a wide range of substituted derivatives obtainable. Hence they are valuable starting materials in any study of the  $\pi$ -allyl system.

The route used to synthesise the dimer depends on the available allylic starting material; alkenes<sup>37</sup>, dienes<sup>38</sup>, allylic halides<sup>39</sup> and alcohols<sup>40</sup> can all be used as shown in equations 2.1, 2.2, 2.3 respectively.



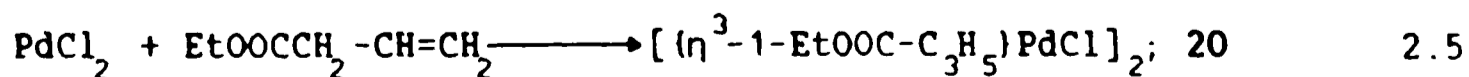
However, most of the above routes result in relatively low yields ( < 50% ). Improvements have been made on the last route, employing allylic halides, by the addition of carbon monoxide<sup>41</sup>, thus forming a hydroxy(carbonyl) $\pi$ -olefin intermediate<sup>42</sup> which rearranges to give the allyl complex.

For small-scale preparations the use of carbon monoxide is not particularly convenient and may be avoided by employing SnCl<sub>2</sub> as a catalyst<sup>43</sup>, equation 2.4.

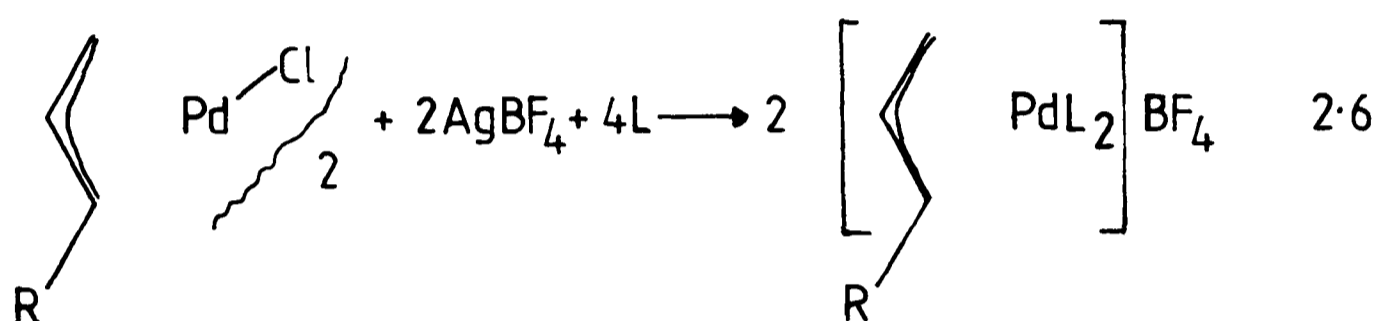


This reaction supposedly involves a Pd(SnCl<sub>3</sub>)<sub>5</sub><sup>3-</sup> intermediate and proceeds in almost quantitative yields for a variety of substituted allyls. When the allyl is substituted in the 1-position, the product obtained is almost always the *syn* isomer<sup>44</sup>, as indicated by <sup>1</sup>H n.m.r. studies. However, the use of large groups can force the substituent into the *anti* position<sup>31</sup>. Thus the 1-*syn*-phenyl- and 1-*syn*-methyl-substituted allyl palladium chloride dimers ( 18 and 19 respectively ) can be readily synthesised from commercially-available cinnamyl- and crotyl-chlorides in high yield.

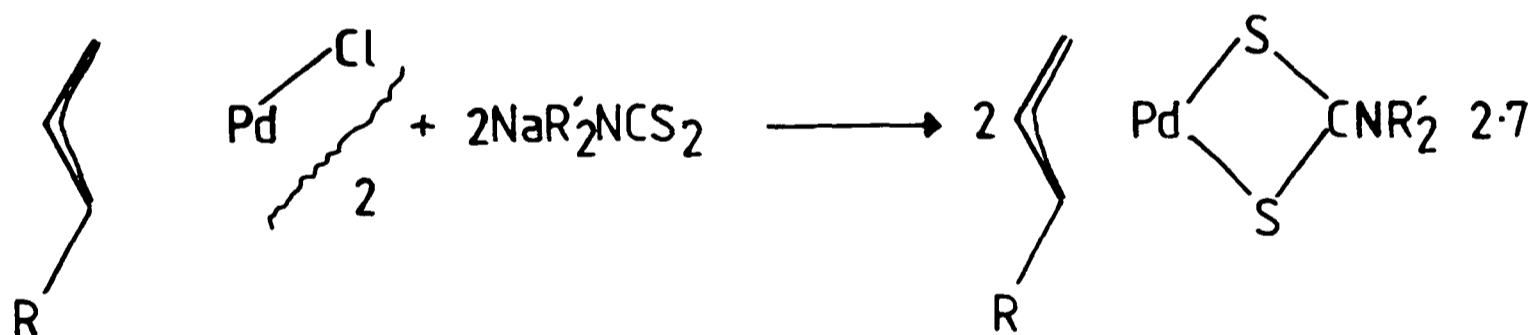
In the case of the ethoxycarbonyl-substituted analogue ( 20 ), the allylic chloride is not commercially available and a modification of the route in equation 2.1 is employed, using the ester ethyl 2-butenate<sup>45</sup>, equation 2.5.



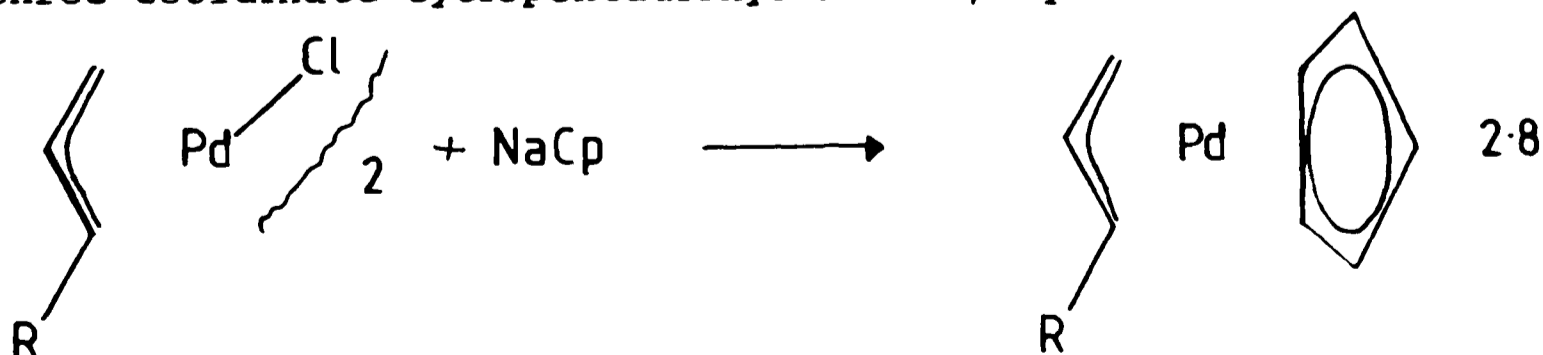
A wide range of reagents will cleave the halogen bridge in these dimeric compounds while preserving the allyl coordination to the metal. Reaction with a silver salt such as  $\text{AgBF}_4$  or  $\text{AgPF}_6$  results in the formation of the coordinatively unsaturated  $[\text{Pd}(\text{allyl})]^+$  species<sup>46</sup>. This can be stabilised by the addition of two neutral, two-electron donor ligands, L, such as phosphines<sup>47</sup>, arsines<sup>47</sup>, dienes<sup>48</sup>, or amines<sup>49</sup>, giving four-coordinate cations, equation 2.6.



Similarly, neutral species can be made by treatment of the dimers with salts of dialkyldithiocarbamates<sup>50</sup> or acetylacetonates<sup>51,52</sup>, again resulting in the formation of planar four-coordinate species, equation 2.7.



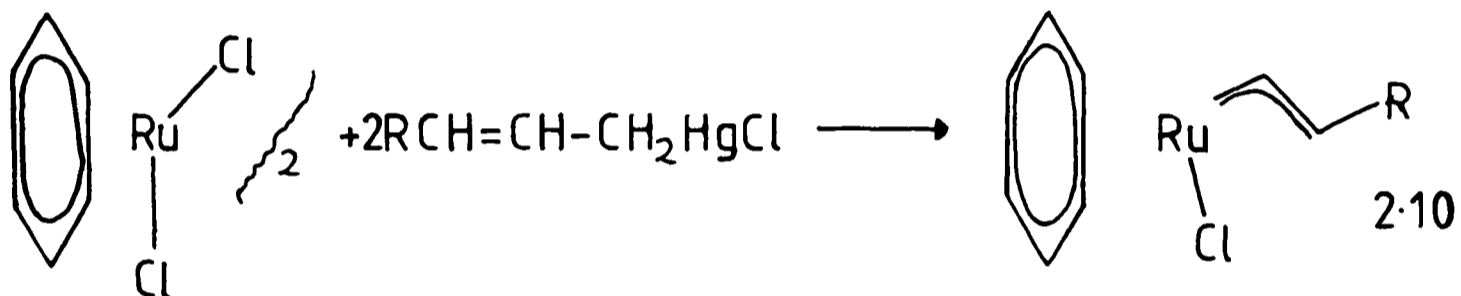
This method may even be used to increase the coordination number of the metal by using the formally three-coordinate cyclopentadienyl anion<sup>51</sup>, equation 2.8.



Reaction of the allyl palladium chloride dimers with metallic mercury results in migration of the allyl to yield  $\sigma$ -allylmercurychlorides in quantitative yields<sup>53</sup>, equation 2.9.



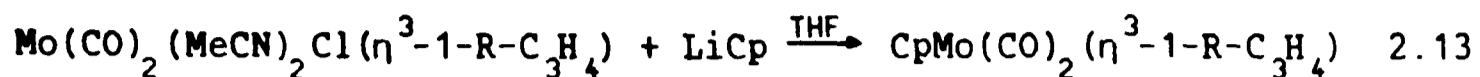
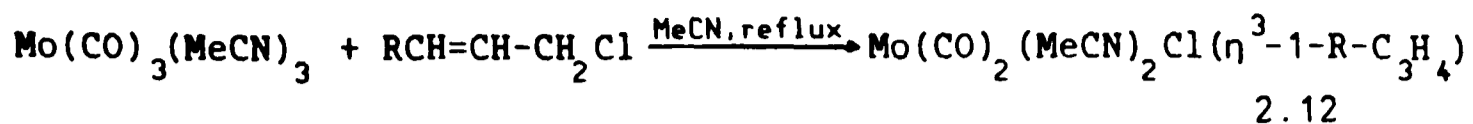
These can then be used as allylating reagents for the synthesis of many platinum group metal  $\pi$ -allyl complexes<sup>54</sup> such as  $(\eta^6\text{-arene})\text{RuCl}(\eta^3\text{-allyl})$  and its derivatives, equation 2.10.



Thus the allyl palladium chloride dimers can give access to four-, five-, and six-coordinate  $\pi$ -allyl complexes.

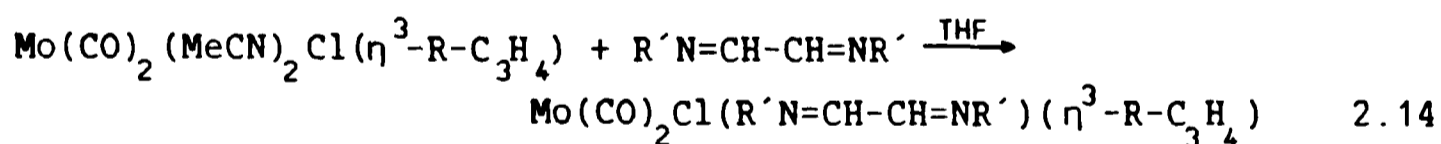
In order to obtain examples of seven coordinate complexes a different approach is required. The most suitable compounds are of the type  $\text{LL}'_2\text{Mo}(\text{CO})_2(\eta^3\text{-allyl})$ , where  $\text{LL}'_2$  is a three-coordinate, six-electron donating, anionic ligand or combination of ligands. Examples where  $\text{LL}'_2$  is the cyclopentadienyl anion were originally synthesised by Hayter<sup>55</sup> and the route was more generally developed by Faller<sup>56</sup>. It is a three stage sequence, equations 2.11-2.13.





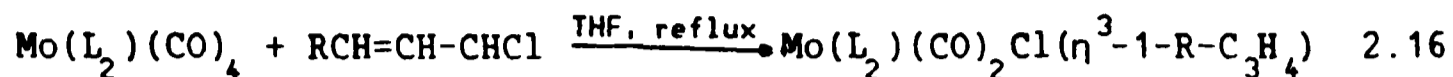
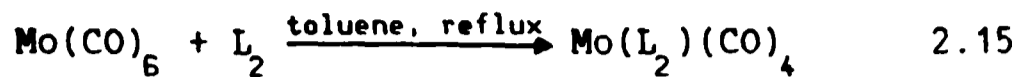
Alternatively, L may be a halide ( or a pseudohalide such as  $\text{NCS}^-$  ), with  $\text{L}'_2$  representing one bidentate or two monodentate donor ligands. In those cases where  $\text{L}'_2$  is a strong  $\pi$ -acceptor ligand such as a phosphite<sup>57</sup>, phosphine<sup>58</sup> or acetylacetonone<sup>59</sup>, the necessary condition of this study that the "backbone" be symmetric is not fulfilled. However in those cases where  $\text{L}'_2$  is not a strong  $\pi$ -acceptor, but is, for example, a diimine<sup>60,61</sup>, diamine<sup>62,63</sup> or diether<sup>64</sup>, the required mirror symmetry is achieved.

The diimine complexes may be prepared by the reaction of the acetonitrile complex formed in equation 2.12 with diimine, which results in displacement of two molecules of acetonitrile, equation 2.14<sup>65</sup>.



Diamines ( e.g. bipy or phen ) and diethers do not displace acetonitrile and a different route is required. The diamine or diether is first coordinated to the metal by substitution of two carbonyl groups from  $\text{Mo(CO)}_6$ , equation 2.15<sup>66</sup>. Reaction of this complex with allyl halide<sup>67</sup> or, in the case of the diether complex, allyl acetate<sup>64</sup> yields the required  $\pi$ -allyl complex, by displacement of a further two

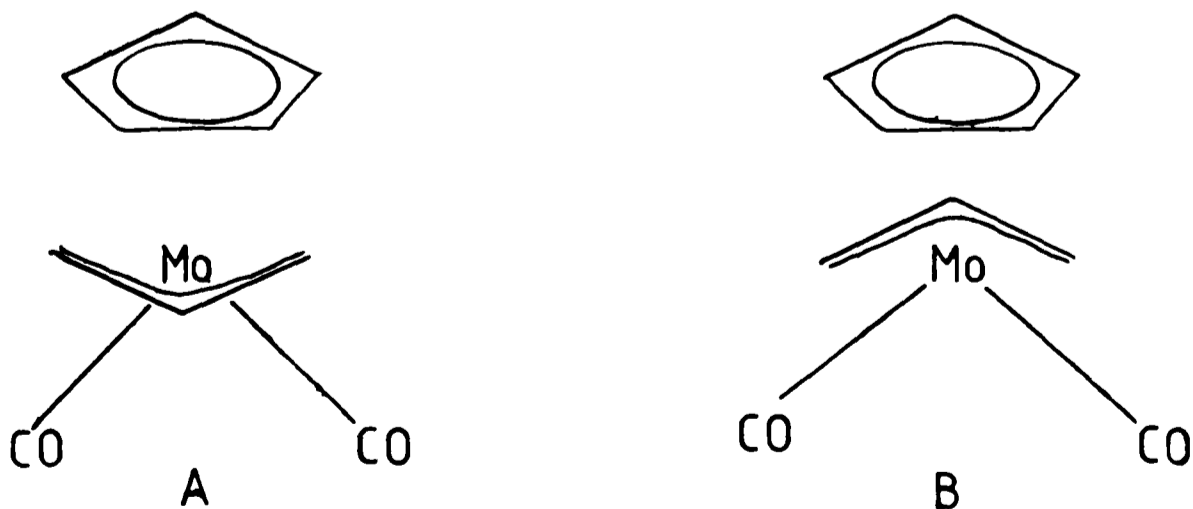
carbonyls, equation 2.16.



Direct metathetical reaction of the halogen derivatives with the salt of a pseudohalogen, such as KNCS, results in formation of the respective pseudohalide complex<sup>67</sup> which is often more soluble than the parent compound. Similarly, cationic complexes, which also possess the required symmetry<sup>68</sup>, can be synthesised by reaction with a suitable counter-ion ( e.g.  $\text{AgBF}_4$  or  $\text{NaBPh}_4$  ) and a neutral 2-electron donating ligand ( e.g. pyridine )<sup>67</sup>.

Unfortunately, all these preparations involve the use of the allylchloride and hence the range of derivatives is severely restricted.

An interesting feature of these seven-coordinate species is that the allyl group can adopt two different conformations with respect to the  $\text{Mo(CO)}_2$  fragment<sup>69</sup>, *endo*, A and *exo*, B.

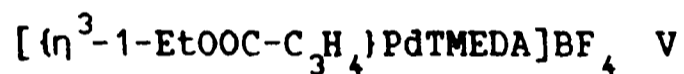
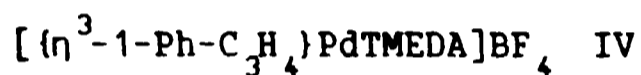
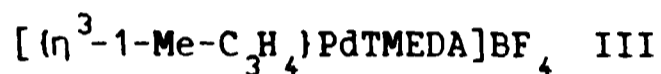
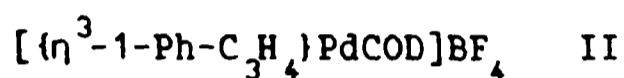
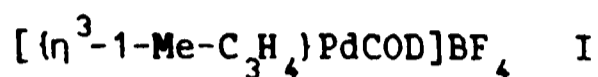


Normally both forms exist in solution, the *endo*:*exo* ratio

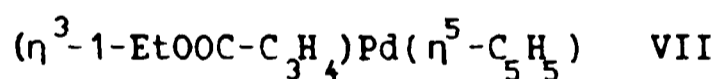
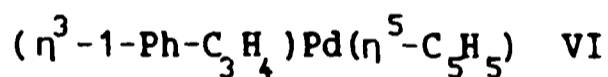


and rate of inter-conversion being dependant on the allylic substituents. The two isomers can be differentiated on the basis of their n.m.r. spectra<sup>56</sup>.

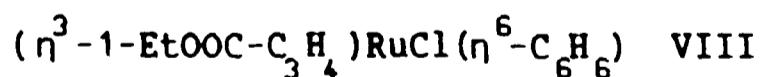
For the purposes of this study the following compounds were synthesised by the appropriate aforementioned routes. The four coordinate ionic complexes:-



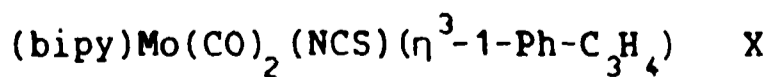
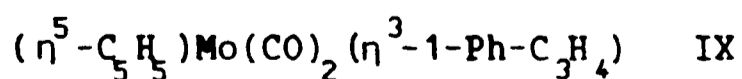
The five coordinate neutral species:-

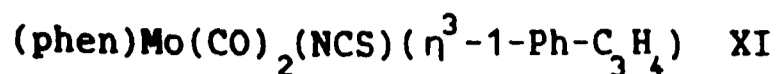


The six-coordinate complex:-



and the seven-coordinate series:-





Complex III has been previously synthesised<sup>49</sup> although the method differed slightly from that used here.

For the purposes of synthesising VIII the  $\sigma$ -allylmercuryhalide  $\text{EtOOC-CH=CH-CH}_2\text{HgCl}$ , VIIIb, was prepared and characterised. The halide precursors to IX, X and XI were prepared but not fully characterised due to their insolubility or sensitivity to air. Their identity was confirmed by full characterisation of the final products and by analogy with previous literature examples<sup>56,67</sup>.

## 2.2 Infra-red spectra:-

Evidence of the  $\pi$ -allylic nature of the complexes is furnished by their infra-red spectra. The carbon-carbon stretching frequencies observed near  $1450\text{cm}^{-1}$  are characteristic of an allylic  $\text{C}\cdots\text{C}$  bond<sup>70</sup>. The exact position will obviously be dependent on the substituents and differentiating between  $\nu(\text{C}\cdots\text{C})$  and bands due to coordinated  $\text{C}_6\text{H}_6$  or Cp (ca.  $1430\text{cm}^{-1}$ )<sup>53</sup> is difficult. Bands due to coordinated and free alkene (as in VIIIb) occur at approximately  $1500\text{-}1550\text{cm}^{-1}$  and  $1620\text{cm}^{-1}$  respectively and are more easily identified.

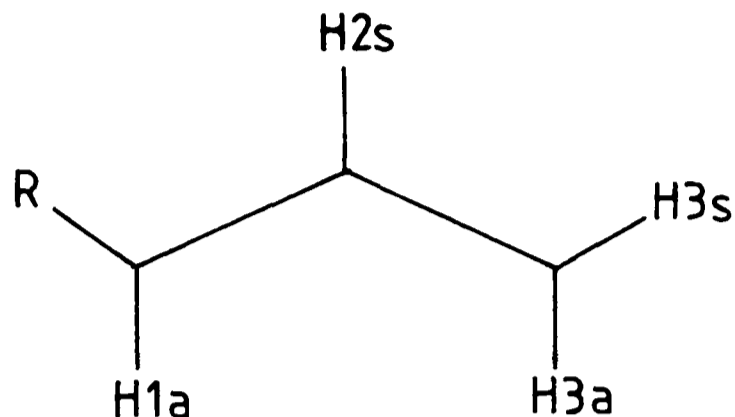
The 1-Ph-allyl complexes give bands at ca.  $1460\text{cm}^{-1}$  and  $1490\text{cm}^{-1}$  while in the ethoxycarbonyl derivatives the stretching frequencies are approximately  $1470\text{cm}^{-1}$  and  $1440\text{cm}^{-1}$ , the exact values depending on the particular compound.

The spectra are also useful for confirming the presence of an uncoordinated carbonyl group in the ethoxycarbonyl derivatives. A characteristic  $\nu(\text{CO})$  band at about  $1700\text{cm}^{-1}$  is observable in the spectra of V, VII, VIIIb and VIII.

The mode of bonding of the NCS group in the seven-coordinate compounds X and XI can also be determined. A sharp  $\nu(\text{NC})$  band at  $2090\text{cm}^{-1}$  and a broad  $\nu(\text{CS})$  at  $830\text{cm}^{-1}$  are both characteristic of an isothiocyanate<sup>71</sup>.

### 2.3 Assignment of $^1\text{H}$ n.m.r. spectra:-

The allyl protons in the  $^1\text{H}$  n.m.r. spectra of all the  $\pi$ -allyl complexes are assigned according to the scheme:-



The number denotes the carbon of attachment whilst the letter indicates their position, *syn* or *anti*, relative to the unique proton H<sub>2s</sub>. The spectra have been assigned on the basis of coupling constants, chemical shifts and analogy with previously recorded spectra of related compounds.

For all compounds, the spectra may be interpreted unequivocally as showing 1-*syn* substitution. This is indicated by the presence of two *trans*  $^3\text{J}$  couplings of ca. 10 - 13Hz (  $^3\text{J}_{(\text{H1a-H2s})}$  and  $^3\text{J}_{(\text{H3a-H2s})}$  ) and only one *cis*  $^3\text{J}$  coupling (  $^3\text{J}_{(\text{H3s-H2s})}$  ) of ca. 7Hz. It is generally well established that *trans* alkene couplings are almost twice as large as *cis*<sup>72</sup>, although in the allyl system the difference is sometimes not so marked.

The presence of only one *cis* coupling allows the resonance from H<sub>3s</sub> to be readily identified, as a doublet with a relatively small coupling constant of approximately 7Hz.

Also readily assignable is H<sub>2s</sub>; coupling with H<sub>1a</sub>, H<sub>3a</sub>

and H3s, it should appear as a doublet of doublets of doublets i.e. eight lines of equal intensity. However, when the  $^3J$  couplings H1a-H2s and H3a-H2s are similar there may be two overlapping signals thus giving six lines of relative intensity 1:1:2:2:1:1. Furthermore, the resonance should occur at the highest frequency of all the allyl protons.

Differentiating between H1a and H3a in the case of the 1-methyl- substituted compounds is trivial since H1a will couple not only with H2s but also with the methyl protons, resulting in a doublet of quartets. However, this is complicated in the spectra of III due to overlap with the doublet due to H3s. Selective decoupling experiments do however confirm the assignment.

In the cases of the 1-phenyl- and 1-ethoxycarbonyl- substituted complexes the assignment is not so straightforward. Both H1a and H3a appear as doublets with a  $^3J$  coupling constant of 10 - 13Hz. However, the signal of H1a should occur at higher frequency than that of H3a due to the shielding effects of both substituents. This is borne out by comparison with reported analogues such as;  $[(\eta^3-1-Ph-C_3H_4)PtCOD]^+$  <sup>73</sup>, 21,  $(\eta^3-1-Ar-C_3H_4)PdAcAc$  <sup>51,74</sup>, 22,  $[(\eta^3-1-Ph-C_3H_4)PdTMEDA]^+$  <sup>49</sup>, 23,  $(\eta^3-1-Ph-C_3H_4)PtCp$  <sup>75</sup>, 24, and  $[(\eta^3-1-EtOOC-C_3H_4)PdCl]_2$  <sup>45</sup>, 20.

In some spectra fine structure is evident, due to either long range or geminal couplings. However this is not well resolved on the lower field spectra and is more readily observed in the high field study ( *vide infra* ).

Compound **VIIIb** was fully characterised by  $^1\text{H}$  n.m.r. spectroscopy since microanalysis was not available due to the presence of toxic mercury which would contaminate the analyser. Satellites due to  $^{199}\text{Hg}$  (  $I=1/2$ , 16.8% abundance ) were obvious on the methylene signal (  $^2J_{(\text{H-Hg})} = 142\text{Hz}$  ) and the spectrum compares favourably with those of analogous  $\sigma$ -bonded allyls such as  $\text{CODPtCl}(\sigma\text{-CH}_2\text{-CH=CHPh)$ , 25<sup>68</sup>.

Only one isomer of each compound in the  $\text{LL}'_2\text{Mo}(\text{CO})_2(\eta^3\text{-1-Ph-C}_3\text{H}_4)$  series was detected on the lower field spectra ( 80 or 200MHz ) but both were observed in the high field study ( *vide supra* ).

## 2.4 High field $^1\text{H}$ n.m.r. studies:-

In order to further resolve the fine structure observed in some of the low-field spectra and probe the effects of differing substituents, high-resolution ( 360MHz ) spectra of the four-coordinate, ionic complexes  $[(\eta^3-1-R-C_3H_4)PdTMEDA]BF_4$ , ( R = Me, Ph, COOEt ); III, IV and V, have been recorded in deuterioacetone. Similar spectra have also been obtained of the seven coordinate compounds, IX, X and XI in order to resolve and assign the signals arising from both isomeric forms.

The effect of allyl substitution: The spectra of III, IV and V, with relevant line narrowed expansions, are shown in Figures 2.1, 2.2 and 2.3 respectively. Data for the allyl resonances are summarised in Table 2.1.

Table 2.1 Spectroscopic data for allyl resonances of complexes  $[(\eta^3-1-R-C_3H_4)PdTMEDA]BF_4$ .

	R		
	Me	Ph	COOEt
$\delta H_{1a}$	3.80	4.64	3.72
$\delta H_{2s}$	5.56	6.34	6.33
$\delta H_{3s}$	3.80	4.04	4.27
$\delta H_{3a}$	3.0	3.36	3.69
$^3J_{(H_{1a}-H_{2s})}$	12.2	11.8	10.3
$^3J_{(H_{3a}-H_{2s})}$	11.4	12.2	13.3
$^3J_{(H_{3s}-H_{2s})}$	7.1	7.2	7.6

Fig. 2.1  $^1\text{H}$  n.m.r. spectrum of  
 $[(\eta^3\text{-1-Me-C}_3\text{H}_4)\text{PdTMEDA}]\text{BF}_4$ .

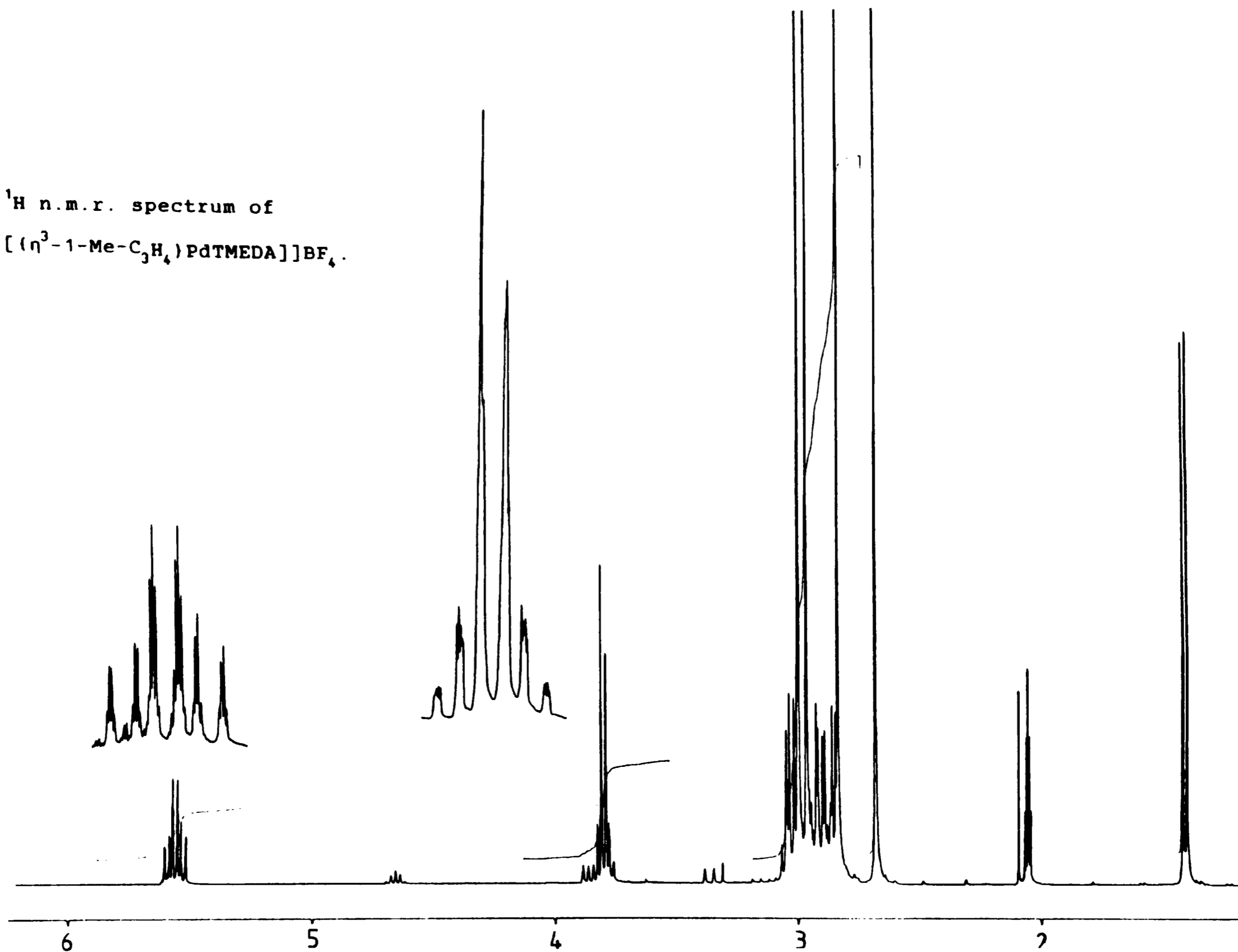




Fig. 2.2  $^1\text{H}$  n.m.r. spectrum of  $[(\eta^3\text{-1-Ph-C}_3\text{H}_4)\text{PdTMEDA}]\text{BF}_4$ .

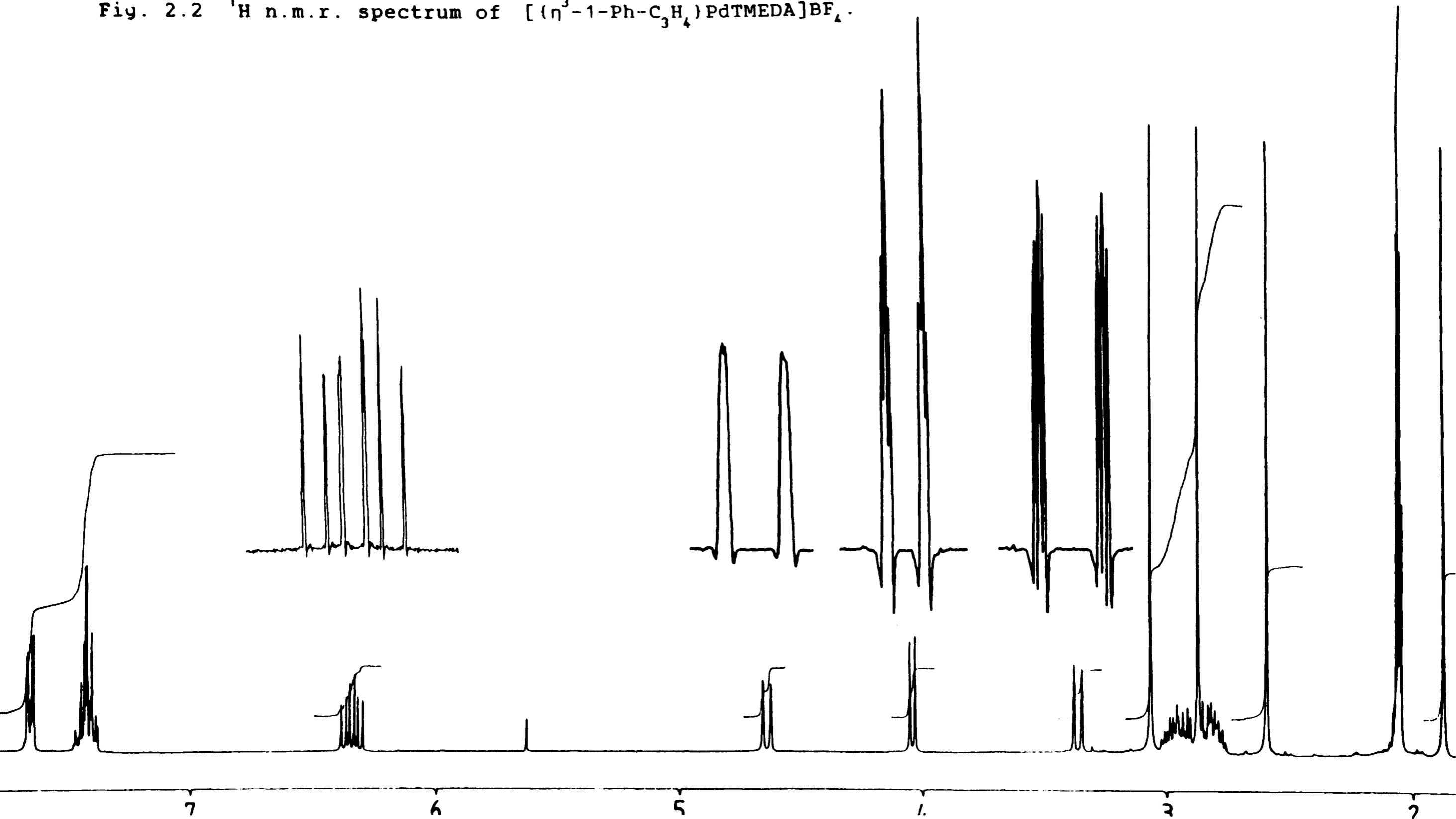
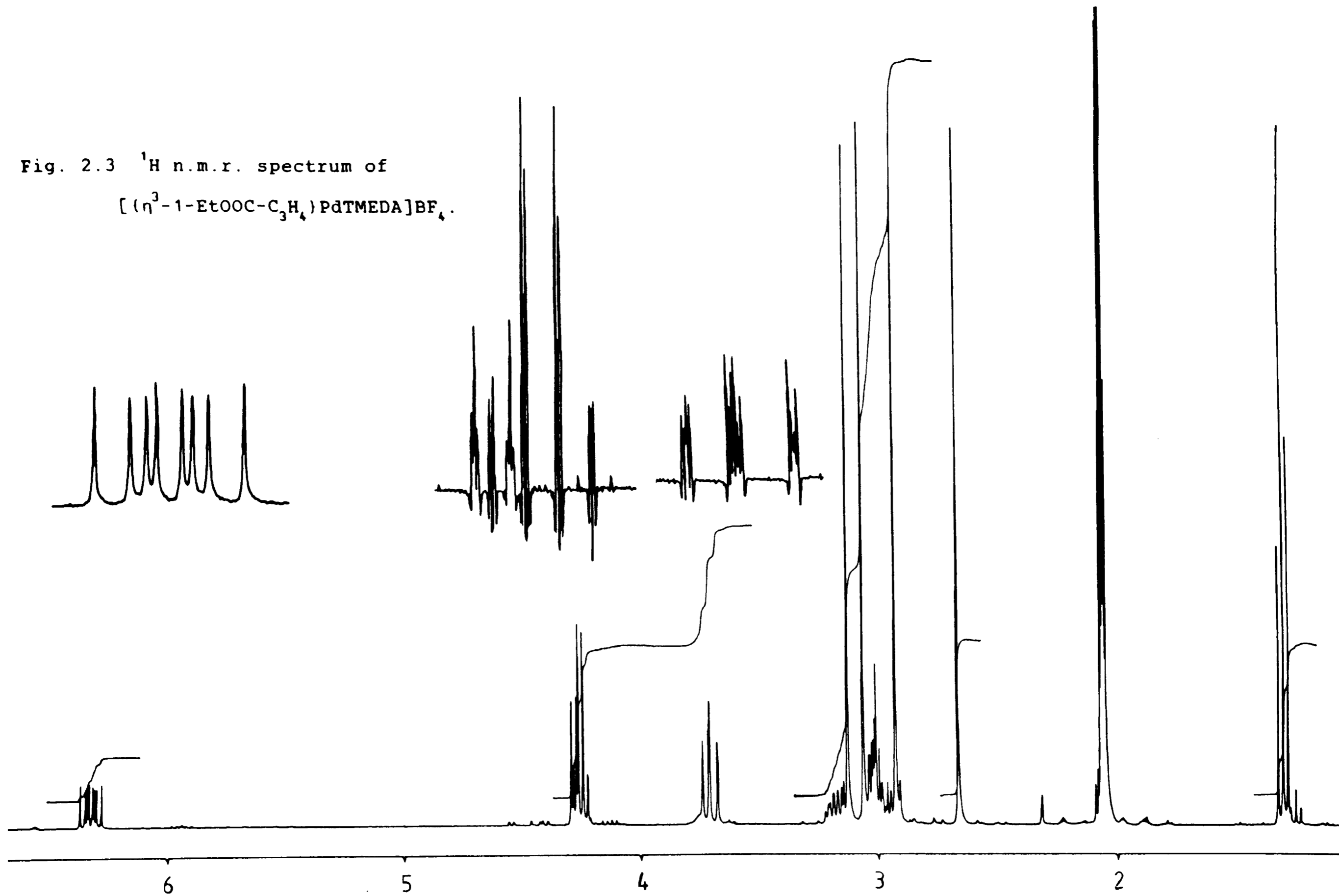


Fig. 2.3  $^1\text{H}$  n.m.r. spectrum of  
 $[(\eta^3\text{-1-EtOOC-C}_3\text{H}_4)\text{PdTMEDA}]\text{BF}_4$ .



All complexes show four sharp singlets, due to the TMEDA methyl groups, which indicates a non-fluxional structure. This is in contrast to the results for the COD analogues, both of palladium ( this work ) and platinum<sup>73</sup> where at room temperature broad signals were observed for the ligand protons. Discernable multiplets, as expected for a non-fluxional structure, were only observed at low temperatures ( ca. 193K ) for these derivatives.

The difference,  $\Delta$ , between the two *trans* coupling constants,  $^3J_{(H1a-H2s)}$  and  $^3J_{(H3a-H2s)}$ , reflects the inductive effect of the substituent. A plot of  $\Delta$  versus  $\sigma^*$ , the Taft inductive parameter<sup>76</sup>, is shown in Figure 2.4. The Taft parameter for the functional group COOEt is not available; instead that for COOMe was used. A value of  $\Delta = 0.0$  can obviously be assigned to the hydride-substituted allyl complex ( R = H ) since this would give an  $AM_2X_2$  type spectrum with identical *trans* couplings. Although the fit is not perfect there is an obvious correlation. The discrepancies may be due to the fact that  $\sigma$  is a kinetic, as opposed to a thermodynamic parameter. A modified parameter  $\sigma^e$ , has been defined<sup>77</sup> based on electrochemical data, and therefore, thermodynamic in nature. For the phenyl group  $\sigma^e$  has a value of +0.9, compared to the +0.6 for  $\sigma^*$  and so the former is clearly in better accord with the other values from this study ( see Figure 2.4 ). Unfortunately, values for the other substituents are not available, apart from methyl for which both  $\sigma^e$  and  $\sigma^*$  are assumed to be 0.0.

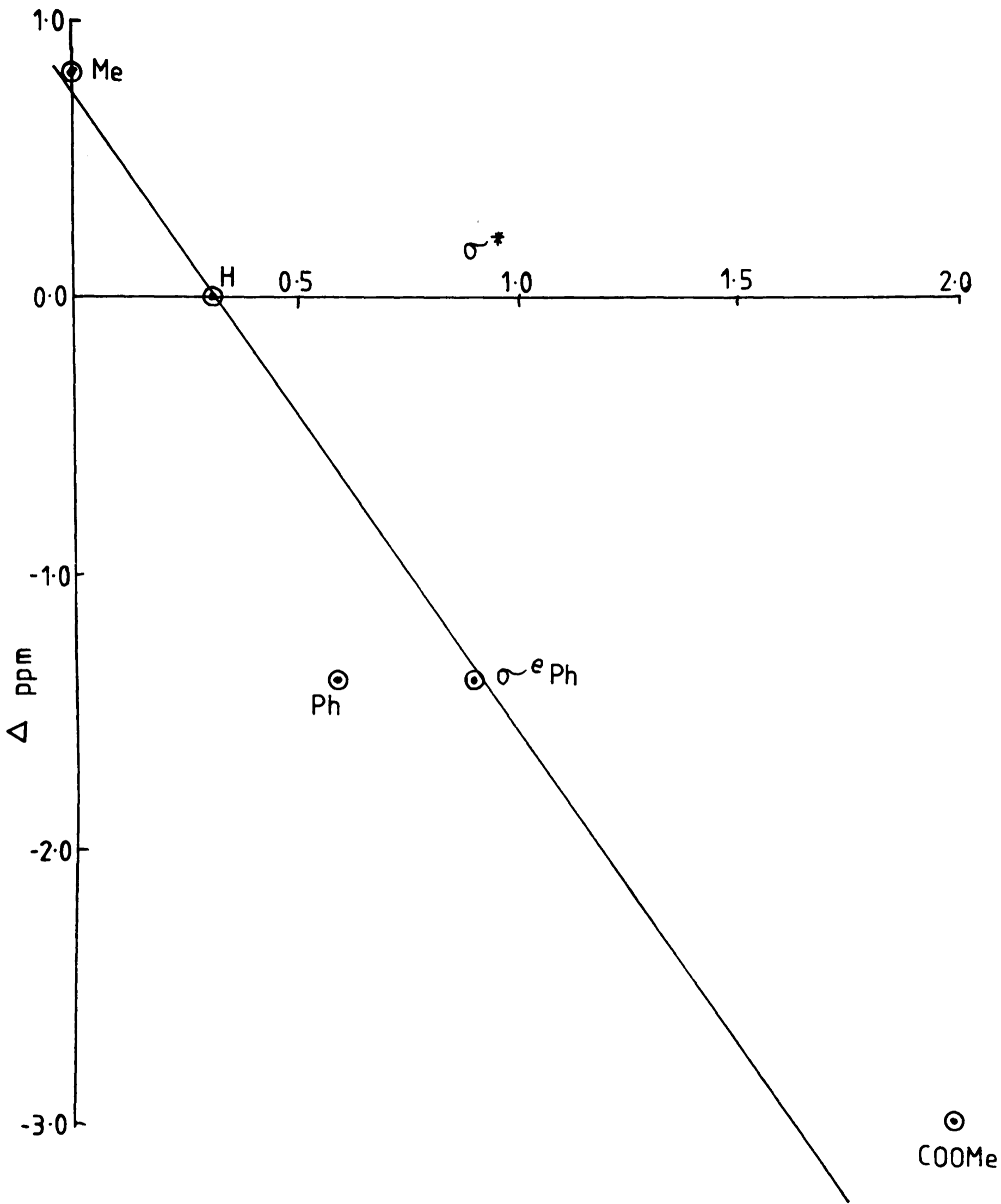


Fig. 2.4 Graph of  $\Delta$  versus  $\sigma^*$ .

The observation that the substituent has an effect- reflected in the coupling constants- on the bonding within the ligand, which correlates to a modest degree with its electronic properties, suggests that any asymmetry in metal/ligand bonding may also be electronic in origin.

R = Me Figure 2.1: The signal due to H3a is obscured by those due to the methyl and methylene groups of TMEDA, but careful examination of the integral, comparison with the low-field spectrum (in which part of the signal was observed) and with the literature spectrum<sup>49</sup> allows it to be located at  $3.0 \pm 0.1\delta$ . However, the  ${}^3J_{(H3a-H2s)}$  coupling constant, along with the other  ${}^3J$  couplings, can be determined from the resonance due to H2s. This appears as an overlapping doublet of doublets of doublets of quartets at  $5.56\delta$ . The quartet splitting is due to long-range coupling with the methyl group protons of the allylic substituent. Selective irradiation of the methyl group signal (at  $1.41\delta$ ) simplifies the H2s resonance to an eight line signal (Figure 2.5) due solely to  ${}^3J$  couplings from which the relevant coupling constants can be extracted. The signals due to H1a and H3s are also superimposed. Since the coupling constant of H1a with the methyl group protons ( $6.1\text{Hz}$ ) is exactly half that of the H1a-H2s *trans* coupling ( $12.2\text{Hz}$ ), the H1a signal appears as a 1:3:4:4:3:1 multiplet, further broadened by long-range coupling (ca.  $0.5-1.0\text{Hz}$ ) to H3s and H3a. Superimposed on this, at the same chemical shift, is the doublet due to H3s ( ${}^3J_{(H3s-H2s)} = 7.1\text{Hz}$ ) giving

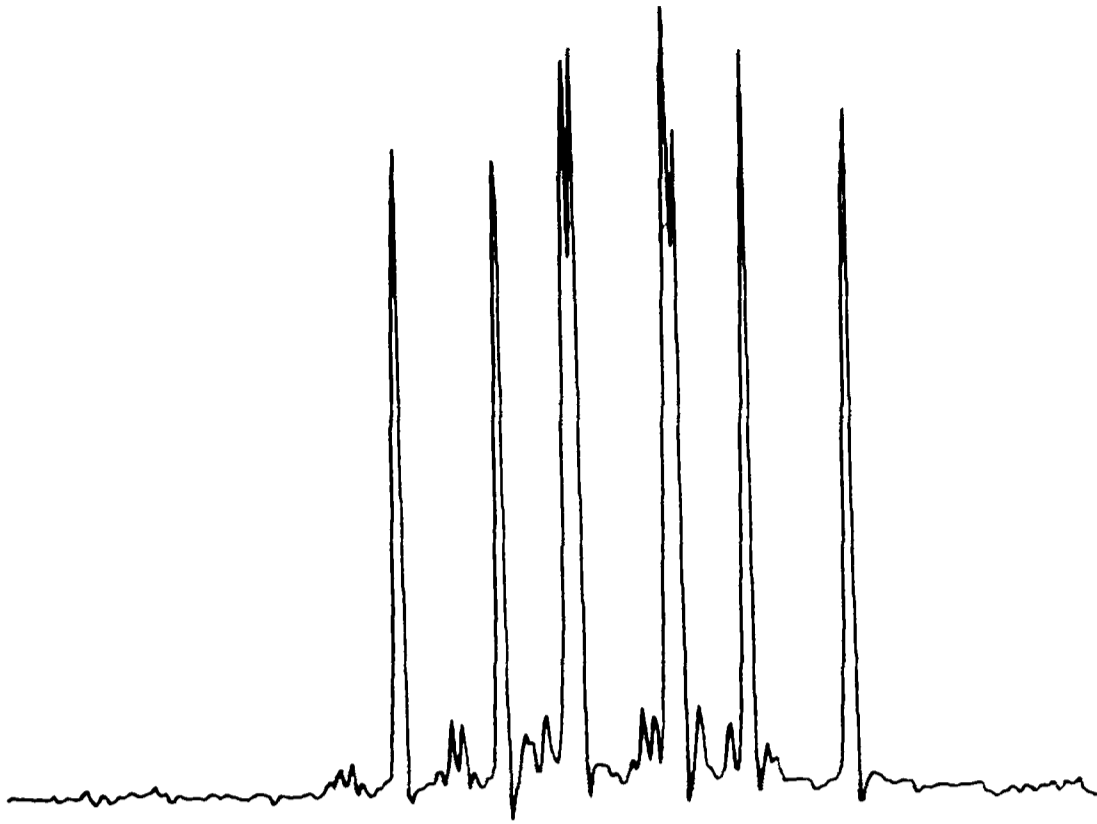


Fig. 2.5 Methyl decoupled H<sub>2</sub>s resonance.

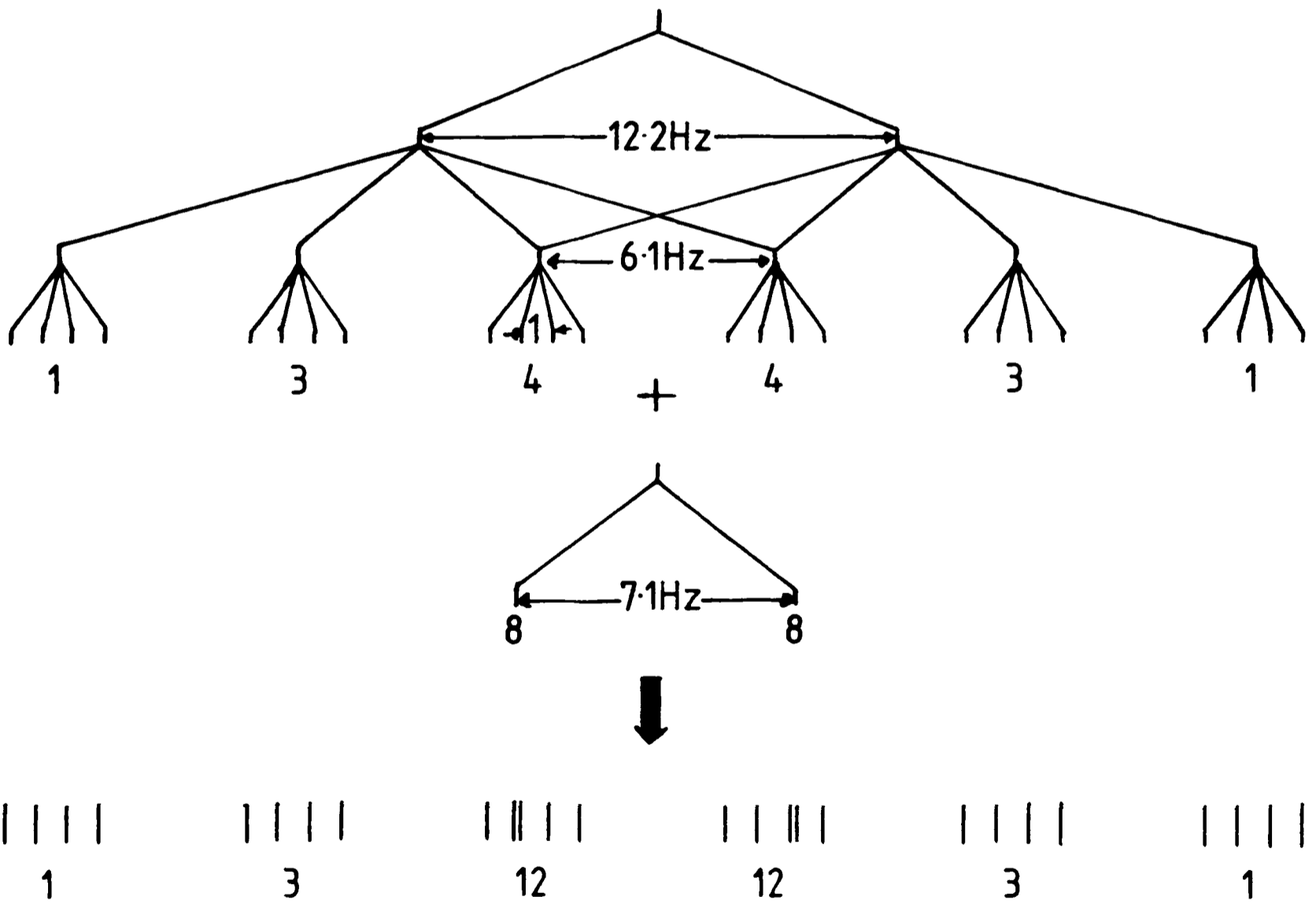


Fig. 2.6 Schematic splitting diagram for H<sub>1a</sub>.

the observed 1:3:12:12:3:1 signal. Figure 2.6 is a schematic diagram of the splitting pattern.

R = Ph Figure 2.2: In this case there are no overlapping signals and analysis is much simpler. The resonance due to H2s ( 6.34 $\delta$  ) is resolved into its expected eight lines, allowing all three  $^3J$  coupling constants to be extracted and checked by comparison with those determined from the other resonances in the spectrum. The intensities of the eight lines are perturbed as a result of the similarity of the two *trans* couplings ( 11.8Hz and 12.2Hz ).

The signal due to H3a ( 3.36 $\delta$  ) is a doublet,  $^3J = 12.2\text{Hz}$ , further split by a  $^2J$  *gem*-coupling with H3s and a long-range  $^4J$  coupling to H1a: both coupling constants are approximately 0.5-1.0Hz. The magnitude of *gem*-coupling depends on the H-C-H angle<sup>78</sup>, a value of 0.5-1.0Hz suggesting an angle of 125 $\pm$ 2°. Equivalent couplings are also observed in the fine structure of the H3s doublet. The long-range couplings to H3a and H3s are not well resolved in the signal of H1a, which appears as a broad doublet with only a slight indication of fine structure.

R = COOEt Figure 2.3: The eight-line doublet of doublets of doublets at 6.33 $\delta$ , due to H2s, is well resolved with each line having an equal intensity since the two *trans*-couplings are markedly inequivalent ( 10.3Hz *cf.* 13.3Hz ).

The signals due to H1a and H3a overlap, the higher frequency one being assigned to H1a. Both doublets are further split by long-range coupling to the other allyl

protons and in the case of H1a, coupling to the ethyl group protons. The coupling between H1a and the methylene protons of the ethyl group is also observed in the CH<sub>2</sub> quartet ( 4.25δ ) which can be resolved into a doublet of quartets ( <sup>5</sup>J = 0.5-1.0Hz ). The H3s doublet ( 4.27δ ) also shows the *gem* and long-range couplings observed for H3a, although accurate measurement is difficult ( <sup>4</sup>J < 0.5Hz ).

Effect of other ligands on allyl conformation: The spectra of IX, X and XI all indicate the presence of two isomers, *endo* and *exo*, which have been detected for the many analogous compounds already studied<sup>56,69</sup>. Figure 2.7 shows the spectrum of XI with the resonances due to the minor isomer indicated. Spectroscopic data for the allyl resonances of IX, X and XI are given in Table 2.2. Due to their relatively low concentrations and to overlapping peaks, not all resonances arising from the minor isomer were fully resolved.

Criteria for differentiating isomers have been established by Faller *et al.*<sup>56</sup>. In the infra-red spectrum the *exo* conformation usually has a carbonyl stretching frequency ca. 10cm<sup>-1</sup> lower than the *endo* form. Also, in the n.m.r. spectrum the *anti* protons are generally at higher field ( by ca. 0.6 p.p.m. ) and there is a larger geminal *syn-anti* coupling observed for the *exo* form than for the *endo* form.



Fig. 2.7  $^1\text{H}$  n.m.r. spectrum of  $(\text{Phen})(\text{NCS})\text{Mo}(\text{CO})_2(\eta^3\text{-1-Ph-C}_3\text{H}_4)$ .

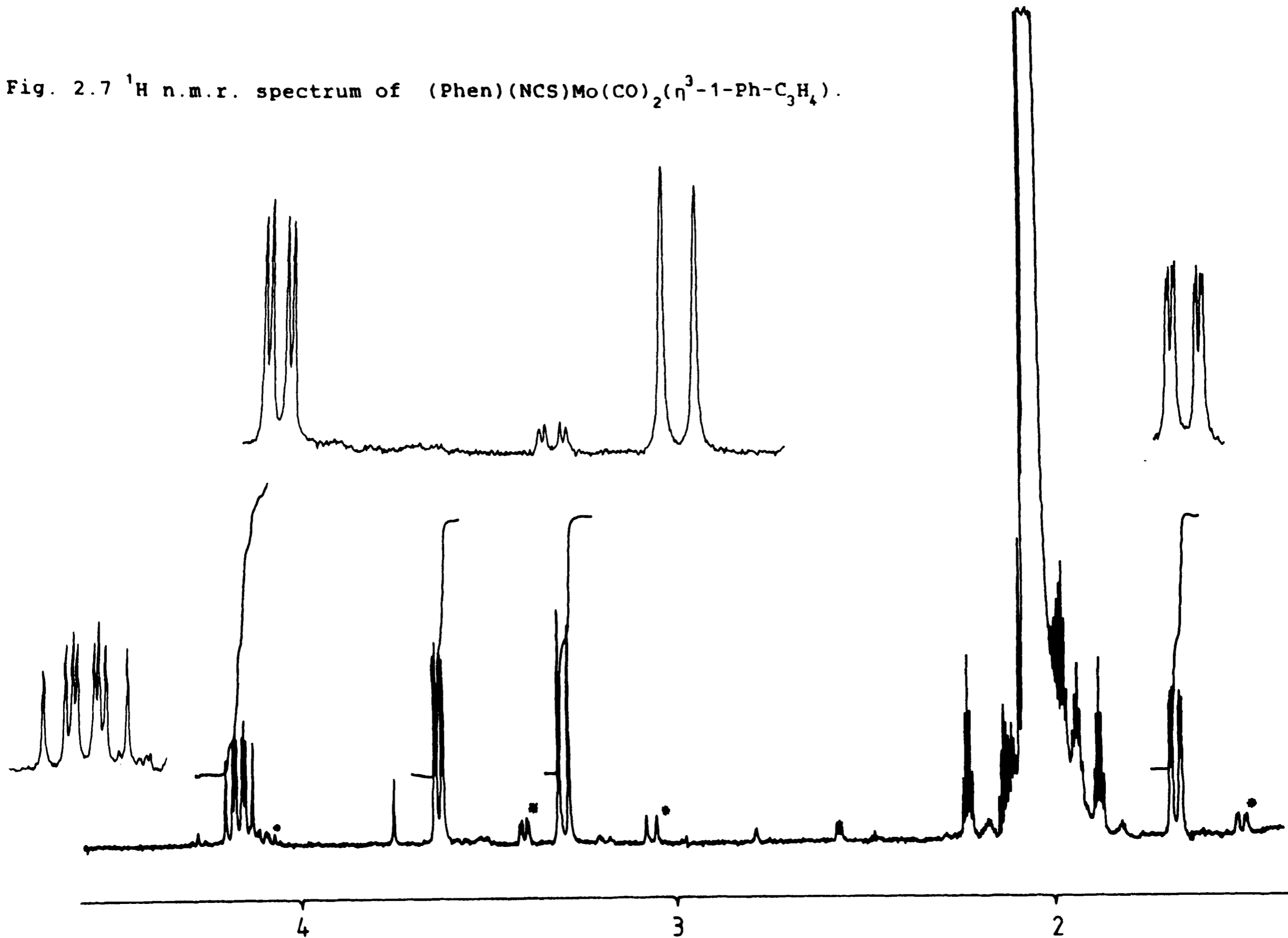


Table 2.2 Spectroscopic data for the allyl resonances  
in complexes  $LL'_2Mo(CO)_2(\eta^3-1-PhC_3H_4)$  IX, X and XI.

	IX		X		XI	
	Major	Minor	Major	Minor	Major	Minor
$\delta H_{1a}$	2.48	2.42	3.24	3.01	3.30	3.07
$\delta H_{2s}$	5.24	5.06	4.15	4.1	4.17	4.06
$\delta H_{3s}$	2.85	2.60	3.45	3.2	3.64	3.41
$\delta H_{3a}$	0.92	0.88	1.59	1.41	1.68	1.50
$^3J_{(H_{1a}-H_{2s})}$	10.6	5	10.1	9.7	10.2	9
$^3J_{(H_{3a}-H_{2s})}$	10.0	7.0	8.9	7	8.8	7
$^3J_{(H_{3s}-H_{2s})}$	7.2	N.R.	6.7	-	6.7	6.5

The infra-red spectra of IX, X and XI do not help in differentiating between the two isomers since, being complexes of low symmetry, the bands are more numerous and overlap considerably such that no peak due to the minor isomer can be detected.

In every case the high-field  $^1H$  n.m.r. spectrum indicates a  $^2J_{(H_{3a}-H_{3s})}$  gem coupling of ca. 1.5-2.0Hz, normally indicative of the *exo* form, for BOTH isomers. The smaller coupling ( $^2J < 0.6Hz$ ) characteristic of the *endo* isomer is not observed.

In all three spectra the resonances for the *anti* protons (  $H_{1a}$  and  $H_{3a}$  ) of the major isomer occur at higher frequency than those of the minor isomer. Although this indicates that the major isomer is, in all cases, the *endo* form, the evidence cannot be considered conclusive, especially in the light of the observed geminal couplings.

CpMo(CO)<sub>2</sub>(η<sup>3</sup>-1-Ph-C<sub>3</sub>H<sub>4</sub>); **IX**: Integration of major and minor isomer peaks indicates a 20:1 *endo:exo* ratio at 298K in deuterioacetone. Owing to the low proportion of the *exo* isomer, the signals due to it are very weak and poorly resolved.

For the major isomer, the similarity between the two *trans* couplings (  $^3J_{(H1a-H2s)}$  and  $^3J_{(H3a-H2s)}$ ; 10.6Hz and 10.0Hz respectively ) results in only six lines ( in the ratio 1:1:2:2:1:1 ) being observed for H2s. The resonances due to H3s and H3a show not only the  $^3J$  couplings with H2s but also a  $^2J$  geminal coupling of 1.3Hz. No additional coupling with H1a is observed, in contrast to the situation in the four coordinate complex **IV**. Similar  $^2J$  couplings have been observed for the *exo* conformation of CpMo(CO)<sub>2</sub>(allyl) species<sup>56</sup>.

(Bipy)Mo(CO)<sub>2</sub>(NCS)(η<sup>3</sup>-1-Ph-C<sub>3</sub>H<sub>4</sub>); **X**: The signals due to the *exo* form are much better resolved here than in **IX**, reflecting a relatively lower *endo:exo* ratio of 5.5:1. However, the signals due to H2s and H3s in the minor isomer overlap with the major isomer peaks of H2s and H1a respectively and cannot be fully analysed. The difference between the  $^3J_{(H1a-H2s)}$  and the  $^3J_{(H3s-H2s)}$  couplings results in the full eight line resonance for H2s being observed (4.15δ). No long-range coupling is observed in the signals of H1a, H3a or H3s, the only fine structure being due to a geminal coupling (  $^2J_{(H3s-H3a)}$  ) of 1.5Hz, again indicative of an *exo* conformation.

(Phen)Mo(CO)<sub>2</sub>(NCS)(n<sup>3</sup>-1-Ph-C<sub>3</sub>H<sub>4</sub>); XI: The spectrum of this compound shows the highest resolution and is shown, along with relevant line-narrowed expansions, in Figure 2.7. The peaks due to the minor isomer are indicated by asterisks. The chemical shifts and coupling constants are almost identical to those obtained for X, as is the *endo:exo* ratio of 5:1. However, some additional fine structure is observed. Observed in the signal of H3a are not only the splittings due to coupling with H2s (<sup>3</sup>J = 8.8Hz) and the geminal H3s (<sup>2</sup>J = 1.9Hz) but also long range coupling to H1a (<sup>4</sup>J ≈ 0.6Hz). No similar long-range coupling to H1a is observed in the signal of H3s. The <sup>4</sup>J<sub>(H1a-H3a)</sub> coupling is not resolved in the signal of H1a, which appears only as a broad doublet (<sup>3</sup>J = 10.2Hz). The geminal coupling for the minor isomer is also readily measurable on this spectrum and the value of 1.8Hz is not significantly different to that derived for the major isomer.

## 2.5 Preliminary crystallographic studies:

Crystals suitable for X-ray diffraction were obtained for compounds I, III, IV, V, VI, VIII and XI. Compound II gave poorly-formed crystals which were found to contain solvent of crystallisation ( dichloromethane ), which was rapidly lost. This was shown by the n.m.r. spectrum ( singlet, 5.80 $\delta$ , 1H ) and the microanalytical results, both techniques indicating a ratio of one solvent molecule per two compound ion-pairs. The use of alternative solvents such as acetone also failed to yield crystals suitable for diffraction work.

The five-coordinate ethoxycarbonyl derivative, VII, is a liquid at ambient temperature and was not studied, although techniques for *in situ* crystal growth from liquid samples have been pioneered at Edinburgh University<sup>79</sup>. This could possibly be the subject of future work.

Crystals of IX are thin plates with very poor optical properties and high solubility ( notably in epoxy adhesive ) which meant that no suitable crystal could be mounted.

Crystals of X, although well formed, were not of sufficient size for study, all dimensions being less than 0.1mm.

Interpretation of single crystal oscillation and Weissenberg photographs<sup>80</sup> of suitable samples indicated the following crystal data:-

Compound I: Orthorhombic unit cell with a volume of approximately 1390Å<sup>3</sup>. From the systematic absences the space group is either  $Cmc2_1$ ,  $Ama2$  ( with an interchange of

axes ) or *Cmcm*. The first two being eight-fold and the last sixteen-fold<sup>81</sup>. For a unique molecule in each asymmetric unit this would result in densities of  $3.28\text{gcm}^{-3}$  and  $6.56\text{gcm}^{-3}$  for *Z* of eight and sixteen respectively. These are unrealistically high and the complex must therefore possess at least mirror symmetry. Refinement of 25 high angle reflections, centred on a CAD4 diffractometer, gave an accurate unit cell of  $a = 8.560(4)\text{\AA}$ ,  $b = 14.940(6)\text{\AA}$  and  $c = 10.926(5)\text{\AA}$ ,  $V = 1397.4\text{\AA}^3$ . Subsequent data collection ( see Chapter 4 ) and analysis of *E* statistics indicated a centrosymmetric space group, therefore it must be the sixteen-fold *Cmcm*. For *Z* = 4, a reasonable density of  $1.64\text{gcm}^{-3}$  is calculated. Thus the molecule must possess four-fold symmetry and be highly disordered. It is highly unlikely that the asymmetry in allyl bonding could be observed in such a structure, even if solution was possible. The study of this compound was therefore abandoned at this point.

Compound III: A tetragonal, body-centred lattice was indicated by the photographs, with an approximate volume of  $780\text{\AA}^3$ . This gives a density of  $1.55\text{gcm}^{-3}$  for *Z* = 2. Since the space group must be at least eight-fold, the complex must again possess four-fold symmetry and be disordered as in I. Further investigation was not, therefore, considered worthwhile.

Compound IV: The photographs indicated an orthorhombic cell of volume  $1810\text{\AA}^3$ , with the systematic absences

indicating the space group is either  $Pca2_1$  or  $Pcam$  ( an alternative setting of  $Pbcm$  ). Data collection and analysis of  $E$  statistics indicated a non-centrosymmetric space group, which was therefore assumed to be the four-fold  $Pca2_1$ . A reasonable density of  $1.56\text{gcm}^{-3}$  is calculated for  $Z = 4$ , i.e. one ion-pair per asymmetric unit.

Compound V: No symmetry was apparent from the photographs, indicating a triclinic cell with a volume of approximately  $890\text{\AA}^3$ . Thus the space group is either  $P1$  or  $P\bar{1}$  ( almost certainly the latter ) with two ion-pairs per cell giving a reasonable density of  $1.31\text{gcm}^{-3}$ .

Compound VI: A monoclinic cell was indicated with a volume of approximately  $1160\text{\AA}^3$ . The observed systematic absence (  $h0l, l = 2n+1$  ) indicates the space group is  $P2/c$ , although the possibility of the most common space group,  $P2_1/c$ , remains open since the condition  $0k0, k = 2n$  is not observable when mounted about  $b$ . This latter space group is far more likely. Both are however, four-fold and a reasonable density of  $1.67\text{gcm}^{-3}$  is calculated for  $Z = 4$ .

Compound VIII: An unusual diffraction pattern was observed here, the symmetry of which indicated an orthorhombic lattice. However, the systematic absences were not consistent with any space group. The conclusion that this was the result of a twinned crystal was supported by the poor optical properties of the crystals and the difficulty in obtaining one that gave discrete spots.

Compound XI: A monoclinic lattice was indicated with a

volume of  $2200\text{\AA}^3$ . Systematic absences uniquely defined the space group as  $P2_1/n$  ( an alternative setting of  $P2_1/c$  ) giving a calculated density of  $1.53\text{gcm}^{-3}$  for  $Z = 4$ .

Thus samples of IV, V, VI and XI were suitable for full three-dimensional crystallographic study since they show no imposed symmetry which would indicate a disordered structure.



## 2.6 Experimental:-

All manipulations described were carried out under an atmosphere of dry, oxygen free nitrogen using standard Schlenk-tube techniques<sup>82</sup>. Solvents were dried and deoxygenated prior to use by standard methods<sup>83</sup>. Hence, pentane and hexane were distilled over sodium wire, tetrahydrofuran over sodium-benzophenone and dichloromethane over calcium hydride. Removal of solvent under reduced pressure refers to the use of a BUCHI type rotary evaporator. Commercially available reagents were used as supplied whilst others were prepared by literature methods, as indicated.

Infra-red spectra were recorded on a Perkin-Elmer P.E. 598 grating spectrophotometer and were referenced against the  $1603\text{cm}^{-1}$  band of polystyrene. Samples were prepared as pressed KBr pellets, or dissolved in dichloromethane in NaCl solution cells ( path length 0.5mm ) or as a liquid film ( KBr plates ).

Routine n.m.r. spectra were recorded on samples held in 5mm tubes using Bruker WP80SY or WP200SY Fourier transform spectrometers with internal [<sup>2</sup>H] lock. Samples for the high field study were sealed, under vacuum, with freshly distilled, thoroughly dried ( 4Å molecular sieves) and degassed deuterioacetone as sole solvent. Spectra were recorded on a Bruker WH360SY Fourier transform spectrometer with internal [<sup>2</sup>H] lock. Chemical shifts  $\delta$ (p.p.m.), were referenced with respect to the residual

solvent protons [  $(\text{CHD}_2)\text{COCD}_3$  in  $(\text{CD}_3)_2\text{CO}$  at 2.06 $\delta$ ,  $\text{CHCl}_3$  in  $\text{CDCl}_3$  at 7.25 $\delta$  and  $\text{C}_6\text{D}_5\text{H}$  in  $\text{C}_6\text{D}_6$  at 7.16 $\delta$  relative to TMS (tetramethylsilane) at 0.0 $\delta$  ]. Positive shifts are to high frequency of TMS. All coupling constants ( J ) are in Hz.

Microanalyses ( C, H and N ) were determined by the departmental analytical service. Melting points were recorded, by the author, on a Kofler hot stage microscope.

For the crystallographic studies single crystals with good optical properties, determined under a polarising microscope, were either sealed in Lindemann tubes, under  $\text{N}_2$ , or mounted on the end of a glass fibre, using low temperature epoxy adhesive. The mounted sample was fixed to a Stoe or Enraf-Nonius Weissenberg goniometer and aligned by oscillation photographs taken over a range of  $\pm 10^\circ$ . Subsequent zero- and first level Weissenberg photographs were taken over a range of  $\pm 110^\circ$  with a film translation of 0.5mm per degree of rotation.

General method for the preparation of complexes of the type  $[(\eta^3\text{-1-R-C}_3\text{H}_4)\text{PdL}_2]\text{BF}_4$  ( R = Me, Ph or EtOOC;  $\text{L}_2$  = COD or TMEDA ).

To a solution of  $[(\eta^3\text{-1-R-C}_3\text{H}_4)\text{PdCl}]_2$ <sup>43,45</sup> ( 0.5mmol ) in  $\text{CH}_2\text{Cl}_2$  ( 10ml ) was added  $\text{AgBF}_4$  ( 0.19g, 1mmol ) and after stirring for 5mins the chelating ligand (  $\text{L}_2$ , 1mmol ) was also added. After a further 1min the solution was filtered and the residue of  $\text{AgCl}$  was washed with  $\text{CH}_2\text{Cl}_2$  ( 2 x 5ml ).

Addition of EtOEt ( 100ml ) to the combined filtrate and washings resulted in the precipitation of a white solid. This was recovered by filtration and further recrystallised from the appropriate solvents. In this manner were prepared:-

$(\eta^4\text{-Cyclo-octa-1,5-diene})(\eta^3\text{-1-methylallyl})\text{palladium(II)}$   
tetrafluoroborate;  $[(\eta^3\text{-1-Me-C}_3\text{H}_4)\text{Pd}(\eta^4\text{-C}_8\text{H}_{12})]\text{BF}_4$ , I.

From  $\text{CH}_2\text{Cl}_2/\text{EtOEt}$  ( 1:3 solvent diffusion at  $-30^\circ\text{C}$  )

Yield:- 0.29g (79%) M.Pt. =  $168^\circ\text{C}$  (dec.)

$^1\text{H}$  n.m.r. [ 200MHz,  $\text{CDCl}_3$ , 298K ]  $\delta$ :

1.77(d, 6.3Hz, 3H,  $\text{CH}_3$ ), 2.2-2.8(m br, 8H,  $\text{CH}_2$ ;COD),  
3.60(d, 13.0Hz, 1H, H3a), 4.67(d, 6.6Hz, 1H, H3s),  
4.87(dt, 6.3, 12.6Hz, 1H, H2a), 5.4-5.6(m br, 1H, CH;COD),  
5.94(ddd, 13.0, 12.6, 6.3Hz, 1H, H2s), 6.1-6.3(m br, 3H, CH;COD).

I.R. (KBr disc):- 1950, 1890, 1485, 1453, 1433, 1380, 1298, 1050br,  
883, 850, 820, 760, 735, 695, 668,  $524\text{cm}^{-1}$ .

Analysis; Found(Calc):- 42.0(41.9)%C, 5.4(5.5)%H

Unit cell:- Orthorhombic;  $a = 8.5$ ,  $b = 14.9$ ,  $c = 11.0\text{\AA}$

Conditions:- hkl,  $h+k = 2n$ ; h0l,  $l = 2n$

( $\eta^4$ -Cyclo-octa-1,5-diene)( $\eta^3$ -1-phenylallyl)palladium(II)

tetrafluoroborate                      methylenechloride                      solvate;

$[(\eta^3-1-Ph-C_3H_4)Pd(\eta^4-C_8H_{12})]BF_4 \cdot 1/2CH_2Cl_2$ , II.

From  $CH_2Cl_2$ /EtOEt ( 1:3 solvent diffusion at  $-30^\circ C$  )

Yield:- 0.30g (74%)    M.Pt. =  $121^\circ C$

$^1H$  n.m.r. [ 200MHz,  $(CD_3)_2CO$ , 193K ]  $\delta$ :

2.2-2.8(m br, 8H,  $CH_2$ ;COD), 3.86(d, 13.0Hz, 1H, H3a),

4.4-4.5(m br, 1H, CH;COD), 5.05(d, 7.3Hz, 1H, H3s),

5.79(d, 12.6Hz, 1H, H1a), 5.80(s, 1H,  $1/2CH_2Cl_2$  solvent),

6.3-6.4(m br, 3H, CH;COD), 6.94(ddd, 7.3, 12.6, 13.0Hz, 1H, H2s),

7.4-7.9(m, 5H, Ph).

I.R. (KBr disc):- 3010, 2935, 2890, 1515, 1490, 1462, 1431, 1103,  
1050br, 875, 757,  $686cm^{-1}$ .

Analysis; Found( Calc):- 46.6(46.8)%C, 4.8(4.9)%H

( $\eta^3$ -1-Methylallyl)(N,N,N',N'-tetramethylethylenediamine)palladium(II)

tetrafluoroborate;  $[(\eta^3-1-Me-C_3H_4)Pd(C_6H_{16}N_2)]BF_4$ ; III:

From  $CH_2Cl_2$ /EtOEt ( 1:3 solvent diffusion )

Yield:- 0.31g (85%)    M.Pt. =  $197-199^\circ C$

$^1H$  n.m.r. [ 80MHz,  $(CD_3)_2CO$ , 298K ]  $\delta$ :

1.42(d, 6.1Hz, 3H,  $CH_3$ ), 2.79(s, 3H, MeN), 2.82(s, 3H, MeN),

2.89(s, 3H, MeN), 2.96(s, 3H, MeN), 3.0(d, n.r., 1H, H3a),

2.79-2.96(m, 4H,  $-CH_2-CH_2-$ ), 3.81(m, 2H, H3s and H1a),

5.61(ddd, n.r., H2s).

I.R. (KBr disc):- 2960, 2875, 2840, 2795, 1460, 1280, 1040br, 955,  
800, 770cm<sup>-1</sup>.

Analysis; Found( Calc):- 33.1(33.0)%C, 6.5(6.3)%H, 7.7(7.7)%N

Unit cell:- Tetragonal; a = 9.1, c = 9.4Å

Conditions:- hkl, h+k+l = 2n.

( $\eta^3$ -1-Phenylallyl)(N,N,N',N'-tetramethylethylenediamine)palladium(II)  
tetrafluoroborate; [ $\eta^3$ -1-Ph-C<sub>3</sub>H<sub>4</sub>]<sub>3</sub>Pd(C<sub>6</sub>H<sub>16</sub>N<sub>2</sub>)<sub>4</sub>BF<sub>4</sub>; IV:

From CH<sub>2</sub>Cl<sub>2</sub>/EtOEt ( 1:3 solvent diffusion )

Yield:- 0.34g (80%) M.Pt. = 164°C

<sup>1</sup>H n.m.r. [ 80MHz, (CD<sub>3</sub>)<sub>2</sub>CO, 298K ]  $\delta$ :

1.88(s, 3H, MeN), 2.59(s, 3H, MeN), 2.6-2.9(m, 4H, -CH<sub>2</sub>-CH<sub>2</sub>-),  
2.87(s, 3H, MeN), 3.06(s, 3H, MeN),  
3.36(ddd, 12.3, <1.0, <1.0Hz, 1H, H3a), 4.03(d, 6.7Hz, 1H, H3s),  
4.64(d, 11.8Hz, 1H, H1a), 6.35(ddd, 12.3, 11.8, 6.7Hz, 1H, H2s),  
7.25-7.75(m, 5H, Ph).

I.R. (KBr disc):- 3010, 2965, 2910, 1490, 1465, 1285, 1050br, 950,  
800, 765cm<sup>-1</sup>.

Analysis; Found( Calc):- 42.1(42.2)%C, 5.7(5.9)%H, 6.8(6.6)%N

Unit cell:- Orthorhombic; a = 11.5, b = 15.9, c = 9.9Å.

Conditions:- Okl, l = 2n; hOl, h = 2n.

( $\eta^3$ -1-Ethoxycarbonylallyl)(N,N,N',N'-tetramethylethylenediamine)

palladium(II)tetrafluoroborate;

$[(\eta^3-1-EtOOC-C_3H_4)Pd(C_6H_{16}N_2)]BF_4 \cdot V$ :

From  $(CH_3)_2CO/EtOEt$  ( 1:3 solvent diffusion )

Yield:- 0.35g (83%) M.Pt. = 124-126°C

$^1H$  n.m.r. [ 80MHz,  $(CD_3)_2CO$ , 298K ]  $\delta$ :

1.31(t, 7.1Hz, 3H,  $CH_3(Et)$ ), 2.66(s, 3H, MeN), 2.92(s, 3H, MeN),  
2.9-3.2(m, 4H,  $-CH_2-CH_2-$ ), 3.06(s, 3H, MeN), 3.12(s, 3H, MeN),  
3.70(d, 13.3Hz, 1H, H3a), 3.72(d, 10.3Hz, 1H, H1a),  
4.25(q, 7.1Hz, 2H,  $CH_2(Et)$ ), 4.27(d, 7.5Hz, 1H, H3s),  
6.32(ddd, 13.3, 10.3, 7.5Hz, 1H, H2s).

I.R. (KBr disc):- 2985, 2900, 1704, 1600, 1510, 1465, 1365, 1313,  
1280, 1258, 1155, 1040br, 955, 865, 805, 770 $cm^{-1}$ .

Analysis; Found( Calc):- 34.2(34.1)%C, 6.1(6.0)%H, 6.8(6.6)%N

Unit cell:- Triclinic;  $a = 9.4$ ,  $d_{010} = 15.2$ ,  $d_{001} = 6.2\text{\AA}$

Conditions:- none.

Preparation of (Cyclopentadienyl)( $\eta^3$ -1-phenylallyl)palladium(II);  
( $\eta^5$ -C<sub>5</sub>H<sub>5</sub>)Pd( $\eta^3$ -1-Ph-C<sub>3</sub>H<sub>4</sub>), VI.

To a solution of [ $(\eta^3$ -1-Ph-C<sub>3</sub>H<sub>4</sub>)PdCl]<sub>2</sub><sup>43</sup> ( 0.25g, 0.5mmol )  
in THF was added a THF solution of NaCp<sup>84</sup> ( 5.0ml, 0.2M ).  
After stirring for 10mins the solvent was removed *in vacuo*  
and the red residue extracted with hexane ( 20ml ). Cooling  
to -30°C deposited red crystals of VI.

Yield:- 0.21g (73%) M.Pt. = 50°C

<sup>1</sup>H n.m.r. [ 80MHz, (CD<sub>3</sub>)<sub>2</sub>CO, 298K ]  $\delta$ :  
2.35(dd, 10.6, 0.9Hz, 1H, H3a), 3.60(d, 6.1Hz, 1H, H3s),  
4.14(d, 10.8Hz, 1H, H1a), 5.55(ddd, 10.8, 10.6, 6.1Hz, 1H, H2s),  
5.56(s, 5H, C<sub>5</sub>H<sub>5</sub>), 7.17-7.58(m, 5H, Ph).

I.R. (KBr disc):- 3040, 3010, 2910, 2840, 1593, 1480, 1449sh, 1425,  
1402, 1330, 1272, 1229, 1174, 1154sh, 1102,  
1068, 1043, 1008, 979, 943, 918, 907, 863,  
830, 806, 753, 691, 614, 590, 582, 528, 436cm<sup>-1</sup>.

Analysis; Found( Calc):- 58.4(58.2)%C, 5.1(4.9)%H.

Unit cell:- monoclinic,  $d_{100} = 14.4$ ,  $b = 5.8$ ,  $d_{001} = 13.7\text{\AA}$ ,  $\beta \approx 90^\circ$ .

Conditions:-  $h0l$ ,  $l = 2n$

Preparation of (Cyclopentadienyl)( $\eta^3$ -1-ethoxycarbonylallyl)  
palladium(II); ( $\eta^5$ -C<sub>5</sub>H<sub>5</sub>)Pd( $\eta^3$ -1-EtOOC-C<sub>3</sub>H<sub>4</sub>), VII.

As above, using [ $(\eta^3$ -EtOOC-C<sub>3</sub>H<sub>4</sub>)PdCl]<sub>2</sub><sup>45</sup>, except:- solvent  
removed from extracts and residue distilled under *vacuo*  
(50°C, 0.1Torr ) onto a dry-ice/acetone cooled ( -78°C )

probe to give a deep red/purple viscous liquid.

Yield:- 0.15g (53%)

$^1\text{H}$  n.m.r. [ 80MHz,  $\text{CDCl}_3$ , 298K ]  $\delta$ :

1.26(t, 7.1Hz, 3H,  $\text{CH}_3(\text{Et})$ ), 2.49(dd, 11.4, 0.9Hz, 1H, H3a),

3.17(d, 9.3Hz, 1H, H1a), 3.74(d, 6.5Hz, 1H, H3s),

4.15(q, 7.1Hz, 2H,  $\text{CH}_2(\text{Et})$ ), 5.73(s, 5H, Cp),

5.79(ddd, 11.4, 9.3, 6.5Hz, 1H, H2s).

I.R. (neat):- 3068, 3043, 2968, 2925, 2900, 2867, 1710, 1638sh,

1613, 1477, 1463, 1441, 1388, 1365, 1340, 1306,

1265, 1252, 1217, 1183, 1156, 1096, 1046, 1014,

982, 917, 864, 833, 771,  $735\text{cm}^{-1}$ .

Analysis:- Not performed.

Preparation of ( $\sigma$ -1-Ethoxycarbonylallyl)mercurychloride,  
( $\sigma$ -1-EtOOC- $\text{C}_3\text{H}_4$ )HgCl; VIIIb:

A solution of [ $(\eta^3$ -1-EtOOC- $\text{C}_3\text{H}_4$ )PdCl] $_2$ <sup>45</sup> ( 0.51g, 1mmol ) in benzene ( 10ml ) was stirred vigorously with metallic mercury ( 10g ) for 60mins after which time the colour had faded. The mixture was filtered and the mercury washed with benzene ( 2 x 5ml ). The combined filtrate and washing were evaporated to dryness in vacuo giving a white solid.

Yield:- 0.32g (92%) M.Pt. = 88-90°C

$^1\text{H}$  n.m.r. [ 80MHz,  $\text{C}_6\text{D}_6$ , 298K ]  $\delta$ :

1.04(t, 7.1, 3H,  $\text{CH}_3(\text{Et})$ ),

1.33(dd+sat., 9.0, 1.1Hz,  $J_{\text{H-Hg}}$  142Hz,  $-\text{CH}_2\text{-HgCl}$ ),

4.08(q, 7.1Hz, 2H,  $\text{CH}_2(\text{Et})$ ), 5.48(dt, 15.3, 1.1Hz, 1H, EtOOC- $\text{CH}=\text{CH}$ -),

6.62(dt, 15.3, 9.0Hz, 1H,  $-\text{CH}=\text{CH}-\text{CH}_2$ -).



I.R. (KBr disc):- 2910, 2953, 2850, 1702, 1623, 1467, 1446, 1388,  
1363, 1318, 1195, 1120cm<sup>-1</sup>.

Analysis:- Not performed.

Preparation of ( $\eta^6$ -Benzene)( $\eta^3$ -1-ethoxycarbonylallyl)  
ruthenium(II)chloride; ( $\eta^6$ -C<sub>6</sub>H<sub>6</sub>)( $\eta^3$ -1-EtOOC-C<sub>3</sub>H<sub>4</sub>)RuCl, VIII:

A solution of ( $\sigma$ -1-EtOOC-C<sub>3</sub>H<sub>4</sub>)HgCl ( VIIIb, 0.35g, 1mmol )  
in MeOH ( 10ml ) was added to a suspension of  
[( $\eta^6$ -C<sub>6</sub>H<sub>6</sub>)RuCl<sub>2</sub>]<sub>2</sub><sup>85</sup> ( 0.25g, 0.5mmol ) in MeOH/H<sub>2</sub>O ( 100ml, 10:1 )  
and stirred for 16hrs. The mixture was filtered and the  
filtrate diluted with H<sub>2</sub>O ( 200ml ). This mixture was  
extracted with CH<sub>2</sub>Cl<sub>2</sub> ( 5 x 50ml ), the extracts dried  
(MgSO<sub>4</sub>) and the solvent removed under reduced pressure.  
Recrystallisation of the residue from CH<sub>2</sub>Cl<sub>2</sub>/hexane ( 1:3  
solvent diffusion ) yielded orange crystals of VIII.

Yield:- 0.18g (55%) M.Pt. = 210°C (dec.)

<sup>1</sup>H n.m.r. [ 80MHz, (CD<sub>3</sub>)<sub>2</sub>CO, 298K ]  $\delta$ :

1.25(t, 7Hz, 3H, CH<sub>3</sub>(Et)), 2.32(d, 12Hz, 1H, H3a),

2.37(d, 8Hz, 1H, H3s), 2.87(d, 10Hz, 1H, H1a),

4.21(q, 7Hz, 2H, CH<sub>2</sub>(Et)), 5.12(ddd, 12,10,8Hz, 1H, H2s),

5.60(s, 6H, C<sub>6</sub>H<sub>6</sub>).

I.R. (KBr disc):- 3040, 2945, 2905, 2853, 1675, 1487, 1433, 1364,  
1300, 1215, 1145, 1047, 916, 868, 849, 805cm<sup>-1</sup>.

Analysis; Found( Calc):- 44.2(44.0)%C, 4.6(4.6)%H.

Unit cell:- Monoclinic? not indexed.

Conditions:-  $hkl$ ,  $h+k = 2n$ ;  $hk0$ ,  $h = 2n$ ;  $00l$ ,  $l = 4n$ ;  $0k0$ ,  $k = 4n$

Preparation of (Cyclopentadienyl)(dicarbonyl)( $\eta^3$ -1-phenylallyl)molybdenum(II);  $\text{CpMo}(\text{CO})_2(\eta^3\text{-1-Ph-C}_3\text{H}_4)$ : IX.

A suspension of  $\text{Mo}(\text{CO})_6$  ( 1.31g, 5mmol ) in MeCN ( 20ml ) was refluxed until it no longer sublimed out of solution (approx. 2hrs. ). The resulting yellow solution was cooled to room temperature and cinnamylchloride ( 1.2ml, 7.5mmol ) added. The mixture was refluxed for a further 18hrs to yield a red solution. Removal of solvent *in vacuo* and washing with EtOEt ( 10ml ) gave 1.8g ( 92% ) of crude  $\text{Mo}(\text{CO})_2(\text{MeCN})_2\text{Cl}(\eta^3\text{-1-Ph-C}_3\text{H}_4)$ , IXb. To a suspension of IXb ( 0.78g, 2mmol ) in THF ( 10ml ) was added a freshly prepared solution of LiCp in THF ( 10ml, 0.2M ) and the mixture stirred for 16hrs. The volume of solvent was reduced to ca. 5ml under vacuum and the brown solution loaded onto an alumina column ( 2.5 x 15cm, Brockman Activity II ). A yellow band was eluted with pentane. Removal of solvent under vacuum and recrystallisation from EtOEt/heptane ( 3:1 slow evaporation ) gave IX.

Yield:- 0.49g (73%)

$^1\text{H}$  n.m.r. [ 80MHz,  $(\text{CD}_3)_2\text{CO}$ , 298K ]  $\delta$ :  
0.9(d br, 10Hz, 1H, H3a), 2.48(d, 10.4Hz, 1H, H1a),  
2.84(d, 7.2Hz, 1H, H3s), 5.13(ddd, 10, 10.4, 7.2Hz, 1H, H2s),  
5.32(s, 5H, Cp), 7.1-7.5(m, 5H, Ph).

I.R. ( $\text{CH}_2\text{Cl}_2$  Sol<sup>n</sup>.):-  $\nu_{\text{CO}}$  1940, 1862 $\text{cm}^{-1}$ .

**Analysis; Found( Calc):- 57.3(57.7)%C, 4.1(4.2)%H.**

**Preparation of (Bipyridyl)(dicarbonyl)(isothiocyanato) (1-phenylallyl)molybdenum(II); (Bipy)Mo(CO)<sub>2</sub>(NCS)( $\eta^3$ -1-Ph-C<sub>3</sub>H<sub>4</sub>); X.**

To a solution of Mo(bipy)(CO)<sub>4</sub><sup>66</sup> ( 0.36g, 1mmol ) in THF ( 20ml ) was added cinnamylchloride ( 2ml ) and the mixture refluxed for 2hrs. The resulting brown precipitate of (bipy)Mo(CO)<sub>2</sub>(Cl)( $\eta^3$ -1-Ph-C<sub>3</sub>H<sub>4</sub>) was filtered off and washed with THF ( 10ml ). It was then suspended in (CH<sub>3</sub>)<sub>2</sub>CO and refluxed, with KNCS ( 0.1g, 1mmol ), for 3hrs. The resulting solution was filtered, added to H<sub>2</sub>O ( 200ml ) and extracted with CH<sub>2</sub>Cl<sub>2</sub> ( 4 x 50ml ). The extracts were dried (MgSO<sub>4</sub>), the solvent removed under reduced pressure and the residue recrystallised from CH<sub>2</sub>Cl<sub>2</sub>/hexane to yield X.

**Yield:- 0.37g (78%)**

**<sup>1</sup>H n.m.r. [ 200MHz, (CD<sub>3</sub>)<sub>2</sub>CO, 298K ]  $\delta$ :**  
1.57(dd, 8.8, 1.9Hz, 1H, H1a), 3.23(d, 10.9Hz, 1H, H3a),  
3.43(dd, 6.6, 1.9Hz, 1H, H3s), 4.14(ddd, 6.6, 8.8, 10.9Hz, 1H, H2s),  
6.85-7.25(m, 5H, Ph), 7.47-8.90(m, 8H, bipy).

**I.R. ( CH<sub>2</sub>Cl<sub>2</sub> sol<sup>n</sup>):-  $\nu_{CN}$  2090,  $\nu_{CO}$  1950 and 1865,  $\nu_{CS}$  825cm<sup>-1</sup>.**

**Analysis; Found( Calc):- 54.4(54.7)%C, 3.6(3.5)%H, 8.9(8.7)%N.**

Preparation of (Dicarbonyl)(isothiocyanato)(phenanthroline)  
( $\eta^3$ -1-phenylallyl)molybdenum(II);

(phen)Mo(CO)<sub>2</sub>(NCS)( $\eta^3$ -1-Ph-C<sub>3</sub>H<sub>4</sub>); XI.

As above using Mo(phen)(CO)<sub>4</sub><sup>66</sup>.

Yield:- 0.45g (89%).

<sup>1</sup>H n.m.r. [ 80MHz, (CD<sub>3</sub>)<sub>2</sub>CO, 298K ]  $\delta$ :

1.68(dd, 9.0, 1.8Hz, 1H, H1a), 3.30(d, 10.2, 1H, H3a),

3.64(dd, 6.7, 1.8Hz, 1H, H3s), 4.16(ddd, 6.7, 9.0, 10.2Hz, 1H, H2s),

7.2-7.5(m, 5H, Ph), 7.8-9.9(m, 8H, phen).

I.R. (CH<sub>2</sub>Cl<sub>2</sub> Sol<sup>n</sup>):-  $\nu_{NC}$  2087,  $\nu_{CO}$  1949 and 1864,  $\nu_{CS}$  845cm<sup>-1</sup>.

Analysis; Found(Calc):- 56.6(56.8)%C, 3.7(3.3)%H, 8.2(8.3)%N.

Unit cell:- Monoclinic a = 17.7, b = 9.5, d<sub>001</sub> = 13.1Å

Conditions:- h0l, h+l = 2n; 0k0, k = 2n



## CHAPTER 3

### STRUCTURAL STUDIES OF ALLYL COMPOUNDS

#### 3.1 Preamble:-

The crystal structures of the four suitable compounds, as synthesised in Chapter 2, have been successfully determined. Compounds with an  $\eta^3$ -1-phenylallyl ligand are;  $[(\eta^3\text{-1-Ph-C}_3\text{H}_4)\text{PdTMEDA}]\text{BF}_4$ , IV ( hereafter PHALPD ),  $(\eta^3\text{-1-Ph-C}_3\text{H}_4)\text{PdCp}$ , VI ( CPPHAL ), and  $(\text{phen})\text{Mo}(\text{CO})_2(\text{NCS})(\eta^3\text{-1-Ph-C}_3\text{H}_4)$ , XI ( MOPHAL ).

Perspective plots, demonstrating the numbering scheme adopted in each case, are given as Figures 3.1, 3.2 and 3.3 with bond lengths and angles in Tables 3.1, 3.2 and 3.3 ( for PHALPD, CPPHAL and MOPHAL respectively ). These, together with  $(\eta^3\text{-1-Ph-C}_3\text{H}_4)\text{Ir}(\text{PPh}_3)_2(\text{H})(\text{Cl})$ , 16<sup>32</sup> ( hereafter IRPHAL ) complete the series of four-, five-, six- and seven-coordinate examples of complexes bearing this ligand.

A single cation of complex V,  $[(\eta^3\text{-1-EtOOC-C}_3\text{H}_4)\text{PdTMEDA}]\text{BF}_4$  ( PDETAL ), the four-coordinate species containing an ethoxycarbonyl- substituted allyl is shown in Figure 3.4 with a similar numbering scheme to that of PHALPD. Bond lengths and angles for PDETAL are given in Table 3.4.

The overall geometry of the compounds and the non-allyl ligands will be discussed under the heading of the appropriate metal/ligand fragments. The metal-ligand bonding and intraligand stereochemistry of the

1-phenylallyls, collating all the available data, and those of the 1-ethoxycarbonylallyl complex will then be discussed. An analysis of intramolecular interligand and intermolecular contacts will conclude the discussion.

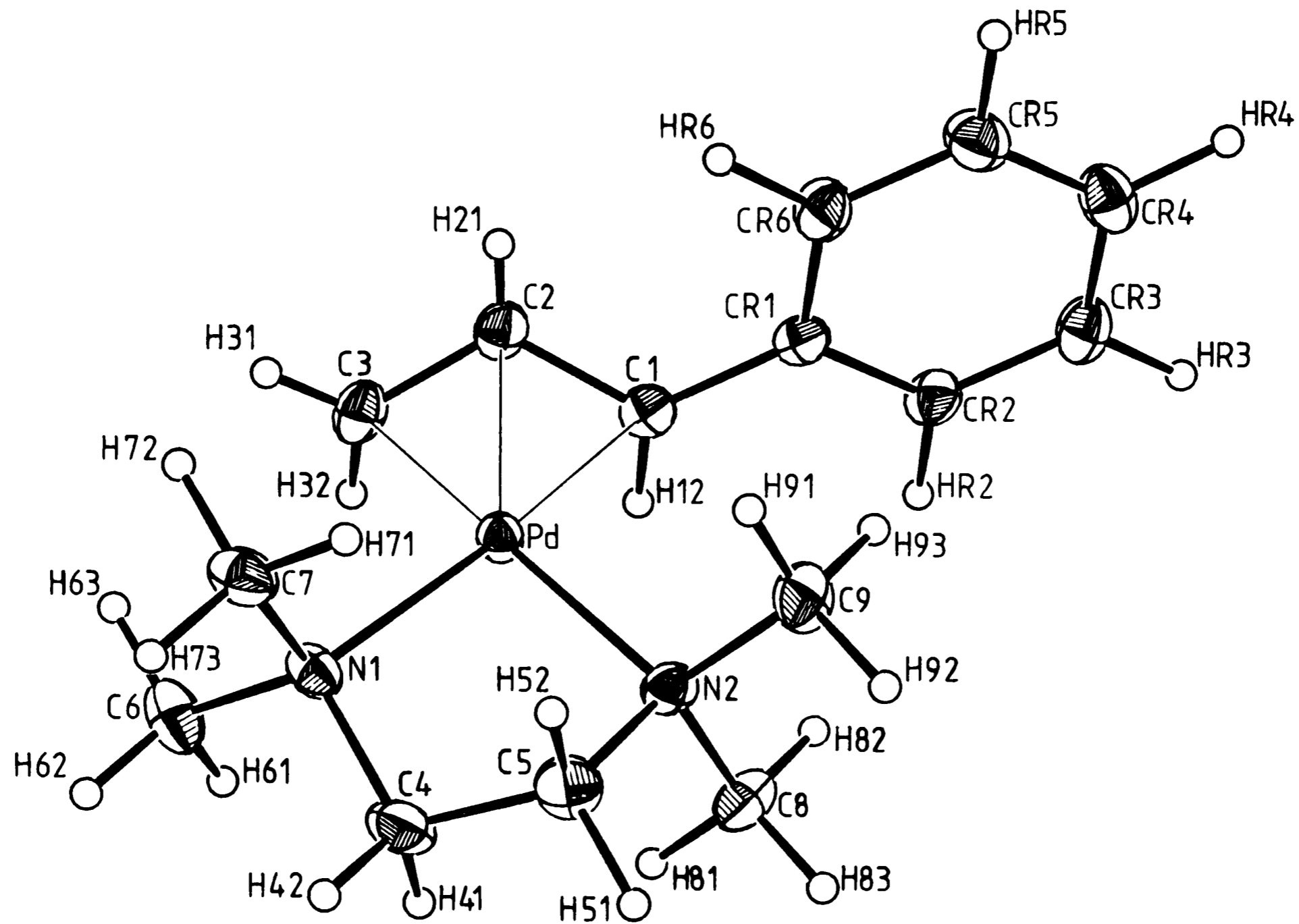


Fig. 3.1 The  $[(\eta^3\text{-1-Ph-C}_2\text{H}_5)\text{PdTMEDA}]^+$  cation, PHALPD.

Table 3.1a Inter-Atomic distances ( Å ) for PHALPD

Pd - C(1)	2.173(3)	CR(5) - CR(6)	1.392(6)
Pd - C(2)	2.125(4)	N(1) - C(4)	1.492(6)
Pd - C(3)	2.124(5)	N(1) - C(6)	1.495(6)
Pd - N(1)	2.146(3)	N(1) - C(7)	1.472(5)
Pd - N(2)	2.138(3)	N(2) - C(5)	1.508(6)
C(1) - C(2)	1.425(5)	N(2) - C(8)	1.478(6)
C(1) - CR(1)	1.467(5)	N(2) - C(9)	1.479(6)
C(2) - C(3)	1.394(6)	C(4) - C(5)	1.501(7)
CR(1) - CR(2)	1.395(6)	B - F(1)	1.366(6)
CR(1) - CR(6)	1.398(6)	B - F(2)	1.378(5)
CR(2) - CR(3)	1.399(6)	B - F(3)	1.380(5)
CR(3) - CR(4)	1.401(6)	B - F(4)	1.387(6)
CR(4) - CR(5)	1.374(7)		
C(1) - H(12)	1.00(3)	C(3) - H(31)	0.93(3)
C(2) - H(21)	0.81(3)	C(3) - H(32)	1.01(3)

Table 3.1b Inter-Bond Angles ( ° ) for PHALPD

C(1) - Pd - C(2)	38.72(15)	CR(4) - CR(5) - CR(6)	121.8(4)
C(1) - Pd - C(3)	69.18(15)	CR(1) - CR(6) - CR(5)	120.1(4)
C(1) - Pd - N(1)	169.03(13)	Pd - N(1) - C(4)	103.61(25)
C(1) - Pd - N(2)	104.06(13)	Pd - N(1) - C(6)	113.1(3)
C(2) - Pd - C(3)	38.29(17)	Pd - N(1) - C(7)	112.19(25)
C(2) - Pd - N(1)	134.90(14)	C(4) - N(1) - C(6)	108.6(3)
C(2) - Pd - N(2)	139.15(15)	C(4) - N(1) - C(7)	111.7(3)
C(3) - Pd - N(1)	101.23(15)	C(6) - N(1) - C(7)	107.7(3)
C(3) - Pd - N(2)	169.18(15)	Pd - N(2) - C(5)	105.8(3)
N(1) - Pd - N(2)	84.57(13)	Pd - N(2) - C(8)	108.5(3)
Pd - C(1) - C(2)	68.84(22)	Pd - N(2) - C(9)	115.0(3)
Pd - C(1) - CR(1)	123.7(3)	C(5) - N(2) - C(8)	110.2(4)
C(2) - C(1) - CR(1)	123.0(3)	C(5) - N(2) - C(9)	108.4(3)
Pd - C(2) - C(1)	72.44(22)	C(8) - N(2) - C(9)	108.8(4)
Pd - C(2) - C(3)	70.8(3)	N(1) - C(4) - C(5)	110.2(4)
C(1) - C(2) - C(3)	119.9(4)	N(2) - C(5) - C(4)	110.6(4)
Pd - C(3) - C(2)	70.9(3)	F(1) - B - F(2)	110.6(4)
C(1) - CR(1) - CR(2)	119.1(3)	F(1) - B - F(3)	109.8(4)
C(1) - CR(1) - CR(6)	122.6(3)	F(1) - B - F(4)	108.9(4)
CR(2) - CR(1) - CR(6)	118.2(4)	F(2) - B - F(3)	109.7(4)
CR(1) - CR(2) - CR(3)	121.4(4)	F(2) - B - F(4)	108.6(4)
CR(2) - CR(3) - CR(4)	119.6(4)	F(3) - B - F(4)	109.3(4)
CR(3) - CR(4) - CR(5)	118.9(4)		
Pd - C(1) - H(12)	90.2(15)	Pd - C(3) - H(31)	109.4(16)
H(12) - C(1) - C(2)	113.1(15)	Pd - C(3) - H(32)	101.8(15)
H(12) - C(1) - CR(1)	121.4(15)	C(2) - C(3) - H(31)	118.7(16)
Pd - C(2) - H(21)	115.6(18)	C(2) - C(3) - H(32)	120.8(15)
C(1) - C(2) - H(21)	119.7(19)	H(31) - C(3) - H(32)	118.9(22)
H(21) - C(2) - C(3)	118.6(19)		



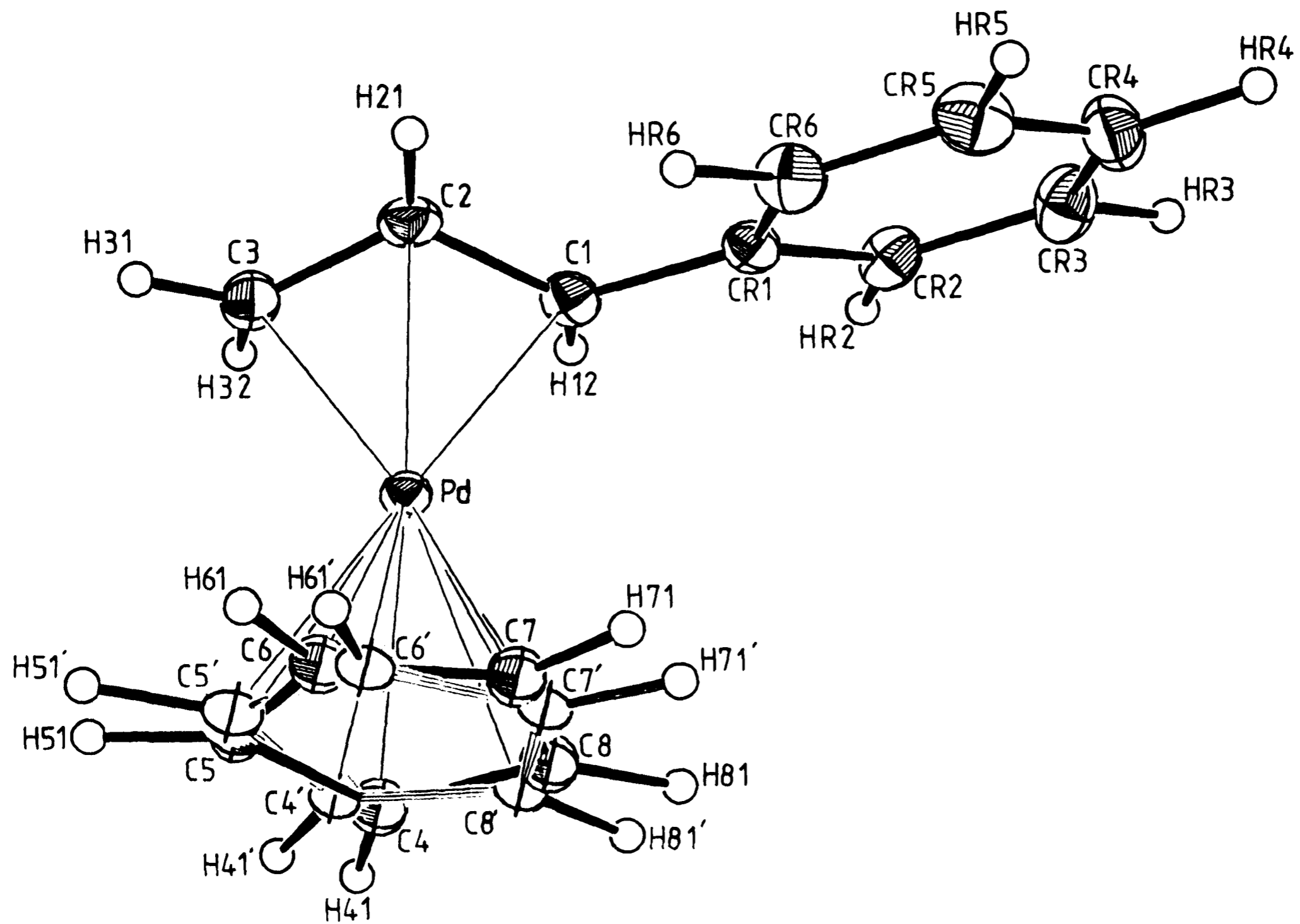


Fig. 3.2 A single molecule of  $(\eta^3\text{-1-Ph-C}_3\text{H}_4)\text{PdCp}$ , CPPHAL, demonstrating the disordered Cp ring.

Table 3.2a Inter-Atomic Distances ( Å ) for CPPHAL

Pd - C(1)	2.1739(23)	CR(1) -CR(2)	1.390(4)
Pd - C(2)	2.079(3)	CR(1) -CR(6)	1.387(4)
Pd - C(3)	2.116(3)	CR(2) -CR(3)	1.382(4)
Pd - C(4)	2.302(8)	CR(3) -CR(4)	1.370(5)
Pd - C(5)	2.302(7)	CR(4) -CR(5)	1.389(5)
Pd - C(6)	2.415(8)	CR(5) -CR(6)	1.394(4)
Pd - C(7)	2.364(8)	C(4) - C(5)	1.454(10)
Pd - C(8)	2.272(8)	C(4) - C(8)	1.410(11)
Pd -C(4')	2.292(6)	C(5) - C(6)	1.411(10)
Pd -C(5')	2.282(8)	C(6) - C(7)	1.401(11)
Pd -C(6')	2.436(7)	C(7) - C(8)	1.466(11)
Pd -C(7')	2.410(6)	C(4') -C(5')	1.446(10)
Pd -C(8')	2.332(6)	C(4') -C(8')	1.400(9)
C(1) - C(2)	1.412(4)	C(5') -C(6')	1.422(10)
C(1) -CR(1)	1.475(3)	C(6') -C(7')	1.395(9)
C(2) - C(3)	1.413(4)	C(7') -C(8')	1.427(9)
C(1) -H(12)	1.02(5)	C(3) -H(31)	0.94(5)
C(2) -H(21)	1.04(4)	C(3) -H(32)	1.21(4)

Table 3.2b Inter-Bond Angles ( ° ) for CPPHAL

C(1) - Pd - C(2)	38.69(10)	C(5') - Pd -C(8')	59.58(24)
C(1) - Pd - C(3)	68.07(10)	C(6') - Pd -C(7')	33.45(22)
C(1) - Pd - C(4)	136.07(21)	C(6') - Pd -C(8')	57.39(22)
C(1) - Pd - C(5)	172.50(18)	C(7') - Pd -C(8')	34.98(21)
C(1) - Pd - C(6)	150.27(19)	Pd - C(1) - C(2)	67.03(14)
C(1) - Pd - C(7)	122.95(19)	Pd - C(1) -CR(1)	120.55(16)
C(1) - Pd - C(8)	115.45(20)	C(2) - C(1) -CR(1)	122.97(21)
C(1) - Pd -C(4')	142.55(16)	Pd - C(2) - C(1)	74.28(15)
C(1) - Pd -C(5')	178.36(20)	Pd - C(2) - C(3)	71.73(16)
C(1) - Pd -C(6')	143.88(17)	C(1) - C(2) - C(3)	116.49(23)
C(1) - Pd -C(7')	120.30(16)	Pd - C(3) - C(2)	68.93(15)
C(1) - Pd -C(8')	119.04(16)	C(1) -CR(1) -CR(2)	118.75(21)
C(2) - Pd - C(3)	39.34(11)	C(1) -CR(1) -CR(6)	123.02(22)
C(2) - Pd - C(4)	164.31(21)	CR(2) -CR(1) -CR(6)	118.20(23)
C(2) - Pd - C(5)	146.80(19)	CR(1) -CR(2) -CR(3)	121.21(25)
C(2) - Pd - C(6)	133.88(20)	CR(2) -CR(3) -CR(4)	120.6(3)
C(2) - Pd - C(7)	135.87(20)	CR(3) -CR(4) -CR(5)	119.2(3)
C(2) - Pd - C(8)	151.88(21)	CR(4) -CR(5) -CR(6)	120.4(3)
C(2) - Pd -C(4')	161.28(17)	CR(1) -CR(6) -CR(5)	120.4(3)
C(2) - Pd -C(5')	142.60(20)	Pd - C(4) - C(5)	71.6(4)
C(2) - Pd -C(6')	134.65(18)	Pd - C(4) - C(8)	70.9(4)
C(2) - Pd -C(7')	140.43(17)	C(5) - C(4) - C(8)	106.7(7)
C(2) - Pd -C(8')	157.38(17)	Pd - C(5) - C(4)	71.6(4)
C(3) - Pd - C(4)	128.75(21)	Pd - C(5) - C(6)	77.1(4)
C(3) - Pd - C(5)	113.88(19)	C(4) - C(5) - C(6)	109.4(6)
C(3) - Pd - C(6)	126.79(20)	Pd - C(6) - C(5)	68.2(4)
C(3) - Pd - C(7)	157.49(20)	Pd - C(6) - C(7)	71.0(4)
C(3) - Pd - C(8)	161.96(21)	C(5) - C(6) - C(7)	107.4(7)
C(3) - Pd -C(4')	122.75(17)	Pd - C(7) - C(6)	75.0(4)
C(3) - Pd -C(5')	113.56(20)	Pd - C(7) - C(8)	68.2(4)
C(3) - Pd -C(6')	133.56(18)	C(6) - C(7) - C(8)	108.9(7)

C(3) - Pd -C(7')	166.45(17)	Pd - C(8) - C(4)	73.2(5)
C(3) - Pd -C(8')	153.34(17)	Pd - C(8) - C(7)	75.0(4)
C(4) - Pd - C(5)	36.8(3)	C(4) - C(8) - C(7)	107.3(7)
C(4) - Pd - C(6)	59.4(3)	Pd -C(4') -C(5')	71.2(4)
C(4) - Pd - C(7)	59.5(3)	Pd -C(4') -C(8')	73.9(4)
C(4) - Pd - C(8)	35.9(3)	C(5') -C(4') -C(8')	107.3(6)
C(5) - Pd - C(6)	34.7(3)	Pd -C(5') -C(4')	72.0(4)
C(5) - Pd - C(7)	58.10(25)	Pd -C(5') -C(6')	78.5(4)
C(5) - Pd - C(8)	60.3(3)	C(4') -C(5') -C(6')	107.4(6)
C(6) - Pd - C(7)	34.1(3)	Pd -C(6') -C(5')	66.6(4)
C(6) - Pd - C(8)	59.6(3)	Pd -C(6') -C(7')	72.3(4)
C(7) - Pd - C(8)	36.8(3)	C(5') -C(6') -C(7')	108.1(6)
C(4') - Pd -C(5')	36.87(24)	Pd -C(7') -C(6')	74.3(4)
C(4') - Pd -C(6')	58.44(22)	Pd -C(7') -C(8')	69.5(3)
C(4') - Pd -C(7')	58.29(21)	C(6') -C(7') -C(8')	108.5(6)
C(4') - Pd -C(8')	35.24(21)	Pd -C(8') -C(4')	70.9(3)
C(5') - Pd -C(6')	34.89(25)	Pd -C(8') -C(7')	75.5(4)
C(5') - Pd -C(7')	58.08(24)	C(4') -C(8') -C(7')	108.3(5)
Pd - C(1) -H(12)	103.9(25)	Pd - C(3) -H(31)	111.8(28)
H(12) - C(1) - C(2)	118.8(26)	Pd - C(3) -H(32)	108.1(20)
H(12) - C(1) -CR(1)	113.4(26)	C(2) - C(3) -H(31)	122.3(28)
Pd - C(2) -H(21)	109.8(24)	C(2) - C(3) -H(32)	122.1(20)
C(1) - C(2) -H(21)	120.4(24)	H(31) - C(3) -H(32)	112.4(34)
H(21) - C(2) - C(3)	121.0(24)		

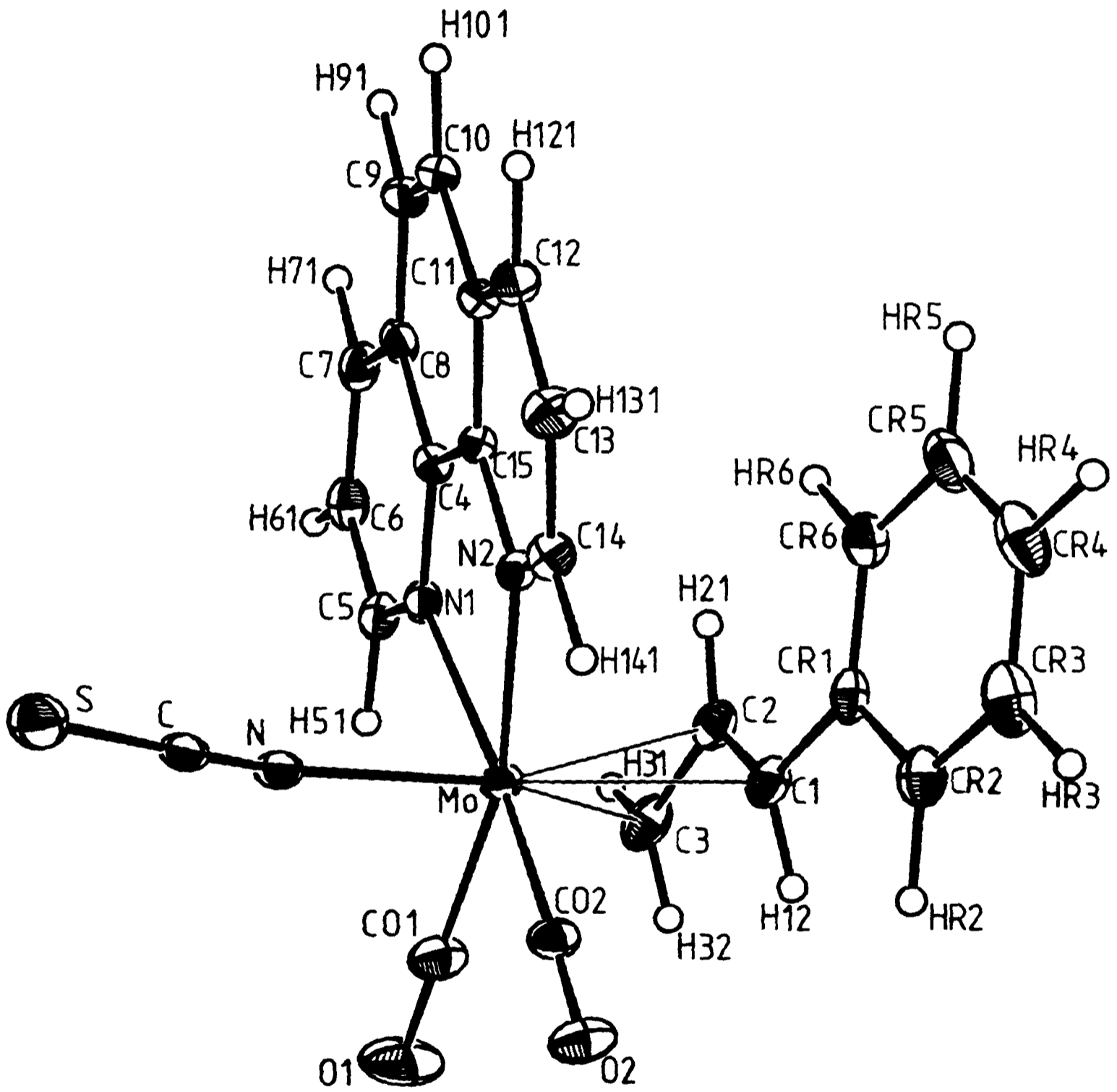


Fig. 3.3 A single molecule of  
 $(\text{Phen})(\text{NCS})\text{Mo}(\text{CO})_2(\eta^3\text{-1-Ph-C}_3\text{H}_4)$ , MOPHAL.

**Table 3.3a Inter-Atomic Distances ( Å ) for MOPHAL**

Mo - N	2.167(3)	C(8) - C(9)	1.433(6)
Mo - N(1)	2.256(3)	C(9) -C(10)	1.341(6)
Mo - N(2)	2.236(3)	C(10) -C(11)	1.437(5)
Mo - C(1)	2.429(4)	C(11) -C(12)	1.408(6)
Mo - C(2)	2.243(4)	C(11) -C(15)	1.399(5)
Mo - C(3)	2.311(5)	C(12) -C(13)	1.362(6)
Mo -CO(1)	1.972(5)	C(13) -C(14)	1.396(6)
Mo -CO(2)	1.943(4)	C(1) - C(2)	1.393(6)
N - C	1.128(5)	C(1) -CR(1)	1.475(6)
C - S	1.632(5)	C(2) - C(3)	1.398(6)
N(1) - C(4)	1.365(5)	CR(1) -CR(2)	1.407(6)
N(1) - C(5)	1.333(5)	CR(1) -CR(6)	1.389(6)
N(2) -C(14)	1.325(5)	CR(2) -CR(3)	1.386(7)
N(2) -C(15)	1.373(5)	CR(3) -CR(4)	1.375(7)
C(4) - C(8)	1.401(5)	CR(4) -CR(5)	1.386(7)
C(4) -C(15)	1.431(5)	CR(5) -CR(6)	1.384(7)
C(5) - C(6)	1.398(6)	CO(1) - O(1)	1.149(6)
C(6) - C(7)	1.377(6)	CO(2) - O(2)	1.160(5)
C(7) - C(8)	1.412(6)		
C(1) -H(12)	0.98(5)	C(3) -H(31)	0.89(5)
C(2) -H(21)	0.93(5)	C(3) -H(32)	0.91(6)

Table 3.3b Inter-Bond Angles (°) for MOPHAL

N	-	Mo	-	N(1)	84.37(12)	N(1)	-	C(4)	-	C(15)	117.5(3)
N	-	Mo	-	N(2)	77.80(12)	C(8)	-	C(4)	-	C(15)	119.8(3)
N	-	Mo	-	C(1)	149.77(14)	N(1)	-	C(5)	-	C(6)	123.4(4)
N	-	Mo	-	C(2)	163.57(14)	C(5)	-	C(6)	-	C(7)	119.1(4)
N	-	Mo	-	C(3)	150.07(15)	C(6)	-	C(7)	-	C(8)	118.9(4)
N	-	Mo	-	CO(1)	88.29(16)	C(4)	-	C(8)	-	C(7)	118.1(4)
N	-	Mo	-	CO(2)	89.29(15)	C(4)	-	C(8)	-	C(9)	118.9(4)
N(1)	-	Mo	-	N(2)	73.90(11)	C(7)	-	C(8)	-	C(9)	123.0(4)
N(1)	-	Mo	-	C(1)	112.98(13)	C(8)	-	C(9)	-	C(10)	121.4(4)
N(1)	-	Mo	-	C(2)	82.34(14)	C(9)	-	C(10)	-	C(11)	120.8(4)
N(1)	-	Mo	-	C(3)	81.34(14)	C(10)	-	C(11)	-	C(12)	123.2(4)
N(1)	-	Mo	-	CO(1)	102.58(15)	C(10)	-	C(11)	-	C(15)	119.0(3)
N(1)	-	Mo	-	CO(2)	173.33(15)	C(12)	-	C(11)	-	C(15)	117.7(3)
N(2)	-	Mo	-	C(1)	83.44(13)	C(11)	-	C(12)	-	C(13)	119.5(4)
N(2)	-	Mo	-	C(2)	89.22(14)	C(12)	-	C(13)	-	C(14)	119.2(4)
N(2)	-	Mo	-	C(3)	122.43(14)	N(2)	-	C(14)	-	C(13)	123.4(4)
N(2)	-	Mo	-	CO(1)	165.88(15)	N(2)	-	C(15)	-	C(4)	117.6(3)
N(2)	-	Mo	-	CO(2)	102.74(15)	N(2)	-	C(15)	-	C(11)	122.5(3)
C(1)	-	Mo	-	C(2)	34.40(15)	C(4)	-	C(15)	-	C(11)	119.9(3)
C(1)	-	Mo	-	C(3)	59.94(16)	Mo	-	C(1)	-	C(2)	65.47(24)
C(1)	-	Mo	-	CO(1)	110.26(17)	Mo	-	C(1)	-	CR(1)	122.0(3)
C(1)	-	Mo	-	CO(2)	71.89(16)	C(2)	-	C(1)	-	CR(1)	125.6(4)
C(2)	-	Mo	-	C(3)	35.71(16)	Mo	-	C(2)	-	C(1)	80.1(3)
C(2)	-	Mo	-	CO(1)	104.00(17)	Mo	-	C(2)	-	C(3)	74.8(3)
C(2)	-	Mo	-	CO(2)	103.54(17)	C(1)	-	C(2)	-	C(3)	116.2(4)
C(3)	-	Mo	-	CO(1)	69.52(18)	Mo	-	C(3)	-	C(2)	69.5(3)
C(3)	-	Mo	-	CO(2)	105.26(17)	C(1)	-	CR(1)	-	CR(2)	118.2(4)
CO(1)	-	Mo	-	CO(2)	79.26(18)	C(1)	-	CR(1)	-	CR(6)	123.9(4)
Mo	-	N	-	C	158.7(3)	CR(2)	-	CR(1)	-	CR(6)	117.9(4)
N	-	C	-	S	177.2(4)	CR(1)	-	CR(2)	-	CR(3)	120.6(4)
Mo	-	N(1)	-	C(4)	115.07(24)	CR(2)	-	CR(3)	-	CR(4)	120.5(5)
Mo	-	N(1)	-	C(5)	127.0(3)	CR(3)	-	CR(4)	-	CR(5)	119.7(5)
C(4)	-	N(1)	-	C(5)	117.7(3)	CR(4)	-	CR(5)	-	CR(6)	120.1(5)
Mo	-	N(2)	-	C(14)	126.8(3)	CR(1)	-	CR(6)	-	CR(5)	121.2(4)
Mo	-	N(2)	-	C(15)	115.50(23)	Mo	-	CO(1)	-	O(1)	177.2(4)
C(14)	-	N(2)	-	C(15)	117.6(3)	Mo	-	CO(2)	-	O(2)	176.7(4)
N(1)	-	C(4)	-	C(8)	122.6(3)						
Mo	-	C(1)	-	H(12)	102.6(31)	Mo	-	C(3)	-	H(32)	107.2(35)
H(12)	-	C(1)	-	C(2)	115.4(32)	C(2)	-	C(3)	-	H(31)	116.9(35)
H(12)	-	C(1)	-	CR(1)	114.4(32)	C(2)	-	C(3)	-	H(32)	122.2(35)
Mo	-	C(2)	-	H(21)	101.9(34)	H(31)	-	C(3)	-	H(32)	116.3(50)
C(1)	-	C(2)	-	H(21)	117.2(34)						
H(21)	-	C(2)	-	C(3)	124.8(34)						
Mo	-	C(3)	-	H(31)	113.8(35)						

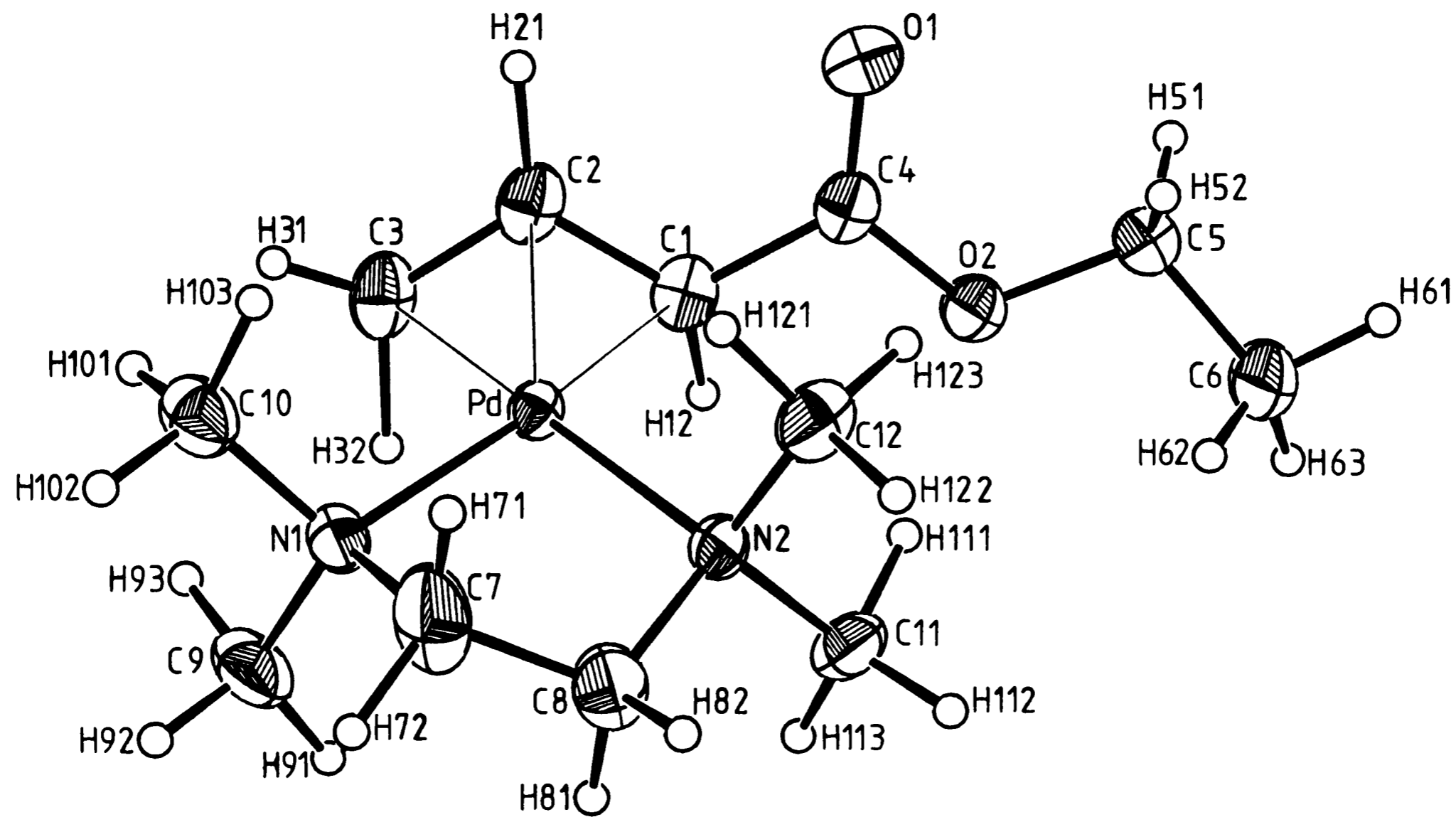


Fig. 3.4 The  $[(\eta^3-1\text{-EtOOC-C}_3\text{H}_4)\text{PdTMEDA}]^+$  cation, PDETAL.

Table 3.4a Inter-Atomic Distances ( Å ) for PDETAL

Pd - C(1)	2.124(4)	N(1) - C(7)	1.491(9)
Pd - C(2)	2.128(4)	N(1) - C(9)	1.452(8)
Pd - C(3)	2.131(4)	N(1) - C(10)	1.476(7)
Pd - N(1)	2.125(3)	N(2) - C(8)	1.493(7)
Pd - N(2)	2.127(3)	N(2) - C(11)	1.465(6)
C(1) - C(2)	1.408(7)	N(2) - C(12)	1.468(6)
C(2) - C(3)	1.388(7)	C(7) - C(8)	1.448(10)
C(1) - C(4)	1.484(6)	B - F(1)	1.366(7)
C(4) - O(1)	1.204(6)	B - F(2)	1.336(8)
C(4) - O(2)	1.323(5)	B - F(3)	1.294(12)
C(5) - C(6)	1.458(11)	B - F(4)	1.339(10)
C(5) - O(2)	1.467(6)		
C(1) - H(12)	1.08(6)	C(3) - H(31)	0.94(6)
C(2) - H(21)	1.20(6)	C(1) - H(12)	1.35(6)

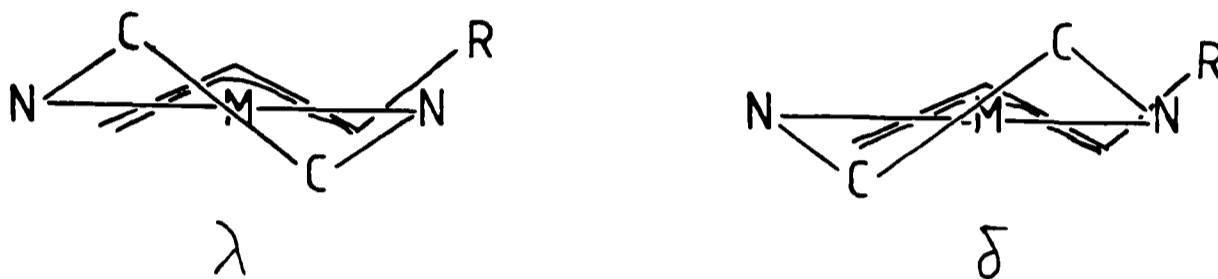
Table 3.4b Inter-Bond Angles ( ° ) for PDETAL

C(1) - Pd - C(2)	38.69(18)	C(4) - O(2) - C(5)	115.8(4)
C(1) - Pd - C(3)	68.32(19)	Pd - N(1) - C(7)	105.2(4)
C(1) - Pd - N(1)	167.54(16)	Pd - N(1) - C(9)	109.6(3)
C(1) - Pd - N(2)	106.03(15)	Pd - N(1) - C(10)	114.3(3)
C(2) - Pd - C(3)	38.03(20)	C(7) - N(1) - C(9)	114.3(5)
C(2) - Pd - N(1)	133.39(17)	C(7) - N(1) - C(10)	105.3(5)
C(2) - Pd - N(2)	139.65(16)	C(9) - N(1) - C(10)	108.3(4)
C(3) - Pd - N(1)	100.35(18)	Pd - N(2) - C(8)	104.6(3)
C(3) - Pd - N(2)	171.85(18)	Pd - N(2) - C(11)	113.6(3)
N(1) - Pd - N(2)	84.67(14)	Pd - N(2) - C(12)	110.8(3)
Pd - C(1) - C(2)	70.8(3)	C(8) - N(2) - C(11)	105.6(4)
Pd - C(1) - C(4)	121.2(3)	C(8) - N(2) - C(12)	114.4(4)
C(2) - C(1) - C(4)	119.7(4)	C(11) - N(2) - C(12)	107.8(4)
Pd - C(2) - C(1)	70.5(3)	N(1) - C(7) - C(8)	112.0(6)
Pd - C(2) - C(3)	71.1(3)	N(2) - C(8) - C(7)	112.4(6)
C(1) - C(2) - C(3)	117.4(4)	F(1) - B - F(2)	111.7(5)
Pd - C(3) - C(2)	70.9(3)	F(1) - B - F(3)	109.4(6)
C(1) - C(4) - O(1)	125.2(4)	F(1) - B - F(4)	109.4(6)
C(1) - C(4) - O(2)	110.0(4)	F(2) - B - F(3)	115.7(7)
O(1) - C(4) - O(2)	124.9(4)	F(2) - B - F(4)	105.5(6)
C(6) - C(5) - O(2)	106.9(5)	F(3) - B - F(4)	104.7(7)
Pd - C(1) - H(12)	103.5(33)	C(5) - C(6) - H(63)	136.6(10)
H(12) - C(1) - C(2)	123.8(33)	N(1) - C(9) - H(91)	121.0(7)
H(12) - C(1) - C(4)	110.7(33)	N(1) - C(9) - H(92)	107.6(6)
Pd - C(2) - H(21)	109.3(30)	N(1) - C(9) - H(93)	99.1(6)
C(1) - C(2) - H(21)	122.7(30)	N(1) - C(10) - H(101)	104.1(5)
H(21) - C(2) - C(3)	115.8(30)	N(1) - C(10) - H(102)	111.2(5)
Pd - C(3) - H(31)	114.1(38)	N(1) - C(10) - H(103)	113.0(6)
Pd - C(3) - H(32)	86.9(25)	N(2) - C(11) - H(111)	97.5(5)
C(2) - C(3) - H(31)	126.3(39)	N(2) - C(11) - H(112)	113.6(5)
C(2) - C(3) - H(32)	120.3(26)	N(2) - C(11) - H(113)	116.6(5)
H(31) - C(3) - H(32)	113.4(46)	N(2) - C(12) - H(121)	110.4(5)
C(5) - C(6) - H(61)	98.7(9)	N(2) - C(12) - H(122)	110.3(5)
C(5) - C(6) - H(62)	90.4(9)	N(2) - C(12) - H(123)	107.7(5)



### 3.2 Pd-TMEDA:-

The palladium-TMEDA fragment is found in the square planar complexes PHALPD ( Figure 3.1 ) and PDETAL ( Figure 3.4 ). The five membered chelate ring, M-N-CH<sub>2</sub>-CH<sub>2</sub>-N, can adopt two configurations,  $\lambda$  and  $\delta$ , shown below<sup>86</sup>.



Figures 3.1 and 3.4 indicate that PHALPD is in the  $\delta$  configuration whilst PDETAL is of the  $\lambda$  form. The  $\lambda$  configuration may be defined as having the C-C bond of the methylene bridge parallel to the C(1)-C(2) bond of the allyl, whereas in the  $\delta$  form it is parallel to the C(2)-C(3) bond.

The carbon atoms in the -CH<sub>2</sub>-CH<sub>2</sub>- bridge are displaced from the metal coordination plane ( defined by Pd, N(1) and N(2) ) by -0.51Å and 0.18Å in PHALPD ( Table 3.5 ). This indicates that the conformation of the ring is moving away from the ideal skew geometry towards an envelope conformation<sup>87</sup> with C(5) approaching the coordination plane. Such deformations are easily accomplished within the magnitude of crystal packing forces and intramolecular steric congestion. Examination of intramolecular contacts ( Table 3.7 ) reveals a very short contact, H(52)...H(71)

Table 3.5 Least-Squares Planes Data for PHALPD

(a) Coefficients

Plane 1: C(1), C(2), C(3).

$$\text{Equation: } 4.8069x + 6.7977y + 7.9628z = 7.5126\text{\AA}.$$

Plane 2: CR(1), CR(2), CR(3), CR(4), CR(5), CR(6).

$$\text{Equation: } 8.8465x + 6.1499y + 4.9058z = 7.9942\text{\AA}.$$

R.M.S. Deviation = 0.004\AA.

Plane 3: Pd, N(1), N(2).

$$\text{Equation: } -4.9589x - 0.9494y + 8.9261z = -0.4849\text{\AA}.$$

(b) Atomic Deviations ( \AA )

Plane 1: Pd 1.6521, H(12) -0.4036, H(21) 0.1875,  
H(31) 0.3130, H(32) -0.5251.

Plane 2: CR(1) -0.0072, CR(2) 0.0076, CR(3) -0.0002,  
CR(4) -0.0076, CR(5) 0.0080, CR(6) -0.0005.

Plane 3: C(1) -0.2523, C(2) 0.3144, C(3) -0.3342,  
C(4) -0.5125, C(5) 0.1842.

(c) Dihedral Angles (°)

Plane 1, Plane 2 27.33

Plane 1, Plane 3 59.53

Plane 2, Plane 3 85.54

Table 3.6 Least-Squares Planes Data for PDETAL

(a) Coefficients

Plane 1: C(1), C(2), C(3).

$$\text{Equation: } 0.7497x + 6.8021y - 8.2218z = -6.7004\text{\AA}.$$

Plane 2: Pd, N(1), N(2).

$$\text{Equation: } 4.4745x - 4.8747y - 0.8630z = -0.9092\text{\AA}.$$

(b) Atomic Deviations ( \AA )

Plane 1: Pd 1.6472, H(12) -0.5601, H(21) 0.4089  
H(31) 0.2439, H(32) -0.3876.

Plane 2: C(1) 0.2315, C(2) -0.4056, C(3) 0.2370,  
C(7) -0.3007, C(8) 0.3338.

(c) Dihedral Angles (°)

Plane 1, Plane 2 118.3

2.095(6)Å, which could be forcing C(5) into the coordination plane.

A similar examination of contacts in PDETAL ( Table 3.8a.) indicates that the ligand is far less strained, the most significant contacts being between the methyl group hydrogens and not involving the methylene groups. This is reflected in the deviations of the bridging carbon atoms from the metal coordination plane ( -0.30Å and 0.33Å for C(7) and C(8) respectively ), resulting in a nearly ideal skew conformation.

The range reported for M-N bond lengths in similar  $d^8$  TMEDA complexes ( M = Pd or Pt ) is 2.045(6)Å<sup>88</sup> - 2.17(2)Å<sup>89</sup>, and the distances in both complexes studied here fall within this range ( 2.146(3)Å and 2.138(3)Å for PHALPD and 2.125(3)Å and 2.127(3)Å in PDETAL ). The lengths however, do reflect the *trans* influence of the other ligands. In  $[(\eta^2-C_2H_4)(Cl)PtTMEDA]^+$ , 26<sup>88</sup>, the Pt-N bond *trans* to Cl is 2.045(6)Å whilst that *trans* to  $\eta^2-C_2H_4$  is 2.128(6)Å. The *trans* influence of  $\eta^3-1-Ph-C_3H_4$  has been observed in IRPHAL, in which the Ir-P bond *trans* to the substituted allyl carbon is shorter than that *trans* to the unsubstituted atom. In PHALPD however, the Pd-N bond *trans* to the substituted carbon is the longer of the two, although the difference is not strictly significant (  $\Delta < 3\sigma$  ). EHMO calculations ( see Chapter 4 ) support this, affording a smaller overlap population for the bond *trans* to the substituent. This apparent reversal of the *trans* influence may be due to

Table 3.7 Significant non-bonded contacts for PHALPD

(a) Intramolecular ( Å )

H(21)....H(31)	2.23(4)
H(21)....HR(6)	2.25(3)
H(93)....CR(1)	2.746(6)
H(93)....CR(6)	2.937(7)
H(41)....H(61)	2.300(7)
H(41)....H(81)	2.214(6)
H(51)....H(83)	2.299(7)
H(52)....H(71)	2.095(6)
H(52)....H(91)	2.269(7)
H(62)....H(73)	2.377(6)
H(63)....H(72)	2.377(6)

(b) Intermolecular

Contact X....H	Symm H	Dist (Å)	Angle A-X....H ( ° )
F(1)....H(52)	x, y, z-1	2.502(7)	148.7(4)
F(2)....H(51)	3/2-x, y, z-1/2	2.346(5)	118.6(3)
F(2)....H(61)	x, y, z	2.517(6)	92.5(2)
F(2)....H(73)	1-x, 2-y, z-1/2	2.514(6)	118.6(3)
F(2)....H(81)	x, y, z	2.477(7)	124.6(3)
F(3)....H(42)	1-x, 2-y, z-1/2	2.496(5)	139.0(3)
F(3)....H(61)	x, y, z	2.437(6)	95.9(3)
F(4)....HR(4)	1-x, 1-y, z-1/2	2.445(6)	116.3(3)
H(31)....H(71)	1/2-x, y, z-1/2	2.34(3)	112.7(16)
CR(2)....HR(5)	1/2-x, y, z-1/2	2.921(7)	
CR(5)....HR(2)	1-x, 1-y, 1/2+z	2.814(7)	

Table 3.8 Significant non-bonded contacts for PDETAL

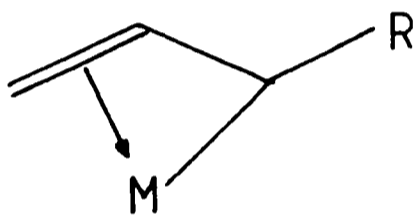
(a) Intramolecular ( Å )

H(52)....H(61)	2.189(10)
H(52)....H(62)	2.102(8)
H(71)....H(82)	2.337(12)
H(72)....H(81)	2.337(10)
H(72)....H(92)	2.336(12)
H(81)....H(113)	2.249(8)
H(82)....H(122)	2.329(8)
H(92)....H(102)	2.371(8)
H(93)....H(101)	2.019(8)
H(111)....H(123)	2.106(6)

(b) Intermolecular.

Contact X....H	Symm H	Dist (Å)	Angle A-X....H ( ° )
F(1)....H(82)	x, y, z	2.311(9)	130.9(3)
F(1)....H(72)	1-x, 1-y, 1-z	2.316(7)	119.2(4)
F(2)....H(121)	1+x, y, z	2.454(8)	143.2(5)
F(3)....H(92)	1-x, 1-y, 1-z	2.342(9)	127.6(8)
H(63)....H(12)	1-x, -y, 2-x	1.87(6)	166.3(19)
O(1)....H(52)	1-x, 1-y, 2-z	2.333(6)	129.9(3)

TMEDA being a pure  $\sigma$ -donor as opposed to a  $\sigma$ -donor/ $\pi$ -acceptor as are the phosphines in IRPHAL. The nature of the *trans* influence is different in each case. The polarisation theory of Grindberg<sup>90</sup> rationalises the *trans* influence of  $\sigma$ -donor ligands. However, it has been shown that  $\sigma$ -donor ligands are not susceptible to the *trans* influence of  $\pi$ -bonding ligands, such as phosphines<sup>91</sup>. From inspection of the C-C bond lengths of a coordinated 1-phenylallyl ligand ( see section 4.5 ), this ligand could be considered as being  $\sigma/\pi$  bound, A.



A

In IRPHAL the phosphine ligand *trans* to the alkene coordinating part of the allyl will be labilised ( due to competition for the available  $\pi$ -electron density ) relative to that *trans* to the substituted carbon. However, in the case of only  $\sigma$ -donor ligands, such as the TMEDA in PHALPD, it will be the Pd-ligand bond *trans* to the substituted carbon that will be relatively the weaker, the alkene part of the allyl having no effect on the *trans* nitrogen. Hence the apparent reversal of the *trans* influence of the 1-phenylallyl ligand is understandable.

There is a good correlation between the average M-N bond length and the N-M-N angle for M-TMEDA complexes ( M

= Pd<sup>49</sup> and Pt<sup>88,89,92</sup> ) as can be seen from Figure 3.5. Both PHALPD and PDETAL obey this correlation with N-Pd-N angles of 84.57(13)° and 84.67(14)° respectively. These lengths and angles are not significantly different to those in the parent species [ $\eta^3$ -C<sub>3</sub>H<sub>5</sub>]PdTMEDA]<sup>+</sup>, 27<sup>49</sup>, ( Pd-N = 2.15(1)Å and 2.16(2)Å, N-Pd-N = 84.6(5)° ) although in this complex the dimethylene bridge shows some sign of disorder.

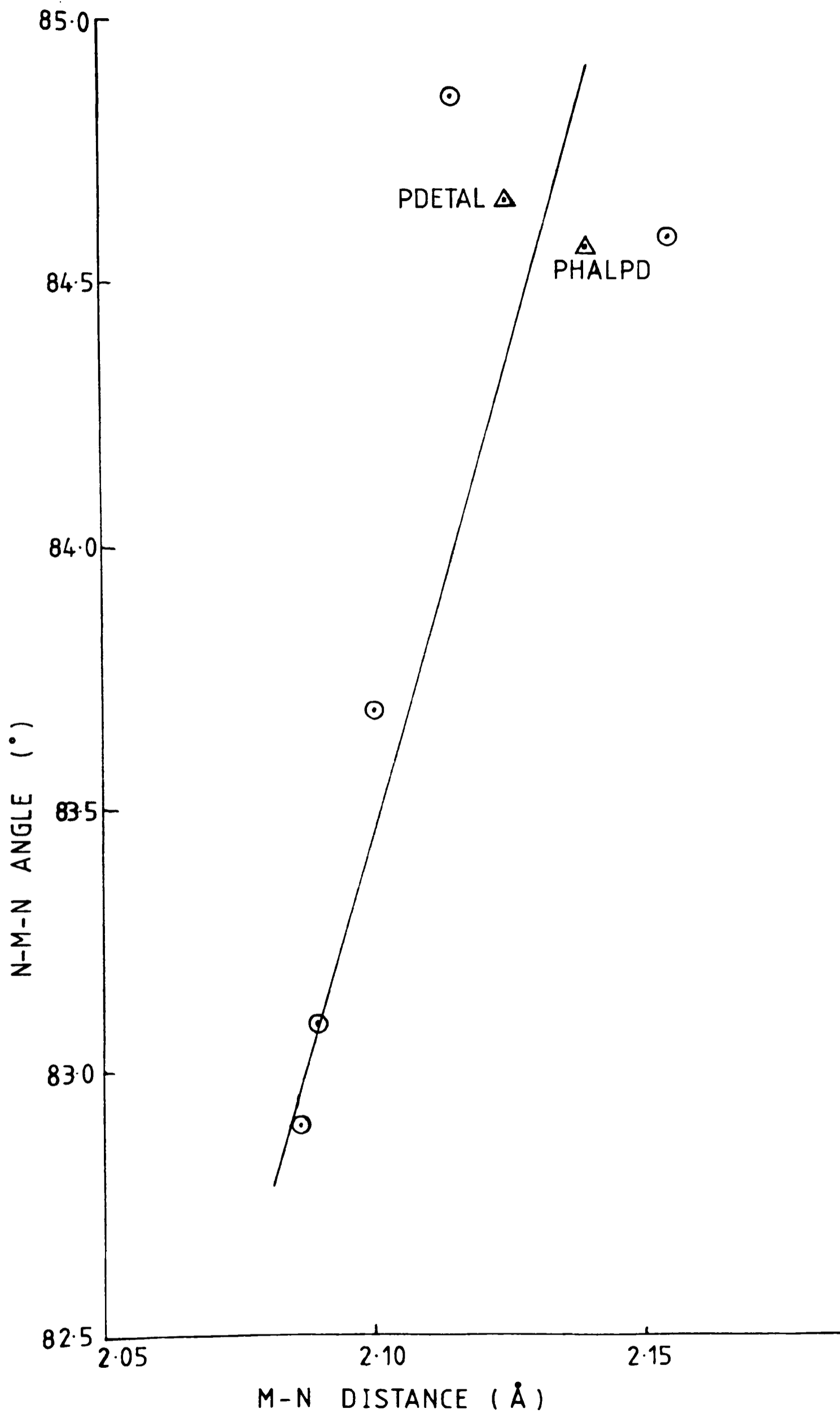


Fig. 3.5 Graph of M-N distance versus N-M-N angle.



### 3.3 Pd-Cp:-

The cyclopentadienyl ring in CPPHAL was found to be severely disordered, and has been modeled as two, isotropic,  $C_5$  rings which were refined with variable, linked site occupation factors (SOF's) and not idealised to regular pentagons. The final ratio of the two SOF's was 54:46, and the major component is indicated by the shaded ellipsoids in Figure 3.2. Atom labels of the minor component (represented by the solid ellipsoids) carry a prime superscript and are numbered according to which carbon from the major component they are nearest.

The two rings are inclined at an angle of  $3.9^\circ$  (Table 3.9) and subtend angles of  $20.4^\circ$  (major) and  $22.2^\circ$  (minor) to the allyl  $C_3$  plane. The last two values compare favourably with the angle of  $20.0^\circ$  found in  $CpPd(\eta^3-C_3H_5)$ , 28<sup>93</sup>.

The bond lengths (Table 3.2a) and angles (Table 3.2b) indicate that the Cp rings are not identical nor symmetrically bonded to the metal atom. The major discrepancies between the two rings involve C(7) and C(8) (and the equivalent atoms C(7') and C(8')). The C(7)-C(8) and C(7')-C(8') distances are  $1.466(11)\text{\AA}$  and  $1.427(9)\text{\AA}$  and these are the only corresponding C-C distances between the two rings that are different.

The asymmetry in the bonding of the rings to the metal is not identical in either case. Two factors will affect the bonding; the *trans* influence of the asymmetric allyl ligand

**Table 3.9 Least-Squares Planes Data for CPPHAL**

**(a) Coefficients**

Plane 1: C(1), C(2), C(3).

Equation:  $2.0758x - 0.2879y + 13.6234z = 2.5669\text{\AA}$ .

Plane 2: CR(1), CR(2), CR(3), CR(4), CR(5), CR(6).

Equation:  $5.6207x + 2.5073y + 11.1026z = 4.3849\text{\AA}$ .

R.M.S. Deviation =  $0.0041\text{\AA}$ .

Plane 3: C(4), C(5), C(6), C(7), C(8).

Equation:  $2.6767x + 1.7392y + 12.8842z = 7.3526\text{\AA}$ .

R.M.S. Deviation =  $0.023\text{\AA}$ .

Plane 4: C(4'), C(5'), C(6'), C(7'), C(8').

Equation:  $1.8185x + 1.9282y + 12.8926z = 7.3525\text{\AA}$ .

R.M.S. Deviation =  $0.0245\text{\AA}$ .

**(b) Atomic Deviations (  $\text{\AA}$  ).**

Plane 1: Pd 1.7285, H(12) -0.5006, H(21) 0.2510,  
H(31) 0.2170, H(32) -0.6254.

Plane 2: CR(1) -0.0056, CR(2) 0.0006, CR(3) 0.0043,  
CR(4) -0.0041, CR(5) -0.0009, CR(6) 0.0058.

Plane 3: Pd -1.9859, C(4) 0.0315, C(5) -0.0300,  
C(6) 0.0169, C(7) 0.0029, C(8) -0.0213.

Plane 4: Pd -2.0115, C(4') 0.0253, C(5') -0.0340,  
C(6') 0.0305, C(7') -0.0147, C(8') -0.0070.

**(c) Dihedral Angles ( $^{\circ}$ )**

Plane 1, Plane 2 33.07

Plane 1, Plane 3 20.43

Plane 1, Plane 4 22.19

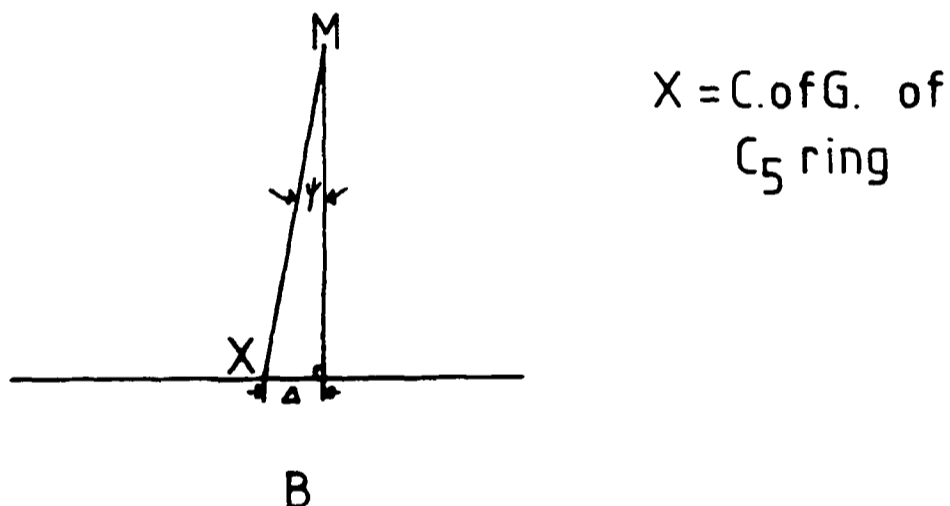
Plane 2, Plane 3 15.81

Plane 2, Plane 4 17.88

Plane 3, Plane 4 3.93

and a slippage of the ring towards a cyclic  $\eta^3$ -allyl function and a free double bond, the complex tending towards a sixteen electron configuration analogous to  $(\eta^3\text{-C}_3\text{H}_5)_2\text{Pd}$ , 29<sup>94</sup>.

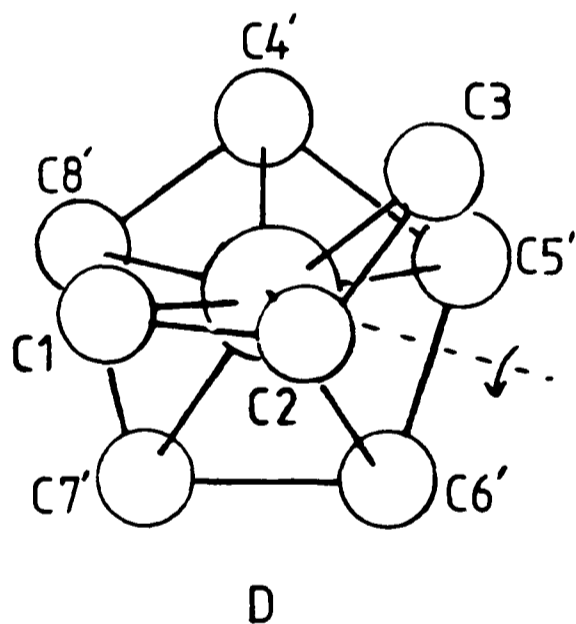
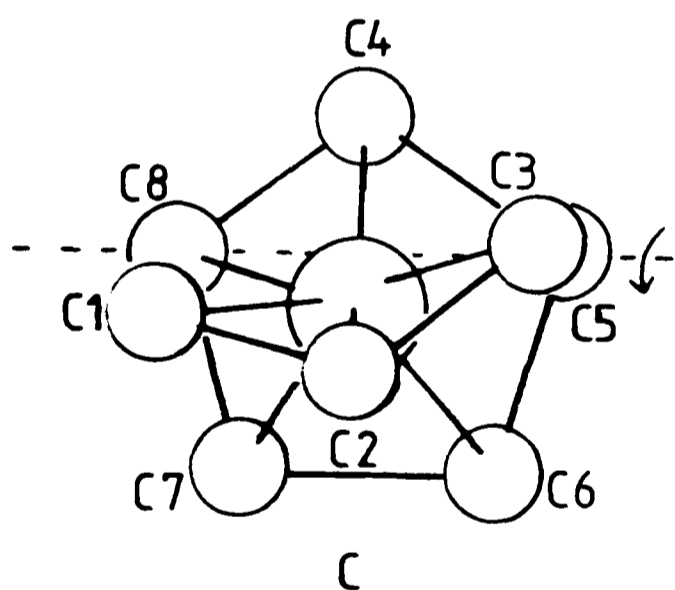
For the major component ring the Pd-C distances are arranged in the order Pd-C(6) > Pd-C(7) > Pd-C(4)  $\approx$  Pd-C(5) > Pd-C(8). This, coupled with the shortest C-C distance being C(6)-C(7), suggests a slippage towards an  $\eta^3$ -allyl ( C(8), C(4) and C(5) ) and free double bond ( C(6) and C(7) ). This would give the predicted, more thermodynamically stable, *trans* configuration of the two allyls<sup>94</sup>. The slippage can be quantified in terms of an angular tilt,  $\psi$ <sup>95</sup>, or a translational slip,  $\Delta$ <sup>96</sup>, B.



Here the values of  $\psi$  and  $\Delta$  are 3.7° and 0.13Å respectively, towards C(4). Consistent with this is the non-planarity of the ring. It is of an envelope conformation, bent about the C(5)...C(8) vector by 5.3°, C.

In the case of the minor component the Pd-C' bond lengths are arranged in the order Pd-C(6') > Pd-C(7') > Pd-C(8') > Pd-C(4')  $\approx$  Pd-C(5') with C(6')-C(7') again being the shortest C'-C' bond distance. As before this suggests a slip

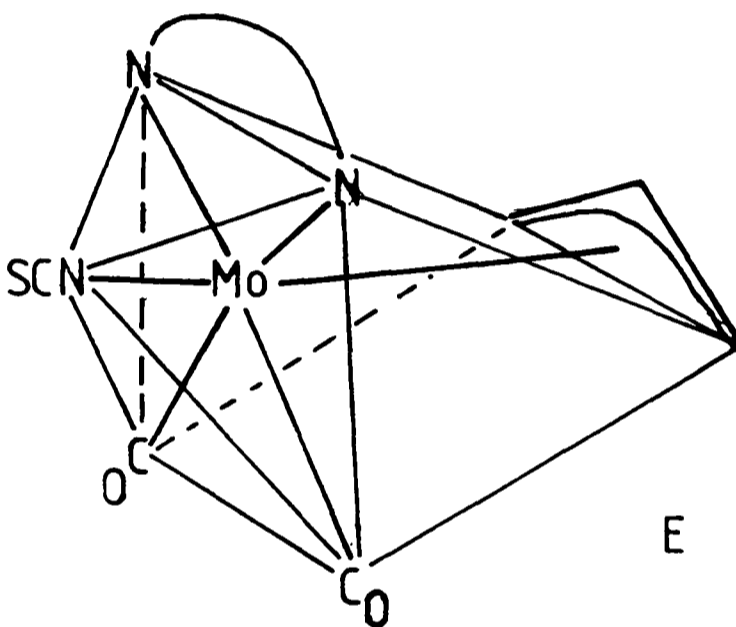
towards a cyclic  $\eta^3$ -function ( C(8'), C(4') and C(5') ) with a free double bond ( C(6') and C(7') ). However, consistent with the *trans* influence expected from the asymmetrically bonded allyl function, Pd-C(8') is the longest Pd-C' bond, unlike the equivalent bond in the major component ring. Also the conformation of the bis-allyl complex that would be formed in the limit of the slipping is not the near perfect *trans* configuration found for the major component. Thus the tilt of the ring is about the C(8')-X vector ( where X is the mid-point of the C(5')-C(6') bond ), D, by 4.6° or a translational slip of 0.16Å. Consistent with this is the conformation of the ring which is puckered about the C(8')-X vector.



Interestingly in the analogous compound, 28<sup>93</sup>, the ring is symmetrically bonded to the metal with average distances of 2.26Å ( Pd-C ) and 1.40Å ( C-C ). However, other examples of palladium compounds with an asymmetrically bonded cyclopentadienyl ring have been studied<sup>97</sup> and in these the other ligands are usually asymmetric.

### 3.4 (Phen)Mo(CO)<sub>2</sub>(NCS):-

As can be seen, from Figure 3.3, the overall geometry of this seven-coordinate species is, perhaps, best described as a 1:4:2 capped trigonal prism<sup>98</sup>. The isothiocyanate occupies the capping position, the bidentate 1,10-phenanthroline and the two carbonyl groups the capped square plane, with the allyl group, which is in the *exo* conformation with respect to the Mo(CO)<sub>2</sub> fragment, along the final edge, E



A similar arrangement has been found in the analogous compounds;  $(\text{bipy})\text{Mo}(\text{CO})_2(\text{NCS})(\eta^3\text{-C}_3\text{H}_5)$ ,  $30^{62}$ ,  
 $(\text{phen})\text{Mo}(\text{CO})_2(\text{NCS})(\eta^3\text{-2-Me-C}_3\text{H}_4)$ ,  $31^{63}$ ,  
 $[(\text{py})(\text{bipy})\text{Mo}(\text{CO})_2(\eta^3\text{-C}_3\text{H}_5)]^+$ ,  $32^{68}$  and other members of the  $\text{LL}'_2\text{Mo}(\text{CO})_2(\text{allyl})$  series<sup>60,61,64</sup>. In all cases, however,  $\text{L}'_2$  is not a strong  $\pi$ -acceptor. As mentioned above, when  $\text{L}'_2$  is a phosphine or similar strong  $\pi$ -acceptor, rearrangement occurs such that  $\text{L}'_2$  is no longer *trans* to the carbonyl groups<sup>57-59</sup>.

In MOPHAL the allyl has an *exo* conformation with respect to the Mo(CO)<sub>2</sub> fragment, consistent with the structures of  $30^{62}$ ,  $31^{63}$ ,  $32^{68}$ ,  $\text{CpMo}(\text{CO})_2(\eta^3\text{-C}_3\text{H}_5)$ ,  $33^{22}$ , and

many other seven coordinate species containing the  $\text{Mo(CO)}_2(\text{allyl})$  moiety<sup>58-61,64,99-103</sup>. The  $\text{C}_3\text{-Mo(CO)}_2$  interplanar angle (  $6.5^\circ$  ) compares favourably with the neutral species 30 and 31 (  $8.3^\circ$  and  $7.6^\circ$  respectively but not with the cationic species 32 (  $13.8^\circ$  ) whilst the phen- $\text{Mo(CO)}_2$  angle (  $12.6^\circ$  ) is similar to that in compounds 30 and 32, (  $15.1^\circ$  and  $14.3^\circ$  respectively ), but is considerably less than that (  $27.5^\circ$  ) in the phenanthroline species 31. For the above mentioned analogous compounds the range of  $\text{Mo-C}_{(\text{carbonyl})}$  distances is  $1.87(4)\text{\AA}$ <sup>61</sup> -  $2.061(8)\text{\AA}$ <sup>68</sup> and the range of OC-Mo-CO angles is  $75(2)^\circ$ <sup>61</sup> -  $82.6(4)^\circ$ <sup>63</sup>. Thus the values of  $1.972(5)\text{\AA}$  and  $1.943(4)\text{\AA}$  for the  $\text{Mo-C}_{(\text{carbonyl})}$  distances ( Table 3.3a ) and  $79.26(18)^\circ$  for the OC-Mo-CO angle ( Table 3.3b ) observed in MOPHAL are quite standard for this type of compound.

The Mo-N(1) and Mo-N(2) bond lengths (  $2.256(3)\text{\AA}$  and  $2.236(3)\text{\AA}$  respectively ) with an associated N(1)-Mo-N(2) angle of  $73.90(11)^\circ$  fit the correlation between the average M-N distance and N-M-N angle observed for a variety of metal-(phen) complexes<sup>104</sup>. All the phenanthroline C-C and C-N distances observed in MOPHAL fall within the range reported for the corresponding distances in the structures reviewed<sup>104</sup>. Furthermore, none of the distances are significantly different to those reported for the free ligand<sup>105</sup>.

The Mo-N bond to the isothiocyanate (  $2.167(3)\text{\AA}$  ) is significantly longer than that in either 30 or 31;

Table 3.10 Least-Squares Planes Data for MOPHAL

(a) Coefficients

Plane 1: C(1), C(2), C(3).

$$\text{Equation: } 2.8944x - 7.7136y + 6.7042z = 4.2975\text{\AA}$$

Plane 2: CR(1), CR(2), CR(3), CR(4), CR(5), CR(6).

$$\text{Equation: } -2.0025x + 8.4368y - 5.4368z = -2.5759\text{\AA}$$

R.M.S. Deviation 0.004\AA

Plane 3: N(1), N(2), C(4), C(5), C(6), C(7), C(8),  
C(9), C(10), C(11), C(12), C(13), C(14),  
C(15).

$$\text{Equation: } 2.0715x + 7.6902y - 8.9856z = -2.3185\text{\AA}$$

R.M.S. Deviation 0.0547\AA

Plane 4: Mo, CO(1), CO(2).

$$\text{Equation: } -1.2428x + 8.0353y - 6.9940z = -1.8149\text{\AA}$$

(b) Atomic Deviations ( \AA )

Plane 1: Mo -2.0415, H(12) 0.3767, H(21) -0.2027,  
H(31) -0.0326, H(32) 0.3554.

Plane 2: CR(1) 0.0022, CR(2) 0.0032, CR(3) -0.0047,  
CR(4) 0.0009, CR(5) 0.0046, CR(6) -0.0061.

Plane 3: Mo -0.1568, N(1) 0.0198, N(2) -0.1017,  
C(4) -0.0403, C(5) 0.0839, C(6) 0.0536,  
C(7) -0.0301, C(8) -0.0457, C(9) -0.0314,  
C(10) 0.0258, C(11) -0.0006, C(12) 0.0709,  
C(13) 0.0784, C(14) -0.0268, C(15) -0.0556.

(c) Dihedral Angles (°)

Plane 1, Plane 2 171.49  
Plane 1, Plane 3 161.72  
Plane 1, Plane 4 173.47  
Plane 2, Plane 3 17.39  
Plane 2, Plane 4 6.21  
Plane 3, Plane 4 12.60

concomitant with this is a short N-C bond ( 1.128(5)Å ). Both facts signify a more weakly bound NCS group in MOPHAL due to the *trans* influence of the 1-phenylallyl ligand. The C-S bond of 1.632(5)Å is not significantly different to those found in either 30 or 31. The non-linearity of the bonding ( Mo-N-C = 158.7(3)° ) is consistent with that in 31 although, as expected the N-C-S bond is nearly linear ( 177.2(4)° ).



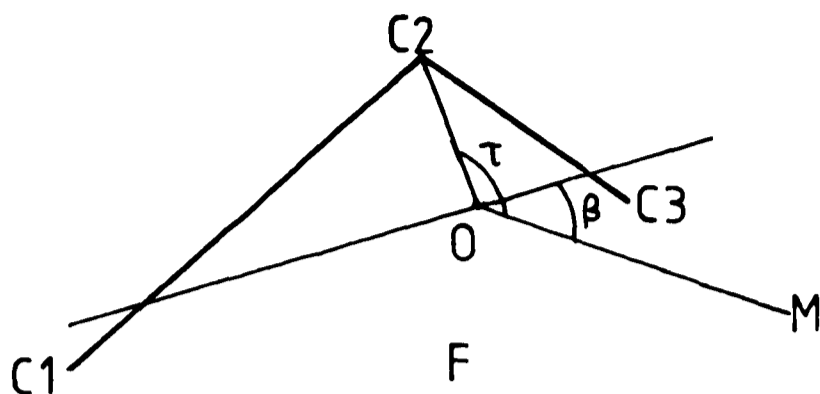
### 3.5 The $\eta^3$ -1-phenylallyl ligand:-

The  $\eta^3$ -1-phenylallyl ligand (  $\eta^3$ -1-Ph-C<sub>3</sub>H<sub>4</sub> ) is contained in the complexes PHALPD, CPPHAL, MOPHAL and in the previously determined IRPHAL<sup>32</sup>. Parameters describing both the metal-ligand bonding and intraligand features for all four structures are summarised in Table 3.11. The numbering system is consistent throughout and is illustrated by any one of Figures 3.1, 3.2 or 3.3. The carbon atom bearing the substituent is C(1), the central allyl carbon is C(2) and the unsubstituted terminal allyl carbon C(3). Allylic hydrogens carry the number of the carbon to which they are bound followed by a number representing the position; 1 for the *syn* and 2 for the *anti* position. Phenyl ring carbon and hydrogen atom labels contain the letter R and are numbered cyclicly with CR(6) *syn* to C(2), hydrogens carrying the number of the carbon to which they are bound.

From Table 3.11 it is obvious that the ligand is not symmetrically bound to the metal, since in all cases M-C(1) is considerably longer than M-C(3). A single parameter defining this asymmetrical bonding has been described by Ibers et al.<sup>106</sup>. It is  $\beta$ , the angle between the vector M-O (where M is the metal atom and O is the centre of gravity of the C<sub>3</sub> fragment ) and a vector parallel to C(1)-C(3), passing through O, F. This parameter accounts for any asymmetry which may also be present in the C-C bond distances.

Table 3.11 Parameters for coordinated  $\eta^3-1\text{-Ph-C}_3\text{H}_4$

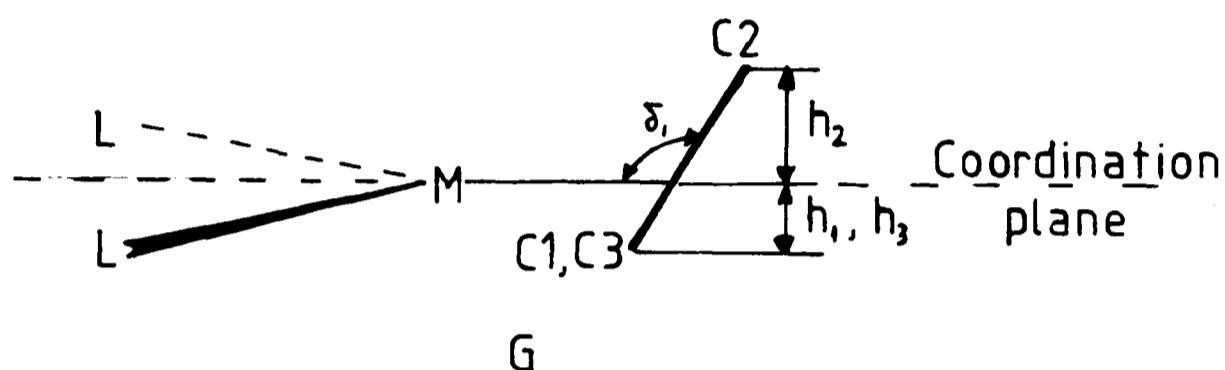
	PHALPD	CPPHAL	IRPHAL	MOPHAL
M-C(1)	2.173(3)	2.1739(23)	2.276(6)	2.429(4)
M-C(2)	2.125(4)	2.079(3)	2.178(6)	2.243(4)
M-C(3)	2.124(5)	2.116(3)	2.196(7)	2.311(5)
$\beta$ (°)	88.88	88.39	88.11	86.72
C(1)-C(2)	1.425(5)	1.412(4)	1.427(8)	1.393(6)
C(2)-C(3)	1.394(6)	1.413(4)	1.378(12)	1.398(6)
C(1)-CR(1)	1.467(5)	1.475(3)	1.483(8)	1.475(6)
C(1)-C(2)-C(3)	119.9(4)	116.49(23)	120.8(8)	116.2(4)
$\theta$ (°)	27.3	33.1	52.6	8.5
HR(6)-H(21)	2.25(3)	2.25(4)	2.53(9)	2.17(7)
C(2)-C(1)-CR(1)	123.0(3)	122.97(21)	120.6(6)	125.6(4)
$\tau$ (°)	117.6	110.86	113.2	101.9
M-O	1.866	1.851	1.954	2.090
$\Delta\text{H}12$ (°)	-23.8	-29.3	-26.0	-22.6
$\Delta\text{H}21$ (°)	13.4	14.0	10.8	12.6
$\Delta\text{H}31$ (°)	19.7	13.3	1.3	2.1
$\Delta\text{H}32$ (°)	-31.3	-31.1	-32.9	-23.0
$\delta_1$ (°)	120.5	-	105.3	-
$h_1$	-0.2523	-	0.3495	-
$h_2$	0.3144	-	0.6899	-
$h_3$	-0.3342	-	-0.2480	-



Thus, when  $\beta < 90^\circ$ , the substituted carbon is tilted away from the metal atom. This is observed for all four cases examined here. In the first three, PHALPD, CPPHAL and IRPHAL there is a good correlation between the angle of bow,  $\beta$ , and the coordination number of the metal. The seven-coordinate complex, MOPHAL, can be omitted from this comparison because of intraligand contacts (*vide infra*) which will affect the angle  $\beta$ . In fact, MOPHAL shows the greatest asymmetry in metal-allyl bonding, having a  $\beta$  angle of  $86.72^\circ$ .

As is commonly found in allyl complexes<sup>106-107</sup>, C(2) is generally the allyl carbon closest to the metal, an exception being PHALPD where it is equidistant with C(3). In all complexes C(2) is tilted away from the metal. This has been defined by the angle  $\tau^{106}$ , the angle between the M-O and O-C(2) vectors, F. If the metal was normal to the  $C_3$  plane the value of  $\tau$  would be  $90^\circ$ . In the complexes studied here  $\tau$  ranges from  $101.9^\circ$  (MOPHAL) to  $117.6^\circ$  (PHALPD) which fits well within the previously reported range of  $97.1^\circ - 132.2^\circ$ <sup>106</sup> for  $\eta^3-C_3H_5$  complexes. With such a wide

range of values being observed for this parameter its usefulness for describing the bonding of the allyl must be questioned. An alternative parameter,  $\delta_1$ , has been defined by Muetterties *et al.*<sup>107</sup>, being the angle between the  $C_3$  plane and the coordination plane of the complex in which the allyl lies, G.

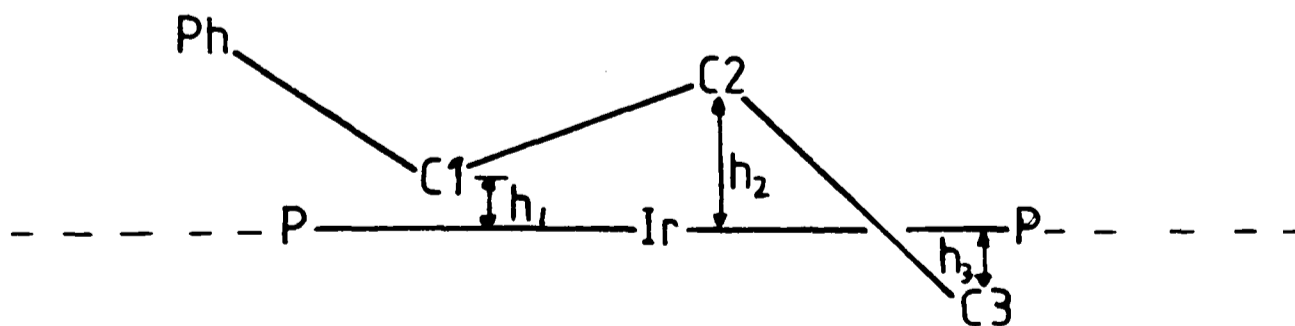


However, this plane can only be accurately defined for complexes of either square planar or octahedral geometry. For  $d^8$  square planar complexes the range reported for  $\delta_1$  is  $105.4^\circ - 126.5^\circ$ , and the value of  $120.5^\circ$  for PHALPD falls within this range. In the unsubstituted analogue,  $27^{49}$ ,  $\delta_1$  is  $114.2^\circ$ . For  $d^6$  octahedral complexes a range of  $105.5^\circ - 134.1^\circ$  is reported, although it is suggested that steric interactions between the allyl and large axial ligands have artificially increased this range. The value for IRPHAL ( $105.3^\circ$ ) slightly extends the lower limit and may reflect the relatively small size of the axial ligands in this complex (H and Cl).

In CPPHAL the coordination plane could be considered as being perpendicular to the  $C_5$  ring, passing through the

palladium. This would result in a value of  $111.3^\circ$  ( averaged over the two, disordered  $C_5$  rings ), well within the range for  $d^8$  complexes.

Also defineable with respect to the coordination plane are  $h_1$ ,  $h_2$  and  $h_3$ , the perpendicular displacements of the allyl carbon atoms. In symmetric allyl complexes, such as 27,  $h_1 \approx h_3$  (  $0.1401\text{\AA}$  and  $0.1502\text{\AA}$  respectively ),  $h_2$  (  $-0.4435\text{\AA}$  in 27 ) is larger and negative, indicating a displacement to the opposite side of the plane. In PHALPD there appears to be a rotation about the allyl-metal vector, as indicated by the non-equivalence of  $h_1$  and  $h_3$  (  $-0.2523\text{\AA}$  and  $-0.3342\text{\AA}$  respectively ). Furthermore, the magnitude of  $h_2$  is less than that of  $h_1$ , indicating that the centre of gravity of the allyl must lie above the  $ML_2$  plane. Thus the rotation is such that the C(1)-C(2) bond is brought towards a position where it would be parallel to the  $ML_2$  plane. In IRPHAL the situation is even more exaggerated. Both  $h_1$  and  $h_2$  are positive whilst  $h_3$  remains negative. This is depicted in H.



H

Again the rotation is such that C(1)-C(2) is nearly parallel

to the  $ML_2$  plane.

Examination of the allylic C-C bond distances in both PHALPD and IRPHAL indicates a greater alkene character in C(2)-C(3), since in both complexes this is significantly shorter than C(1)-C(2). This localisation of the double bond character and the rotation about the metal-allyl vector supports the  $\sigma$ - $\pi$  bonding mode of the allyl. In square planar alkene complexes, such as  $26^{88}$ , the C=C vector is perpendicular to the coordination plane of the metal. In these allyl complexes, the C-C bond with the greater double bond character ( C(2)-C(3) ), A, clearly is moving towards the position perpendicular to the  $ML_2$  plane. The displacement is, however, restricted by C(1) which also needs to remain coordinated.

The observed allylic angle C(1)-C(2)-C(3),  $\alpha$ , is not significantly different from the ideal value of  $120^\circ$  for an  $sp^2$  type carbon atom in either PHALPD or IRPHAL. However, in the case of CPPHAL and MOPHAL the values of  $\alpha$  are experimentally equivalent (  $116.49(23)^\circ$  and  $116.2(4)^\circ$  ) and are considerably different to those in the four- and six-coordinate complexes. Examination of the allylic C-C bond lengths reveals that that there is no localisation of the double bond character ( in both CPPHAL and MOPHAL C(1)-C(2) = C(2)-C(3) ) and this delocalisation may be affecting the value of  $\alpha$ .

Ibers *et al.*<sup>106</sup> have found an approximate correlation between the metal-O distance,  $D'$ , and  $\alpha$  ( for an

unsubstituted allyl ligand ) dependant on the electron configuration of the metal. Only the  $d^6$  complex, IRPHAL, fits this correlation, all other complexes having allyl angles considerably smaller than expected for the distance  $D'$ , although it is reasonable to expect the angle to be reduced by the steric effect of the substituent.

The 1-phenylallyl ligand is not planar in any example studied. The dihedral angle,  $\theta$ , between the allyl and the phenyl planes ranges from  $8.5^\circ$  ( MOPHAL ) to  $52.6^\circ$  ( IRPHAL ). Certainly in the case of the former there are interligand effects which constrain the conformation ( *vide supra* ) and this may also apply in IRPHAL although the authors make no mention of any. The values of  $27.3^\circ$  and  $33.1^\circ$  for PHALPD and CPPHAL would seem more reasonable. The twist is a result of the short, repulsive, nonbonding interaction between HR(6) and H(21), which in an idealised planar structure would be  $\approx 1.7\text{\AA}$ . The twisting relieves this considerably ( to  $2.25\text{\AA}$  in PHALPD and CPPHAL ), although in the case of MOPHAL, where the ligand is not so twisted, slight elongation of the contact to  $2.17(7)\text{\AA}$  is achieved by a widening of the C(2)-C(1)-CR(1) angle to  $125.6(4)^\circ$ . A similar widening, to  $123^\circ$ , is observed in PHALPD and CPPHAL. Only in IRPHAL, where the H...H contact is  $2.53(9)\text{\AA}$ , due to the large twist, is a near-normal  $sp^2$ -type angle of  $120.6(6)^\circ$  observed.

The twist also results in a loss of conjugation between the  $\pi$ -systems of the phenyl ring and the allyl. This is reflected in the C(1)-CR(1) bond which has an average value

of 1.475Å, considerably longer than would be expected if the systems were conjugated.

The allyl hydrogens do not lie in the allylic  $C_3$  plane. Although the positions of hydrogen atoms, as determined by the x-ray diffraction method, are notoriously inaccurate<sup>108</sup>, more faith can be put in the angular deviations from the plane. In all complexes studied here the *anti* hydrogens ( H(12) and H(32) ) are bent away from the metal by an angle of between 22.6° and 32.9°. Surprisingly little variation is found in the angular deviation of H(21), which is involved in the H(21)...HR(6) non-bonded contact. It is bent towards the metal ( and also HR(6) ) by an angle of between 10.8° and 14.0°. A greater variation is found in the deviation of H(31), which, although consistently bent towards the metal, is so in the wide range of 1.3°-19.7°. Deviations similar to these have been observed for a number of other allyl complexes which have been accurately studied<sup>96,109-113</sup>. The reason may be traced to rehybridisation of the allyl orbitals upon complex formation<sup>114</sup> ( see Chapter 4 ).



### 3.6 The $\eta^3$ -1-ethoxycarbonylallyl ligand:-

In the complex containing the  $\eta^3$ -1-ethoxycarbonylallyl ligand, PDETAL, the substituted carbon, C(1), appears to be closer to the metal than is C(3) ( Pd-C(1) = 2.124(4)Å, Pd-C(3) = 2.131(4)Å ) although the difference is not strictly, statistically significant. This results in a  $\beta$  angle of 90.32°. Also C(2) does not appear to be nearer the metal than the other allyl carbons ( Pd-C(2) = 2.128(4)Å ). Examples where this has been previously observed normally involve bulky substituents on C(2) which interact with the other ligands, such as [Me<sub>2</sub>Ga(N<sub>2</sub>C<sub>5</sub>H<sub>7</sub>)(O(CH<sub>2</sub>)<sub>2</sub>NH<sub>2</sub>)]Mo(CO)<sub>2</sub>( $\eta^3$ -2-Me-C<sub>3</sub>H<sub>4</sub>), 34<sup>113</sup>, ( $\eta^5$ -C<sub>9</sub>H<sub>7</sub>)Mo(CO)<sub>2</sub>( $\eta^3$ -2-Me-C<sub>3</sub>H<sub>4</sub>), 35<sup>115</sup>, and CpMo(RNC)<sub>2</sub>( $\eta^3$ -RNC.C(CH<sub>2</sub>Bu<sup>t</sup>).CNR) ( R = 2,6-Me<sub>2</sub>-C<sub>6</sub>H<sub>3</sub> ), 36<sup>116</sup>. In PDETAL this results in  $\tau$  and  $\delta_1$  angles of 117.6° and 118.3°. The value of  $\tau$  is the same as that found in PHALPD although  $\delta_1$  is somewhat different. The similarity between the values of  $\tau$  and  $\delta_1$  for PDETAL suggests that the allyl is bound more symmetrically across the metal coordination plane with the centre of gravity of the allyl very nearly in that plane. This is confirmed by the displacements  $h_1$ ,  $h_2$  and  $h_3$  ( 0.2315Å, -0.4056Å and 0.2370Å respectively ). These are similar to the values observed in the unsubstituted allyl complex, 27, and indicate that there is no rotation about the metal-allyl vector, as was found in the 1-phenylallyl complexes.

The C-C bond lengths ( 1.408(7)Å and 1.388(7)Å ) are not significantly different and are very similar to those of

other allyl complexes, although they could indicate more double bond character between C(2) and C(3) as was found in PHALPD and IRPHAL. The allyl angle,  $\alpha$  (  $117.4(4)^\circ$  ), is again smaller than expected from the value of  $D'$  (  $1.860\text{\AA}$  ) and again may be due to the substituent. The value observed in 12,  $105.7(4.3)^\circ$ , reflects the disubstitution of the allyl. However, the difference is not strictly significant owing to the very large errors in the structural determination of 12. In fact none of the corresponding molecular dimensions between PDETAL and 12 are different owing to the large errors and little can be deduced from comparison of the two structures.

As with the 1-phenylallyls and the other determinations previously discussed, the allyl hydrogens do not lie in the  $C_3$  plane. The *anti* hydrogens H(12) and H(32) are bent away from the metal, by  $31.2^\circ$  and  $16.7^\circ$  respectively and the *syn* hydrogens are bent towards the metal, by  $19.9^\circ$  ( H(21) ) and  $15.0^\circ$  ( H(31) ).

### 3.7 Interligand steric interactions:-

In the case of the 1-phenylallyl ligand the lengthening of the Pd-C(1) bond, relative to Pd-C(3), could obviously be the result of steric interaction between the phenyl ring and the other ligands. Figures 3.6-3.8 present space filling diagrams of PHALPD, CPPHAL and MOPHAL respectively.

Figure 3.6 indicates that there may be an interaction between the phenyl ring and hydrogens of the TMEDA methyl groups in PHALPD. A detailed analysis for significant contacts ( Table 3.7 ) reveals the relevant non-bonded interactions H(93)...CR(1) and H(93)...CR(6) of 2.746(6)Å and 2.937(7)Å respectively ( sum of van der Waals radii for H and aromatic carbon = 3.05Å ). However, these relatively large distances suggest the interactions, if present, are weak and may not, therefore, cause the observed asymmetry in the metal-allyl bond lengths.

This contention is further supported by the space filling diagram of CPPHAL, Figure 3.7. Here it is clear that there are NO interligand contacts, and yet the complex shows the same asymmetry in metal-allyl bond lengths as does PHALPD.

The situation is different however in MOPHAL, Figure 3.8. The diagram indicates a severe interaction between the phenyl substituent and part of the phenanthroline ligand. The two aromatic systems are nearly parallel ( interplanar angle = 17.4°, Table 3.10 ) and the centroids of the two six membered rings ( CR(1)-CR(6) and N(2), C(15), C(11), C(12), C(13)

and C(14) ) are separated by only 4.062(5)Å ( Table 3.12 ). This results in some degree of graphitic packing<sup>117</sup>. This clearly affects the twisting of the phenyl ring (  $\theta$  is only 8.5° ) and may also be affecting the Mo-C(1) bond length, resulting in the large value of  $\beta$  observed.

In PDETAL C(1) lies closer to the metal than does C(3), and this is obviously in spite of any possible steric interactions. Examination of the space filling diagram, Figure 3.9, and analysis of contacts however, reveals there are no significant interactions between the substituent and the TMEDA methyl groups, as there were in PHALPD. This presumably allows the substituted end of the allyl to approach closer to the metal, if electronically preferred.

The large angle of  $\theta$  observed for IRPHAL may be due to steric interactions between the allyl substituent and the phenyl rings of the phosphine ligands. However, no attempt has been made to analyse these and the authors make no mention of any such interactions.

Table 3.12 Significant non-bonded contacts for MOPHAL

(a) Intramolecular ( Å )

H(21)....HR(6)	2.17(7)
Cent(3)..Cent(4)	4.062(5)

(b) Intermolecular

Contact X....H	Symm	Dist (Å)	Angle A-X....H ( ° )
S....C(5)	x, 1+y, z	3.632(4)	
S....C(6)	x, 1+y, z	3.420(4)	
S....H(91)	-x, 1-y, 1-z	2.923(4)	59.2(3)
S....H(101)	1/2+x, 3/2-y, z	2.787(4)	93.7(3)
O(2)...H(131)	1/2+x, 3/2-y, z	2.520(5)	110.6(4)
O(2)...H(12)	1-x, 1-y, 2-z	2.4(5)	55.2(23)
O(2)...CR(5)	1/2-x, 1/2+y, 2-z	3.104(5)	112.2(4)
Cent(1)..Cent(2)	-x, 1-y, 1-z	3.726(5)	

Cent(1) is the centroid of N(1), C(4), C(5), C(6), C(7), C(8).

Cent(2) " " " " C(4), C(8), C(9), C(10), C(11), C(15).

Cent(3) " " " " N(2), C(15), C(11), C(12), C(13), C(14).

Cent(4) " " " " CR(1), CR(2), CR(3), CR(4), CR(5), CR(6).

Table 3.13 Significant non-bonded contacts for CPPHAL

(a) Intra-molecular ( Å )

H(21)....HR(6)	2.25(4)
----------------	---------

(b) Inter-molecular.

Contact X....H	Symm	Dist (Å)	Angle A-X....H ( ° )
CR(2)....CR(5)	x, 1+y, z	3.597(4)	
H(51')...H(71')	x, 1+y, z	2.269(8)	124.0(6)
H(41)....HR(6)	x, 1+y, z	2.259(8)	104.9(7)
H(81)....HR(3)	1-x, 1/2+y, 1/2-z	2.197(8)	142.5(7)

### 3.8 Crystal packing:-

Figures 3.10 and 3.11 show one unit cell and its contents for PHALPD and PDETAL respectively, hydrogen atoms having been omitted for clarity. Intermolecular contacts are given in Tables 3.7b and 3.8b. Both compounds exist as reasonably well separated ion-pairs. Notably there is no graphitic type packing between the phenyl rings of related cations in PHALPD and only minimal HR...CR contacts exist. In PDETAL the carbonyl oxygen participates in a short hydrogen bonding interaction with H(52) of 2.333(6)Å ( sum of van der Waals radii = 2.6Å ) with angles of 129.9(3)° ( at O(1) ) and 175.8(6)° ( at H(52) ) and there is a short repulsive H(63)...H(12) interaction of 1.87(6)Å ( sum of van der Waals radii = 2.4Å ), the interactions being to a cation across an inversion centre at 0.5, 0.5, 1.0.

In CPPHAL ( Figure 3.12 ) the molecules appear to be even more isolated and this is borne out by the intermolecular contacts ( Table 3.13b ). The only significant interactions are H...H repulsive contacts, the shortest being 2.197(8)Å between H(81) and HR(3) at 1-x, 1/2+y, 1/2-z. Again there is no graphitic packing between the phenyl rings.

The situation in MOPHAL however is quite different. The ring systems of the phenanthroline interact, as can be seen in the central region of the packing diagram ( Figure 3.13 ). The ring; N(1), C(4), C(5), C(6), C(7) and C(8) is parallel to, and within contact distance of ( centroid-centroid separation = 3.726(5)Å ) the ring; C(4), C(8), C(9), C(10), C(11) and C(15),

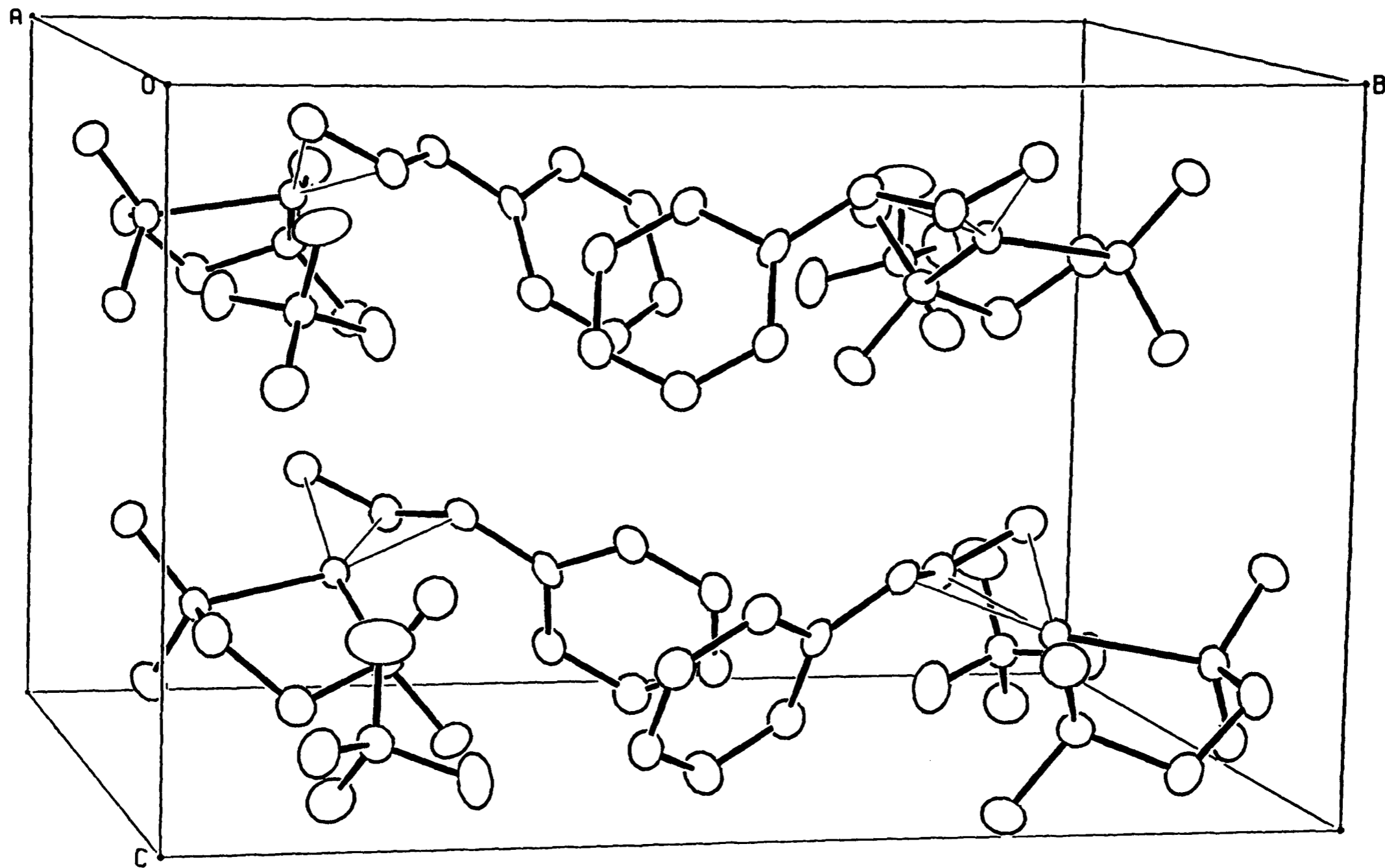


Fig. 3.10 Packing diagram of  $[(\eta^3-1-Ph-C_3H_4)PdTMEDA]BF_4$ .

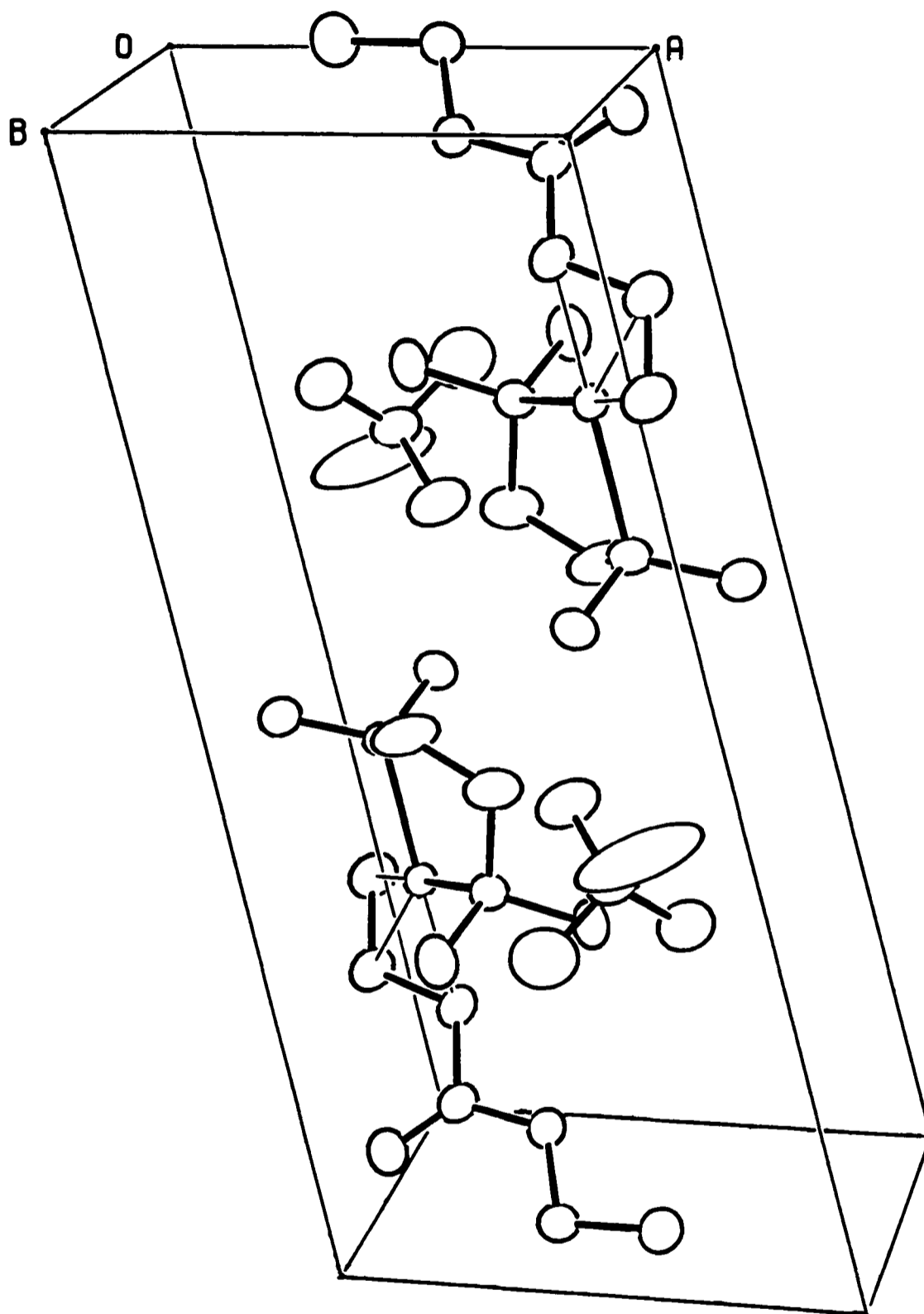


Fig. 3.11 Packing diagram of  $[(\eta^3-1\text{-EtOOC-C}_3\text{H}_4)\text{PdTMEDA}]\text{BF}_4$



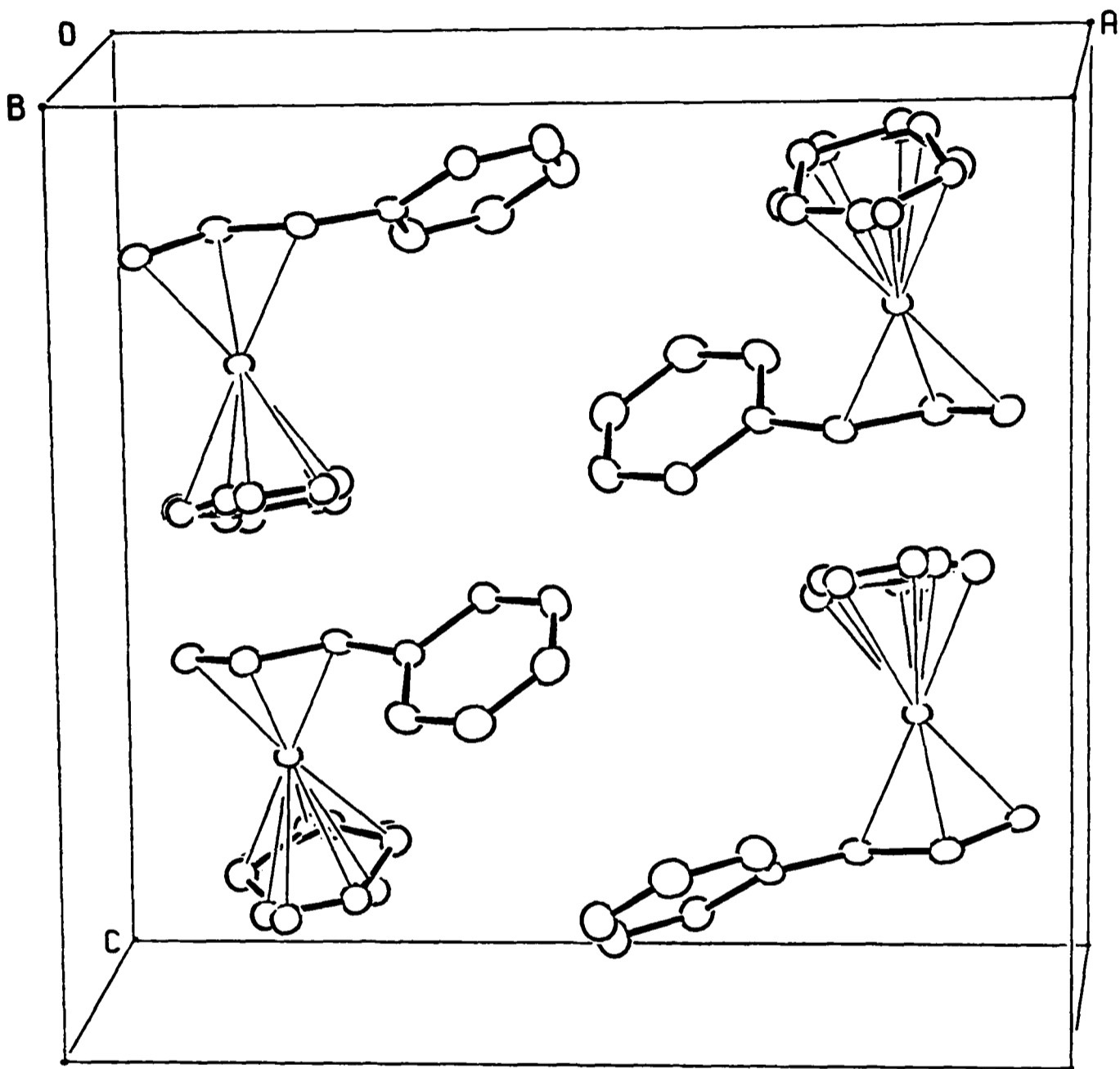


Fig. 3.12 Packing diagram of  $(\eta^3\text{-1-Ph-C}_3\text{H}_4)\text{PdCp}$ .

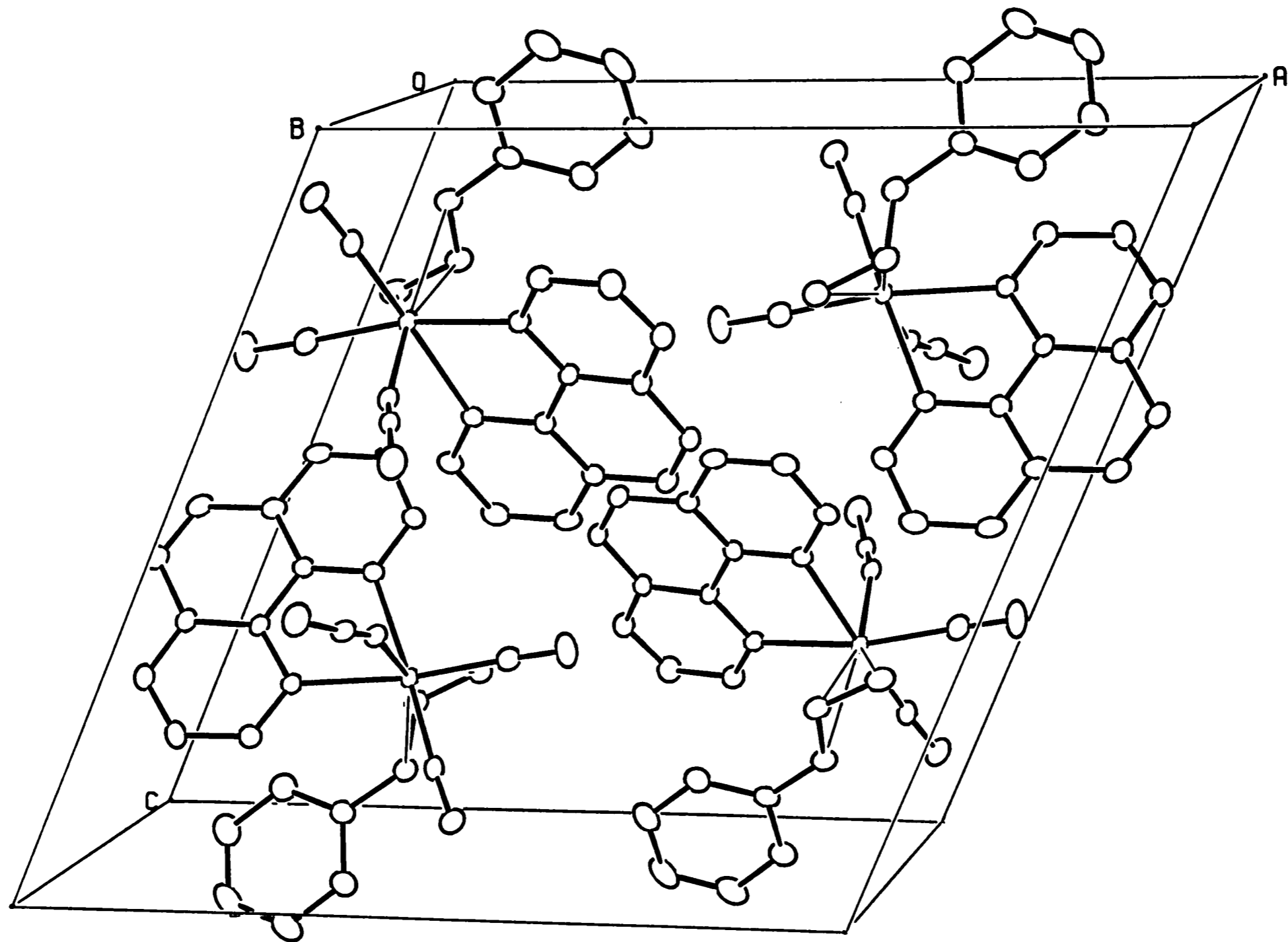


Fig. 3.13 Packing diagram of  $(\text{Phen})(\text{NCS})\text{Mo}(\text{CO})_2(\eta^3\text{-1-Ph-C}_3\text{H}_4)$ .

across an inversion centre at 0.0, 0.5, 0.5. Thus the molecules pack as head-to-tail pairs. A similar arrangement is found in (phen)MoO<sub>2</sub>(Cl)<sub>2</sub>, 37<sup>118</sup>. Other contacts, tabulated in Table 3.12b, involve the sulphur and the carbonyl oxygen O(2) but are of minor consequence.

### 3.9 Experimental:-

Standard data collection and reduction procedure: The suitable crystalline sample ( see Chapter 2 ) was transferred to an Enraf-Nonius CAD4 diffractometer, equipped with ULT-1 low temperature apparatus and using graphite-monochromated Mo-K $\alpha$  X-radiation (  $\lambda_{\alpha 1} = 0.70926\text{\AA}$ ,  $\lambda_{\alpha 2} = 0.71354\text{\AA}$  ). The crystal was optically centred and 25 relatively low angle reflections located and centred ( program SEARCH ). Their angular settings were used to generate the first unit cell and orientation matrix ( INDEX ). If this did not correspond to that known, as determined by preliminary photography, the matrix was appropriately modified ( TRANS ).

This matrix was then used to collect a shell (  $\theta_h$  ) of relatively high angle data. From these data were selected 25 strong reflections covering all of reciprocal space (employing equivalents as given by space group symmetry). These were then accurately centred ( SETANG ) to generate, upon least-squares refinement, accurate cell dimensions and orientation matrix.

The crystal was then slowly cooled to the temperature, T, required for data collection. Upon equilibration the centring of the crystal was checked optically. The 25 reflections were recentred and used to generate the final cell dimensions and the orientation matrix used in data collection.

Intensity data were collected, over the range  $\theta_d$ , in

unique segments of reciprocal space, using  $\omega$ -2 $\theta$  scans in 96 steps with the  $\omega$  scan width being set by  $A + B \cdot \tan\theta$ . After a rapid prescan, only those reflections considered sufficiently intense ( $I > C\sigma(I)$ ), were remeasured such that their final net intensity had  $I > D\sigma(I)$ , subject to a maximum measuring time  $t_{\max}$  ( s ).

Two orientation and two intensity control reflections were monitored every 200 reflections and 3600s respectively to determine any significant decay, movement of the crystal or source variance during the period of data collection,  $T_{(\text{tot})}$  ( X-ray hrs. ).

The effects of absorption ( where significant ) were reduced by means of correction factors estimated from a  $\psi$  scan of one strong reflection at  $\chi = 90^\circ$ <sup>119</sup>; Lorentz and polarisation corrections were also applied ( CADABS<sup>120</sup> ) to the  $N_c$  data collected.

Rejection of systematic absences and merging of equivalent reflections ( affording  $R_{\text{merg}}$  ) yielded  $N_d$  unique data of which  $N$  with  $F_o > E\sigma(F_o)$  were used for structure solution and refinement.

Except where stated this procedure was followed throughout this study. Crystal data and data collection parameters for PHALPD, PDETAL, CPPHAL and MOPHAL are listed in Table 3.14 and 3.15 respectively.

In the case of MOPHAL an alternative setting (  $P2_1/a$  ) of the photographically determined space group (  $P2_1/n$  ) was indexed on the CAD4 and was used for data collection,

Table 3.14 Crystal Data

	PHALPD	PDETAL	CPPHAL	MOPHAL
<b><u>M</u></b>	426.5	422.5	288.7	507.4
<b>a/A</b>	11.326(4)	7.3076(23)	14.2255(19)	15.658(4)
<b>b/A</b>	16.048(5)	8.0643(23)	5.8203(11)	9.473(3)
<b>c/A</b>	9.950(3)	15.632(4)	13.837(5)	15.666(6)
<b><math>\alpha/^\circ</math></b>	90.0	89.255(22)	90.0	90.0
<b><math>\beta/^\circ</math></b>	90.0	78.834(22)	91.287(21)	113.95(3)
<b><math>\gamma/^\circ</math></b>	90.0	76.812(20)	90.0	90.0
<b><math>V/\text{Å}^3</math></b>	1808.6	879.4	1145.4	2123.9
<b><math>D_c/\text{gcm}^{-3}</math></b>	1.566	1.595	1.674	1.587
<b>F(000)</b>	864	428	576	1024
<b><math>\mu(\text{Mo-K}\alpha)/\text{cm}^{-1}</math></b>	10.48	10.85	15.43	7.18
<b>Space Group</b>	$Pca2_1$	$P\bar{1}$	$P2_1/c$	$P2_1/a$
<b>Z</b>	4	2	4	4

**Table 3.15 Data Collection Parameters**

	<b>PHALPD</b>	<b>PDETAL</b>	<b>CPPHAL</b>	<b>MOPHAL</b>
$\theta_h$ (°)	14.0-15.0	12.0-13.0	15.0-16.0	12.0-13.0
T (K)	185	185	185	185
$\theta_d$ (°)	1.0-30.0	1.0-30.0	1.0-30.0	1.0-30.0
quad	h k l -h -k -l	h $\pm$ k $\pm$ l	h k $\pm$ l h -k $\pm$ l	h k $\pm$ l -h -k $\pm$ l
A	0.80	0.80	0.80	0.80
B	0.35	0.35	0.35	0.35
C	0.5	0.5	0.5	0.5
D	50	50	50	50
$t_{max}$	90	90	90	90
$t_{tot}$	133	133	144	200
$N_c$	5936	5502	7541	8279
$R_{merg}$	0.0633	0.0162	0.0169	0.0219
$N_d$	5206	5110	3331	3734
N	4431	4429	3064	3014
E	2	2	2	2
Abs. Corr.	No	No	Yes	No

solution and refinement of the structure.

Structure solution and refinement: The metal atom position was found by Patterson synthesis with all other heavy atoms being located from subsequent, post-refinement difference Fourier maps. All non-H atoms ( except where stated ) were allowed anisotropic thermal motion and the model was refined by full matrix least-squares. A weighting scheme of the type  $w = 1/[\sigma(F_o) + G(F_o)^2]$  was applied to the structure factors, giving no unusual variation of the root mean square deviation of a reflection of unit weight versus parity group,  $(\sin\theta)/\lambda$ ,  $F_o$ ,  $h$ ,  $k$  or  $l$ .

Allylic hydrogen atoms were located in a difference Fourier map and their positions refined. Methyl functions were treated as rigid groups with a C-H distance of 1.08Å and H-C-H angle of 109.5°, pivoting about the carbon atom position, the final X-C-H angles being checked for chemical sensibility. Methylene hydrogens were given similar geometric parameters and were constrained to lie in the plane bisecting the heavy atom angle, X-C-Y, with X/Y-C-H obtuse. Aromatic hydrogens were constrained to lie in the plane of the polyene function on the external bisector of the C-C-C angle at C-H = 1.08Å. All hydrogens were given a fixed isotropic temperature factor of  $U = 0.06\text{Å}^2$ .

Refinement of the  $N_p$  variables gave the agreement factors  $R$ ,  $R_w$  and  $S$ , with min. and max. residues (  $e\text{Å}^{-3}$  ) observed in the final  $\Delta F$  synthesis.



Solution and refinement of all structures was accomplished using the SHELX76 program package<sup>121</sup> implemented on the ICL 2972 computer at Edinburgh University. Throughout, neutral atomic scattering factors were employed<sup>122,123</sup>. Molecular geometry calculations were performed using XANADU<sup>124</sup>, CALC<sup>125</sup> and the XRAY76 program package<sup>126</sup>. Single molecule and packing diagrams were constructed using ORTEPII<sup>127</sup>, with thermal ellipsoids drawn at the 30% probability level except for H atoms which were given an artificial radius of 0.1Å for clarity. Space filling diagrams were drawn using the SCHAKAL<sup>128</sup> program.

Parameters for structure solution and final agreement factors are given in Table 3.16. Final atomic coordinates for PHALPD, PDETAL, CPPHAL and MOPHAL are given in Tables 3.17-3.20 respectively, anisotropic thermal parameters being given in Appendix 1. Lists of structure factors ( h, k, l, 10Fo, 10Fc ) are available from the author on request.

In the case of PHALPD, which crystallised in a non-centrosymmetric space group, the alternative hand of the molecule was tested for by inverting all positional parameters. Upon examination of the agreement factors no unambiguous assignment of the hand could be made.

The cyclopentadienyl ligand in CPPHAL showed a large degree of disorder. This was modeled as two independent, C<sub>5</sub> rings, employing isotropic carbon atoms. The population parameters of the five carbon atoms in each ring were constrained to be the same, although the ratio of the two

**Table 3.16 Refinement and Final Agreement Factors.**

	<b>PHALPD</b>	<b>PDETAL</b>	<b>CPPHAL</b>	<b>MOPHAL</b>
<b>G</b>	0.01097	0.0019	0.000983	0.000545
<b>N<sub>p</sub></b>	231	226	144	292
<b>R</b>	0.0311	0.0452	0.0267	0.0362
<b>R<sub>w</sub></b>	0.0554	0.0616	0.0453	0.0399
<b>S</b>	0.6114	0.9894	0.9687	0.8699
<b>min</b>	-1.25	-0.91	-0.57	-0.45
<b>max</b>	1.26	1.31	0.62	0.43

rings was allowed to refine such that the total occupancy over the ten positions was equivalent to five full carbon atoms. The final ratio obtained was 54:46.

Table 3.17 Fractional Coordinates of Atoms  
with Standard Deviations for PHALPD

	x	y	z
Pd	0.39985(2)	0.77262(1)	0.25000
C(1)	0.3467(3)	0.65017(22)	0.1792(4)
C(2)	0.2473(4)	0.70400(25)	0.1932(5)
C(3)	0.2463(4)	0.78092(25)	0.1281(5)
CR(1)	0.3612(3)	0.57353(18)	0.2578(5)
CR(2)	0.4341(4)	0.51048(25)	0.2084(4)
CR(3)	0.4476(4)	0.43501(25)	0.2771(4)
CR(4)	0.3879(4)	0.4225(3)	0.3988(5)
CR(5)	0.3183(5)	0.4854(3)	0.4487(5)
CR(6)	0.3033(4)	0.56025(25)	0.3801(4)
N(1)	0.4377(3)	0.90184(19)	0.2847(3)
N(2)	0.5682(3)	0.75170(24)	0.3413(3)
C(4)	0.5686(4)	0.9038(3)	0.3003(5)
C(5)	0.6081(4)	0.8354(3)	0.3930(6)
C(6)	0.4044(5)	0.9564(3)	0.1690(5)
C(7)	0.3774(4)	0.9340(3)	0.4051(4)
C(8)	0.6506(4)	0.7212(3)	0.2373(7)
C(9)	0.5677(4)	0.6921(3)	0.4548(5)
B	0.5136(4)	0.8227(3)	-0.1405(4)
F(1)	0.5657(4)	0.8121(3)	-0.2631(4)
F(2)	0.59570(21)	0.84708(25)	-0.0463(4)
F(3)	0.4256(3)	0.88201(17)	-0.1497(4)
F(4)	0.4646(3)	0.74759(20)	-0.1002(4)
H(12)	0.3912(20)	0.6593(20)	0.0937(22)
H(21)	0.1999(21)	0.6957(19)	0.2525(22)
H(31)	0.1972(21)	0.8229(19)	0.1613(21)
H(32)	0.2816(21)	0.7874(19)	0.0353(21)
HR(2)	0.4810	0.52014	0.1152
HR(3)	0.5036	0.38669	0.2366
HR(4)	0.3966	0.3644	0.4526
HR(5)	0.2739	0.4765	0.5437
HR(6)	0.2470	0.60814	0.4214
H(41)	0.6095	0.8953	0.2032
H(42)	0.5948	0.9632	0.3415
H(51)	0.7032	0.8361	0.3997
H(52)	0.5707	0.8458	0.4915
H(61)	0.4473	0.9343	0.0789
H(62)	0.4319	1.0196	0.1892
H(63)	0.3098	0.9547	0.1553
H(71)	0.3998	0.8958	0.4908
H(72)	0.2831	0.9324	0.3895
H(73)	0.4050	0.9974	0.4234
H(81)	0.6517	0.7642	0.1538
H(82)	0.6221	0.6606	0.2027
H(83)	0.7383	0.7163	0.2793
H(91)	0.5076	0.7139	0.5314
H(92)	0.6556	0.6874	0.4963
H(93)	0.5396	0.6317	0.4195

**Table 3.18 Fractional Coordinates of Atoms  
with Standard Deviations for PDETAL**

	x	y	z
Pd	0.12041(4)	0.16249(3)	0.76001(2)
C(1)	0.1063(7)	0.0791(5)	0.8900(3)
C(2)	-0.0598(7)	0.0624(6)	0.8611(3)
C(3)	-0.0346(8)	-0.0328(6)	0.7847(4)
C(4)	0.0899(6)	0.1998(5)	0.9635(3)
C(5)	0.2658(7)	0.3038(7)	1.0542(3)
C(6)	0.4672(10)	0.2857(16)	1.0581(6)
O(1)	-0.0562(5)	0.2956(5)	0.99905(23)
O(2)	0.2593(4)	0.1860(4)	0.98473(20)
N(1)	0.1267(5)	0.1923(5)	0.62425(22)
N(2)	0.3049(5)	0.3347(4)	0.74399(21)
C(7)	0.2158(13)	0.3399(11)	0.6010(4)
C(8)	0.3684(10)	0.3416(9)	0.6476(3)
C(9)	0.2307(9)	0.0343(9)	0.5771(4)
C(10)	-0.0643(8)	0.2412(7)	0.6009(3)
C(11)	0.4805(6)	0.2730(7)	0.7781(4)
C(12)	0.2060(7)	0.5000(5)	0.7875(4)
B	0.6629(10)	0.7441(7)	0.6744(4)
F(1)	0.5947(6)	0.6634(5)	0.61524(23)
F(2)	0.7585(8)	0.6332(6)	0.7236(3)
F(3)	0.7548(17)	0.8514(14)	0.6347(4)
F(4)	0.5153(12)	0.8403(10)	0.7300(5)
H(12)	0.234(9)	-0.023(8)	0.885(4)
H(21)	-0.211(9)	0.163(8)	0.881(4)
H(31)	-0.126(9)	-0.029(8)	0.749(4)
H(32)	0.133(9)	-0.144(8)	0.755(4)
H(51)	0.1882	0.2716	1.1158
H(52)	0.2035	0.4331	1.0394
H(61)	0.4517	0.3912	1.1028
H(62)	0.4959	0.3270	0.9918
H(63)	0.5847	0.1838	1.0684
H(71)	0.1069	0.4563	0.6172
H(72)	0.2735	0.3326	0.5318
H(81)	0.4846	0.2325	0.6257
H(82)	0.4182	0.4570	0.6332
H(91)	0.3696	-0.0311	0.5887
H(92)	0.2399	0.0566	0.5083
H(93)	0.1286	-0.0431	0.5983
H(101)	-0.1237	0.1309	0.6157
H(102)	-0.0530	0.2656	0.5322
H(103)	-0.1567	0.3505	0.6385
H(111)	0.4135	0.2640	0.8454
H(112)	0.5699	0.3638	0.7737
H(113)	0.5674	0.1497	0.7536
H(121)	0.0674	0.5437	0.7700
H(122)	0.2906	0.5932	0.7692
H(123)	0.1878	0.4830	0.8570

**Table 3.19 Fractional Coordinates of Atoms  
with Standard Deviations for CPPHAL**

	<b>x</b>	<b>y</b>	<b>z</b>
Pd	0.16303(1)	0.59064(2)	0.30294(1)
C(1)	0.22209(17)	0.4954(4)	0.16505(15)
C(2)	0.13038(20)	0.4091(4)	0.17720(19)
C(3)	0.05891(20)	0.5733(5)	0.19156(19)
CR(1)	0.30580(16)	0.3465(4)	0.16139(15)
CR(2)	0.38174(20)	0.4177(4)	0.10742(20)
CR(3)	0.46061(19)	0.2813(6)	0.09862(21)
CR(4)	0.46569(24)	0.0709(5)	0.1428(3)
CR(5)	0.39087(24)	-0.0030(5)	0.19767(22)
CR(6)	0.31151(23)	0.1350(5)	0.20730(20)
C(4)	0.1887(7)	0.8760(11)	0.4157(5)
C(5)	0.1096(4)	0.7376(14)	0.4460(4)
C(6)	0.1416(7)	0.5168(12)	0.4728(4)
C(7)	0.2377(6)	0.5064(14)	0.4531(4)
C(8)	0.2675(5)	0.7291(17)	0.4150(4)
C(4')	0.1655(5)	0.8735(9)	0.4183(4)
C(5')	0.1052(5)	0.6892(15)	0.4497(5)
C(6')	0.1640(6)	0.4998(10)	0.4748(4)
C(7')	0.2558(5)	0.5549(11)	0.4501(4)
C(8')	0.2571(4)	0.7861(13)	0.4159(4)
H(12)	0.230(3)	0.649(8)	0.130(3)
H(21)	0.120(3)	0.237(7)	0.194(3)
H(31)	-0.000(3)	0.533(7)	0.216(3)
H(32)	0.057(3)	0.756(7)	0.150(3)
HR(2)	0.37917	0.5828	0.07177
HR(3)	0.51880	0.3409	0.05652
HR(4)	0.52697	-0.0364	0.1349
HR(5)	0.39439	-0.1680	0.23327
HR(6)	0.25415	0.0766	0.25084
H(41)	0.1874	1.0562	0.3972
H(51)	0.0374	0.7950	0.4478
H(61)	0.0998	0.3807	0.5029
H(71)	0.2825	0.3585	0.4643
H(81)	0.3370	0.7727	0.3909
H(41')	0.1439	1.0463	0.4000
H(51')	0.0294	0.6946	0.4535
H(61')	0.1414	0.3409	0.5073
H(71')	0.3157	0.4415	0.4559
H(81')	0.3184	0.8781	0.3922

**Table 3.20 Fractional Coordinates of Atoms  
with Standard Deviations for MOPHAL**

	x	y	z
Mo	0.30636(2)	0.48136(3)	0.75808(2)
N	0.26740(22)	0.6759(4)	0.67882(22)
C	0.2400(3)	0.7869(5)	0.6598(3)
S	0.19823(8)	0.94502(11)	0.62706(9)
N(1)	0.19621(21)	0.3833(3)	0.62913(20)
N(2)	0.16897(20)	0.5315(3)	0.76321(20)
C(4)	0.10701(25)	0.3926(4)	0.62320(24)
C(5)	0.2101(3)	0.3107(4)	0.5630(3)
C(6)	0.1387(3)	0.2408(4)	0.4901(3)
C(7)	0.0487(3)	0.2477(4)	0.4846(3)
C(8)	0.0310(3)	0.3285(4)	0.55141(25)
C(9)	-0.0610(3)	0.3506(4)	0.5475(3)
C(10)	-0.0759(3)	0.4342(4)	0.6093(3)
C(11)	0.00098(24)	0.4985(4)	0.68492(25)
C(12)	-0.0106(3)	0.5882(4)	0.7511(3)
C(13)	0.0659(3)	0.6481(4)	0.8191(3)
C(14)	0.1546(3)	0.6157(4)	0.8236(3)
C(15)	0.09192(24)	0.4754(4)	0.69226(24)
C(1)	0.3327(3)	0.3496(4)	0.8996(3)
C(2)	0.3028(3)	0.2680(4)	0.8187(3)
C(3)	0.3654(3)	0.2546(5)	0.7762(3)
CR(1)	0.2787(3)	0.3772(4)	0.9561(3)
CR(2)	0.3242(3)	0.4442(4)	1.0431(3)
CR(3)	0.2776(4)	0.4690(4)	1.1002(3)
CR(4)	0.1856(4)	0.4299(5)	1.0723(4)
CR(5)	0.1395(4)	0.3642(5)	0.9867(3)
CR(6)	0.1861(3)	0.3373(4)	0.9298(3)
CO(1)	0.4187(3)	0.4750(5)	0.7308(3)
CO(2)	0.3943(3)	0.5867(4)	0.8635(3)
O(1)	0.48563(23)	0.4756(4)	0.7175(3)
O(2)	0.44997(19)	0.6491(3)	0.92453(20)
H(12)	0.400(4)	0.356(5)	0.934(3)
H(21)	0.239(4)	0.245(5)	0.790(3)
H(31)	0.346(4)	0.205(5)	0.723(3)
H(32)	0.428(4)	0.260(5)	0.809(4)
H(51)	0.2801	0.3056	0.5659
H(61)	0.1539	0.1822	0.4388
H(71)	-0.0073	0.1923	0.4301
H(91)	-0.1197	0.2989	0.4937
H(101)	-0.1465	0.4534	0.6020
H(121)	-0.0796	0.6093	0.7479
H(131)	0.0580	0.7198	0.8691
H(141)	0.2146	0.6617	0.8792
HR(2)	0.3962	0.4766	1.0655
HR(3)	0.3137	0.5195	1.1671
HR(4)	0.1495	0.4502	1.1169
HR(5)	0.0672	0.3339	0.9643
HR(6)	0.1497	0.2844	0.8639

## CHAPTER 4

### MOLECULAR ORBITAL STUDIES ON ALLYL COMPLEXES

#### 4.1 Preamble:-

The results of the structural analyses ( Chapter 3 ) of PHALPD, CPPHAL and MOPHAL and of the previously studied complex ( IRPHAL<sup>32</sup> ) indicate that the  $\eta^3$ -1-phenylallyl ligand is not symmetrically bound in metal complexes. The substituted carbon, C(1), is further from the metal than is C(3), ( i.e.  $\beta < 90^\circ$  ), even in the absence of any intramolecular steric interactions. Furthermore, the study of an  $\eta^3$ -1-ethoxycarbonylallyl complex, PDETAL, indicates that C(1) is nearer the metal than C(3) (  $\beta > 90^\circ$  ), against any possible intramolecular steric hinderance, although the result is not strictly significant. A change in the intraligand bonding, as a function of differing electronic properties of the substituent, has also been observed in the n.m.r. studies ( Chapter 2 ). These factors indicate that the observed asymmetric bonding may be a function of an electronic effect of the substituent.

To probe this phenomenon, semi-quantitative, approximate, EHMO calculations<sup>129</sup> have been performed on idealised models of the complexes studied crystallographically. The calculations were performed using the ICON8 program package developed by Hoffmann and co-workers<sup>130</sup>, implemented, by the author, on the Edinburgh ICL 2972 computer. The analysis is based on a fragment



molecular orbital approach<sup>131</sup>, in conjunction with symmetry arguments<sup>132</sup>.

The four-coordinate square planar complexes, PHALPD and PDETAL, have been studied, for simplicity, as their square planar  $[(\text{allyl})\text{Pd}(\text{NH}_3)_2]^+$  analogues. No simplification, apart from idealising the geometry, of the five-coordinate complex was either necessary or appropriate. The six-coordinate species, IRPHAL<sup>32</sup>, was simplified, due to computational expediency to the octahedral  $(\text{allyl})\text{Ir}(\text{PH}_3)_2(\text{H})(\text{Cl})$ . It must be remembered that neither the electronic nor steric properties of  $\text{PPh}_3$  and  $\text{PH}_3$  are identical, but the change is necessary and is standard procedure in these types of calculations. In the case of the seven-coordinate MOPHAL, the phenanthroline ligand was not simplified since this was not computationally required. The possible effects of the large  $\pi$  system, in a position where interligand interactions could occur, makes simplification anyway inappropriate.

The geometrical parameters used are given in Table 4.1 and the orbital exponents, taken from the literature<sup>14,133,134</sup>, in Table 4.2. All calculations were performed using the modified Wolfsberg-Helmholtz formula<sup>135</sup>. The interpretation is based on the frontier orbitals of the allyl anion and the cationic metal fragments.

**Table 4.1 Geometrical Parameters for Idealised Models.**

**(a) Bond Lengths ( Å ).**

C-C(allyl)	1.39
C-C(aromatic)	1.395
C-C	1.49
C-N	1.49
C-O	1.30
C=O	1.20
C=O(carbonyl)	1.15
N=C	1.20
C-F	1.35
C-S	1.60
Z-C	1.21
C-H	1.09
N-H	1.10
P-H	1.42
M-C <sub>(allyl)</sub>	2.20
M-C <sub>(carbonyl)</sub>	1.97
M-N	2.12
M-P	2.31
M-H	1.55
M-Cl	2.55

**(b) Interbond Angles ( ° ).**

C-C-C	120.0
A-B-Y(trig)	120.0
A-B-Y(tet)	109.5
L-M-L(cis)	90.0
M-N-C	180.0
N-C-S	180.0

Z = Centroid of C<sub>5</sub> ring

Table 4.2 Orbital Coefficients ( eV )

Orbital	$H_{ii}$	$\zeta_1$	$\zeta_2$	$c_1^a$	$c_2^a$	
Pd	4d	-12.02	5.983	2.613	0.5535	0.6701
	5s	-7.32	2.190			
	5p	-3.75	2.152			
Ir	5d	-12.17	5.796	2.557	0.6698	0.5860
	6s	-11.36	2.500			
	6p	-4.50	2.200			
Mo	4d	-10.50	4.540	1.900	0.6097	0.6097
	5s	-8.34	1.960			
	5p	-5.24	1.920			
Cl	3s	-30.00	2.033			
	3p	-15.00	2.033			
	3d	-9.00	2.033			
S	3s	-20.00	1.817			
	3p	-13.30	1.817			
	3d	-8.00	1.500			
P	3s	-18.60	1.600			
	3p	-14.00	1.600			
	3d	-7.00	1.400			
C	2s	-21.40	1.625			
	2p	-11.40	1.625			
N	2s	-26.00	1.950			
	2p	-13.40	1.950			
O	2s	-32.30	2.275			
	2p	-14.80	2.275			
F	2s	-40.00	2.425			
	2p	-18.10	2.425			
H	1s	-13.60	1.300			

(a) Contraction coefficients used in the double  $\zeta$  expansion.

## 4.2 Metal fragment orbitals:-

The frontier orbitals of  $ML_2$ <sup>136</sup>,  $ML_3$ <sup>137</sup>,  $ML_4$ <sup>138</sup> and  $ML_5$ <sup>14,139</sup> fragments have been analysed by Hoffmann *et al.* For completeness, representations of the orbitals together with their relative energies, for the fragments used in this study, are given in Figure 4.1. Contour plots, drawn using the PSI program package<sup>140</sup>, are given in Appendix 2 for comparison. The fragments may be derived by sequential loss of ligands from an octahedral  $ML_6$  type complex<sup>141</sup>.

In an  $ML_6$  complex the six, octahedral, metal orbitals which interact strongly with the incoming ligands are formed by hybridisation of the s, p,  $dx^2-y^2$  and  $dz^2$  orbitals. The remaining, dxy, dxz and dyz orbitals do not enter into any ligand  $\sigma$ -bonding and are referred to as the non-bonding  $t_{2g}$  set.

Removal of one ligand generates an  $MXL_2Y_2$  type fragment and leaves one metal hybrid, of  $a'$  symmetry, pointing towards the vacant coordination site. This gives a total of four non-bonding orbitals. Since in  $(phen)Mo(CO)_2(NCS)^+$  ( or other  $d^4 ML_5$  metal fragment such as  $CpMo(CO)_2^+$  ) there are only four d electrons, only two of these orbitals are occupied, which leaves the highest orbital of the  $t_{2g}$  set unoccupied. This is the antisymmetric  $a''$  orbital, also orientated towards the now vacant coordination site. See below.

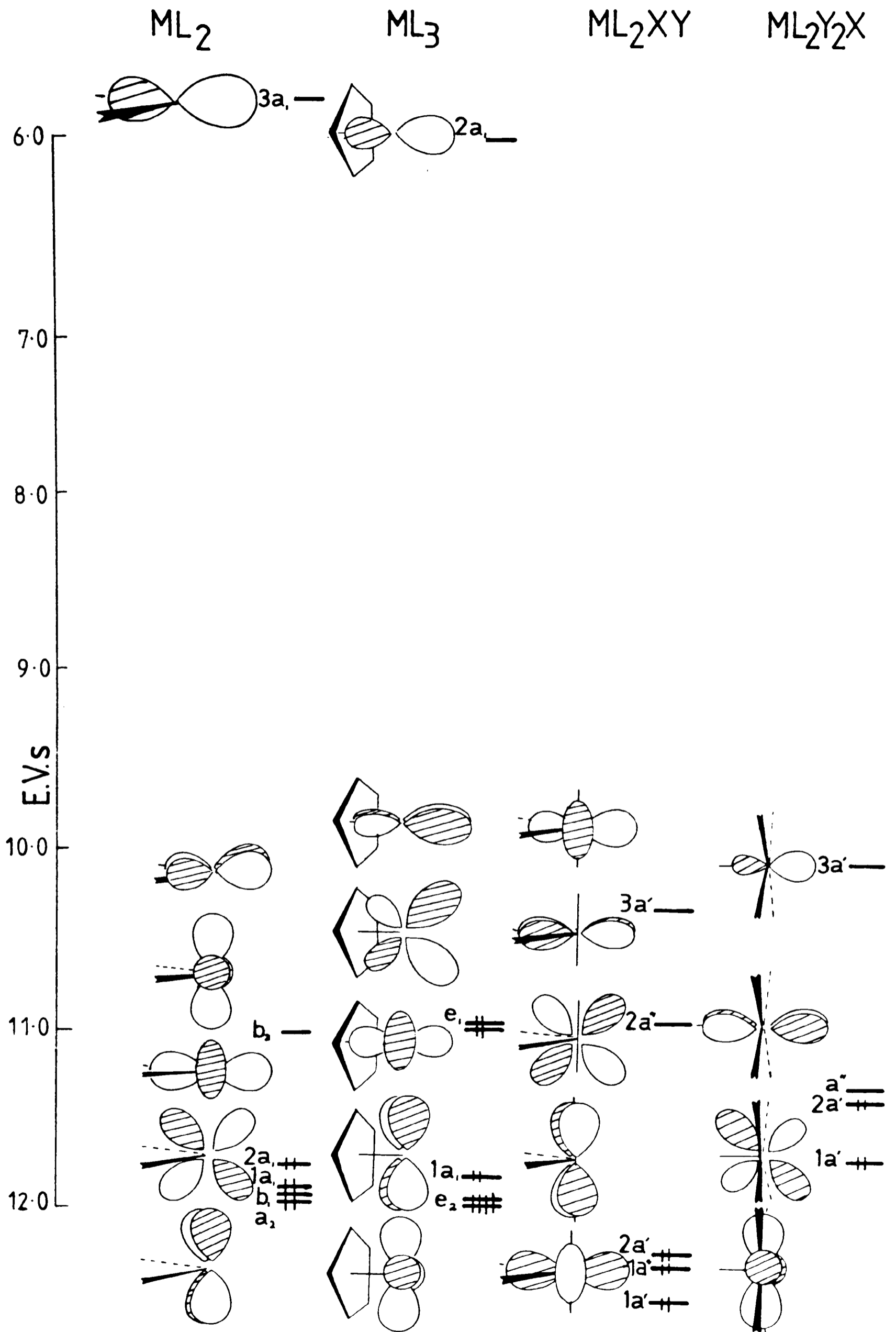
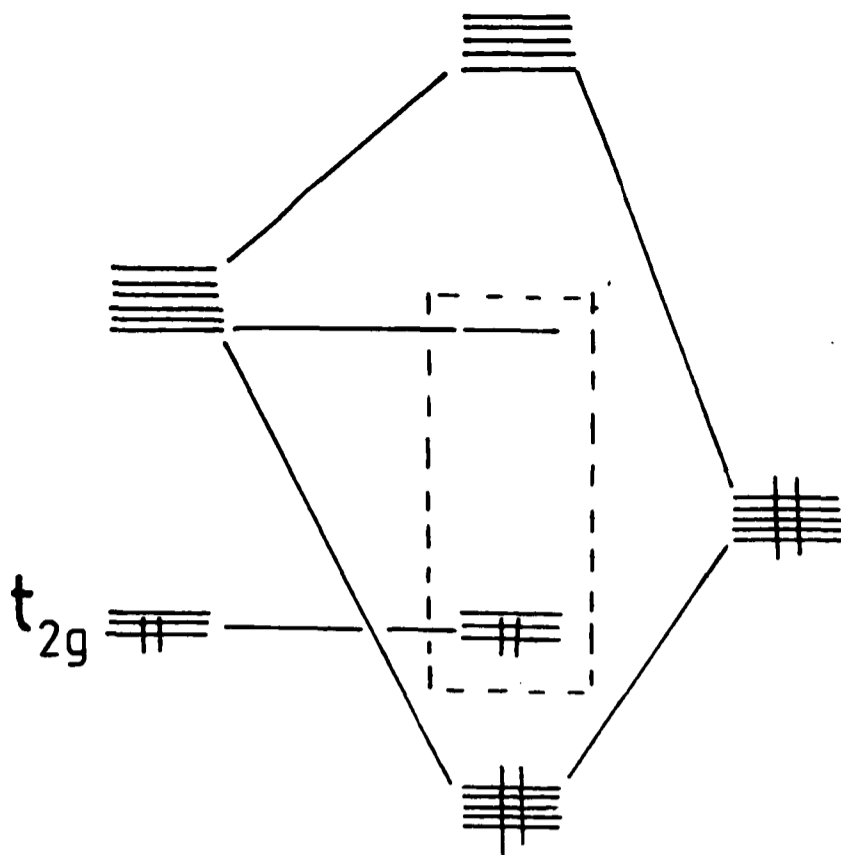


Fig. 4.1 Metal fragment frontier orbitals.

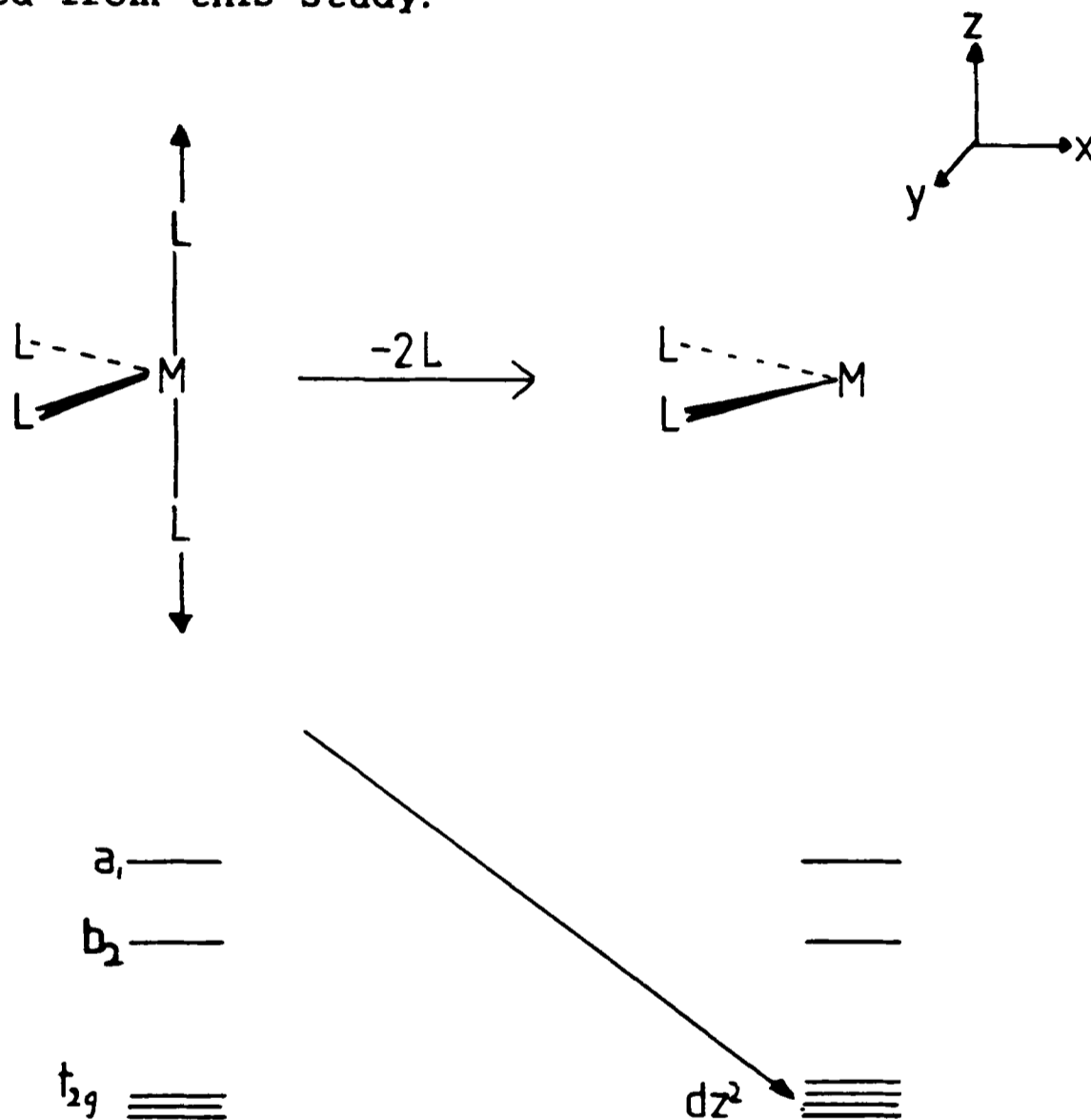


In the  $ML_2XY$  fragment two *cis* ligands have been removed which leaves two hybrids ( one of  $a'$  symmetry and the other  $a''$  ) directed towards the vacant sites, and the  $t_{2g}$  set non-bonding. In a  $d^6$  fragment, such as  $Ir(PH_3)_2(H)(Cl)^+$ , the  $t_{2g}$  set will be fully occupied leaving the  $a'$  and  $a''$  type hybrids empty.

To generate an  $ML_3$  fragment ( in this study a conical,  $C_{5v}$ ,  $PdCp^+$ ,  $d^8$  moiety), three *fac* ligands are removed. This leaves three metal hybrids plus the  $t_{2g}$  set non-bonding. The eight  $d$  electrons fill the  $t_{2g}$  set and half fill the degenerate  $e_1$  set. Thus a high lying ( due to a large amount of  $p$  character )  $a_1$  type orbital and half the  $e_1$  set, one component of which has  $a''$  symmetry, are vacant.

The  $ML_2$  fragment is generated from the  $ML_2XY$  fragment by removal of the two *trans* ligands (  $X$  and  $Y$  ). Thus if

they are said to lie along the z axis, with the generated  $ML_2$  fragment in the xy plane, the  $dz^2$  and pz orbitals will become non-bonding. The newly generated, non-bonding,  $dz^2$  orbital will be at the same energy level as the  $t_{2g}$  set, whilst the pz orbital will be much higher in energy and may be disregarded from this study.



The high lying  $a_1$  ( again with a substantial amount of p character ) and the antisymmetric orbital ( labeled  $b_2$  since the fragment is  $C_{2v}$  symmetry ) remain unoccupied, the eight electrons filling the  $t_{2g}$  set and the non-bonding  $dz^2$  orbital.

The term isolobal, coined by Hoffmann *et al.*, can be used to describe fragments if; the number, symmetry properties, approximate energy, extent in space and occupancy of the

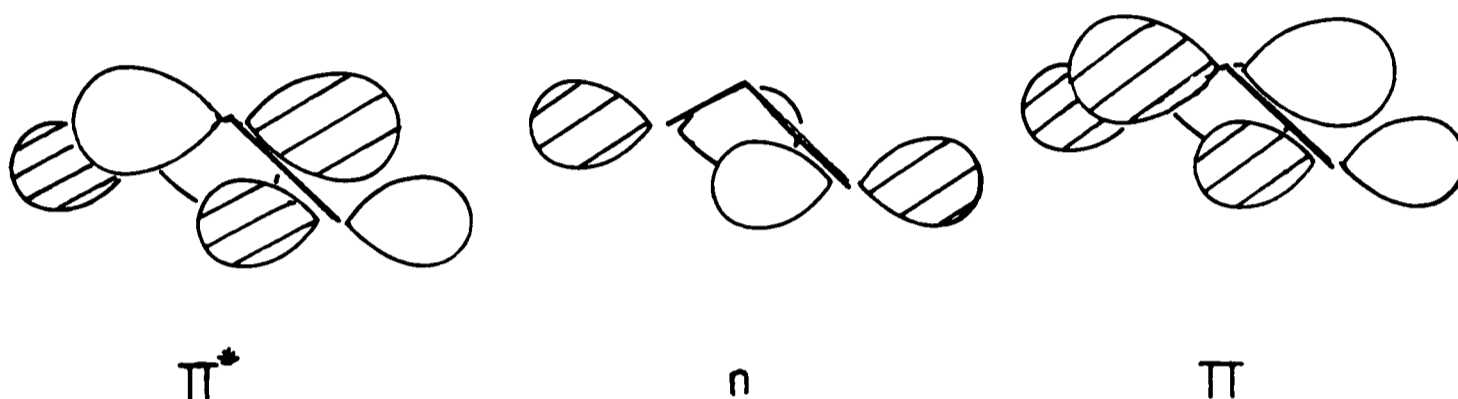
frontier orbitals are similar<sup>114</sup>. They need not be identical, only similar. This analogy has been used to relate many organic and inorganic moieties and has become a powerful tool in modern chemistry.

In that all the fragments discussed here have an vacant  $a_1$  and a potentially vacant  $a''$  orbital they may be considered as isolobal.



### 4.3 Allyl anion orbitals:-

The allyl anion ( $C_3H_5^-$ ) has four  $\pi$  electrons in three  $\pi$  orbitals. These can conveniently be labeled as the filled, bonding  $\pi$ , the unfilled, anti-bonding  $\pi^*$ , both of  $a_1$  type symmetry and intermediate in energy, the  $a''$  symmetry, filled non-bonding  $n$  orbital.



For the planar ligand these M.O.'s will be totally  $p_z$  in character. However, the non-planarity of substituents which occurs upon complexation, is well documented ( see Chapter 3 ), and results from rehybridisation at carbon, pointing the  $\pi$ -M.O.'s towards the metal centre<sup>114</sup>. To simplify the calculations and the interpretation of the results, the allyl substituents ( including hydrogen atoms ) were assumed to lie in the  $C_3$  plane. This slight simplification should not affect the arguments put forward since it is maintained throughout the study. Initially only the orbitals of  $C_3H_5^-$  will be used. Later the modifications caused by the substituents will be considered.

#### 4.4 Interaction of metal fragments with allyl<sup>-</sup>:-

In all cases the major metal-ligand interactions, as indicated by calculated overlaps, are those between;

- (1) the high, empty,  $a_1$  or  $a'$  metal orbital and the low lying, filled, allyl  $\pi$  orbital,
- (2) the empty anti-symmetric metal orbital (  $a''$ ,  $b_2$  or  $e_1$  ) and the filled allyl  $n$  orbital.

This situation is analogous to that reported by Kettle and Mason<sup>142</sup> and since the metal fragments are isolobal, will be observed in all examples studied. Owing to the poor energy match between the empty metal  $a_1$  or  $a'$  orbital and the allyl  $\pi$  orbital, their interaction is relatively small and the antisymmetric combination is found to be the more dominant. For example, in the  $ML_2$ -(allyl) case overlap populations are 0.1303 for the  $3a_1/\pi$  combination and 0.2541 for the  $b_2/n$ . All other possible interactions are very weak in comparison.

Upon complexation the overall symmetry, for all species, is  $C_s$ . This not only lifts the degeneracy of the  $CpPd^+$  frontier orbitals but also allows mixing of all symmetric type fragment orbitals into  $a'$  molecular orbitals and all anti-symmetric fragment orbitals into  $a''$  M.O.'s, which further complicates the analysis.

ML<sub>5</sub>-(allyl):- This is the simplest case and can be understood with reference to the interaction diagram, Figure 4.2.

The primary interaction is between metal a" and allyl n, a two electron, two orbital, stabilising combination. This, as expected due to the similarity of the metal fragment frontier orbitals, is in accord with that reported by Hoffmann et al.<sup>14</sup> for CpMo(CO)<sub>2</sub>-(allyl).

The metal 1a' and 2a' orbitals interact weakly with the ligand π orbital in a six electron, three orbital destabilising manner. However, this is mitigated by allowed mixing of the empty metal 3a' and allyl π\* orbitals, stabilising the antibonding combinations.

In fact, the primary a' type interaction, between 3a' and π is weak compared to the other systems due to conjugation of the metal orbital with the phenanthroline and carbonyl π-systems.

ML<sub>4</sub>-(allyl):- As can be seen from the interaction diagram, Figure 4.3, this situation is more complex.

Again the primary interaction is between the metal a" orbitals and the allyl non-bonding, n, orbital. There are now two metal a" orbitals which mix in the complex, this leading to the three orbital, four electron stabilising interaction shown below.

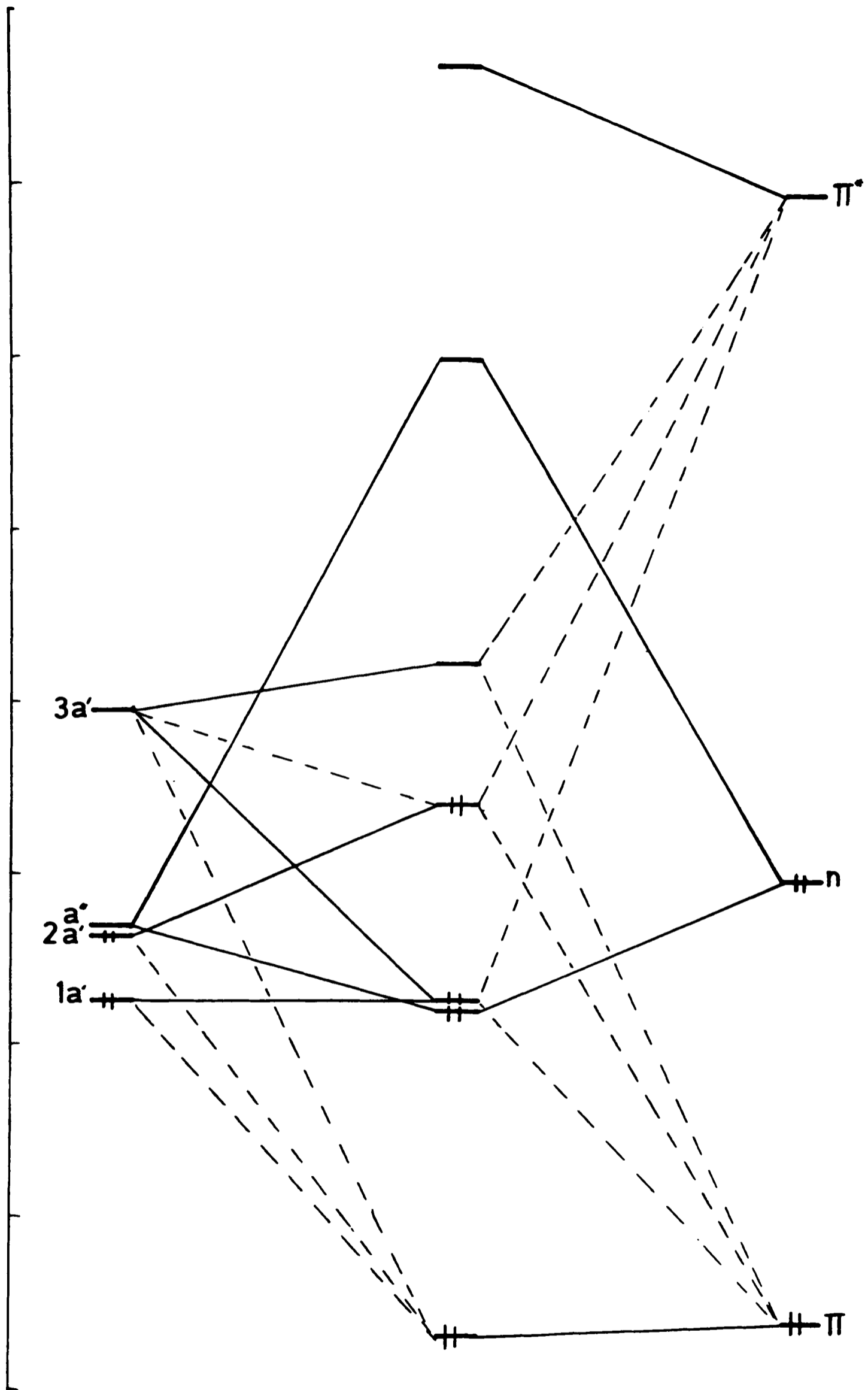


Fig. 4.2 (Phen)(NCS)Mo(CO)<sub>2</sub>-(allyl) interaction diagram

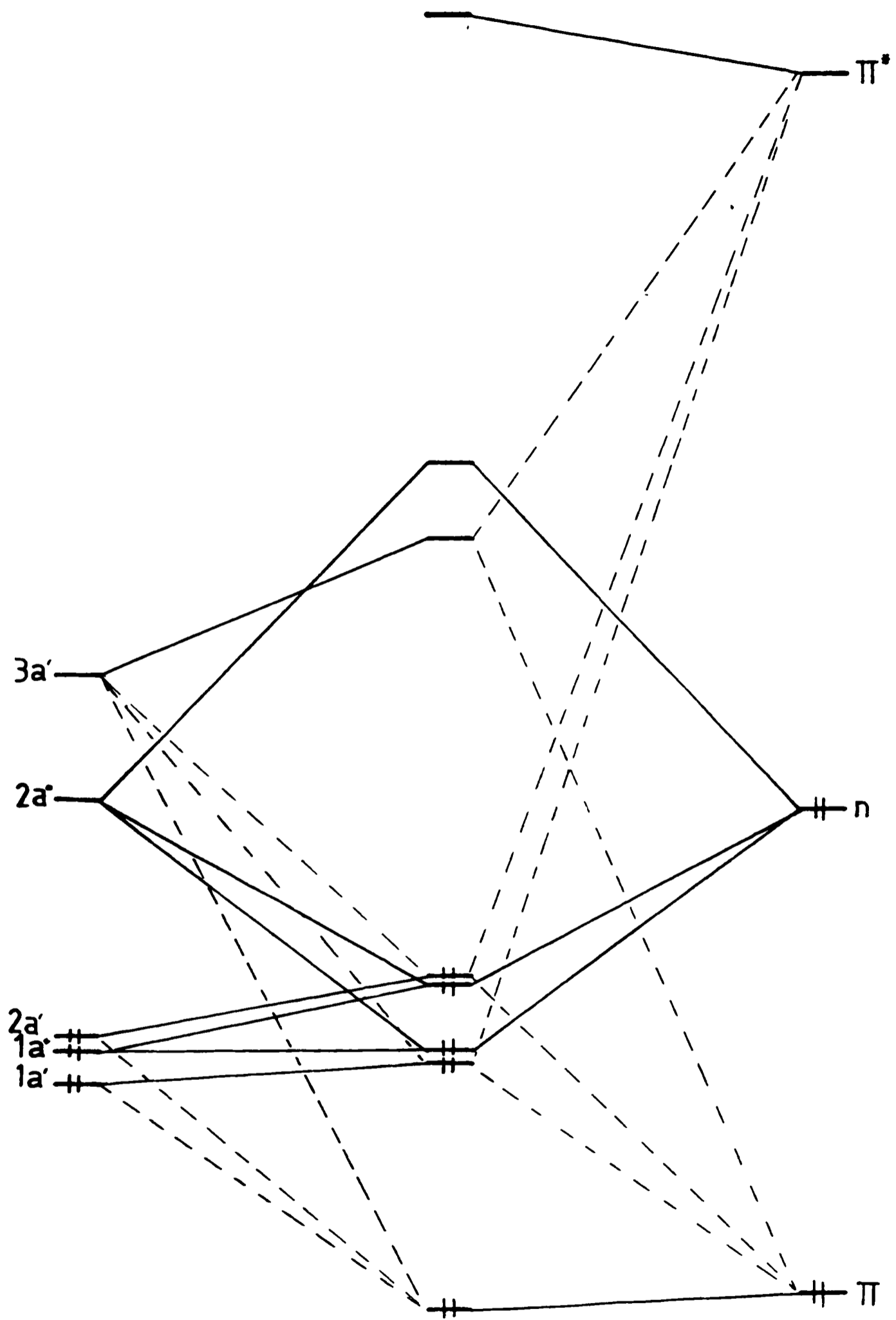
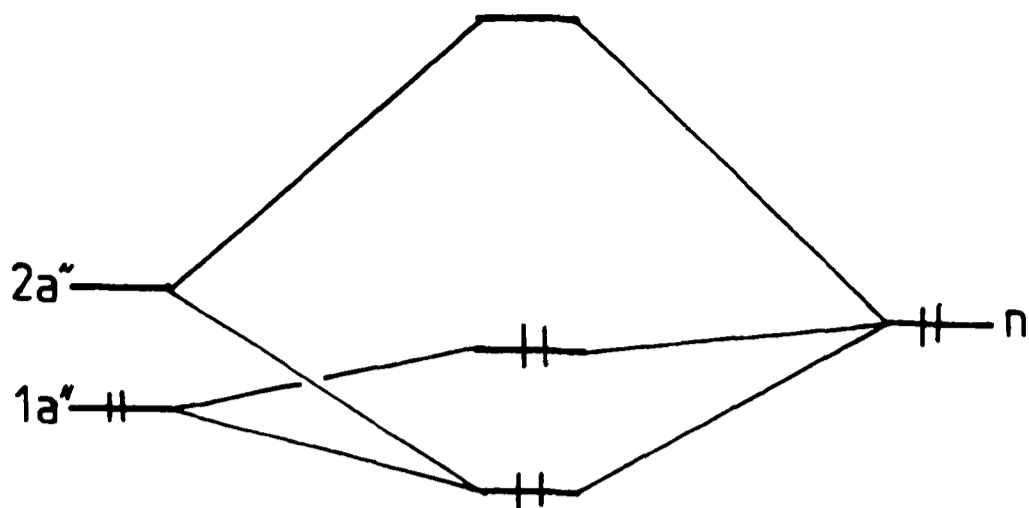
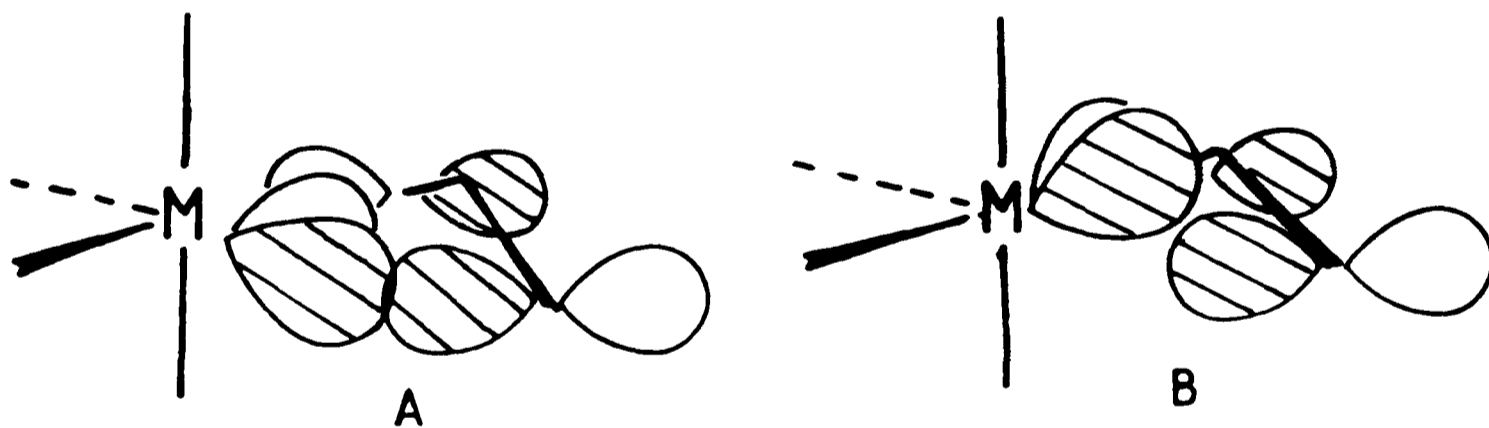


Fig. 4.3  $\text{Ir}(\text{PH}_3)_2(\text{H})(\text{Cl})\text{-(allyl)}$  interaction diagram.



The effect of mixing the  $1a''$  with the  $2a''$  is to reorientate the metal hybrid orbitals thus formed; one component towards the allyl orbital, which is concentrated on the terminal carbons, **A**, and the other away from it, **B**. The former will obviously interact more strongly with the allyl and will be the more stable of the two bonding M.O.s.



The  $a'$  interactions are almost identical to those in previous example. The weak six electron destabilising combinations between the filled metal  $1a'$  and  $2a'$  with the filled allyl  $\pi$  orbital are again mitigated by mixing in of the unoccupied metal  $3a$  and allyl  $\pi^*$ . However, the primary  $a$  interaction is not, in this case, substantially reduced by

conjugation of the metal orbital with other ligands.

ML<sub>3</sub>-(allyl):- The symmetry of the metal fragment ( C<sub>5v'</sub> CpPd<sup>+</sup> ) is reduced to C<sub>s</sub> upon complexation. It is the anti-symmetric ( with respect to the mirror plane of the complex ) components of e<sub>1</sub> and e<sub>2</sub> that participate in the same three orbital four electron interaction with allyl π, as observed previously ( see Figure 4.4 ). The symmetric components and 1a<sub>1</sub> form a four orbital, eight electron destabilising interaction with allyl π, again mitigated by 2a<sub>1</sub> and π\*. The energy match of the 2a<sub>1</sub> metal orbital with the allyl π is poor and this considerably reduces the interaction but overlap calculations still indicate it is the dominant a' combination.

ML<sub>2</sub>-(allyl):- This is almost identical to the ML<sub>4</sub> case, from which the metal fragment was derived. The additional a<sub>1</sub> metal orbital mixes with the other occupied a<sub>1</sub> orbitals, as represented by the broad band in Figure 4.5. These interact weakly with the allyl π orbital in a destabilising mode, again mitigated by 3a<sub>1</sub> and π\* in common with the other systems. The major a' interaction, 3a<sub>1</sub>/π, is again relatively small due to the poor energy match.

The mixing of a<sub>2</sub> and b<sub>2</sub> gives the same type of anti-symmetric interaction as was found in ML<sub>4</sub>-(allyl) and ML<sub>3</sub>-(allyl) systems.

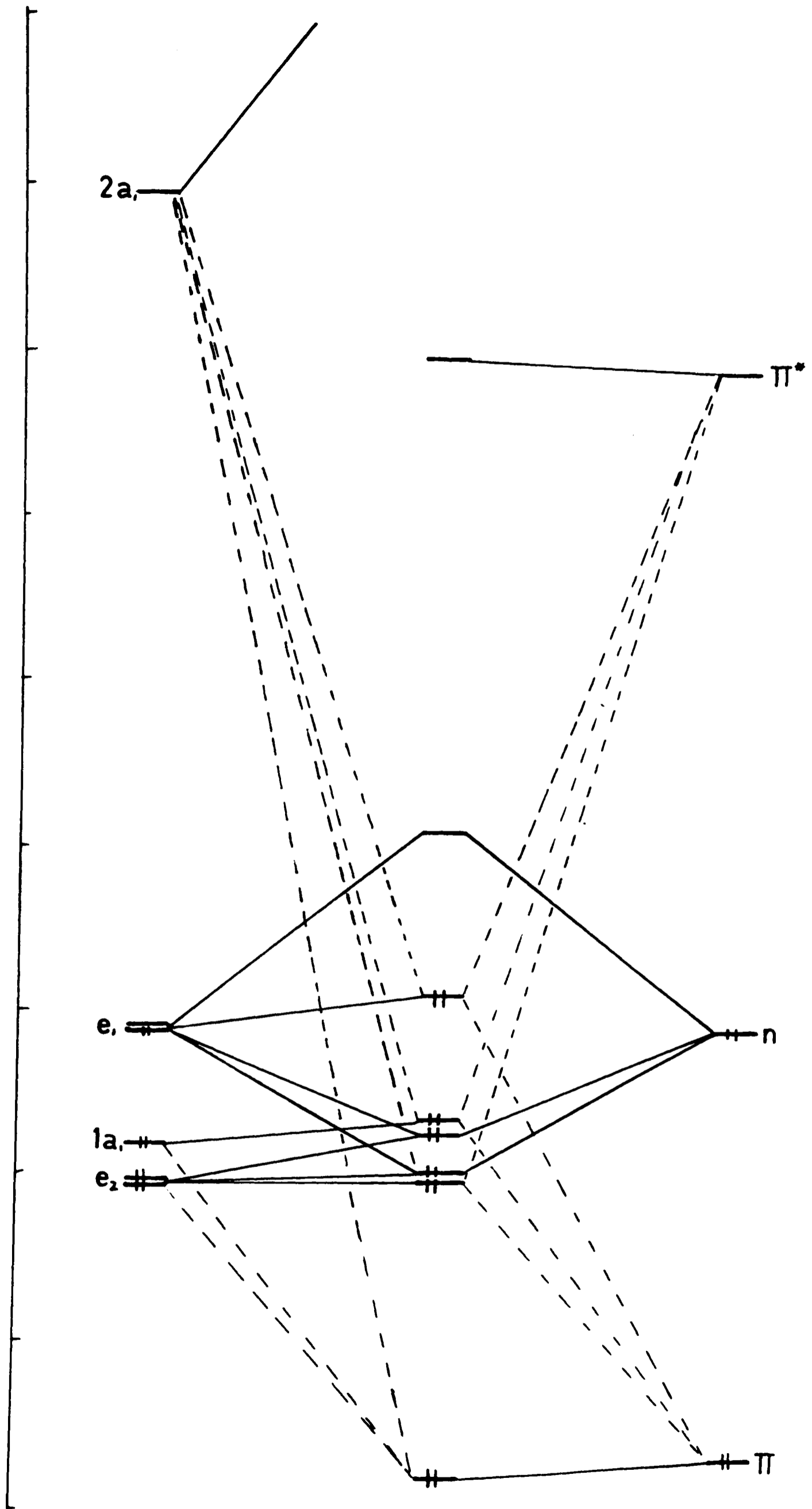


Fig. 4.4 CpPd-(allyl) interaction diagram.



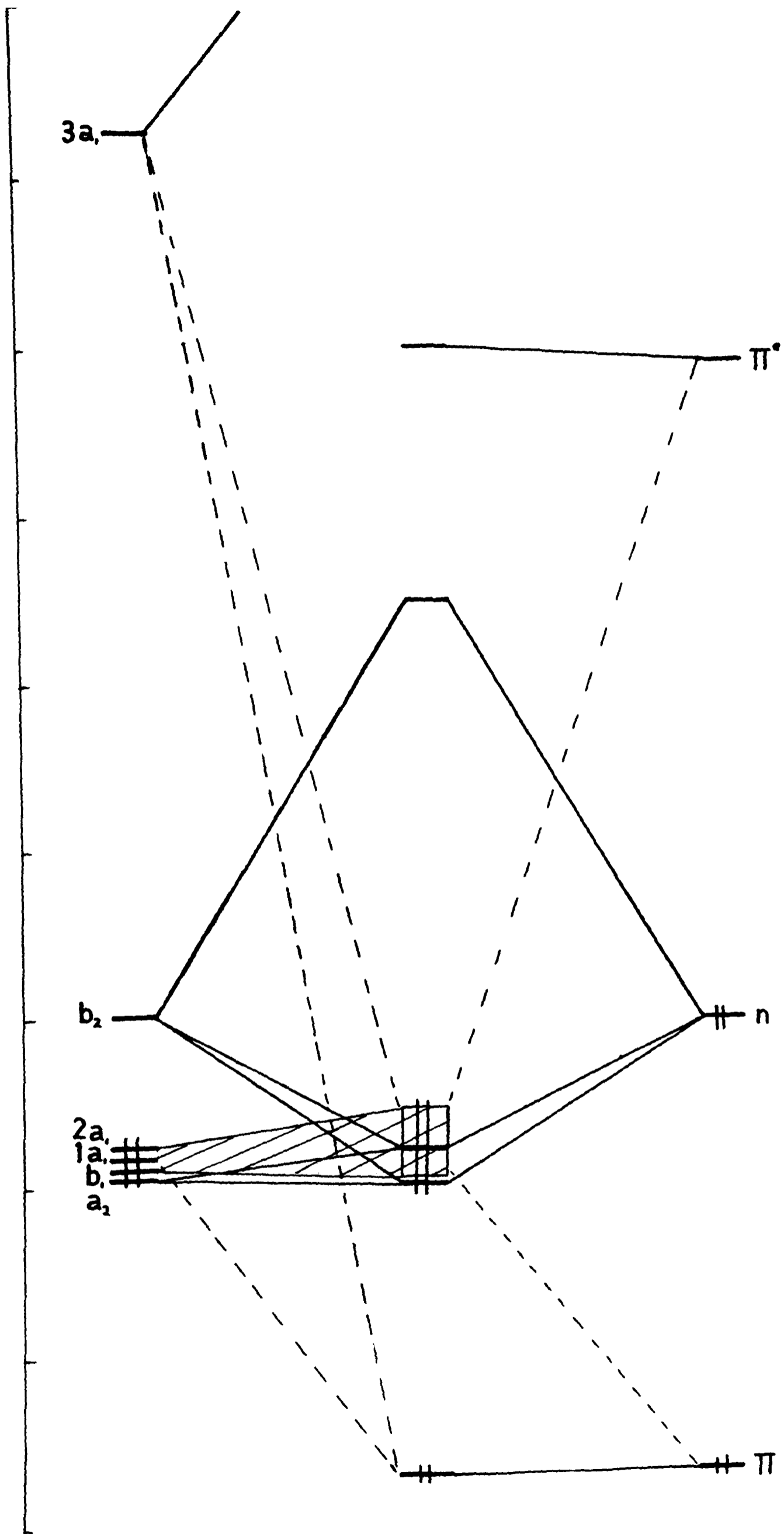


Fig. 4.5  $\text{Pd}(\text{NH}_3)_2$ -(allyl) interaction diagram

#### 4.5 Effects of substitution:-

Ph-C<sub>3</sub> twist:- In all the  $\eta^3$ -1-phenylallyl complexes studied the phenyl ring and allyl C<sub>3</sub> framework were not coplanar, the dihedral angle ( $\theta$ , positive for a counter-clockwise rotation about the CR(1)-C(1) vector), between the two planes ranging from 8.5° (MOPHAL) to 52.6° (IRPHAL)<sup>32</sup>. Certainly in the case of the former and possibly for the latter, there are interligand steric interactions which could contribute towards these extreme values (see Chapter 3). For the two complexes where interligand steric effects are minimal, viz. PHALPD and CPPHAL, the values of  $\theta$  observed are 27.3° and 33.1° respectively.

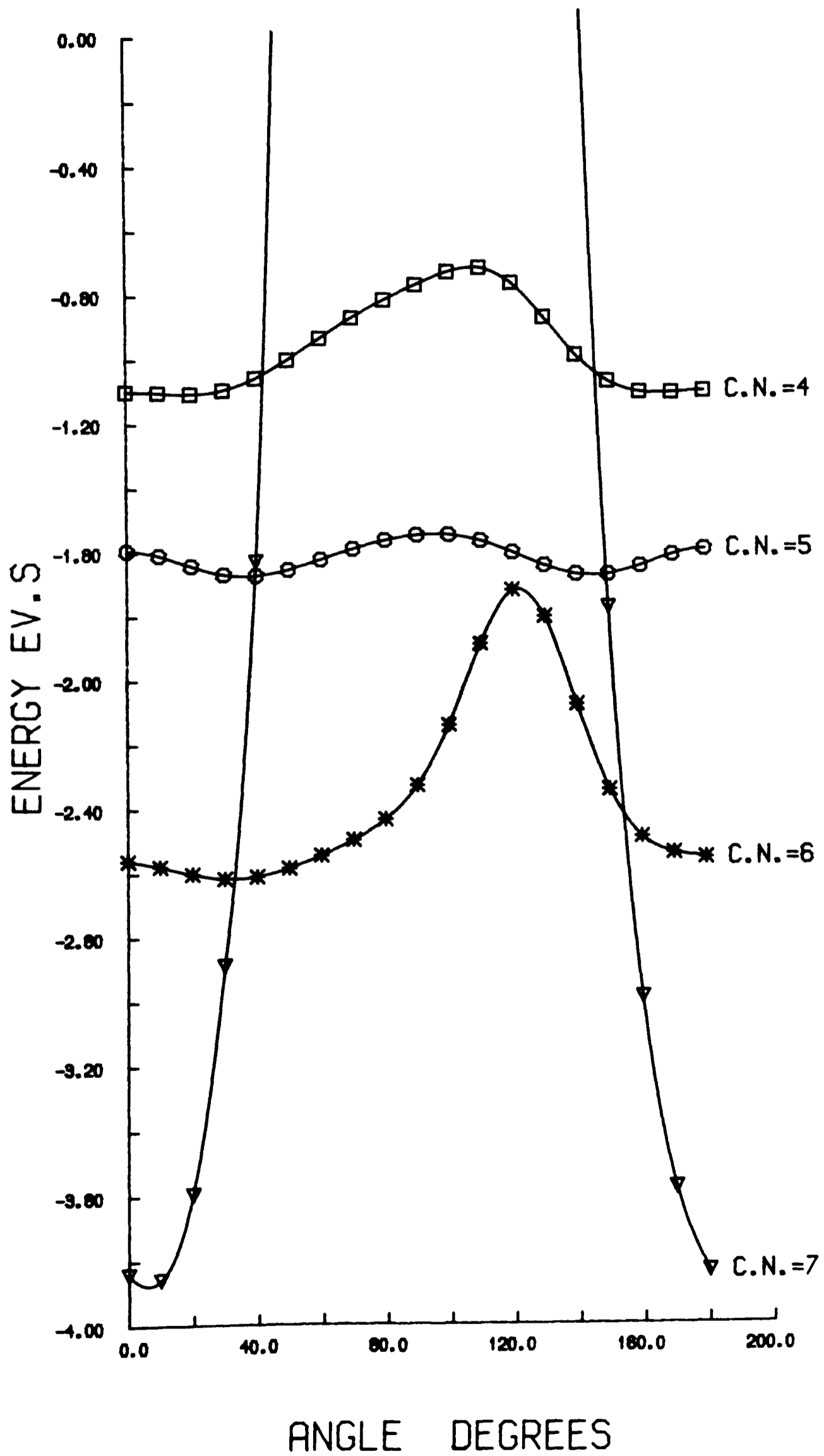
There are two obvious, competing, intraligand effects;

- (1) The requirement to reduce the repulsive H...H contact between the 2-*syn* allyl hydrogen (H(21)) and the adjacent phenyl hydrogen (HR(6)), which, in a completely planar ligand would be 1.7Å.
- (2) The stabilisation obtained by conjugation of the two  $\pi$  systems at  $\theta = 0^\circ$ .

Calculation of an energy profile for various  $\theta$  values indicates a minimum at 10° for an uncomplexed 1-Ph-C<sub>3</sub>H<sub>4</sub><sup>-</sup> ligand, and this value presumably represents the best compromise between the two factors above.

The results of similar calculations for the four-, five-, six- and seven-coordinate complexes used in this study are shown in Figure 4.6. The energy scale is not absolute,

Fig. 4.6 Graph of total energy versus  $\theta$ .



indicating only the magnitude of each profile, with each curve set to its own origin.

Immediately obvious is the very large barrier to rotation for the seven-coordinate complex, with a minimum at  $7^\circ$ . This compares very favourably with the observed value. Obviously both electronic and steric effects are playing an important role in constraining the position of the phenyl ring. The very large barrier is obviously a function of the interligand steric interactions which occur at larger values of  $\theta$ , although the exact position of the minimum is probably more a function of the electronic conjugation between the systems. This also illustrates the necessity of using the phenanthroline ligand in the idealised model instead of a simplification, where the interaction of the  $\pi$ -systems would not be modelled.

The curves for the four- and six- coordinate models show minima at  $20^\circ$  and  $32^\circ$  respectively. Both are relatively flat over a large range ( ca.  $-10^\circ < \theta < 60^\circ$  ) before a large rise in the profile. Within this range steric and crystal packing forces could be expected to have a large effect on the value of  $\theta$ . Neither model is identical to the crystallographically studied compound, although the correlation between the observed and calculated values of  $\theta$  is reasonable, particularly for the four-coordinate model.

The curve for the five-coordinate complex is very flat with a maximum barrier to rotation of  $12\text{kJmol}^{-1}$  and with two minima, of almost identical energy, at  $\pm 35^\circ$ . This

indicates the lack of interligand interactions and corresponds very well with the observed structure, where  $\theta = 33.1^\circ$ .

Obviously if it were only the two factors outlined above that were affecting the twist, all calculated and observed values of  $\theta$  should be approximately  $10^\circ$  ( barring interligand steric interactions ). Therefore it appears that metal-ligand interactions also play a part.

The nine  $\pi$  orbitals of the ligand, in two conformations,  $\theta = 0^\circ$  and  $30^\circ$ , are shown in Figure 4.7. As can be seen they are very similar, although the orbitals are more heavily localised on the phenyl ring in the twisted form, particularly the bonding  $\pi$  orbitals. This has the effect of reducing the four electron destabilising  $a'/\pi$  and the two electron, stabilising  $a'/\pi$  interactions, two competing effects. Therefore, the calculated values of  $\theta$  in the complexes must represent a compromise between all three factors outlined above, namely intraligand steric, intraligand bonding and metal-ligand bonding.

$n^3$ -1-Phenylallyl asymmetry:- The  $\pi^*$  orbitals of the allyl ligand are not significantly involved in metal-ligand bonding. Thus any asymmetry due to the substituent should be observed in changes in the  $n$  and/or  $\pi$  orbitals of the substituted ligand.

The  $n$  orbital of the 1-phenylallyl anion ( Figure 4.7 ) is effectively unaltered from that in the unsubstituted moiety, the coefficients on the two terminal allyl carbons being

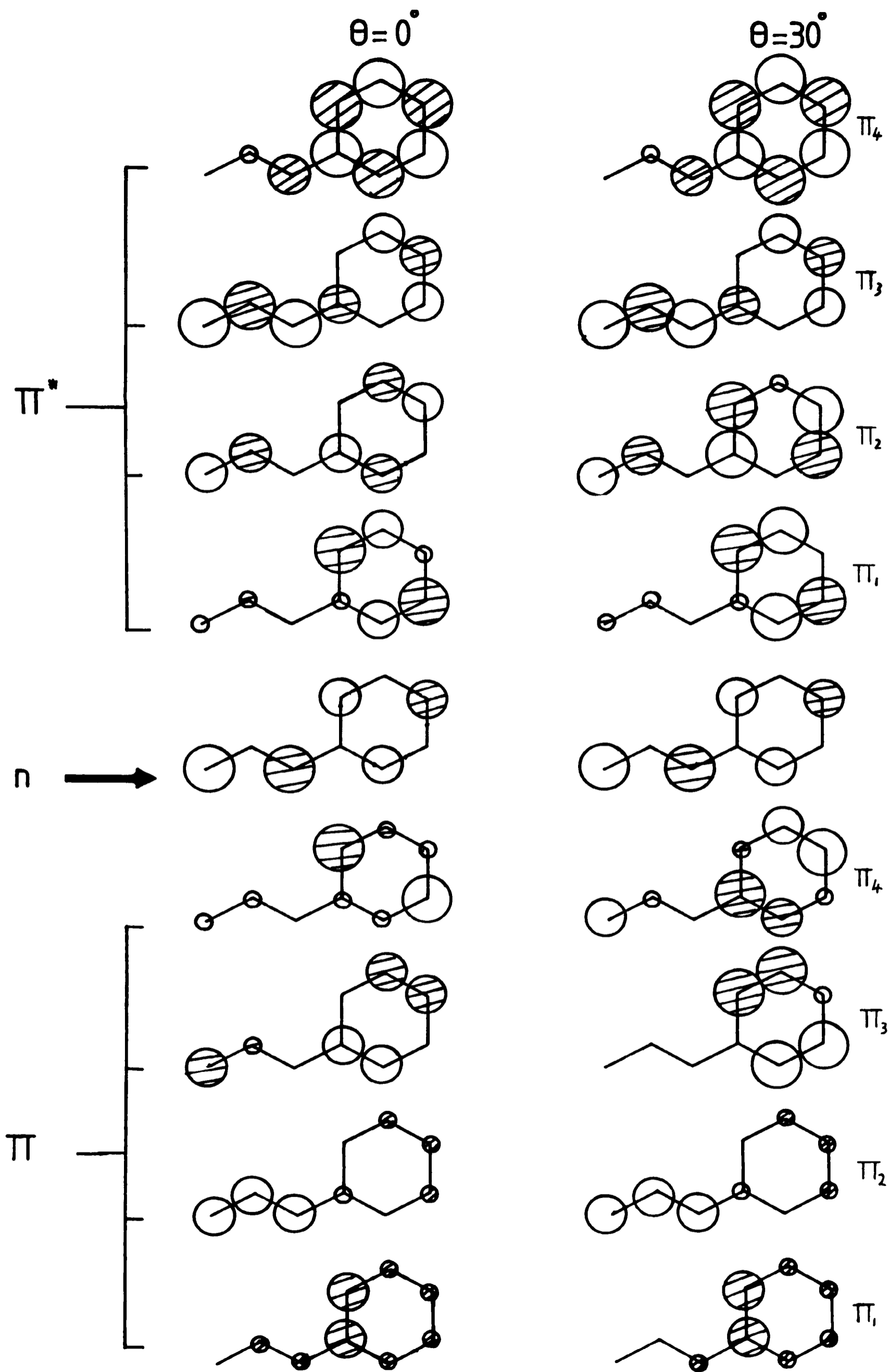


Fig. 4.7 1-Phenylallyl anion  $\pi$ -orbitals.

almost identical ( in magnitude ) and there being nodes at the central allyl and the bonding substituent carbon atom. Hence this orbital will cause no asymmetry in the bonding of a complex.

The  $\pi$  ligand orbitals are, however, altered. The highest,  $\pi_4$ , is localised between carbons C(3) and C(2), with a node near C(1) and an out of phase component on the bonding substituent carbon atom. Since this interacts with a radially symmetrical  $a'$  type orbital in a two electron bonding mode ( the four electron antibonding  $a'/\pi$  interactions are reduced to insignificant proportions by the twisting ) this will seek to maximise overlap. Thus C(3) should be more strongly bound and be closer to the metal than C(1). This is, in fact, observed in all the crystal structures. The other  $\pi$  orbitals are effectively evenly delocalised over the allyl framework and the energy match with metal orbitals is poor. Thus there is little interaction and they will have no effect on the asymmetry.

$\eta^3$ -1-Ethoxycarbonylallyl asymmetry:- In the case of the 1-ethoxycarbonyl- substituted allyl anion the  $\pi$  system, whose orbitals are shown in Figure 4.8, consists of the allyl function and the carbonyl group.

Again the  $\pi^*$  orbitals, which do not significantly contribute to allyl-metal bonding may be ignored, as may the  $\pi_1$  orbital since this is almost entirely localised on the carbonyl group.

The higher  $\pi_2$  orbital however is delocalised evenly over

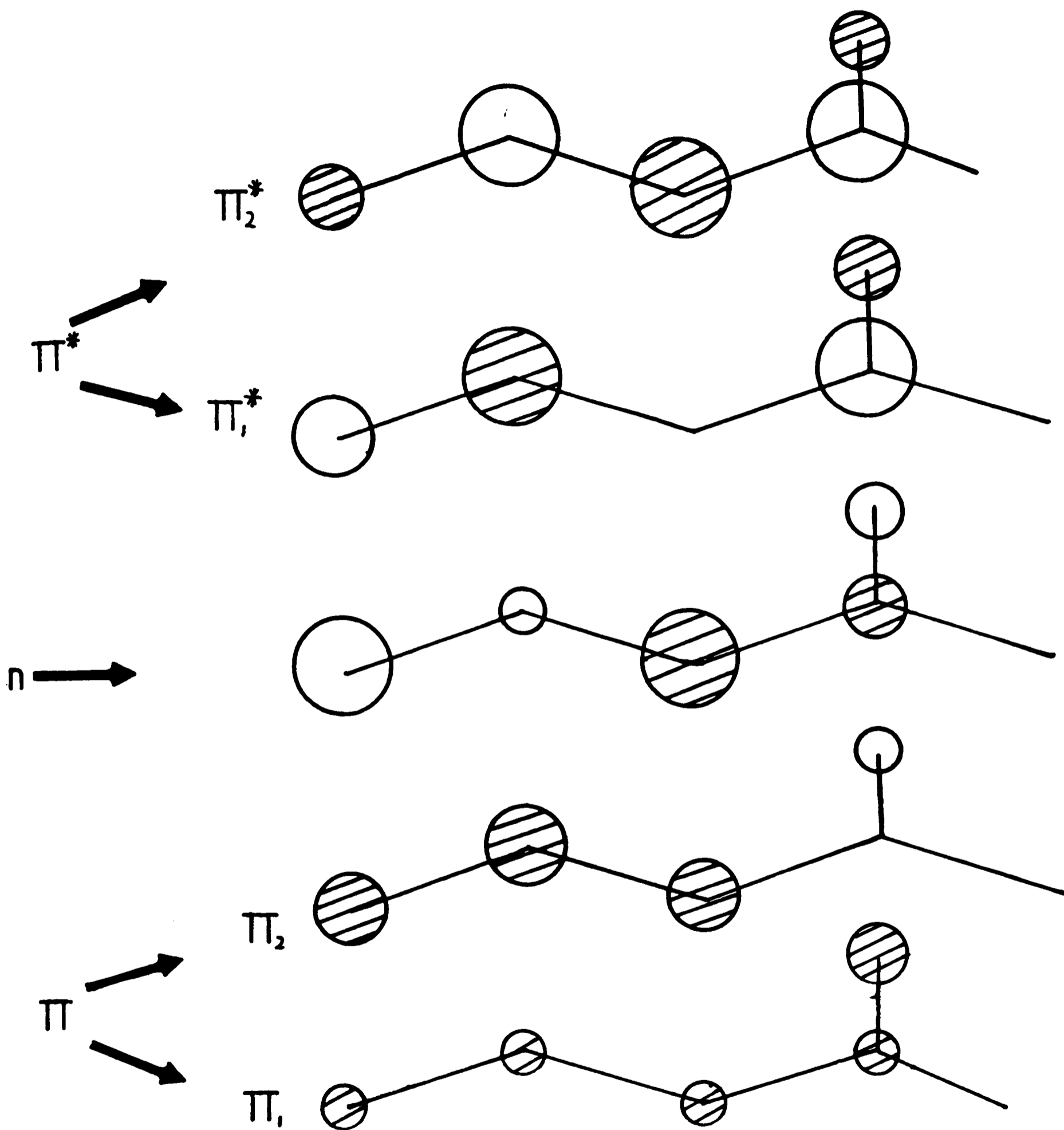
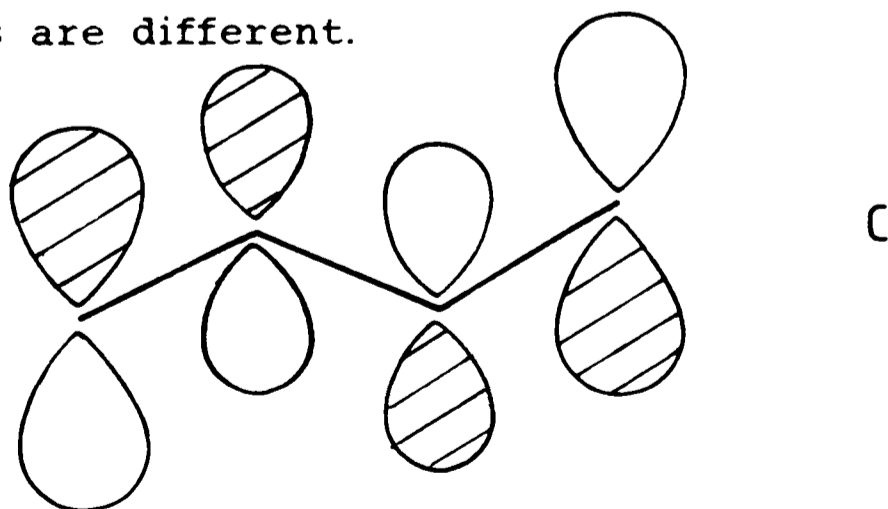


Fig. 4.8 1-Ethoxycarbonylallyl anion  $\pi$ -orbitals.



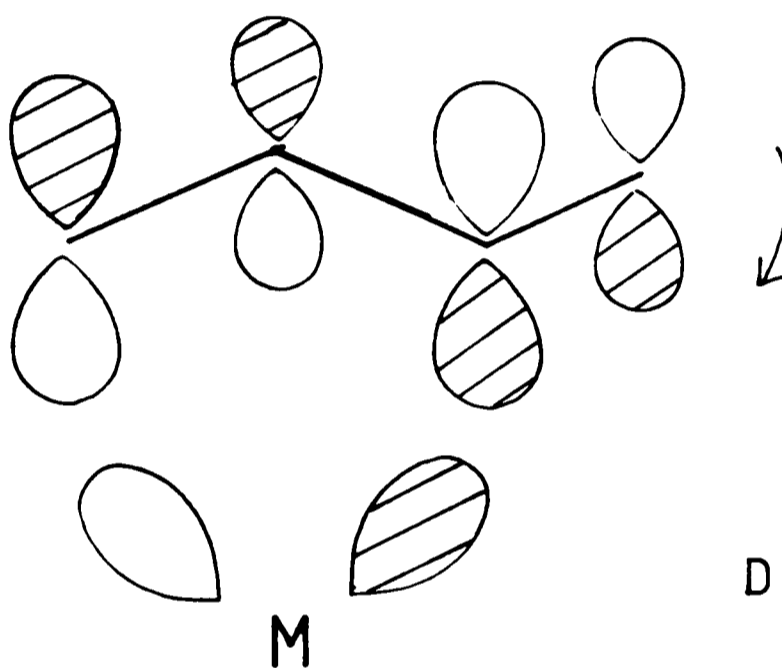
the allyl  $C_3$  framework with a small, in phase, contribution on the carbon of the carbonyl group. This results in a four atom,  $\pi$ , bonding orbital. As the major interaction of this orbital is with the empty  $a'$  metal orbital, a two electron, two orbital stabilising combination, overlap could be maximised by a slight slip of the metal towards the substituted end of the allyl. However, overlap between the radially symmetrical  $a'$  orbital and the orbital on the substituent carbon will be minimal due to the lateral separation. The interaction will not, however, oppose any distortion which brings the substituted end of the allyl closer to the metal, but is unlikely to be the driving force.

Rather, the major contribution to metal-ligand asymmetric bonding comes from the change in the non-bonding  $n$  orbital. Again the  $\pi$ -system is extended to the substituent by the in-phase  $C(1)$ - $C(\text{subs})$  combination, there is also a slight contribution on  $C(2)$  that is in-phase with  $C(3)$ . This orbital is therefore similar to the  $1a''$  orbital ( HOMO ) of butadiene,  $C$ , which also has two in-phase combinations, although the relative coefficients in the two orbitals are different.



This allyl  $n$  orbital interacts with the  $a''$  metal orbital,

which is mainly  $dxz$  in character with an angle of ca.  $90^\circ$  between the lobes. The angle subtended at the metal by the allyl function (  $C(1)-M-C(3)$  ) is in the region of  $70^\circ$ . Thus, the metal orbital will interact to a significant extent with the component of the orbital on the substituent. In order to maximise overlap for this stabilising interaction a movement of the allyl substituent towards the metal could be expected, D.



Thus, in a complex,  $C(1)$  would be expected to lie somewhat closer to the metal atom than would  $C(3)$ , and this is entirely consistent with the observed asymmetry in PDETAL.

Other substituents:- As has been shown the  $\pi$ -system of the ethoxycarbonylallyl tends towards that of butadiene. Thus if the substituent was  $^+CH_2$  ( effectively transforming the allyl into *trans* butadiene ), it would be reasonable to expect an  $\eta^4$  bonded ligand. The complexes  $CpFe(PPh_3)(\eta^3-F_2C=C(CF_3)=C(CF_3)_2)$ ,  $38^{143}$  and

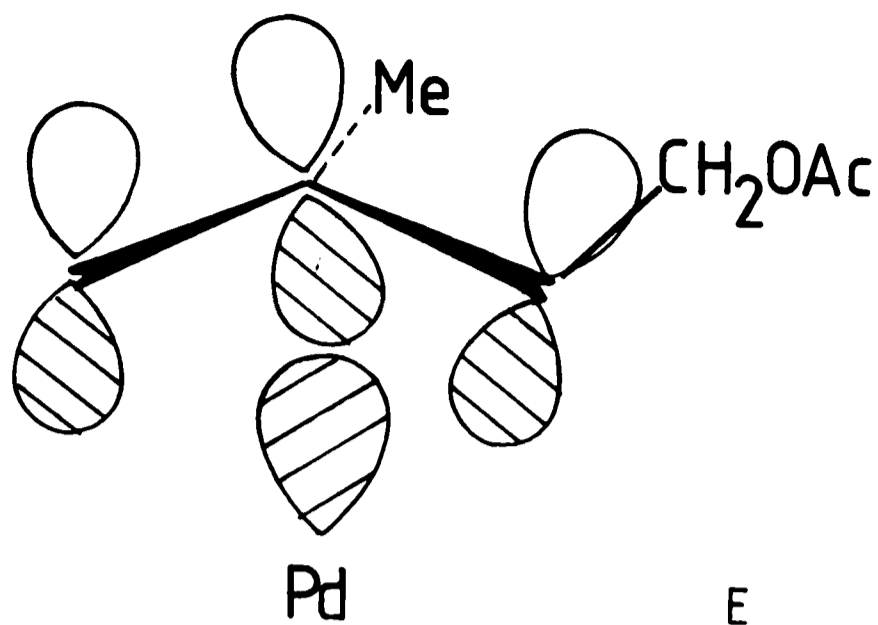
$(\text{CO})_3\text{Fe}(\eta^3\text{-}(\text{O})\text{C}=\text{C}(\text{COOMe})\text{-CH}(\text{COOMe}))$ , 39<sup>144</sup>, may be considered as approaching this situation. In both complexes the allylic carbon which forms part of the external, unsaturated function (  $\text{C}=\text{O}$  and  $\text{C}=\text{C}(\text{CF}_3)_2$  ) is significantly closer to the metal atom than the other allyl terminal carbon.

Other substituents with  $\pi$ -acceptor characteristics ( e.g.  $\text{CN}$  ) produce a similar change in the allyl  $\pi$ -system to the ethoxycarbonyl function and would be expected to bind with the substituted terminal carbon closer to the metal than the unsubstituted one.

Analysis of the  $\pi$ -orbitals of allyls substituted with a  $\pi$ -donor, such as  $\text{NH}_2$  or  $\text{F}$ , reveals that they are similar to those of the 1-phenylallyl. The highest  $\pi$  orbital is localised between  $\text{C}(2)$  and  $\text{C}(3)$ , thus bringing the unsubstituted end closer to the metal. Furthermore, with  $\text{NH}_2$  or  $\text{F}$  substituents, the non-bonding,  $n$ , orbital is anti-bonding across  $\text{C}(1)\text{-X}$ , opposing any distortion that would bring the substituted carbon closer to the metal, exactly the reverse of the situation with  $\pi$ -acceptor substituents.

The only other accurately studied example of an asymmetrically substituted allyl complex, 12, shows that the allyl binds with the substituted carbon being the nearer to the metal of the two terminal carbons. Analysis of the three  $\pi$ -orbitals for this ligand indicates only the bonding,  $\pi$ , orbital is significantly altered. On the face of the allyl to which the metal binds, this is localised between  $\text{C}(1)$  and

C(2), E.



Since this interacts with the metal  $a'$  type orbital, in a manner that seeks maximum overlap, the substituted end should bind closer than the unsubstituted end,  $\beta > 90^\circ$ , as is found.

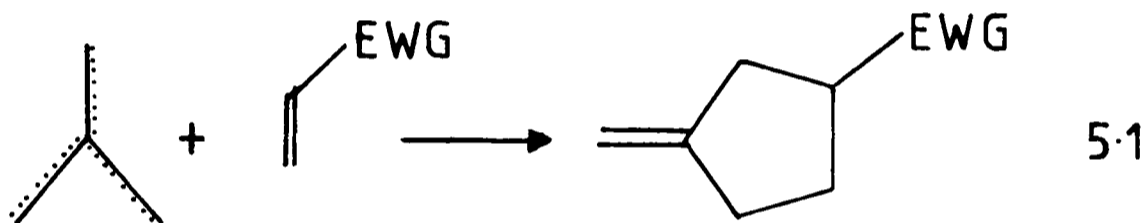
For a 1-methyl- substituted allyl, a substituent with only  $\sigma$ -donor characteristics, the  $\pi$  bonding orbital is again the only one that is significantly altered relative to the unsubstituted ligand. Analogous to the  $\pi$ -donor-substituted allyls, it is localised between C(2) and C(3) with an out of phase combination on the substituent. Thus the 1-methylallyl ligand would be expected to bind with the substituted carbon atom further from the metal,  $\beta < 90^\circ$ .

## CHAPTER 5

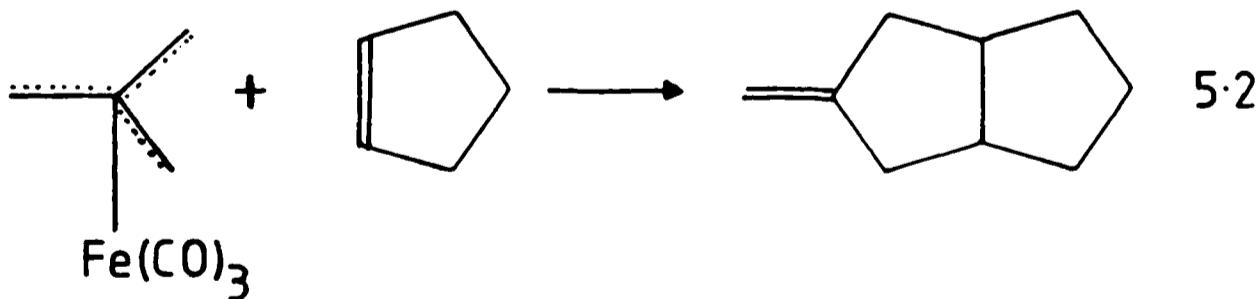
### STRUCTURAL STUDIES ON CPMOL<sub>2</sub>-(ENE) SPECIES

#### 5.1 Introduction:-

The Trimethylenemethane moiety, C(CH<sub>2</sub>)<sub>3</sub> ( TMM ), both in the form of its metastable radical and stabilised in transition metal complexes, has been involved as an intermediate in synthetic organic chemistry. Its main use is in the formation of cyclopentanoids, by cycloaddition to an alkene. This has been performed, in the absence of a metal substrate, by *in situ*. generation of the radical<sup>145</sup>, equation 5.1.



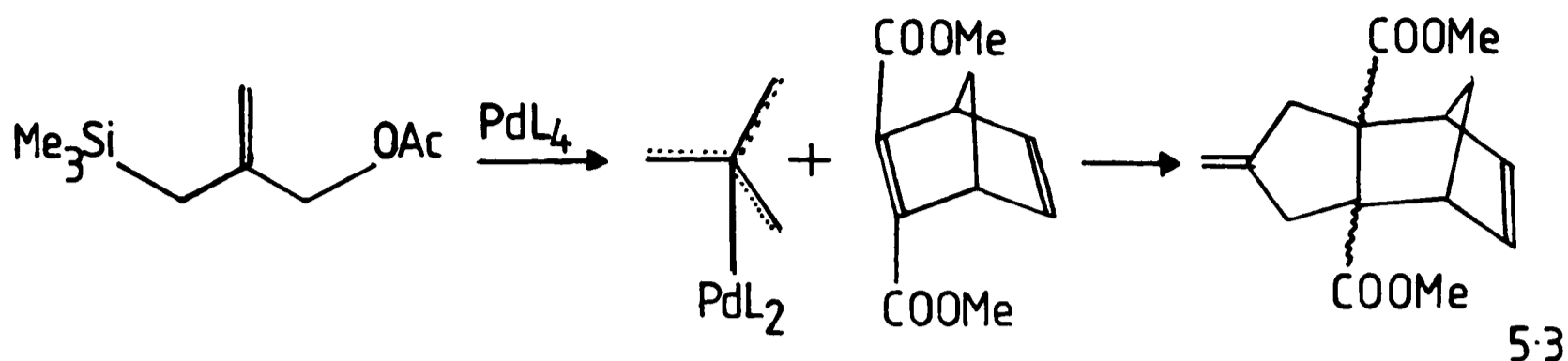
Stable, preformed, TMM complexes undergo similar reactions, equation 5.2.



However, in both systems yields have proved to be low.

More recently TMM complexes generated *in situ*, in a manner analogous to that in the palladium-allyl system ( Chapter 1 ), have been involved in catalytic

cycloadditions<sup>147</sup>, equation 5.3.



In these cases the palladium-TMM complex can neither be stabilised nor isolated.

The TMM moiety is also of interest from a theoretical view point since every connectivity to the central carbon atom has partial multiple bond character. This gives the central carbon the maximum possible "free valency index" as defined by Huckel Molecular Orbital theory. It may also be regarded as a three-fold rotational polyene, for which barriers to rotation<sup>148,149</sup> and conformational preferences<sup>150</sup> in transition metal complexes have been calculated. The mechanism of its formation by ring opening of methylene cyclopropane has also been studied, both from the theoretical view point<sup>134,150,151</sup> and by synthetic/spectroscopic experiments<sup>150,151</sup>.

With the exception of a number of iron species, there is a general paucity of stable TMM containing species, despite its intrinsic interest. Complexes are known, apart from those of iron, only for chromium<sup>152</sup>, molybdenum<sup>151</sup>, tantalum<sup>153</sup>, osmium<sup>154</sup> and iridium<sup>154</sup>. Full structural characterisations have only been carried out for six iron species<sup>155-160</sup>, the chromium<sup>152</sup> and iridium<sup>154</sup> examples.

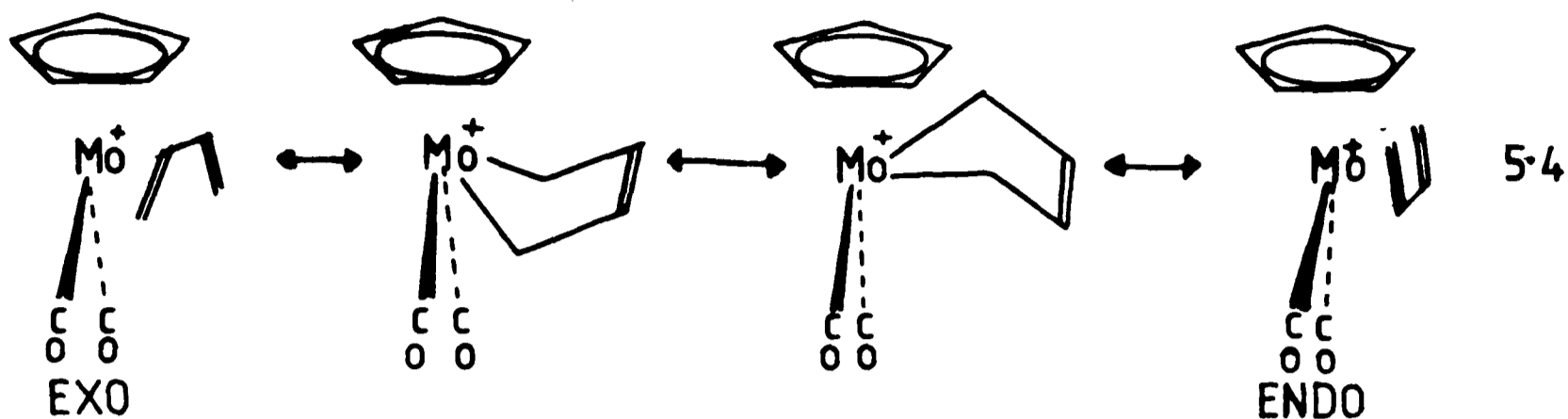
An initial structural characterisation of  $[(\eta^4\text{-C}(\text{CH}_2)_3)\text{Mo}(\text{CO})_2(\eta^5\text{-C}_5\text{Me}_5)]\text{BF}_4$ , ( TRIMET ), synthesised by Green et al.<sup>151</sup>, was carried out by D. M. Sharaiha<sup>161</sup>. However, this was not completed since only the non-hydrogen atoms were located.

The completion of this study was therefore undertaken in order to extend the series of structurally characterised compounds.

The addition of  $\text{H}^-$  to TRIMET was observed to yield  $(\eta^3\text{-2-Me-C}_3\text{H}_4)\text{Mo}(\text{CO})_2\text{Cp}^*$ , **40**<sup>151</sup>, the Cp analogue of which ( CPMOME ), has also been subjected to a full crystallographic study. This was performed to determine the preferred solid state stereochemistry, since, in solution, there is an equilibrium between the *endo* and *exo* forms<sup>56</sup>. Moreover, the *endo* conformation inferred from that of TRIMET, from solution techniques and from a theoretical study<sup>14</sup>, is in contrast to that ( *exo* ) of many previously studied examples of 7 coordinate  $\text{LL}'_2\text{Mo}(\text{CO})(\text{allyl})$  complexes (see Chapter 3 ).

Isomeric to the TMM moiety is butadiene,  $\text{CH}_2=\text{CH}-\text{CH}=\text{CH}_2$ , complexes of which have proved useful in the synthesis of natural products<sup>162</sup>, since, like allyl complexes, they are subject to regiospecific nucleophilic attack<sup>163</sup>. Also of interest is the conformational preferences of butadiene complexes and the mechanism of their intramolecular rearrangements<sup>164</sup>. In the  $[\text{CpMo}(\text{CO})_2(\text{diene})]^+$  system a metallacyclopentadiene intermediate has been proposed in

the interconversion of *endo* and *exo* forms, scheme 5.4, as well as a pure rotation type mechanism<sup>165</sup>.



For the  $[\text{CpMo}(\text{CO})_2(\text{diene})]^+$  system, assignment of isomers could be made on the basis of spectroscopic studies<sup>165</sup>. However, in the neutral  $\text{CpMo}(\text{Cl})_2(\text{diene})$  system<sup>166</sup> this could not be accomplished due to the paramagnetism of the compounds. Furthermore, insufficient data could be obtained from the e.s.r. spectra, even though hyperfine splitting by some of the butadiene hydrogens was observed.

Thus a full three-dimensional crystallographic study of  $\text{CpMo}(\text{CO})_2(\eta^4\text{-C}_4\text{H}_6)$ , CPMOBUT, supplied by J. L. Davidson et al.<sup>166</sup>, was undertaken to determine the stereochemistry.



## 5.2 Solid State Structure of $[(\eta^4\text{-C}(\text{CH}_2)_3)\text{Mo}(\text{CO})_2(\eta^5\text{-C}_5\text{Me}_5)]\text{BF}_4$ ; TRIMET.

Figure 5.1 is a perspective view of the cation demonstrating the adopted numbering scheme. Interatomic distances and angles are given in Tables 5.1a and 5.1b respectively. The cation has approximate  $C_s$  symmetry about a plane passing through Mo, C(11), C(44), C(3) and C(8), and bisecting the OC-Mo-CO angle. Only the C(11)-C(22) and C(11)-C(33) distances violate this symmetry to any significant degree,  $\Delta = 0.070(23)\text{\AA}$ .

In common with the other structurally characterised TMM complexes<sup>152,154-160</sup>, the  $\eta^4\text{-C}(\text{CH}_2)_3$  ligand is not planar. The symmetry is reduced from  $D_{3h}$  symmetry, by a pyramidalisation which results in the central carbon atom (C(11)) being further from the metal than it would be in the planar structure. It does not, however, become more distant than the outer carbon atoms ( Mo-C(11) 2.213(11)\AA, Mo-C(22) 2.326(16)\AA, Mo-C(33) 2.358(10)\AA, Mo-C(44) 2.393(13)\AA ). Concomitant with this bending of the carbon framework is a bending back of the hydrogens of the methylene groups (Table 5.2 ).

These features can be quantified by two angular parameters  $\gamma$  and  $\psi$ <sup>151</sup>. The former is the angle between a plane perpendicular to the  $C_{(\text{central})}$ -metal vector and the  $C_{(\text{central})}$ - $C_{(\text{outer})}$  vector. The latter is the angle between the  $C_{(\text{central})}$ - $C_{(\text{outer})}$  vector and the  $\text{CH}_2$  plane,  $A$ .

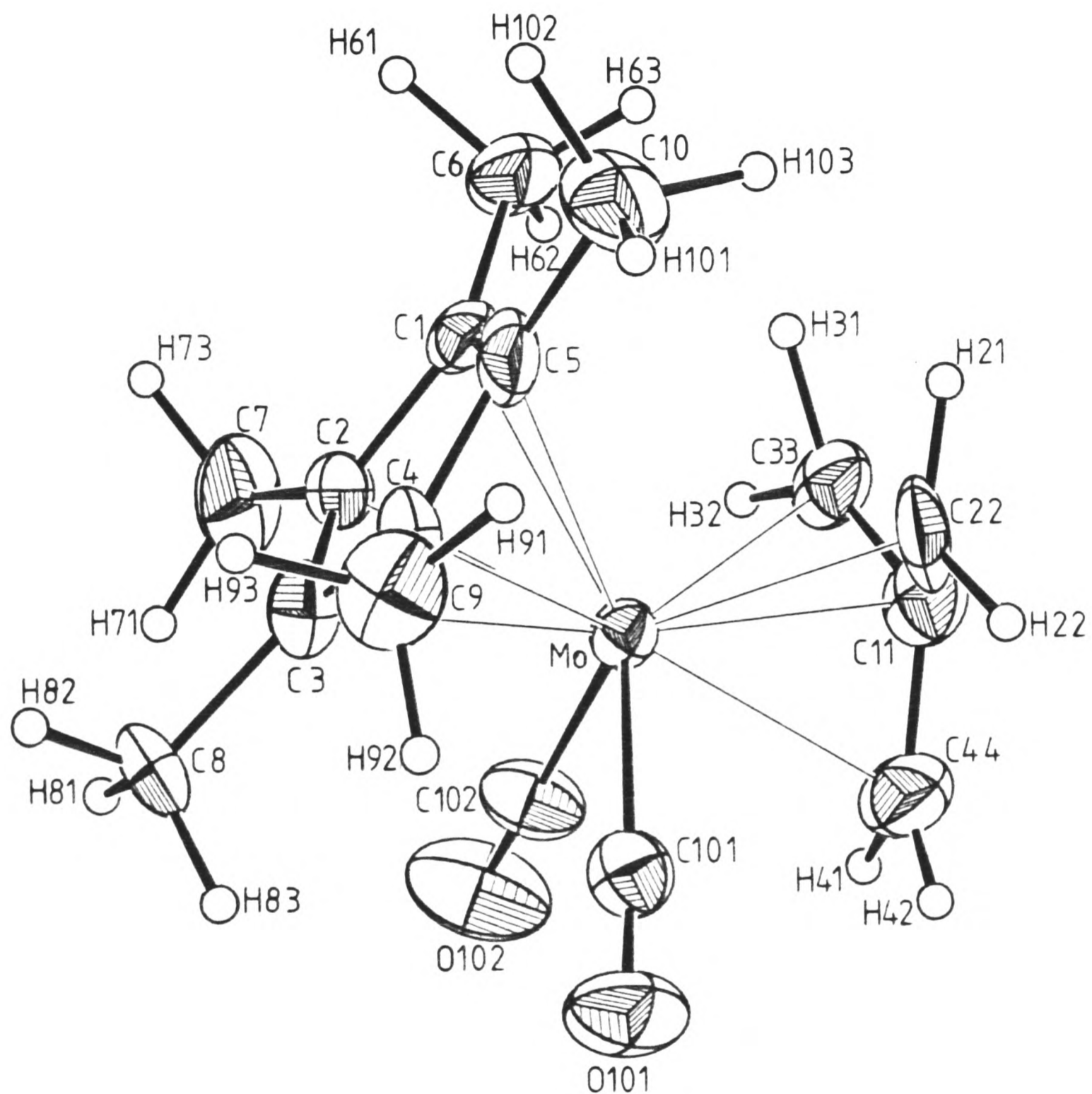


Fig. 5.1 The  $[(\eta^4\text{-C}(\text{CH}_2)_3)\text{Mo}(\text{CO})_2(\eta^5\text{-C}_5\text{Me}_5)]^+$  Cation, TRIMET

Table 5.1a Inter-Atomic Distances ( Å ) for TRIMET

Mo - C(1)	2.374(10)	C(5) - C(10)	1.518(16)
Mo - C(2)	2.313(9)	C(101)-O(101)	1.121(12)
Mo - C(3)	2.297(10)	C(102)-O(102)	1.115(14)
Mo - C(4)	2.318(9)	C(11) - C(22)	1.462(16)
Mo - C(5)	2.349(10)	C(11) - C(33)	1.392(15)
Mo -C(101)	2.023(10)	C(11) - C(44)	1.402(17)
Mo -C(102)	2.032(10)	B - F(1)	1.29(3)
Mo -C(11)	2.213(11)	B - F(2)	1.401(23)
Mo -C(22)	2.326(12)	B - F(3)	1.41(5)
Mo -C(33)	2.358(10)	B - F(4)	1.38(3)
Mo -C(44)	2.393(13)	B - F(5)	1.44(4)
C(1) - C(2)	1.429(13)	B - F(6)	1.46(3)
C(1) - C(5)	1.396(14)	B - F(7)	1.38(5)
C(1) - C(6)	1.472(15)	B - F(8)	1.52(7)
C(2) - C(3)	1.433(13)	B - F(9)	1.38(4)
C(2) - C(7)	1.477(16)	B -F(10)	1.43(4)
C(3) - C(4)	1.400(13)	B -F(11)	1.342(25)
C(3) - C(8)	1.503(14)	B -F(12)	1.37(5)
C(4) - C(5)	1.465(13)	B -F(13)	1.39(5)
C(4) - C(9)	1.476(15)	B -F(14)	1.46(7)
C(22) -H(21)	1.06(8)	C(33) -H(32)	1.01(8)
C(22) -H(22)	0.99(8)	C(44) -H(41)	1.06(9)
C(33) -H(31)	1.16(8)	C(44) -H(42)	0.90(10)

Table 5.1b Inter-Bond Angles ( ° ) for TRIMET.

C(1) - Mo - C(2)	35.5(3)	C(102) - Mo - C(44)	77.6(4)
C(1) - Mo - C(3)	59.6(3)	C(11) - Mo - C(22)	37.5(4)
C(1) - Mo - C(4)	60.0(3)	C(11) - Mo - C(33)	35.3(4)
C(1) - Mo - C(5)	34.4(3)	C(11) - Mo - C(44)	35.2(4)
C(1) - Mo - C(101)	138.9(4)	C(22) - Mo - C(33)	62.0(4)
C(1) - Mo - C(102)	107.8(4)	C(22) - Mo - C(44)	60.3(4)
C(1) - Mo - C(11)	110.2(4)	C(33) - Mo - C(44)	61.0(4)
C(1) - Mo - C(22)	101.0(4)	Mo - C(1) - C(2)	70.0(5)
C(1) - Mo - C(33)	82.0(3)	Mo - C(1) - C(5)	71.9(6)
C(1) - Mo - C(44)	142.9(4)	Mo - C(1) - C(6)	128.9(7)
C(2) - Mo - C(3)	36.2(3)	C(2) - C(1) - C(5)	106.7(8)
C(2) - Mo - C(4)	59.8(3)	C(2) - C(1) - C(6)	127.2(9)
C(2) - Mo - C(5)	58.1(3)	C(5) - C(1) - C(6)	125.7(9)
C(2) - Mo - C(101)	120.4(4)	Mo - C(2) - C(1)	74.6(5)
C(2) - Mo - C(102)	78.7(4)	Mo - C(2) - C(3)	71.3(5)
C(2) - Mo - C(11)	137.1(4)	Mo - C(2) - C(7)	130.4(7)
C(2) - Mo - C(22)	136.3(4)	C(1) - C(2) - C(3)	108.4(8)
C(2) - Mo - C(33)	102.2(3)	C(1) - C(2) - C(7)	123.7(9)
C(2) - Mo - C(44)	150.5(4)	C(3) - C(2) - C(7)	126.6(9)
C(3) - Mo - C(4)	35.3(3)	Mo - C(3) - C(2)	72.5(5)
C(3) - Mo - C(5)	58.8(3)	Mo - C(3) - C(4)	73.2(5)
C(3) - Mo - C(101)	85.4(4)	Mo - C(3) - C(8)	127.9(7)
C(3) - Mo - C(102)	86.1(4)	C(2) - C(3) - C(4)	109.2(8)
C(3) - Mo - C(11)	169.1(4)	C(2) - C(3) - C(8)	124.9(9)
C(3) - Mo - C(22)	136.7(4)	C(4) - C(3) - C(8)	125.2(9)
C(3) - Mo - C(33)	138.0(3)	Mo - C(4) - C(3)	71.5(5)
C(3) - Mo - C(44)	155.7(4)	Mo - C(4) - C(5)	72.8(5)
C(4) - Mo - C(5)	36.6(3)	Mo - C(4) - C(9)	130.9(7)
C(4) - Mo - C(101)	79.1(4)	C(3) - C(4) - C(5)	105.6(8)
C(4) - Mo - C(102)	120.3(4)	C(3) - C(4) - C(9)	128.2(9)
C(4) - Mo - C(11)	138.3(4)	C(5) - C(4) - C(9)	124.7(9)
C(4) - Mo - C(22)	101.6(4)	Mo - C(5) - C(1)	73.8(6)
C(4) - Mo - C(33)	135.8(3)	Mo - C(5) - C(4)	70.6(5)
C(4) - Mo - C(44)	149.2(4)	Mo - C(5) - C(10)	131.0(7)
C(5) - Mo - C(101)	110.4(4)	C(1) - C(5) - C(4)	110.1(8)
C(5) - Mo - C(102)	136.8(4)	C(1) - C(5) - C(10)	125.6(9)
C(5) - Mo - C(11)	110.9(4)	C(4) - C(5) - C(10)	123.4(9)
C(5) - Mo - C(22)	83.1(4)	Mo - C(101) - O(101)	177.2(9)
C(5) - Mo - C(33)	99.2(4)	Mo - C(102) - O(102)	177.0(10)
C(5) - Mo - C(44)	143.2(4)	Mo - C(11) - C(22)	75.5(6)
C(101) - Mo - C(102)	88.9(4)	Mo - C(11) - C(33)	78.0(6)
C(101) - Mo - C(11)	102.5(4)	Mo - C(11) - C(44)	79.4(7)
C(101) - Mo - C(22)	89.9(4)	C(22) - C(11) - C(33)	115.5(10)
C(101) - Mo - C(33)	136.4(4)	C(22) - C(11) - C(44)	111.8(10)
C(101) - Mo - C(44)	76.4(4)	C(33) - C(11) - C(44)	119.4(10)
C(102) - Mo - C(11)	101.3(4)	Mo - C(22) - C(11)	67.1(6)
C(102) - Mo - C(22)	136.9(4)	Mo - C(33) - C(11)	66.7(6)
C(102) - Mo - C(33)	90.8(4)	Mo - C(44) - C(11)	65.4(7)
Mo - C(22) - H(21)	113.8(43)	C(11) - C(33) - H(32)	137.9(47)
Mo - C(22) - H(22)	120.4(48)	H(31) - C(33) - H(32)	92.1(61)
C(11) - C(22) - H(21)	105.4(43)	Mo - C(44) - H(41)	105.2(48)
C(11) - C(22) - H(22)	110.4(49)	Mo - C(44) - H(42)	113.6(61)
H(21) - C(22) - H(22)	123.0(65)	C(11) - C(44) - H(41)	126.4(48)
Mo - C(33) - H(31)	98.9(39)	C(11) - C(44) - H(42)	136.9(62)
Mo - C(33) - H(32)	92.8(46)	H(41) - C(44) - H(42)	96.1(77)
C(11) - C(33) - H(31)	126.0(40)		

Table 5.2 Least-Squares Planes Data for TRIMET.

(a) Coefficients.

Plane 1: C(1), C(2), C(3), C(4), C(5).  
Equation:  $-2.9995x - 3.5302y + 21.0512z = 2.7520\text{\AA}$   
R.M.S. Deviation =  $0.0058\text{\AA}$

Plane 2: Mo, C(101), C(102).  
Equation:  $7.7163x + 3.3768y - 16.9964z = -0.4068\text{\AA}$

Plane 3: C(22), H(21), H(22)  
Equation:  $5.6507x + 8.9912y - 11.8264z = 2.0309\text{\AA}$

Plane 4: C(33), H(31), H(32).  
Equation:  $9.6977x + 7.5523y - 5.1488z = 3.9052\text{\AA}$

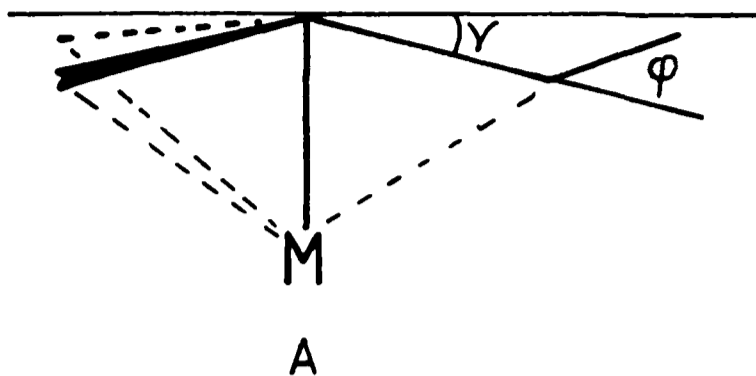
Plane 5: C(44), H(41), H(42).  
Equation:  $9.5259x + 3.7807y - 13.4771z = 2.0640\text{\AA}$

(b) Atomic Deviations (  $\text{\AA}$  ).

Plane 1: Mo	-1.9893,	C(1)	0.0022,	C(2)	-0.0065,	
	C(3)	0.0082,	C(4)	-0.0067,	C(5)	0.0027,
	C(6)	0.1549,	C(7)	0.2352,	C(8)	0.2262,
	C(9)	0.2423,	C(10)	0.2432.		

(c) Dihedral Angles (  $^{\circ}$  )

Plane 1, Plane 2	156.4
Plane 1, Plane 3	142.9
Plane 1, Plane 4	124.3
Plane 1, Plane 5	144.5
Plane 2, Plane 3	31.0
Plane 2, Plane 4	37.5
Plane 2, Plane 5	12.2
Plane 3, Plane 4	25.8
Plane 3, Plane 5	30.4
Plane 4, Plane 5	27.7



Parameters for the coordinated TMM ligand in TRIMET and in other complexes are given in Table 5.3. It is apparent that the metal-TMM<sub>(carbon)</sub> bond lengths in TRIMET are all considerably longer than corresponding distances in the other complexes. However, the carbon-carbon distances and values of  $\gamma$  are all within the previously determined ranges. The previously determined range of values of  $\phi$  is large (  $0^\circ$  to  $57^\circ$  ), note the differences in the two sets of values for the independent molecules of  $(\text{TMM})\text{Cr}(\text{PPh}_3)(\text{CO})_3$  41<sup>152</sup> (  $37^\circ$ - $57^\circ$  and  $8^\circ$ - $13^\circ$  ). These deviations, especially in ambient temperature studies, are subject to rather large errors and their reliability must be questioned. However, the value of  $-15^\circ$  ( i.e. bent towards the metal ) for the C(33) methylene group in TRIMET seems unusual. Analysis of intramolecular contacts ( Table 5.4 ) reveals three short, repulsive, contacts H(31)...H(63) 2.03(9)Å, H(31)...H(62) 2.05(8)Å and H(21)...H(103) 2.07(8)Å which may be affecting the hydrogen positions.

As is common with the Cp ligand, the Cp<sup>\*</sup> is not symmetrically bound to the metal: Mo-C(1)  $\approx$  Mo-C(5) >

Table 5.3 Parameters for coordinated TMM

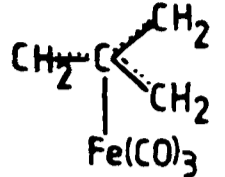
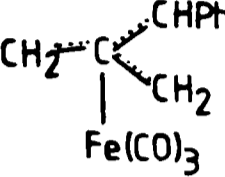
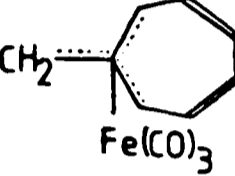
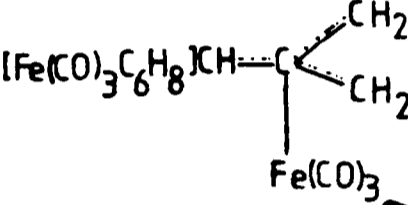
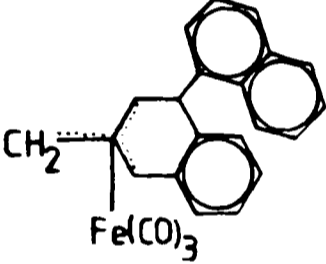
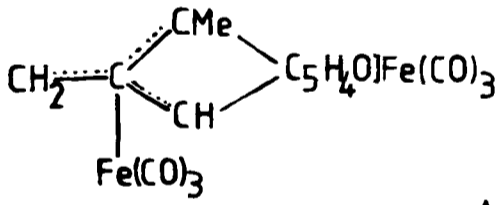
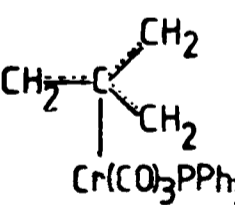
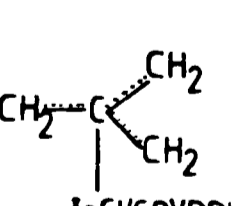
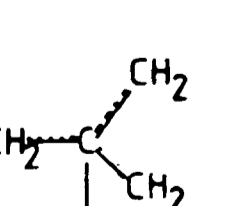
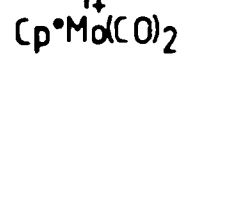
Compound	M-C <sub>(term)</sub>	M-C <sub>(cent)</sub>	C-C	γ	φ	REF.
	2.123(5)	1.938(5)	1.437(3)	13.6	14.4	155
	2.098(11) 2.118(10) 2.162(9)	1.932(10)	1.405(13) 1.406(13) 1.436(12)	13.9 13.0 11.7	36.7 37.1 -0.1	156
	2.120(3) 2.192(3) 2.175(3)	1.946(2)	1.428(5) 1.405(4) 1.412(4)	13.9 10.1 11.0	23.4 14.8 15.9	157
	2.12(1) 2.12(1) 2.17(1)	1.94(1)	1.42(2) 1.45(2) 1.43(1)	13.5 14.1 11.4		158
	2.10(2) 2.11(2) 2.11(2)	1.95(2)	1.41(4) 1.37(4) 1.42(4)	14.4 13.3 14.3		159
	2.206(6) 2.143(6) 2.123(8)	1.943(6)	1.428(9) 1.408(10) 1.417(10)	9.8 12.3 13.4	20.2 19.1 14.9	160
	2.242(13) 2.207(14) 2.247(14)	2.030(12)	1.424(18) 1.429(19) 1.414(20)	11.2 11.9 10.8	45.0 56.5 37.0	152
	2.234(14) 2.218(15) 2.231(13)	2.028(12)	1.418(19) 1.405(21) 1.398(19)	11.4 11.8 11.1	11.3 12.5 8.6	
	2.288(15) 2.201(12) 2.173(15)	2.053(12)	1.50(2) 1.46(2) 1.43(2)	11.6 14.6 15.2		154
	2.326(12) 2.358(10) 2.393(13)	2.213(11)	1.462(16) 1.392(15) 1.402(17)	14.6 12.0 10.6	55.1 -15.7 6.1	

Table 5.4 Significant Non-bonded Contacts for TRIMET.

(a) Intramolecular ( Å )

H(61)...H(91)	1.928(17)
H(31)...H(72)	2.04(8)
H(31)...H(73)	2.03(9)
H(101)...H(81)	1.992(17)
H(21)...H(93)	2.07(8)

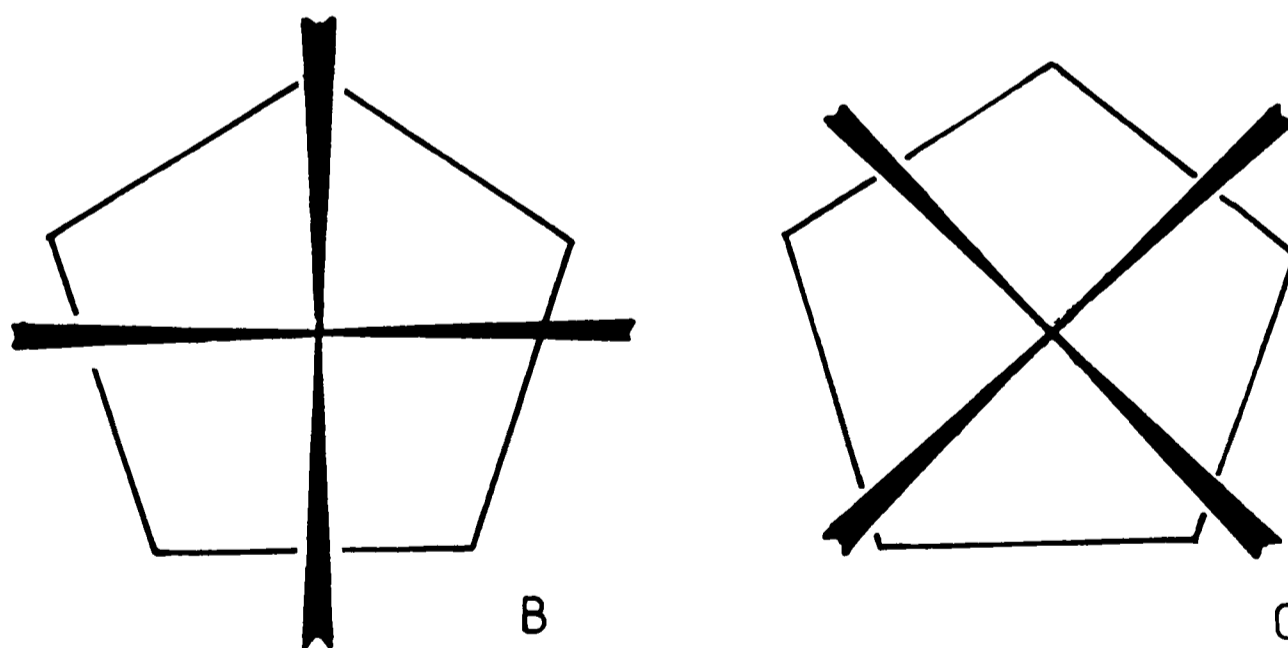
(b) Intermolecular

Contact X...H	Symm H	Dist (Å)	Angle A-X...H (°)
F(8)...H(72)	$x, -1+y, z$	1.94(7)	126.9(8)
F(10)...H(21)	$1/2-x, -1/2+y, z$	2.13(9)	139.1(12)
F(14)...H(61)	$-x, -1/2+y, 1/2-z$	2.20(7)	135.6(8)
F(9)...H(72)	$x, -1+y, z$	2.21(4)	118.1(7)
F(12)...H(32)	$x, -1+y, z$	2.24(9)	168.4(12)
F(7)...H(63)	$1/2-x, -1/2+y, z$	2.32(5)	132.2(7)
F(7)...H(73)	$-x, -1/2+y, 1/2-z$	2.27(5)	142.8(7)
F(5)...H(42)	$-x, -y, -z$	2.32(10)	107.4(13)
F(2)...H(32)	$x, -1+y, z$	2.38(8)	143.0(8)
F(2)...H(41)	$-x, -y, -z$	2.49(9)	114.7(9)
F(4)...H(63)	$1/2-x, -1/2+y, z$	2.44(3)	123.8(7)



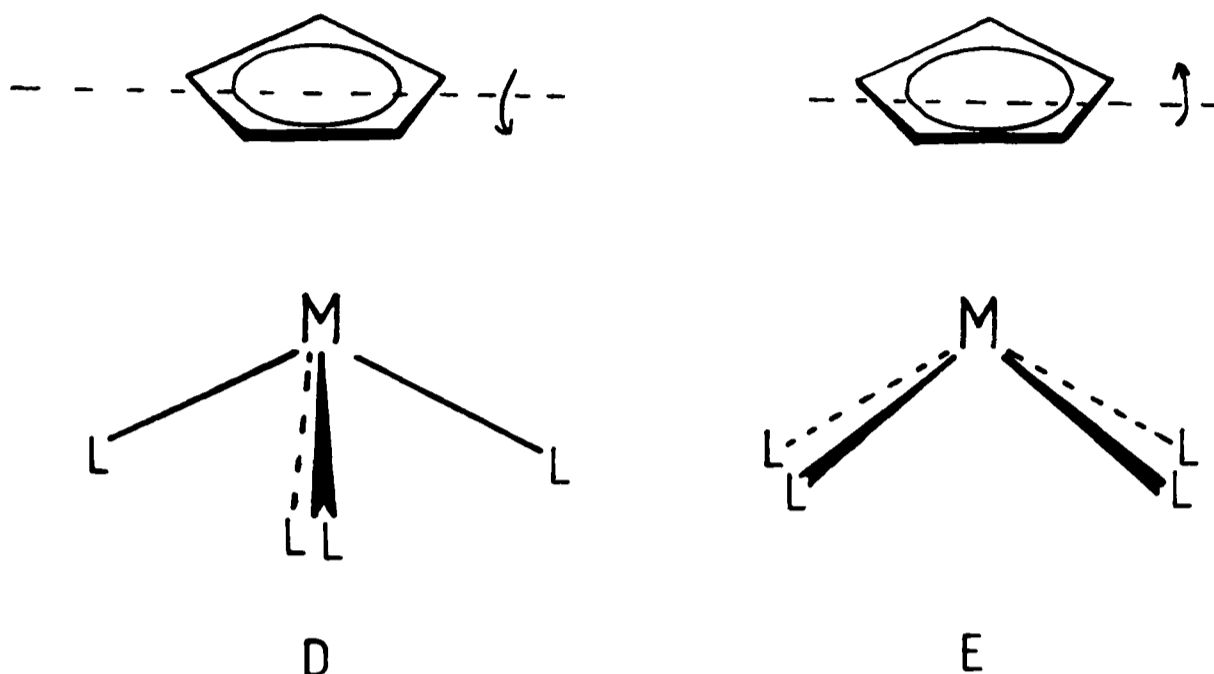
Mo-C(2)  $\approx$  Mo-C(4) > Mo-C(3) indicating the ligand is tipped away from C(22) and C(33). This asymmetry in the Cp\* coordination can be quantified in terms of the parameters  $\psi$  and  $\Delta$  ( see Chapter 3 ). In TRIMET their values are 2.4° and 0.08Å respectively, the slip of the metal across the C<sub>5</sub> face being towards C(3). This could be a consequence of the intramolecular H...H contacts already mentioned. However, it is also consistent with the electronic reason proposed by Kubacek, Hoffmann and Havlas<sup>167</sup>.

In CpML<sub>4</sub> complexes ( such as TRIMET, the TMM being a bidentate ligand ) the four ligands can take two, different, limiting orientations with respect to the Cp ring. In the eclipsed form one ring carbon atom lies directly over a ligand, B, whilst the staggered form, C, corresponds to a rotation of 45° of the ML<sub>4</sub> fragment from this position.



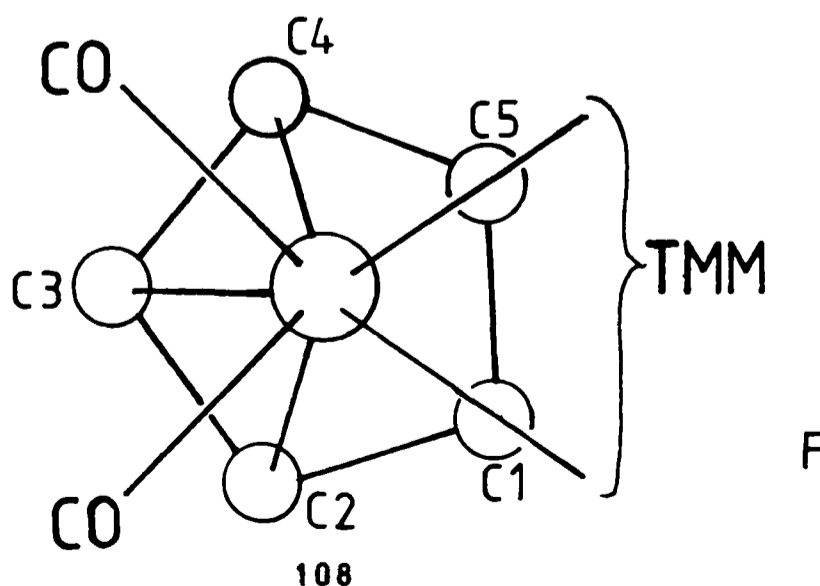
In each case a different component of the Cp e<sub>2</sub> set interacts with the metal b<sub>2</sub> orbital. This results in the carbon directly over a ligand being less strongly bound to the metal in the eclipsed form B, whilst in the staggered

form C, the carbon directly over the bisector of two of the ligands is more strongly bound. Thus the rings tilt in opposite directions in each case, as shown in D and E.



The eclipsed conformation is observed in  $\text{CpMo}(\text{CO})_3(\text{C}_3\text{F}_7)$ , **42**<sup>168</sup>,  $[\text{CpMo}(\text{CO})_3]_2$ , **43**<sup>169</sup>,  $\text{CpMo}(\text{CO})_3(\text{C}_2\text{H}_5)$ , **44**<sup>170</sup> and  $[\text{Cp}_2\text{Mo}_2\text{H}(\text{P}(\text{CH}_3)_2)(\text{CO})_4]$ , **45**<sup>171</sup> all of which show the expected tilt. Examples of the staggered geometry are;  $\text{CpMo}(\eta^3\text{-C}(\text{Me})_3\text{C}(\text{O})\text{O})(\text{CO})(\text{Bu}^t\text{NC})$ , **46**<sup>98</sup> and  $\text{CpNb}(\text{CO})_4$ , **47**<sup>172</sup> which also exhibit the appropriate expected direction of tilt.

The geometry in TRIMET is of the staggered type, C(3) lying directly above the bisector of the carbonyl groups, F.



Thus C(3) should be the closest to the metal with C(5) and C(1) furthest away, as is, in fact, observed. This could be termed as a slippage towards a cyclic  $\eta^3$ -allyl type function ( C(2), C(3) and C(4) ) and an uncoordinated double bond ( C(1)-C(5) ). The shortest C-C intraring distance being C(1)-C(5) further supports this. The slight non-planarity of the ring ( Table 5.2 ) is also consistent, the pentagon being of an envelope conformation, bent about C(2)...C(4) by 1.4°. The limit of this type of distortion is seen in  $\text{CpW(CO)}_2(\eta^3\text{-C}_5\text{H}_5)$ , **48**<sup>173</sup>, in which one  $\text{C}_5\text{H}_5$  ring is only  $\eta^3$ -coordinated, leaving a free double bond. Here the ring is also of an envelope conformation, bent by 19.6°.

Further corroborative evidence that the slippage in TRIMET is electronically induced rather than sterically comes from the deviations of the methyl groups from the  $\text{C}_5$  plane. Those involved in the H...H contacts, C(6) and C(10), are not bent out of the plane any more than the others, as might be expected if the distortion was sterically induced. The methyl groups are all depressed out of the  $\text{C}_5$  plane, away from the metal, by 5.9°, 9.4°, 8.4°, 9.8° and 9.2° for C(6), C(7), C(8), C(9) and C(10) respectively. A theoretical study on  $\text{M(CH)}_n$  fragments<sup>114</sup> suggests that the substituents on an  $\eta^5\text{-C}_5$  ring should lie in the plane of the ring. However, structural determinations of other  $(\eta^5\text{-C}_5\text{Me}_5)\text{-metal}$  complexes<sup>174,175</sup> shows that the methyl groups are depressed out of the  $\text{C}_5$  plane, away from the metal, as is found here.

The bond lengths within the  $\text{Mo(CO)}_2$  function are quite

normal and maintain the  $C_s$  symmetry of the complex. However, the CO-Mo-CO angle (  $88.9^\circ$  ) is very large for this type of complex.

The  $BF_4$  counter ion is severely disordered, the fluorine atoms occupying fourteen independent positions with SOF's ranging from 0.1-0.55. All F atoms were given a fixed, isotropic, thermal parameter (  $U = 0.10\text{\AA}^2$  ) and the final SOF's were refined. Figure 5.2 shows the ion with the spheres representing atoms scaled to the SOF at each site, the lower right-hand sphere representing one full fluorine for scaling. The B-F distances all fall in the range 1.29(3)-1.52(7)\AA but the disorder cannot be interpreted in terms of separate intersecting tetrahedra- a more accurate description may be that it is tending towards a spherical ion.

Figure 5.3 shows one unit cell and contents projected almost onto the (001) plane. There are no unusual features and intermolecular contacts, which are of little stereochemical significance, are listed in Table 5.4.

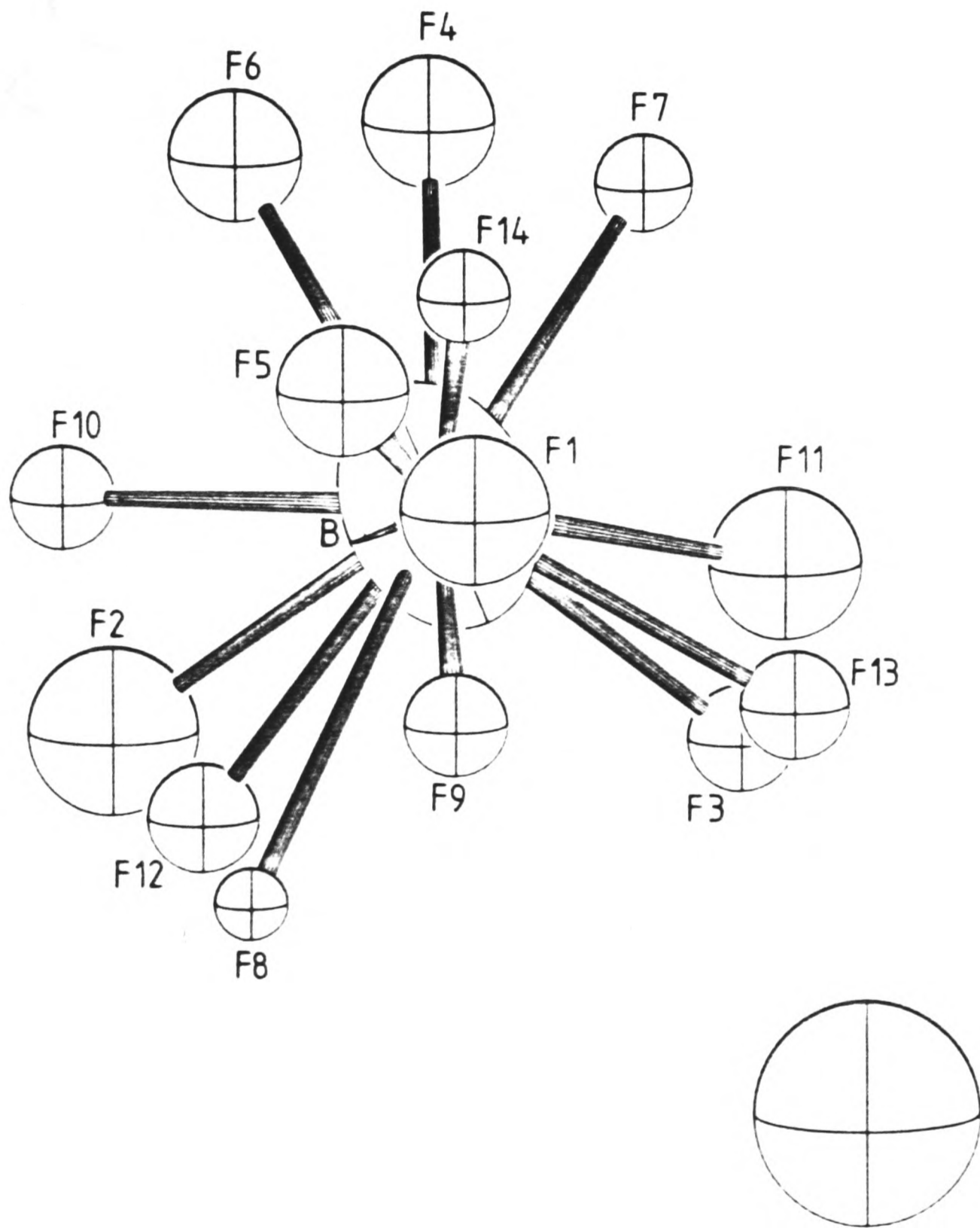


Fig. 5.2 The Disordered  $\text{BF}_4^-$  Anion.

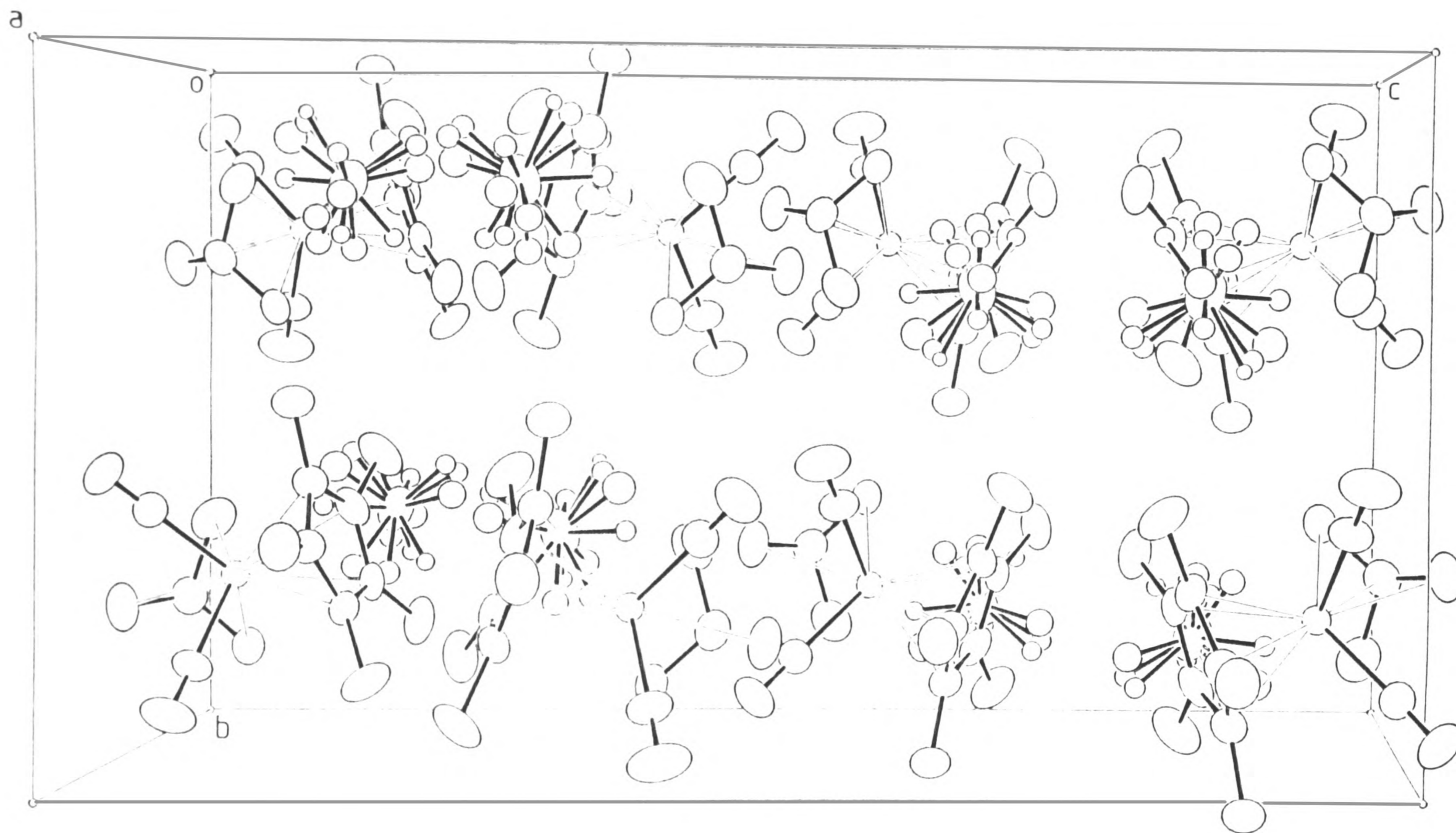


Fig. 5.3 Packing Diagram of  $[(\eta^4\text{-C}(\text{CH}_2)_3)\text{Mo}(\text{CO})_2(\eta^5\text{-C}_5\text{Me}_5)]\text{BF}_4$ .

### 5.3 Solid State Structure of $\text{CpMo(CO)}_2(\eta^3\text{-2-Me-C}_3\text{H}_4)$ ; CPMOME:-

Figure 5.4 is a numbered, perspective view of a single molecule of CPMOME. Bond lengths and angles are given in Tables 5.5a and 5.5b respectively.

The observed *endo* conformation is directly analogous to the *syn* conformation of TRIMET, suggesting that the hydride addition takes place without any major stereochemical change. It is also consistent with the major solution isomer<sup>56</sup> and the predicted conformation for 33<sup>14</sup>, although the crystal structure of 33 shows it to be in the *exo* conformation<sup>22</sup>. This would appear to cast some doubt on the validity of the model used in the theoretical study. Only the compounds 34<sup>113</sup>, 35<sup>115</sup> and 48<sup>113</sup> show the same *endo* configuration as CPMOME and this may be rationalised in terms of the steric requirements of the relatively large ligands on the metal and the substituents on the allyl. Analogous 2-methylallyl complexes<sup>60,63,100,101</sup>, including a gallate complex<sup>109</sup> related to 48, have the *exo* stereochemistry.

Calculation shows that, if CPMOME were in the alternative *exo* geometry, there would be a repulsive H(Me)...H(Cp) contact less than 2.4Å ( the sum of the van der Waals radii ). In the observed *endo* stereochemistry there is no such intramolecular steric congestion.

In contrast to many of the  $\eta^3$ -allyl complexes previously studied, in which the central carbon atom is closest to the metal, the three Mo-C<sub>(allyl)</sub> distances are equal ( Mo-C(1)

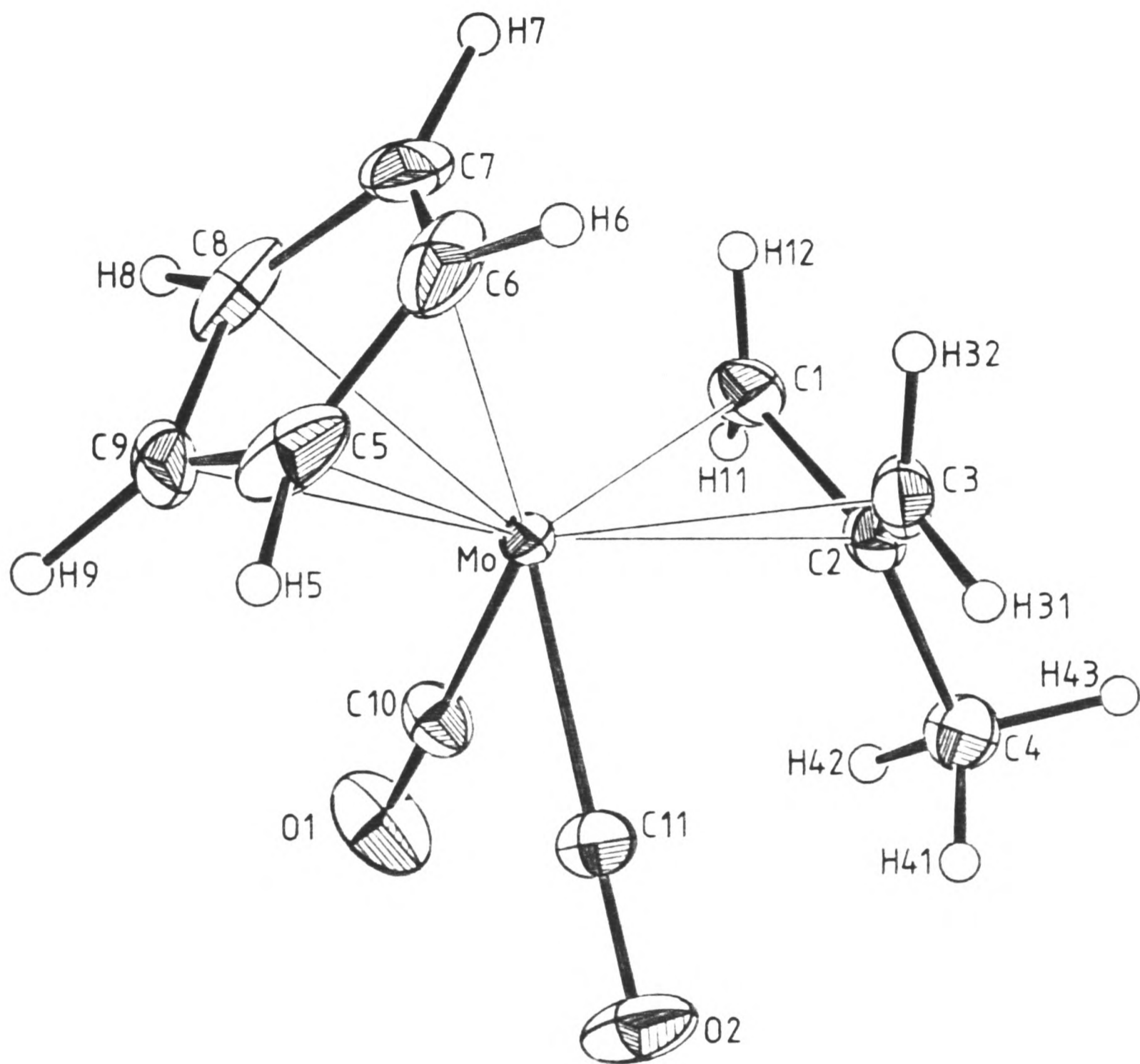


Fig 5.4 Single Molecule of  $(\eta^5\text{-C}_5\text{H}_5)\text{Mo}(\text{CO})_2(\eta^3\text{-2-Me-C}_3\text{H}_4)$ , CPMOME.



Table 5.5a Inter-Atomic Distances ( Å ) for CPMOME

Mo - C(1)	2.3146(25)	C(1) - C(2)	1.407(3)
Mo - C(2)	2.3169(20)	C(2) - C(3)	1.403(3)
Mo - C(3)	2.3175(22)	C(2) - C(4)	1.497(3)
Mo - C(5)	2.333(3)	C(5) - C(6)	1.393(4)
Mo - C(6)	2.377(3)	C(5) - C(9)	1.390(4)
Mo - C(7)	2.358(3)	C(6) - C(7)	1.365(4)
Mo - C(8)	2.318(3)	C(7) - C(8)	1.399(4)
Mo - C(9)	2.306(3)	C(8) - C(9)	1.406(4)
Mo -C(10)	1.9615(22)	C(10) - O(1)	1.147(3)
Mo -C(11)	1.9563(19)	C(11) - O(2)	1.156(3)
C(1) -H(11)	0.99(3)	C(4) -H(43)	0.96(3)
C(1) -H(12)	0.88(3)	C(5) - H(5)	0.86(3)
C(3) -H(31)	1.06(3)	C(6) - H(6)	1.07(3)
C(3) -H(32)	0.94(3)	C(7) - H(7)	0.82(3)
C(4) -H(41)	0.98(3)	C(8) - H(8)	0.66(3)
C(4) -H(42)	0.96(3)	C(9) - H(9)	0.88(3)

Table 5.5b Inter-Bond Angles ( ° ) for CPMOME

C(1) - Mo - C(2)	35.36(8)	C(7) - Mo - C(8)	34.81(10)
C(1) - Mo - C(3)	62.09(8)	C(7) - Mo - C(9)	58.08(10)
C(1) - Mo - C(5)	143.90(10)	C(7) - Mo - C(10)	127.50(10)
C(1) - Mo - C(6)	110.83(10)	C(7) - Mo - C(11)	148.21(9)
C(1) - Mo - C(7)	87.64(10)	C(8) - Mo - C(9)	35.40(10)
C(1) - Mo - C(8)	98.68(10)	C(8) - Mo - C(10)	96.27(10)
C(1) - Mo - C(9)	133.62(10)	C(8) - Mo - C(11)	140.93(9)
C(1) - Mo - C(10)	82.32(9)	C(9) - Mo - C(10)	94.37(10)
C(1) - Mo - C(11)	118.11(8)	C(9) - Mo - C(11)	105.93(9)
C(2) - Mo - C(3)	35.25(7)	C(10) - Mo - C(11)	77.36(8)
C(2) - Mo - C(5)	146.32(9)	Mo - C(1) - C(2)	72.41(13)
C(2) - Mo - C(6)	117.28(9)	Mo - C(2) - C(1)	72.23(13)
C(2) - Mo - C(7)	111.07(9)	Mo - C(2) - C(3)	72.40(12)
C(2) - Mo - C(8)	132.69(9)	Mo - C(2) - C(4)	120.96(15)
C(2) - Mo - C(9)	167.94(9)	C(1) - C(2) - C(3)	116.45(19)
C(2) - Mo - C(10)	88.81(8)	C(1) - C(2) - C(4)	121.27(20)
C(2) - Mo - C(11)	86.11(7)	C(3) - C(2) - C(4)	122.08(19)
C(3) - Mo - C(5)	111.54(9)	Mo - C(3) - C(2)	72.35(12)
C(3) - Mo - C(6)	88.40(9)	Mo - C(5) - C(6)	74.50(18)
C(3) - Mo - C(7)	98.65(9)	Mo - C(5) - C(9)	71.50(17)
C(3) - Mo - C(8)	132.81(9)	C(6) - C(5) - C(9)	107.9(3)
C(3) - Mo - C(9)	144.88(9)	Mo - C(6) - C(5)	71.11(18)
C(3) - Mo - C(10)	120.48(8)	Mo - C(6) - C(7)	72.49(18)
C(3) - Mo - C(11)	79.85(8)	C(5) - C(6) - C(7)	109.0(3)
C(5) - Mo - C(6)	34.40(11)	Mo - C(7) - C(6)	74.01(18)
C(5) - Mo - C(7)	57.18(10)	Mo - C(7) - C(8)	71.03(17)
C(5) - Mo - C(8)	57.94(11)	C(6) - C(7) - C(8)	108.1(3)
C(5) - Mo - C(9)	34.86(10)	Mo - C(8) - C(7)	74.16(17)
C(5) - Mo - C(10)	124.01(10)	Mo - C(8) - C(9)	71.85(17)
C(5) - Mo - C(11)	93.49(9)	C(7) - C(8) - C(9)	107.7(3)
C(6) - Mo - C(7)	33.50(10)	Mo - C(9) - C(5)	73.64(17)
C(6) - Mo - C(8)	56.92(10)	Mo - C(9) - C(8)	72.75(17)
C(6) - Mo - C(9)	57.41(10)	C(5) - C(9) - C(8)	107.4(3)
C(6) - Mo - C(10)	150.82(10)	Mo - C(10) - O(1)	176.61(21)
C(6) - Mo - C(11)	115.04(9)	Mo - C(11) - O(2)	178.18(18)
Mo - C(1) - H(11)	118.5(20)	Mo - C(5) - H(5)	114.6(21)
Mo - C(1) - H(12)	103.6(22)	H(5) - C(5) - C(6)	120.7(21)
H(11) - C(1) - H(12)	122.0(30)	H(5) - C(5) - C(9)	131.1(21)
H(11) - C(1) - C(2)	110.0(20)	Mo - C(6) - H(6)	122.4(18)
H(12) - C(1) - C(2)	119.9(22)	C(5) - C(6) - H(6)	134.6(18)
Mo - C(3) - H(31)	115.4(17)	H(6) - C(6) - C(7)	116.4(18)
Mo - C(3) - H(32)	102.8(19)	Mo - C(7) - H(7)	128.6(21)
C(2) - C(3) - H(31)	121.0(17)	C(6) - C(7) - H(7)	132.3(21)
C(2) - C(3) - H(32)	120.2(19)	H(7) - C(7) - C(8)	118.7(21)
H(31) - C(3) - H(32)	114.6(25)	Mo - C(8) - H(8)	126.6(27)
C(2) - C(4) - H(41)	114.1(18)	C(7) - C(8) - H(8)	124.7(27)
C(2) - C(4) - H(42)	111.2(18)	H(8) - C(8) - C(9)	127.1(27)
C(2) - C(4) - H(43)	106.7(18)	Mo - C(9) - H(9)	118.8(19)
H(41) - C(4) - H(42)	104.4(26)	C(5) - C(9) - H(9)	124.8(19)
H(41) - C(4) - H(43)	106.4(25)	C(8) - C(9) - H(9)	127.8(19)
H(42) - C(4) - H(43)	114.1(25)		

2.3146(25)Å, Mo-C(2) 2.3169(20)Å, Mo-C(3) 2.3175(22)Å ) although they are within the expected range. However, examples are known in which the central carbon is equidistant ( PHALPD and PDETAL ) or even the most distant from the metal, 34<sup>113</sup>, 35<sup>115</sup> and 36<sup>116</sup> ( see Chapter 3 ).

The ligand itself is not planar, the methyl and hydrogen substituents all lying out of the allyl C<sub>3</sub> plane ( Table 5.6 ). The methyl group is tilted towards the metal by 4.2°, this, where sterically permitted, is a common feature for this ligand<sup>16,63,113,115,176,177</sup> and deviations up to 12° have been reported<sup>110</sup>. Similarly the hydrogens *syn* to the methyl group ( H(11) and H(31) ) are also tilted towards the metal ( by 5.8° and 9.8° respectively ) whilst those in the *anti* positions ( H(12) and H(32) ) are bent away from the metal ( by 30.7° and 30.0° respectively ). As has already been shown (Chapter 3 ) similar deviations are commonly observed in allyl complexes.

The Cp ring is not symmetrically bound to the metal; metal-carbon distances are in the order Mo-C(6) > Mo-C(7) > Mo-C(5) > Mo-C(8) > Mo-C(9) and examination of the C<sub>5</sub>-ML<sub>4</sub> orientation suggests it is of the eclipsed conformation, H.

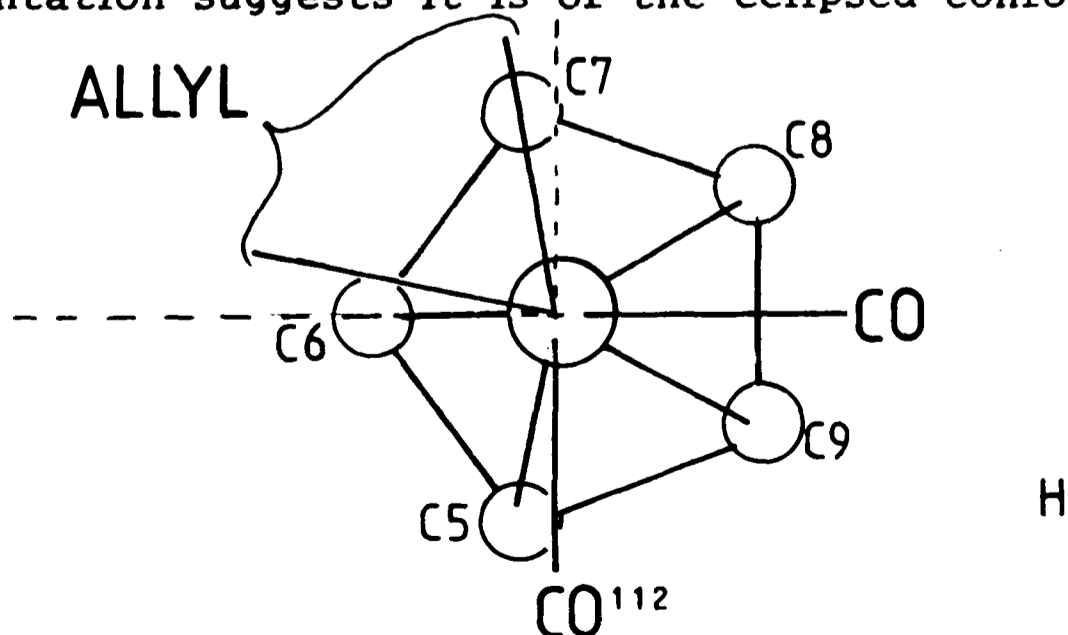


Table 5.6 Least-Squares Planes Data for CPMOME

(a) Coefficients.

Plane 1: C(1), C(2), C(3).

$$\text{Equation: } -1.3590x + 9.4574y + 9.0836z = 4.2242\text{\AA}$$

Plane 2: C(1), C(2), C(3), C(4), C(5).

$$\text{Equation: } 1.8338x - 9.8905y + 6.9447z = 1.8252\text{\AA}$$

R.M.S. deviation = 0.0046\AA

Plane 3: Mo, C(10), C(11).

$$\text{Equation: } -2.2332x + 11.7796y + 2.5851z = 1.5619\text{\AA}$$

(b) Atomic Deviations ( \AA ).

Plane 1: Mo -1.8925, C(4) -0.1114, H(11) -0.1011,  
H(12) 0.4593, H(31) -0.1812, H(32) 0.4737.

Plane 2: Mo -2.0155, C(5) -0.0053, C(6) 0.0066,  
C(7) -0.0053, C(8) 0.0019, C(9) 0.0021.

(c) Dihedral Angles ( ° )

Plane 1, Plane 2 106.5  
Plane 1, Plane 3 32.0  
Plane 2, Plane 3 138.3

Due to the restricted "bite" of the allyl ligand ( $C(1)-Mo-C(3) = 62.09(8)^\circ$ ) the projections of the carbonyl groups, through the metal centre (dotted lines in H) are the best indication of the ligand orientation. This suggests that C(6) is the eclipsed ring carbon atom and hence should be the weakest bond, as is in fact observed. The values of  $\psi$  and  $\Delta$  are  $2.3^\circ$  and  $0.08\text{\AA}$ , representing a slip of the metal across the  $C_5$  face, away from C(6). There are however some indications of rotational disorder in the ring. The final thermal parameters (Appendix 3) for the ring carbon atoms are high and the three highest residuals in the final  $\Delta F$  synthesis lie between atoms C(8) and C(9), C(9) and C(5), and C(5) and C(6). Refinement of a model using two independent rings (as performed for CPPHAL, Chapter 3) would not converge satisfactorily, and thus the current model was adopted. The rings were not idealised to regular pentagons since this would obscure the asymmetric bonding within the ligand, an important feature of these complexes.

In CPMOME the  $Mo(CO)_2$  is typical of this moiety having standard bond lengths and angles, and it subtends an angle of  $32^\circ$  with the allyl  $C_3$  fragment and  $138.3^\circ$  with the Cp ring. This latter value is significantly less than that for TRIMET ( $156.4^\circ$ ), presumably reflecting the differing steric requirements of Cp and Cp\*.

Figure 5.5 is a view of one unit cell and contents viewed almost down the unique axis  $b$  to demonstrate the monoclinic angle  $\beta$ . As may be seen, the complex exists as

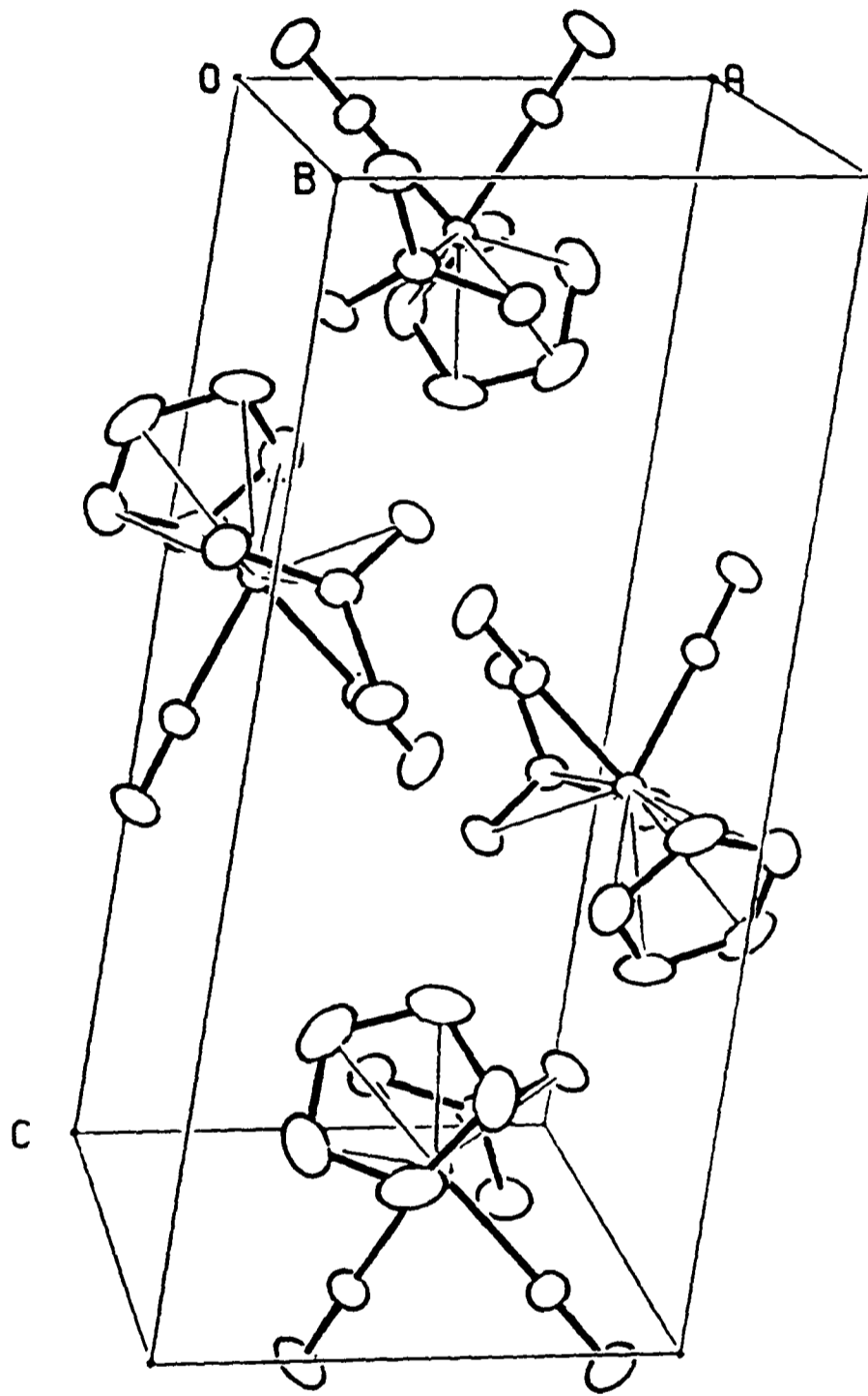


Fig. 5.5 Packing Diagram of  $(\eta^5\text{-C}_5\text{H}_5)\text{Mo}(\text{CO})_2(\eta^3\text{-2-Me-C}_3\text{H}_4)$ .

isolated discrete molecules. The only significant contact being between O(2) and H(6) at  $-1/2+x, 1/2-y, -1/2+z$ , a distance of 2.50(3)Å with an angle of 113.1(9)° at the oxygen.

#### 5.4 Solid state structure of $(\eta^4\text{-C}_4\text{H}_6)\text{Mo}(\text{Cl})_2(\eta^5\text{-C}_5\text{H}_5)$ : CPMOBUT:-

A perspective view of the molecule, demonstrating the numbering scheme is presented in Figure 5.6. Table 5.7 lists interatomic distances and interbond angles.

The complex has nearly  $C_s$  symmetry about the plane that bisects the Cl-Mo-Cl angle. Only the Cp ring violates this to any significant degree, although the thermal parameters ( Appendix 3 ) indicate there may be some rotational disorder, which, as in the case of CPMOME, has not been modeled.

The conformation of the coordinated *cis*-butadiene ligand to the  $\text{Mo}(\text{Cl})_2$  fragment is *endo*<sup>165</sup>. This is consistent with other reported  $\text{CpMX}_2(\text{diene})$  structures  $\text{CpNb}(\text{Cl})_2(\eta^4\text{-C}_4\text{H}_2\text{Me}_4)$ , 49<sup>178</sup> and  $[\text{CpMo}(\text{dppe})(\eta^4\text{-C}_6\text{H}_8)]^+$ , 50<sup>179</sup> and is also that conformation predicted by EHMO calculations ( Chapter 6 ).

Within the diene moiety the C(2)-C(3) bond ( 1.364(5)Å ) is shorter than either the C(1)-C(2) or C(3)-C(4) bonds ( 1.413(5)Å and 1.406(6)Å respectively ). This contrasts with the lengths found in the free ligand<sup>180</sup> but is consistent with a large number of coordinated diene fragments that have been structurally studied<sup>181-185</sup>. However, in contrast to the norm, the  $\text{M}-\text{C}_{(\text{outer})}$  bonds are shorter than the  $\text{M}-\text{C}_{(\text{inner})}$  ( 2.236(4)/2.231(4)Å cf. 2.320(4)/2.319(4)Å ). This feature may be expressed as a tilt of the butadiene, out of the plane parallel to the  $\text{Mo}(\text{Cl})_2$  fragment, by 30.7° ( Table 5.8 ). A similar trend in  $\text{M}-\text{C}_{(\text{diene})}$  bond distances has been observed in  $\text{Cp}_2\text{Zr}(\text{diene})$  complexes<sup>186</sup> and has been



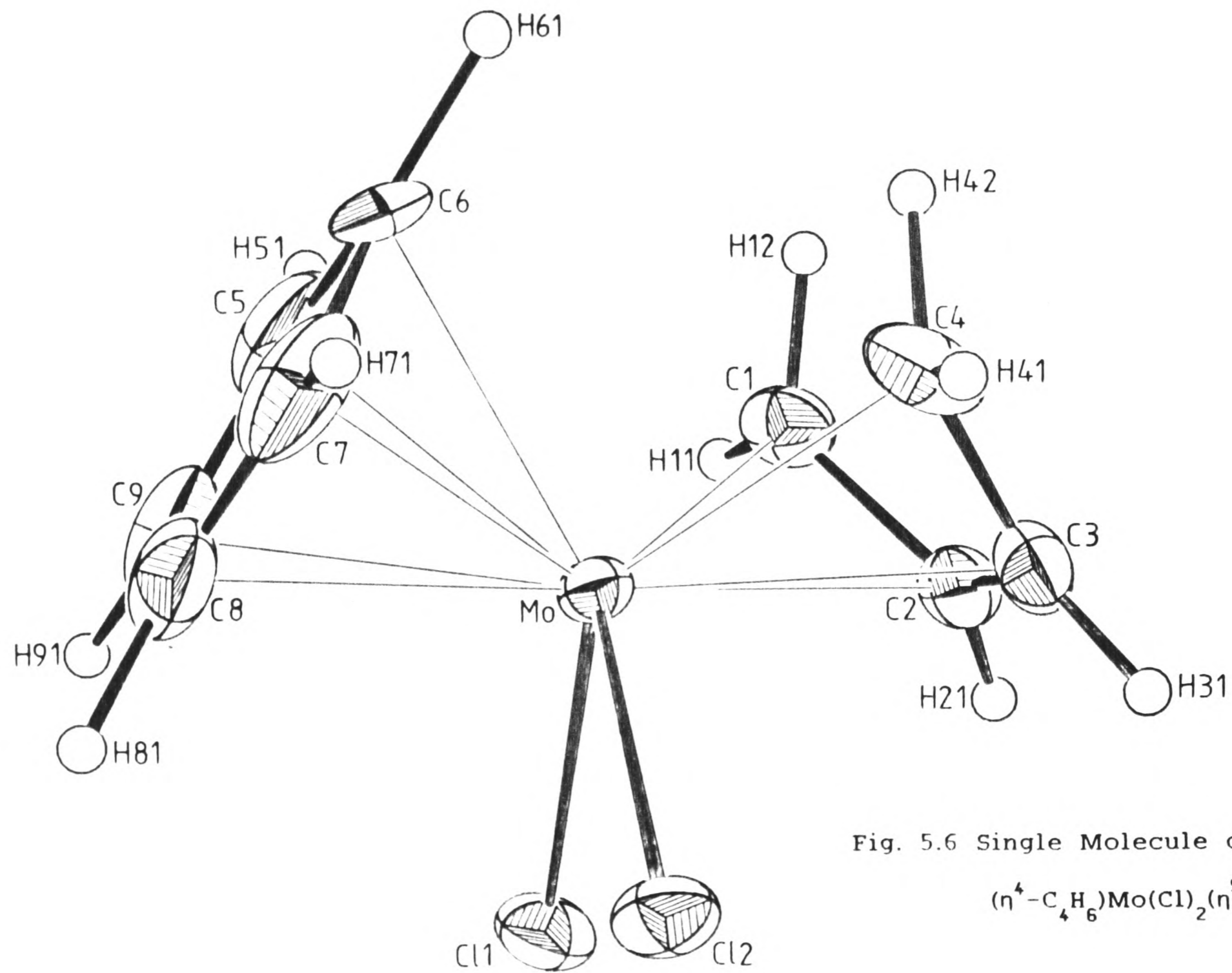


Fig. 5.6 Single Molecule of  
 $(\eta^4\text{-C}_4\text{H}_6)\text{MoCl}_2(\eta^5\text{-C}_5\text{H}_5)$ , CPMOBUT.

Table 5.7a Inter-Atomic Distances ( Å ) for CPMOBUT.

Mo - Cl(1)	2.4352(10)	Mo - C(9)	2.351(6)
Mo - Cl(2)	2.4333(9)	C(1) - C(2)	1.413(5)
Mo - C(1)	2.236(4)	C(2) - C(3)	1.364(5)
Mo - C(2)	2.320(4)	C(3) - C(4)	1.406(6)
Mo - C(3)	2.319(4)	C(5) - C(6)	1.388(9)
Mo - C(4)	2.231(4)	C(5) - C(9)	1.286(8)
Mo - C(5)	2.326(6)	C(6) - C(7)	1.530(9)
Mo - C(6)	2.285(7)	C(7) - C(8)	1.344(7)
Mo - C(7)	2.291(6)	C(8) - C(9)	1.334(7)
Mo - C(8)	2.308(5)		
C(1) - H(11)	0.96(5)	C(3) - H(31)	0.95(5)
C(1) - H(12)	0.97(5)	C(4) - H(41)	0.86(5)
C(2) - H(21)	0.77(5)	C(4) - H(42)	1.02(5)

Table 5.7b Inter-bond Angles ( ° ) for CPMOBUT.

Cl(1) - Mo - Cl(2)	86.24(3)	C(3) - Mo - C(9)	166.61(17)
Cl(1) - Mo - C(1)	84.33(10)	C(4) - Mo - C(5)	113.15(18)
Cl(1) - Mo - C(2)	78.43(10)	C(4) - Mo - C(6)	83.20(20)
Cl(1) - Mo - C(3)	101.50(10)	C(4) - Mo - C(7)	90.76(18)
Cl(1) - Mo - C(4)	137.44(11)	C(4) - Mo - C(8)	124.30(16)
Cl(1) - Mo - C(5)	98.90(15)	C(4) - Mo - C(9)	139.82(18)
Cl(1) - Mo - C(6)	133.77(17)	C(5) - Mo - C(6)	35.03(23)
Cl(1) - Mo - C(7)	130.57(14)	C(5) - Mo - C(7)	59.60(20)
Cl(1) - Mo - C(8)	96.61(12)	C(5) - Mo - C(8)	55.37(19)
Cl(1) - Mo - C(9)	80.90(14)	C(5) - Mo - C(9)	31.92(20)
Cl(2) - Mo - C(1)	140.16(10)	C(6) - Mo - C(7)	39.07(22)
Cl(2) - Mo - C(2)	104.07(10)	C(6) - Mo - C(8)	58.61(21)
Cl(2) - Mo - C(3)	80.78(10)	C(6) - Mo - C(9)	56.71(22)
Cl(2) - Mo - C(4)	86.43(11)	C(7) - Mo - C(8)	33.98(18)
Cl(2) - Mo - C(5)	140.00(15)	C(7) - Mo - C(9)	57.23(20)
Cl(2) - Mo - C(6)	124.45(17)	C(8) - Mo - C(9)	33.25(18)
Cl(2) - Mo - C(7)	86.97(14)	Mo - C(1) - C(2)	75.19(22)
Cl(2) - Mo - C(8)	84.67(12)	Mo - C(2) - C(1)	68.72(21)
Cl(2) - Mo - C(9)	112.59(14)	Mo - C(2) - C(3)	72.87(23)
C(1) - Mo - C(2)	36.09(13)	C(1) - C(2) - C(3)	119.4(4)
C(1) - Mo - C(3)	63.49(14)	Mo - C(3) - C(2)	72.93(23)
C(1) - Mo - C(4)	75.11(15)	Mo - C(3) - C(4)	68.63(23)
C(1) - Mo - C(5)	79.77(18)	C(2) - C(3) - C(4)	118.3(4)
C(1) - Mo - C(6)	88.56(20)	Mo - C(4) - C(3)	75.43(24)
C(1) - Mo - C(7)	127.45(17)	Mo - C(5) - C(6)	70.9(4)
C(1) - Mo - C(8)	134.83(15)	Mo - C(5) - C(9)	75.1(4)
C(1) - Mo - C(9)	103.96(17)	C(6) - C(5) - C(9)	110.8(6)
C(2) - Mo - C(3)	34.19(14)	Mo - C(6) - C(5)	74.1(4)
C(2) - Mo - C(4)	62.96(14)	Mo - C(6) - C(7)	70.7(3)
C(2) - Mo - C(5)	115.85(17)	C(5) - C(6) - C(7)	103.6(5)
C(2) - Mo - C(6)	118.50(20)	Mo - C(7) - C(6)	70.3(3)
C(2) - Mo - C(7)	150.17(17)	Mo - C(7) - C(8)	73.7(3)
C(2) - Mo - C(8)	169.49(15)	C(6) - C(7) - C(8)	102.7(5)
C(2) - Mo - C(9)	136.24(17)	Mo - C(8) - C(7)	72.3(3)
C(3) - Mo - C(4)	35.94(15)	Mo - C(8) - C(9)	75.1(3)
C(3) - Mo - C(5)	135.42(18)	C(7) - C(8) - C(9)	112.3(5)
C(3) - Mo - C(6)	115.75(20)	Mo - C(9) - C(5)	73.0(4)
C(3) - Mo - C(7)	125.48(17)	Mo - C(9) - C(8)	71.6(3)
C(3) - Mo - C(8)	155.87(15)	C(5) - C(9) - C(8)	110.5(5)
Mo - C(1) - H(11)	116.8(30)	Mo - C(3) - H(31)	125.5(28)
Mo - C(1) - H(12)	115.0(31)	C(2) - C(3) - H(31)	120.7(28)
H(11) - C(1) - H(12)	103.8(43)	H(31) - C(3) - C(4)	120.8(28)
H(11) - C(1) - C(2)	120.5(30)	Mo - C(4) - H(41)	119.4(33)
H(12) - C(1) - C(2)	124.0(31)	Mo - C(4) - H(42)	105.0(26)
Mo - C(2) - H(21)	119.8(37)	C(3) - C(4) - H(41)	113.0(33)
C(1) - C(2) - H(21)	119.4(37)	C(3) - C(4) - H(42)	117.3(26)
H(21) - C(2) - C(3)	120.1(37)	H(41) - C(4) - H(42)	118.9(42)

Table 5.8 Least-Squares Planes Data for CPMOBUT

(a) Coefficients

Plane 1: C(1),C(2),C(3),C(4).

Equation:  $0.0435X + 3.9077Y + 10.6581Z = 8.3813\text{\AA}$

R.M.S. Deviation =  $0.0028\text{\AA}$

Plane 2: C(5), C(6), C(7), C(8), C(9).

Equation:  $-0.0385X + 8.4649Y + 1.6687Z = -2.5545\text{\AA}$

R.M.S. Deviation =  $0.0012\text{\AA}$

Plane 3: Mo, Cl(1), Cl(2).

Equation:  $-3.1544x + 7.9997y + 6.7937z = 3.3535\text{\AA}$

(b) Atomic Deviations (  $\text{\AA}$  )

Plane 1: Mo -1.7676, C(1) -0.0018, C(2) 0.0036,  
C(3) -0.0035, C(4) 0.0018, H(11) -0.1819,  
H(12) 0.6564, H(21) -0.1345, H(31) -0.0840,  
H(41) -0.1195, H(42) 0.6399.

Plane 2: Mo 1.9904, C(5) 0.0003, C(6) 0.0007,  
C(7) -0.0014, C(8) 0.0018, C(9) -0.0013

(c) Dihedral angles (  $^\circ$  )

Plane 1, Plane 2 69.4  
Plane 1, Plane 3 38.8  
Plane 2, Plane 3 30.7

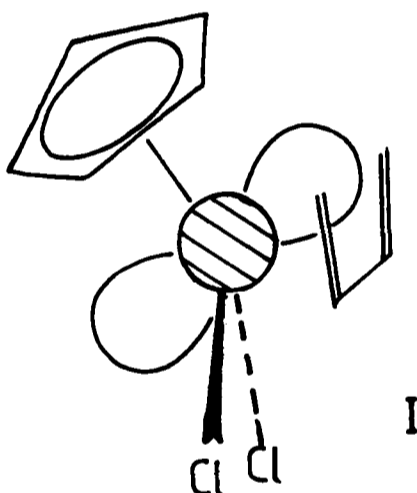
interpreted as an approach towards a  $\sigma^2, \pi$ - bonding mode for the diene. In CPMOBUT the the distortion is not as marked as in the zirconium species, but it does represent distortion towards a metallacyclopentene along pathway 5.4. The tilt is also reproduced by overlap populations in the theoretical study ( Chapter 6 ) where, even in the parallel form where the angle of tilt is  $0^\circ$ , there are indications of stronger bonds to the outer carbon atoms ( C(1) and C(4) ). Upon tilting to the experimentally observed geometry the difference in C-C overlaps changes such that the C(2)-C(3) bond becomes stronger whilst the C(1)-C(2) and C(3)-C(4) bonds weakens. However, the calculations still indicate that the inner bond is weaker than the outer two, in contrast to the inference from the crystallographic results. This may be due to the fact that the model, using planar  $sp^2$  type carbon atoms, is inappropriate. In the crystallographically determined structure none of the hydrogen atoms lie in the  $C_4$  plane. The four *syn* hydrogens ( H(11), H(21), H(31), H(41) ) are bent towards the metal by between  $5^\circ$  and  $11^\circ$ , whilst those in the *anti* positions ( H(12) and H(42) ) bend away, by  $42^\circ$  and  $39^\circ$  respectively. These compare well with the EHMO-calculated values<sup>183</sup> (  $18^\circ$  for *syn* and  $38^\circ$  for *anti* ) and with other structurally characterised coordinated butadienes<sup>182-184</sup>. This has been interpreted as

(a) a twist about the C-C bond

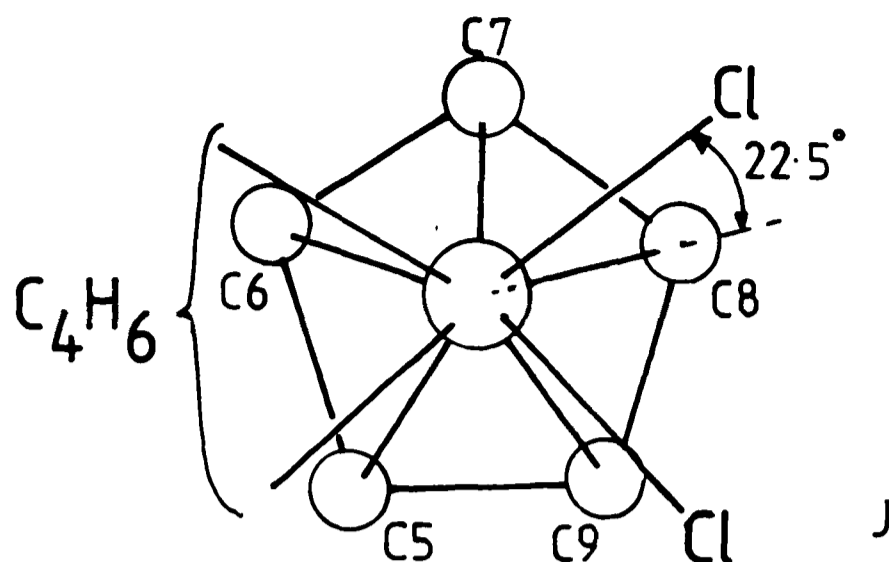
(b) significant  $sp^3$  character of the peripheral carbon atoms.

Both these effects would result in reduction of conjugation within the diene and lead to the relative C-C bond lengths observed. Intramolecular steric interactions have little effect, the H-anti...H-anti contact being 2.24(7)Å and the three H-syn...H-syn contacts being 2.28(7)Å, 2.24(7)Å and 2.23(6)Å ( Table 5.9 ).

The Cl-M-Cl angle ( 86.24(3)° ) is significantly less than that found in the sixteen electron species 49<sup>178</sup> and this may be readily explained by the fact that the seventeenth electron in CPMOBUT occupies an orbital that is bonding between the two chlorine atoms, I.



As with both TRIMET and CPMOME the cyclopentadienyl ligand is not symmetrically bound to the metal. The Mo-C bond lengths are in the order Mo-C(9) > Mo-C(5) > Mo-C(8) > Mo-C(7) ≈ Mo-C(6). Analysis of the Cp-ML<sub>4</sub> conformation reveals that it is neither a true staggered nor eclipsed conformation. The ring appears to be rotated by ≈ 22.5° from the eclipsed geometry, J.



However, the general direction of the slippage seems to be towards a point on the C(6)-C(7) bond, by 0.12Å (  $\Delta$  ), corresponding to a tilt (  $\Psi$  ) of 3.4°, with C(9) lifting away from the metal. The fact that the longest C-C ring distance is C(6)-C(7) is consistent with this. Similar, previously reported, structures are CPMOME, 42<sup>168</sup>, 43<sup>169</sup>, 44<sup>170</sup>, 45<sup>171</sup>.

In CPMOBUT the  $C_5 - Mo(Cl)_2$  interplanar angle ( 149.3° ) is intermediate between that for TRIMET and CPMOME.

Figure 5.7 is a perspective view of the contents of one unit cell. There are significant intermolecular hydrogen-chlorine contacts ( Table 5.9 ) in the range 2.72-2.85Å ( sum van der Waals radii = 3.0Å ) between molecules related by the inversion centre and the *n*-glide plane.

Table 5.9 Significant Non-Bonded Contacts for CPMOBUT

(a) Intramolecular ( Å )

Cl(1).....H(21)	2.82(5)
H(11).....H(21)	2.28(7)
H(12).....H(42)	2.25(7)
H(21).....H(31)	2.24(7)
H(31).....H(41)	2.23(7)

(b) Intermolecular

Contact Cl...H	Symm H	Dist.(Å)	Angle Mo-Cl...H (°)
Cl(1)...H(31)	-X,-Y,-Z	2.85(5)	98.8(9)
Cl(1)...H(12)	X-0.5,0.5-Y,Z-0.5	2.72(5)	148.4(11)
Cl(1)...H(42)	X-0.5,0.5-Y,Z-0.5	2.76(5)	117.2(9)
Cl(2)...H(61)	X-0.5,0.5-Y,Z-0.5	2.773(6)	107.40(15)



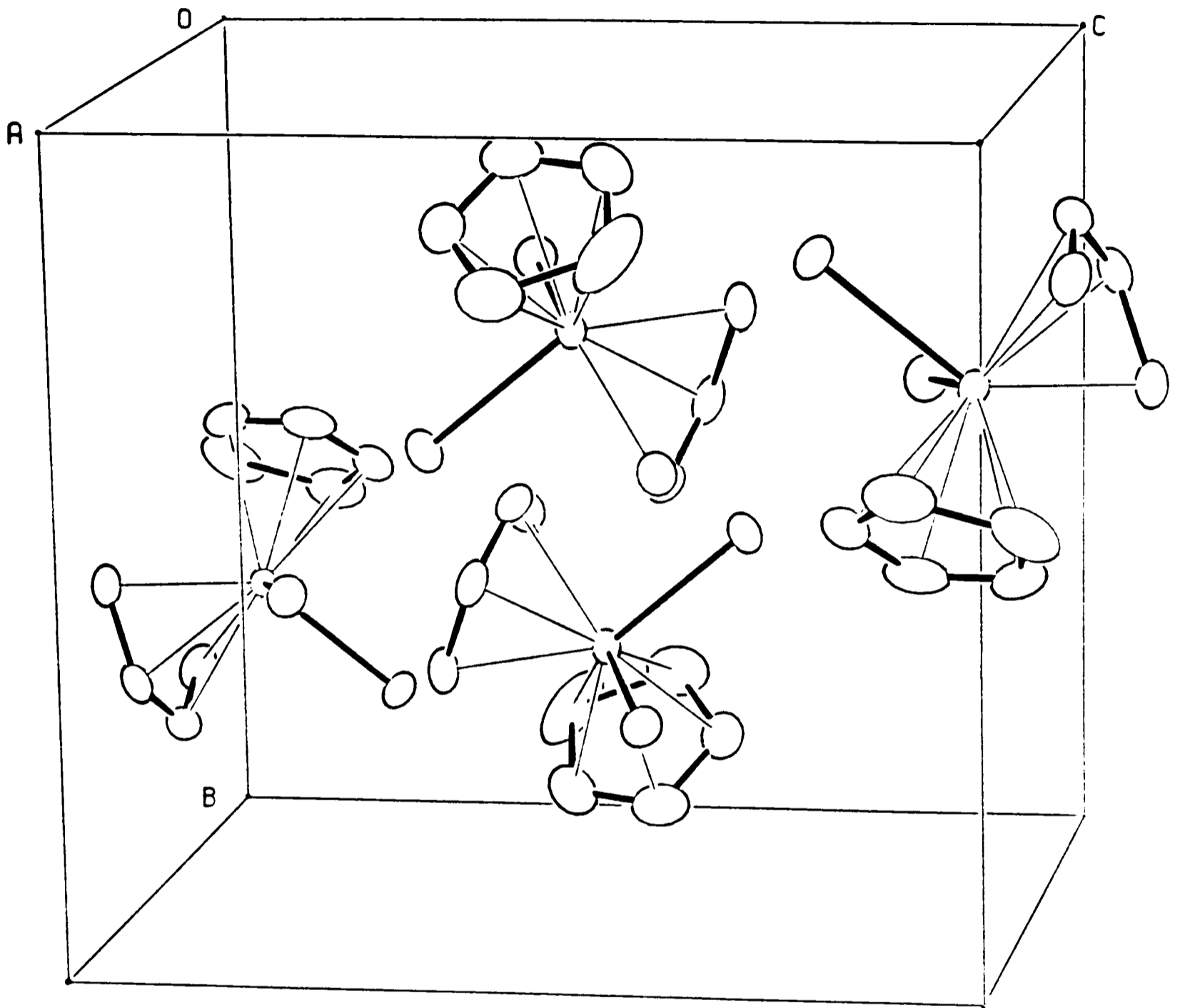


Fig. 5.7 Packing Diagram of  $(\eta^4\text{-C}_4\text{H}_6)\text{Mo}(\text{Cl})_2(\eta^5\text{-C}_5\text{H}_5)$ .

## 5.5 Experimental:-

The sample of  $\text{CpMo(CO)}_2(\eta^3\text{-2-Me-C}_3\text{H}_4)$  was prepared by the literature method<sup>56</sup> in a manner analogous to IX (Chapter 2). Crystals were obtained from diethyl ether/heptane (1:3 slow evaporation). Preliminary crystallographic studies, data collection and reduction and structure solution and refinement for CPMOME and CPMOBUT were carried out as outlined above (Chapters 2 and 3). The relevant parameters are given in Tables 5.11, 5.12 and 5.13. Final atomic coordinates are given in Tables 5.14 and 5.15 for CPMOME and CPMOBUT respectively with thermal parameters in Appendix 3.

In the case of CPMOME the cyclopentadienyl ring showed some degree of disorder. However, attempts to model this as two independent  $\text{C}_5$  rings as was performed for CPPHAL (Chapter 3) would not lead to satisfactory refinement. The three highest residuals in the final  $\Delta F$  synthesis occur between C(8) and C(9), C(9) and C(5) and C(5) and C(6). Also the thermal parameters for the ring carbons are large, the direction of the elongation being tangential to the ring (see Figure 5.4). All hydrogen positions (including Cp H's) were located in a  $\Delta F$  map and were subsequently refined with other parameters with a fixed temperature factor of  $U = 0.04\text{\AA}^2$ .

The data collection and initial solution of the structure of TRIMET was performed by D. M. Sharaiha<sup>161</sup> at The City University, London, using diffractometer data

(recorded at 268±1K ) provided by M. B. Hursthouse, Queen Mary College, University of London. Data collection parameters for this study are given, for comparative purposes, in Table 5.12; crystal data and final agreement factors are given in Tables 5.11 and 5.13 respectively.

The disordered fluorines of the  $\text{BF}_4$  counter-ion were given a fixed thermal parameter ( $U = 0.10\text{\AA}^2$ ) and the SOF's of the fourteen partial atoms were refined, giving a sum of 3.9. TMM hydrogen atoms were located in a  $\Delta F$  synthesis to which the contribution from low-angle reflections were artificially enhanced and refined with a fixed temperature factor of  $U = 0.08\text{\AA}^2$ . Final positional parameters and SOF's are listed in Table 5.16 with refined thermal parameters in Appendix 3.

Table 5.10 Crystal Data

	CPMOME	CPMOBUT	TRIMET
<b>M</b>	272.2	286.0	427.7
<b>a/Å</b>	6.1105(9)	8.1480(20)	12.822(2)
<b>b/Å</b>	12.7885(22)	10.824(3)	12.311(3)
<b>c/Å</b>	13.7247(24)	11.5059(25)	22.660(4)
<b>α/°</b>	90.0	90.0	90.0
<b>β/°</b>	98.787(13)	96.304(20)	90.0
<b>γ/°</b>	90.0	90.0	90.0
<b>V/Å<sup>3</sup></b>	1059.9	1008.6	3576.9
<b>D<sub>c</sub>/gcm<sup>-3</sup></b>	1.705	1.883	1.583
<b>F(000)</b>	544	564	1728
<b>μ(Mo-Kα)/cm<sup>-1</sup></b>	10.83	17.42	6.9
<b>Space Group</b>	<i>P2<sub>1</sub>/n</i>	<i>P2<sub>1</sub>/n</i>	<i>Pbca</i>
<b>Z</b>	4	4	8

Table 5.11 Data Collection Parameters

	CPMOME	CPMOBUT	TRIMET
$\theta_h$ (°)	17.0-18.0	11.0-12.0	14.0-15.0
T (K)	188	185	268
$\theta_d$ (°)	1.0-30.0	1.0-30.0	1.5-27.0
quad	h k l -h -k ±1	h k ±1 -h -k ±1	h k l
A	0.80	0.80	0.85
B	0.35	0.35	0.35
C	0.5	0.5	1.0
D	33	50	33
$t_{max}$	90	90	60
$t_{tot}$	115	143	45
$N_c$	6998	6574	8393
$R_{merg}$	0.0218	0.0381	-
$N_d$	3083	2944	3893
N	2869	2716	2747
E	2	2	2
Abs. Corr.	No	Yes	No

Table 5.12 Refinement and Final Agreement Factors.

	CPMOME	CPMOBUT	TRIMET
G	0.0004524	0.000424	0.035
$N_p$	163	127	256
R	0.0250	0.0367	0.0674
$R_w$	0.0469	0.0532	0.0983
S	0.9764	1.2321	1.56
min	-1.08	-0.87	-0.67
max	0.41	1.21	0.68

**Table 5.13 Fractional Coordinates of Atoms  
with Standard Deviations for CPMOME**

	x	y	z
Mo	0.46349(2)	0.19301(1)	0.12509(1)
C(1)	0.2065(4)	0.29750(17)	0.18619(19)
C(2)	0.3405(4)	0.36310(14)	0.13794(14)
C(3)	0.5683(4)	0.36159(16)	0.17359(17)
C(4)	0.2461(5)	0.42399(19)	0.04816(18)
C(5)	0.7513(4)	0.07415(24)	0.16929(24)
C(6)	0.7330(5)	0.12972(20)	0.25498(24)
C(7)	0.5294(6)	0.11132(22)	0.28080(17)
C(8)	0.4165(4)	0.04157(21)	0.21231(25)
C(9)	0.5559(6)	0.01847(18)	0.14263(19)
C(10)	0.2145(3)	0.16906(18)	0.01913(16)
C(11)	0.5812(3)	0.24101(15)	0.00806(14)
O(1)	0.0755(3)	0.15168(19)	-0.04488(17)
O(2)	0.6451(3)	0.27005(18)	-0.06222(14)
H(11)	0.237(6)	0.2885(23)	0.251(3)
H(12)	0.052(6)	0.2984(19)	0.151(3)
H(31)	0.618(5)	0.3539(22)	0.2412(23)
H(32)	0.683(5)	0.3974(22)	0.1336(23)
H(41)	0.343(5)	0.4280(22)	-0.0021(23)
H(42)	0.113(5)	0.3921(23)	0.0150(23)
H(43)	0.227(5)	0.4946(22)	0.0695(22)
H(5)	0.863(5)	0.0828(23)	0.1395(22)
H(6)	0.840(6)	0.1808(21)	0.302(3)
H(7)	0.476(5)	0.1252(22)	0.3303(23)
H(8)	0.321(5)	0.0187(24)	0.2168(22)
H(9)	0.528(5)	-0.0228(23)	0.0908(22)

**Table 5.14 Fractional Coordinates of Atoms  
with Standard Deviations for CPMOBUT**

	x	y	z
Mo	0.72797(3)	0.26401(2)	0.52076(2)
Cl(1)	0.44563(12)	0.22449(9)	0.43620(8)
Cl(2)	0.74390(10)	0.40730(8)	0.35943(7)
C(1)	0.6220(5)	0.2513(4)	0.6915(3)
C(2)	0.5778(5)	0.3704(4)	0.6485(3)
C(3)	0.6977(6)	0.4484(4)	0.6188(3)
C(4)	0.8624(5)	0.4072(4)	0.6337(3)
C(5)	0.8038(8)	0.0633(5)	0.5752(5)
C(6)	0.9400(9)	0.1401(7)	0.5971(5)
C(7)	0.9729(5)	0.1835(5)	0.4752(6)
C(8)	0.8534(6)	0.1265(4)	0.4051(4)
C(9)	0.7569(7)	0.0569(4)	0.4649(5)
H(11)	0.539(6)	0.189(5)	0.698(4)
H(12)	0.702(7)	0.236(4)	0.759(5)
H(21)	0.486(6)	0.386(5)	0.630(4)
H(31)	0.670(6)	0.526(4)	0.583(4)
H(41)	0.929(6)	0.456(5)	0.604(4)
H(42)	0.902(5)	0.363(4)	0.710(4)
H(51)	0.7449	0.0154	0.6418
H(61)	1.0070	0.1637	0.6803
H(71)	1.0685	0.2446	0.4513
H(81)	0.8373	0.1360	0.3112
H(91)	0.6538	0.0027	0.4262



**Table 5.15 Fractional Coordinates of Atoms  
with Standard Deviations for TRIMET**

	x	y	z	SOF
Mo	0.01524(6)	0.24354(5)	0.07924(3)	1.0000
C(1)	0.0534(8)	0.2567(8)	0.1815(4)	1.0000
C(2)	-0.0527(7)	0.2863(9)	0.1709(4)	1.0000
C(3)	-0.1066(7)	0.1932(7)	0.1483(4)	1.0000
C(4)	-0.0365(6)	0.1066(7)	0.1431(4)	1.0000
C(5)	0.0635(7)	0.1481(9)	0.1647(4)	1.0000
C(6)	0.1339(9)	0.3221(11)	0.2112(5)	1.0000
C(7)	-0.1004(10)	0.3879(10)	0.1926(7)	1.0000
C(8)	-0.2228(6)	0.1850(10)	0.1407(5)	1.0000
C(9)	-0.0598(10)	-0.0091(8)	0.1322(5)	1.0000
C(10)	0.1570(9)	0.0760(11)	0.1774(6)	1.0000
C(101)	-0.0644(7)	0.1454(8)	0.0236(4)	1.0000
O(101)	-0.1120(6)	0.0916(7)	-0.0059(4)	1.0000
C(102)	-0.0844(8)	0.3660(8)	0.0584(5)	1.0000
O(102)	-0.1425(7)	0.4303(7)	0.0475(5)	1.0000
C(11)	0.1541(8)	0.2879(9)	0.0264(5)	1.0000
C(22)	0.1717(8)	0.1747(10)	0.0431(5)	1.0000
C(33)	0.1586(8)	0.3627(9)	0.0724(4)	1.0000
C(44)	0.0755(10)	0.2977(13)	-0.0163(5)	1.0000
B	0.0572(7)	-0.3231(13)	0.1621(6)	1.0000
F(1)	-0.0419(19)	-0.3068(22)	0.1669(12)	0.4314
F(2)	0.0826(15)	-0.3899(15)	0.1142(9)	0.5538
F(3)	0.091(4)	-0.394(4)	0.2069(22)	0.2238
F(4)	0.115(3)	-0.2286(23)	0.1608(12)	0.3358
F(5)	-0.041(3)	-0.272(3)	0.1479(15)	0.3320
F(6)	0.1157(24)	-0.2377(21)	0.1324(12)	0.3323
F(7)	0.113(4)	-0.244(3)	0.1920(24)	0.1779
F(8)	0.009(5)	-0.424(6)	0.134(4)	0.1009
F(9)	-0.042(3)	-0.366(4)	0.1650(19)	0.2077
F(10)	0.111(3)	-0.331(3)	0.1072(18)	0.2075
F(11)	0.1042(17)	-0.3481(16)	0.2133(9)	0.4542
F(12)	0.074(4)	-0.413(3)	0.1275(20)	0.2326
F(13)	0.065(3)	-0.380(4)	0.2147(22)	0.2313
F(14)	-0.034(6)	-0.252(5)	0.168(3)	0.1644
H(21)	0.234(6)	0.177(6)	0.074(4)	1.0000
H(22)	0.172(6)	0.128(6)	0.008(4)	1.0000
H(31)	0.195(6)	0.348(6)	0.119(4)	1.0000
H(32)	0.117(6)	0.427(6)	0.087(4)	1.0000
H(41)	0.033(6)	0.369(6)	-0.027(5)	1.0000
H(42)	0.050(7)	0.257(6)	-0.046(5)	1.0000

**Table 5.15b Calculated H-atom Coordinates**

	<b>x</b>	<b>y</b>	<b>z</b>
H(61)	0.1206	0.3205	0.2582
H(62)	0.1316	0.4051	0.1957
H(63)	0.2094	0.2874	0.2016
H(71)	-0.1809	0.3910	0.1786
H(72)	-0.0588	0.4567	0.1748
H(73)	-0.0969	0.3902	0.2402
H(81)	-0.2584	0.2638	0.1465
H(82)	-0.2535	0.1294	0.1732
H(83)	-0.2399	0.1549	0.0970
H(91)	0.0123	-0.0542	0.1293
H(92)	-0.1024	-0.0172	0.0913
H(93)	-0.1062	-0.0405	0.1681
H(101)	0.1442	-0.0040	0.1593
H(102)	0.1679	0.0700	0.2246
H(103)	0.2257	0.1114	0.1576

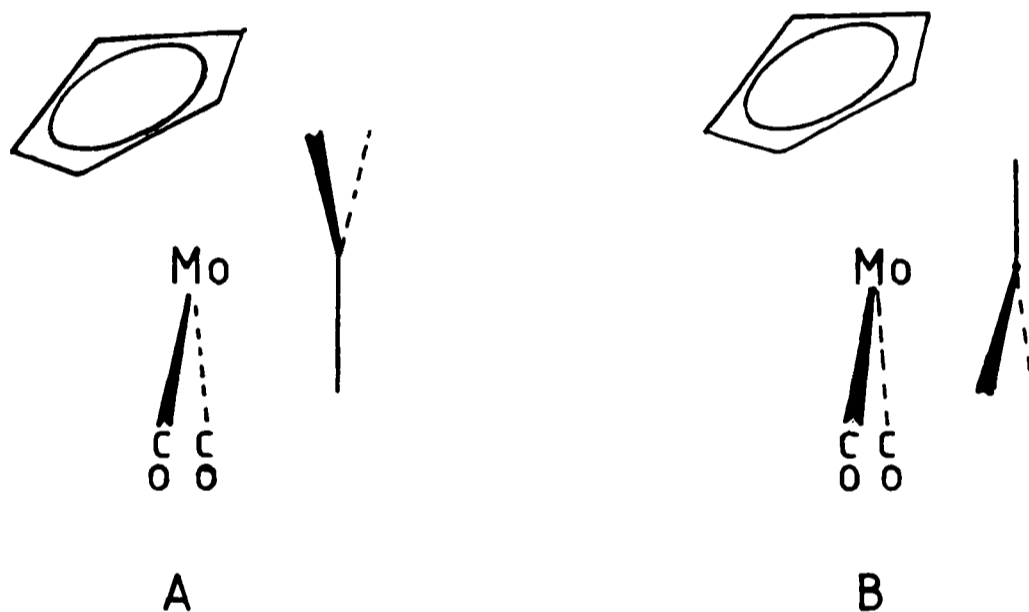
## CHAPTER 6

### MOLECULAR ORBITAL STUDIES ON $\text{CPMO}(\text{L})_2-(\text{C}_4\text{H}_6)$ SPECIES

#### 6.1 Introduction:-

In the complex  $(\eta^4-\text{C}(\text{CH}_2)_3)\text{Fe}(\text{CO})_3$ , 51, the TMM adopts a staggered conformation with respect to the  $\text{Fe}(\text{CO})_3$  fragment<sup>155</sup>, it is pyramidal<sup>155</sup> and there is a large barrier to ligand rotation<sup>187</sup>. Albright and Hoffmann<sup>148</sup> have determined the electronic origins of these features.

In TRIMET there are also two possible limiting conformations, *syn*, A, and *anti*, B, with respect to the  $\text{Mo}(\text{CO})_2$  fragment, which maintain the  $\text{C}_s$  symmetry of the complex.



That observed in the crystal structure ( Chapter 5 ) is *syn*. The TMM is pyramidal and in the case of the Cp analogue, the barrier to rotation is ca.  $41.4\text{kJmol}^{-1}$ .

Similarly, as was noted in scheme 5.4, there are two possible conformations of  $\text{CpMo}(\text{Cl})_2(\eta^4-\text{C}_4\text{H}_6)$ , *endo* and *exo*<sup>165</sup>, that observed being the *endo* form.

To probe the electronic origins of these features EHMO calculations<sup>129</sup> have been carried out on idealised,  $\text{C}_s$

symmetry, models of  $\text{CpMo(CO)}_2\text{TMM}$  and  $\text{CpMo(Cl)}_2(\eta^4\text{-C}_4\text{H}_6)$  according to the parameters in Table 6.1. TRIMET was simplified to the Cp analogue for computational ease. The method of interpretation was similar to that used for the allyl system ( Chapter 4 ) employing a fragment molecular orbital approach<sup>131</sup> and symmetry arguments<sup>132</sup>. Again all calculations were performed using the modified Wolfsberg-Helmholtz formula<sup>135</sup> and orbital coefficients from Table 4.2. The analysis is based on the frontier orbitals of the metal fragments (  $\text{CpMoL}_2$  ) and the ligands ( TMM and butadiene ).

Table 6.1 Geometrical Parameters for  $\text{CpMoL}_2-(\text{C}_4\text{H}_6)$  species.

(a) Bond Lengths ( Å ).

Mo-Z	2.02
Mo-Cl	2.43
Mo-C(O)	1.97
Mo-C <sub>(term)</sub>	2.36
Mo-C <sub>(cent)</sub>	1.90 ( flat TMM )
Mo-C <sub>(cent)</sub>	2.2132 ( bent TMM )
Mo-Cent <sub>(But)</sub>	2.20
C-Z	1.21
C-C <sub>(But)</sub>	1.37
C-C <sub>(TMM)</sub>	1.40
C-O	1.15
C-H	1.09

(b) Interbond Angles ( ° ).

L-Mo-L	90.0
Z-Mo-Cent	126.7
L-Mo-Cent	90.0
C-C-C	120.0
$\text{C}_4\text{-Mo(L)}_2$	0.0 ( unless otherwise stated ).
$\gamma$	12.0
$\psi$	12.0

Z = Centroid of  $\text{C}_5$  ring.

Cent = C. of G. of  $\text{C}_4$  fragment.

## 6.2 Metal fragment orbitals:-

The frontier orbitals of the metal fragments are, as may be expected, very similar. Those of  $\text{CpMo(CO)}_2^+$  have been reported previously<sup>14,139</sup> whereas those of  $\text{CpMo(Cl)}_2$  have not. Both may be derived by the same method as was used to generate the  $\text{MXY}_2\text{L}_2$  fragment used previously ( Chapter 4 ). Representations of the orbitals of both fragments are given in Figure 6.1, together with their relative energies. Contour plots, drawn with the PSI program package<sup>140</sup>, are given in Appendix 4.

As can be seen from Figure 6.1 there is a marked destabilisation of the  $1a'$ ,  $a''$  and  $2a'$  orbitals, with an interchange in the order of  $a''$  and  $2a'$ , on going from the dicarbonyl to the dihalide. The orbitals most affected are of the appropriate orientation for  $\pi$  interaction with the ligands ( Cl and CO ). The  $1a'$  orbital ( in the dicarbonyl species ) is 88%  $dx^2-y^2$  in character, whilst the  $2a'$  is 90%  $dyz$ , and  $a''$  is 92%  $dxz$ . It is the greater  $\pi$ -acceptor characteristics of the carbonyl groups that stabilises these orbitals relative to those in the dihalide species.

Both fragments possess a  $3a'$  orbital that is mainly  $dz^2/pz$  in character, an  $a''$  orbital that is almost totally  $dxz$  and a  $1a'$  that is a  $dx^2-dy^2/dz^2$  hybrid. Only the  $2a'$  orbital is significantly different in the two species, having a large amount of  $dx^2-y^2$  character in the dihalide, not present in the dicarbonyl, as well as contributions from  $dyz$  and  $dz^2$  that are present in both.

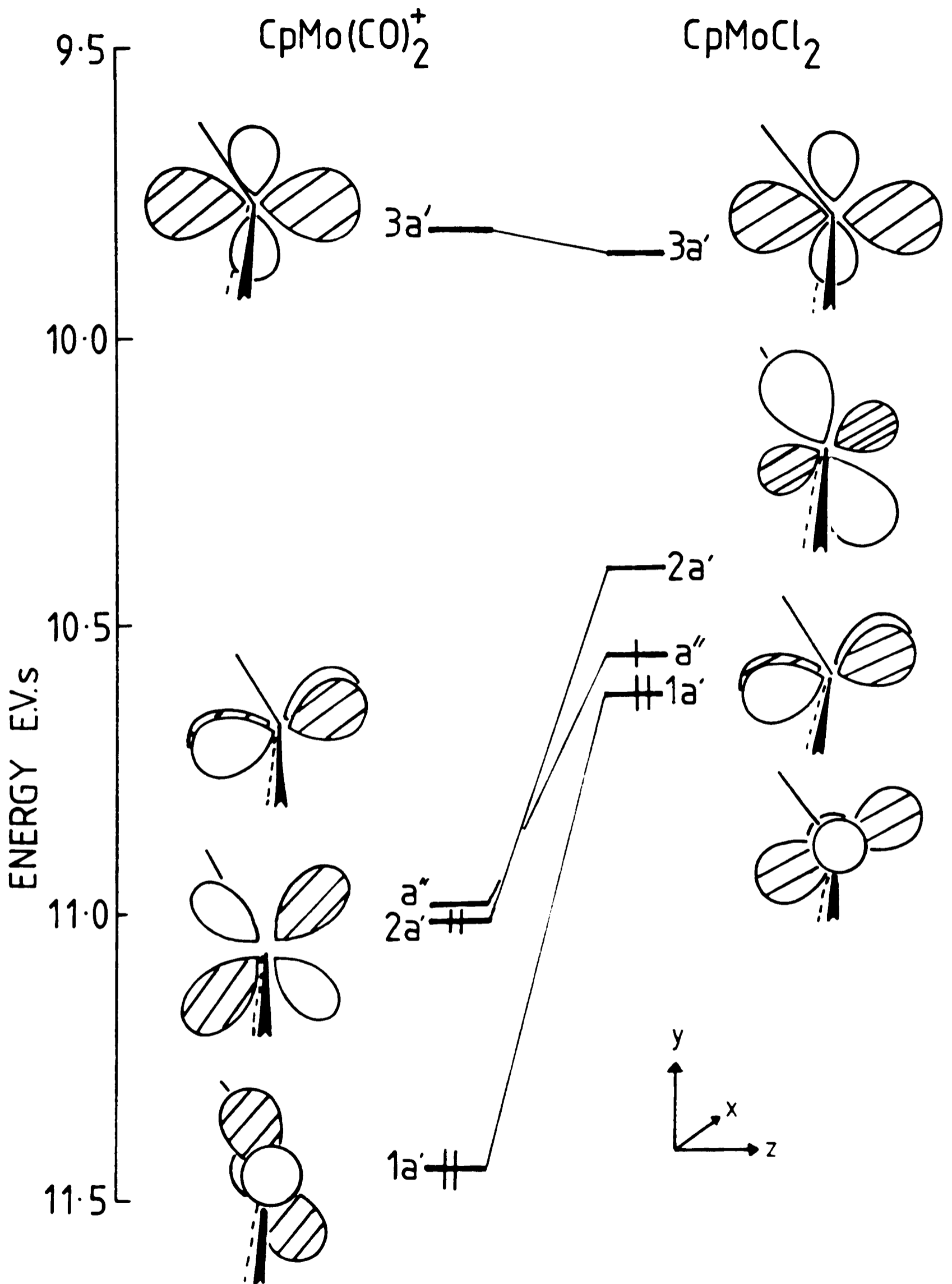


Fig. 6.1  $\text{CpMoL}_2$  Fragment Orbitals.

### 6.3 Ligand orbitals:-

The  $\pi$ -orbitals of both  $C_4H_6$  ligands, TMM ( planar ) and *cis*-butadiene, are shown in Figure 6.2, labelled in the  $C_s$  symmetry of the ultimate complex. Both are four-orbital, four-electron  $\pi$ -systems. In the case of butadiene there are two symmetric type orbitals, one of which is filled (  $1a'$  ) and the other empty (  $2a'$  ). Likewise, there are two antisymmetric orbitals, one filled and one empty (  $1a''$  and  $2a''$  respectively ).

In TMM there is a filled, symmetric, bonding  $1a'$  orbital, and an unfilled, symmetric, antibonding  $3a'$ . Intermediate in energy is the half filled, degenerate pair  $a''/2a'$  which has it's origins in the  $e''$  pair of  $D_{3h}$  TMM.

In the case of butadiene the nonplanarity of the H-substituents with the  $C_4$  framework results in a rehybridisation of the  $\pi$ -orbitals towards the coordinated metal<sup>114</sup>. This was not modelled in the present study.

In the case of TMM there is a non-planarity of the carbon skeleton as well as of the H-substituents, which results in a similar rehybridisation of the  $\pi$ -orbitals. Since this represents a major stereochemical feature which may be electronic in origin, both the flat and pyramidal forms of the ligand were studied.

All discussion is based on the ligand approaching the metal fragment from the positive  $z$  direction with the mirror plane of the complex coincident with the  $yz$  plane of the coordinate system.



TMM

BUTADIENE

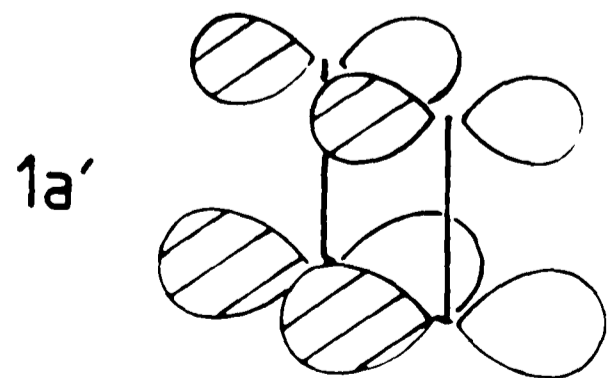
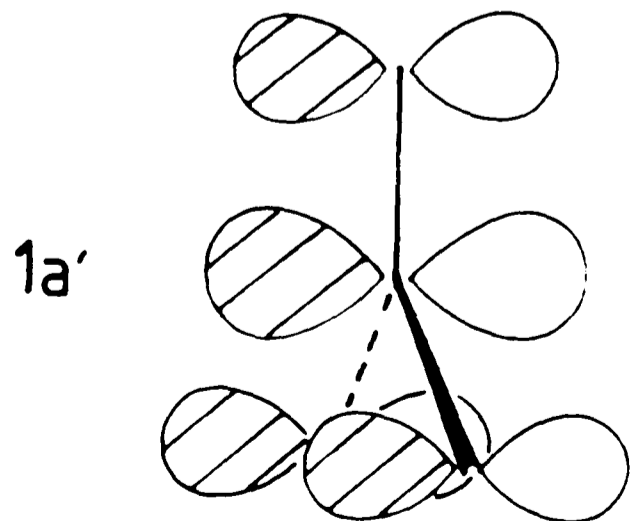
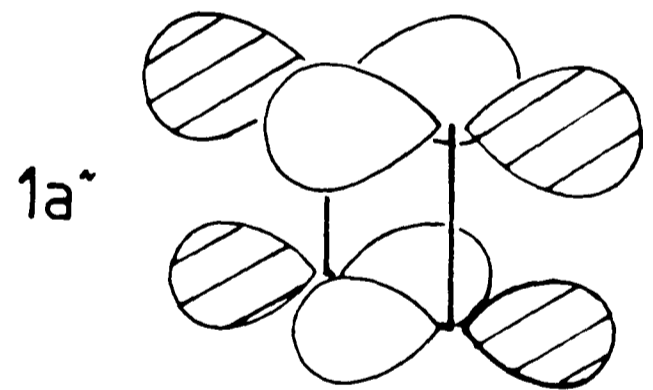
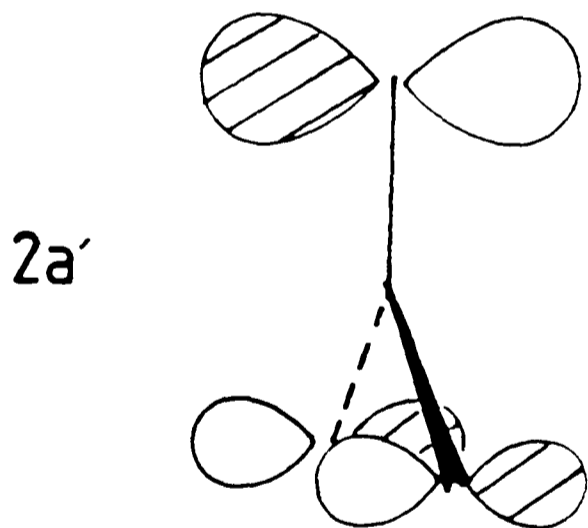
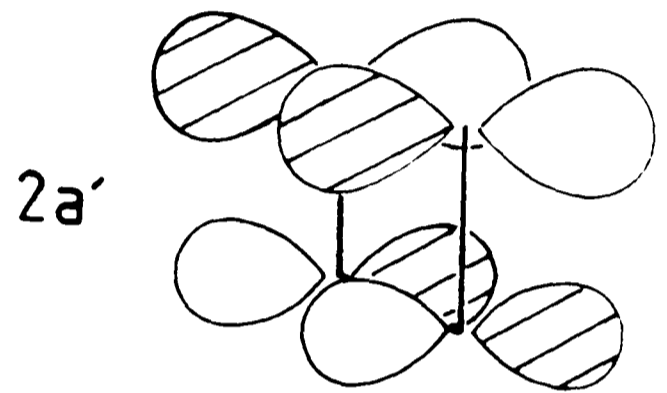
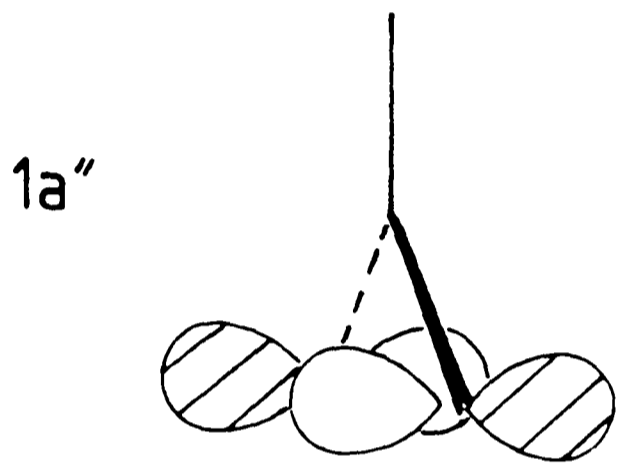
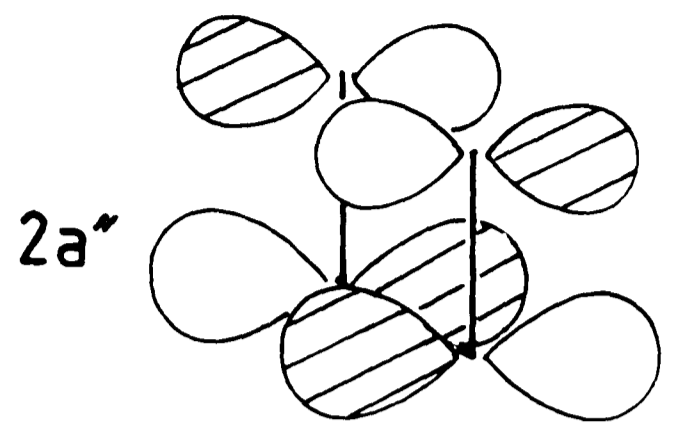
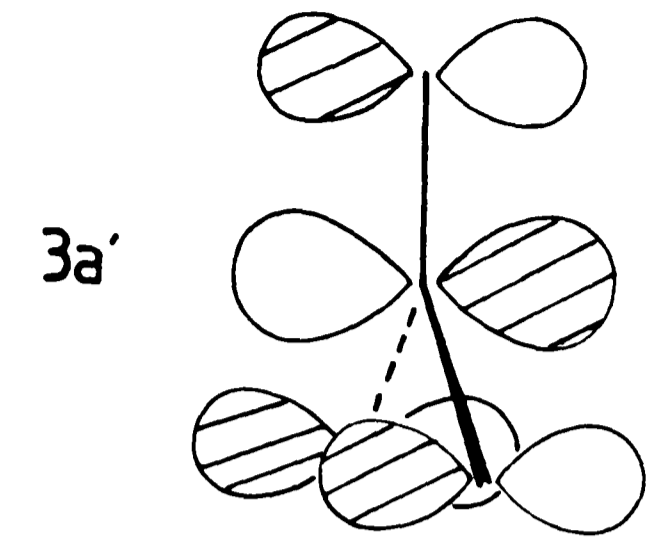


Fig 6.3 C<sub>4</sub>H<sub>6</sub> Ligand π-Orbitals.

#### 6.4 CpMo(CO)<sub>2</sub>-TMM interaction:-

Overlap calculations indicate that the important metal/ligand interactions are the  $3a'/3a'$ ,  $3a'/1a'$ ,  $a''/a''$ ,  $2a'/2a'$  and  $1a'/2a'$  combinations.

The  $3a'/3a'$  interaction is between two unfilled orbitals and therefore will have no stereochemical consequences.

That between  $3a'$  ( metal ) and  $1a'$  ( ligand ) is a two electron bonding interaction, but due to the metal orbital being radially symmetrical about the z axis, since it is mainly  $dz^2$  in character, it will have practically no stereochemical preference.

The underlying reasons for the species adopting the *syn* conformation lie in the  $a''/a''$ ,  $2a'/2a'$  and  $1a'/2a'$  combinations and an interaction diagram is shown in Figure 6.3 for both *syn* and *anti* conformations.

The antisymmetric combination,  $a''/a''$ , a two orbital, two electron bonding interaction, is very similar in both forms. However, the metal orbital is localised slightly above the xz plane due to mixing of some dxy character into the mainly dxz orbital. Thus, this hybrid will interact more strongly with the TMM  $a''$  orbital when the ligand is in the *syn* orientation with the carbons bearing the  $\pi$ -orbital components above the xz plane. This is observed as a slight stabilisation of the resultant M.O. in the *syn*, relative to the *anti* geometry.

It is in this  $a''/a''$  interaction that the reason for the pyramidalisation is apparent. The rehybridised orbitals,

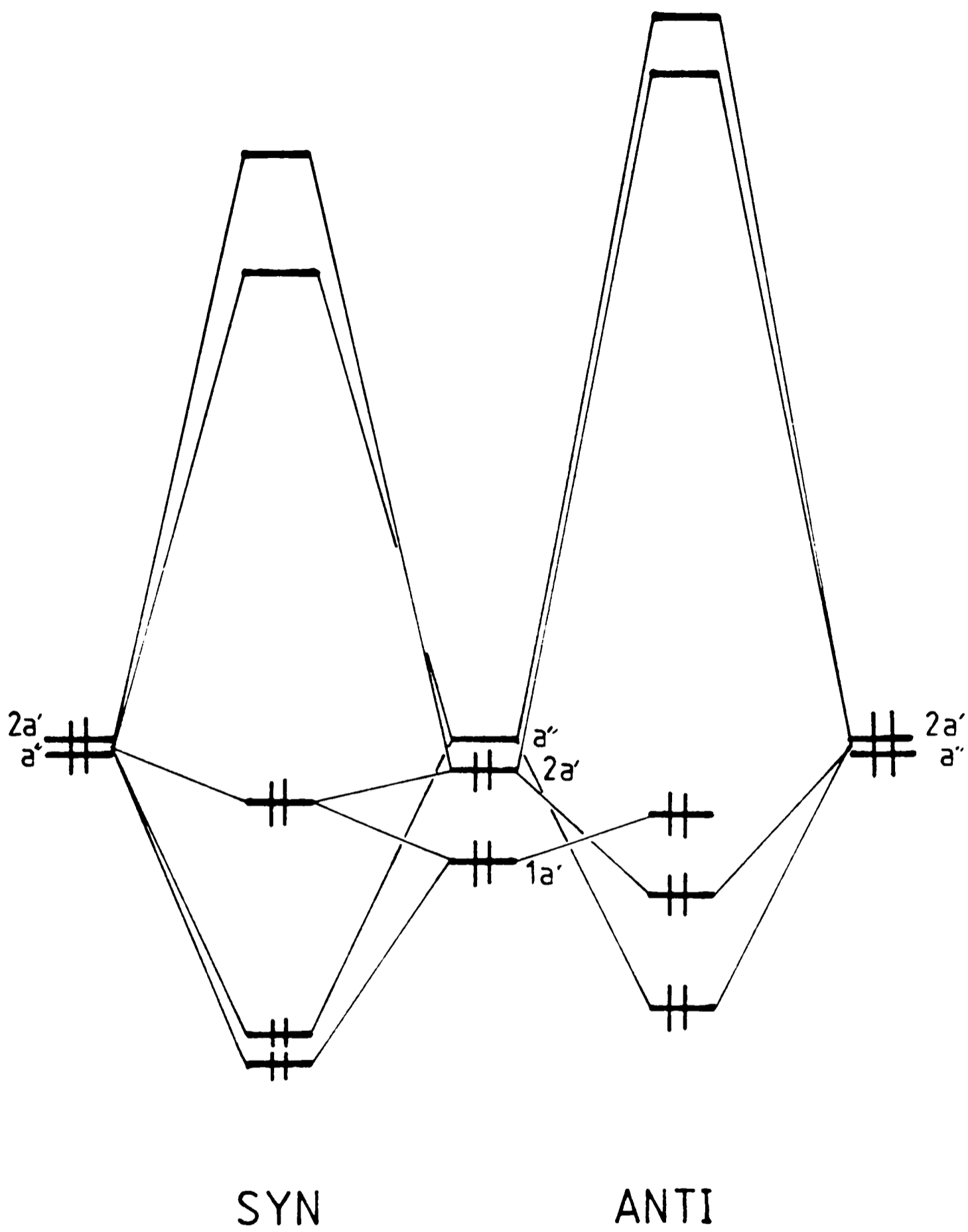
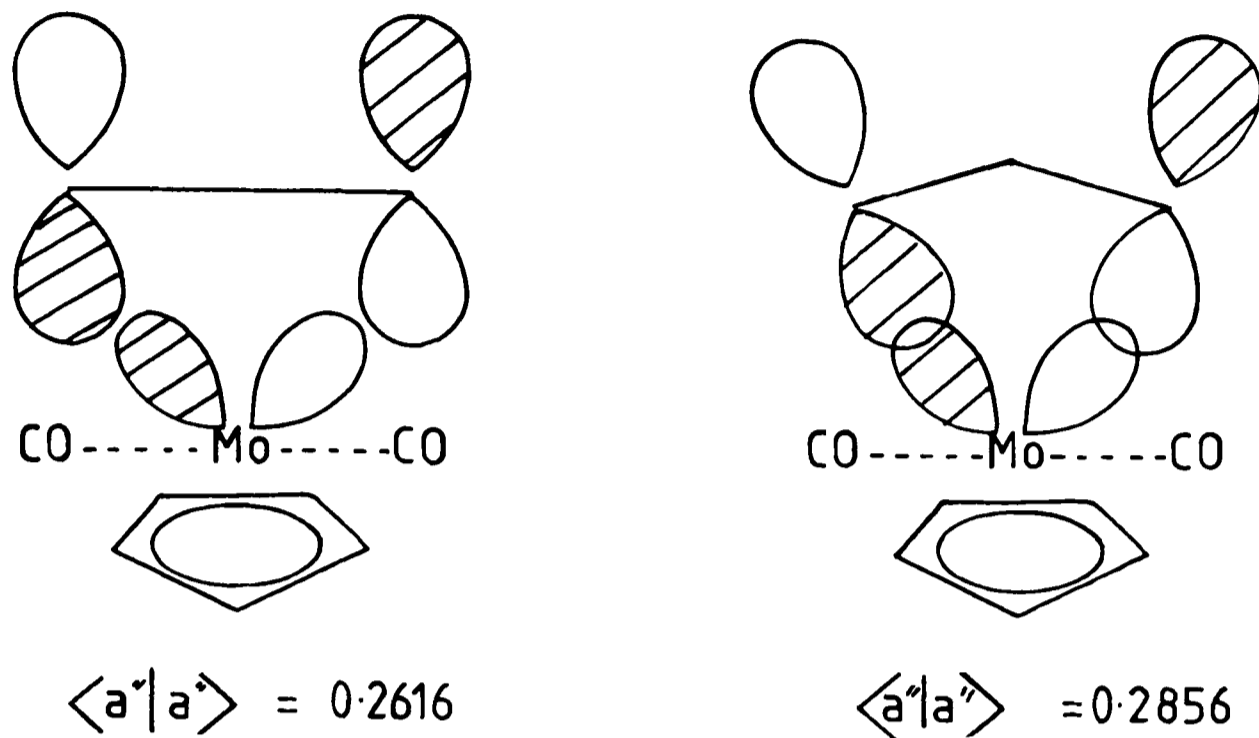


Fig. 6.3 CpMo(CO)<sub>2</sub>-TMM Interaction Diagram.

directed towards the metal, will achieve a greater overlap with the metal orbitals radiating from the coordinated centre, as shown below.



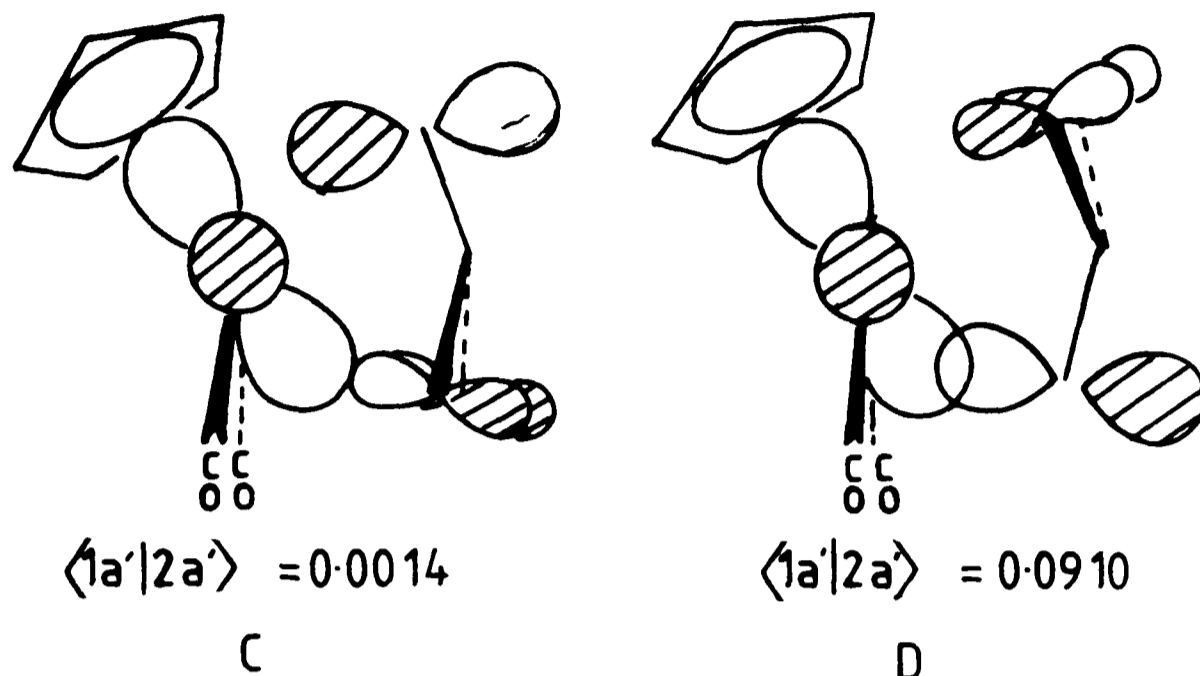
This will apply not only to the  $a''/a'$  interaction but also the  $2a'/2a'$  and will occur in both *syn* and *anti* configurations. A similar effect is observed in  $51^{148}$ .

In the *syn* geometry the metal  $2a'$  and  $1a'$  mix to interact with the TMM  $2a'$  orbital, resulting in a three orbital, four electron stabilising combination. However, in the *anti* configuration the  $1a'/2a'$  interaction is lost, leaving the metal  $1a'$  essentially non-bonding.

The  $2a'/2a'$  stabilising combination prefers the *anti* configuration slightly due to the metal orbital being more heavily localised above the  $xz$  plane, as is the TMM orbital, hence achieving a greater overlap.

The  $1a'/2a'$  interaction, which does not seem to benefit from the pyramidalisation since it is more tangential in nature, is highly susceptible to *syn/anti* interconversion. The

overlap for the *anti* form, C, is almost negligible, whilst that in the *syn* conformation, D, is highly significant.



The net effect of these interactions is to favour the *syn* form over the *anti* as is clearly demonstrated by plotting total energy versus  $\theta$ , the angle of ligand rotation about the z axis (  $0^\circ = \text{anti}$ ,  $60^\circ = \text{syn}$  ), Figure 6.4. Curve 1 represents the planar,  $D_{3h}$ , ligand whilst curve 2 is for the pyramidalised,  $C_{3v}$ , form. The energy scale, in e.V.s, is not absolute, representing only the relative energies along the profile. However, both curves are set to the same origin for comparison. The curves are roughly parallel, the difference representing the stabilisation due to the puckering of the ligand, ca.  $19\text{kJmol}^{-1}$ . The energy difference between the two forms, *anti-syn*, is  $190.2\text{kJmol}^{-1}$  for the flat ligand and  $195.2\text{kJmol}^{-1}$  for the puckered form. However, this does not represent the barrier to rotation since the *anti* conformer is metastable, lying in a shallow potential well. The least stable geometry corresponds to one arm of the

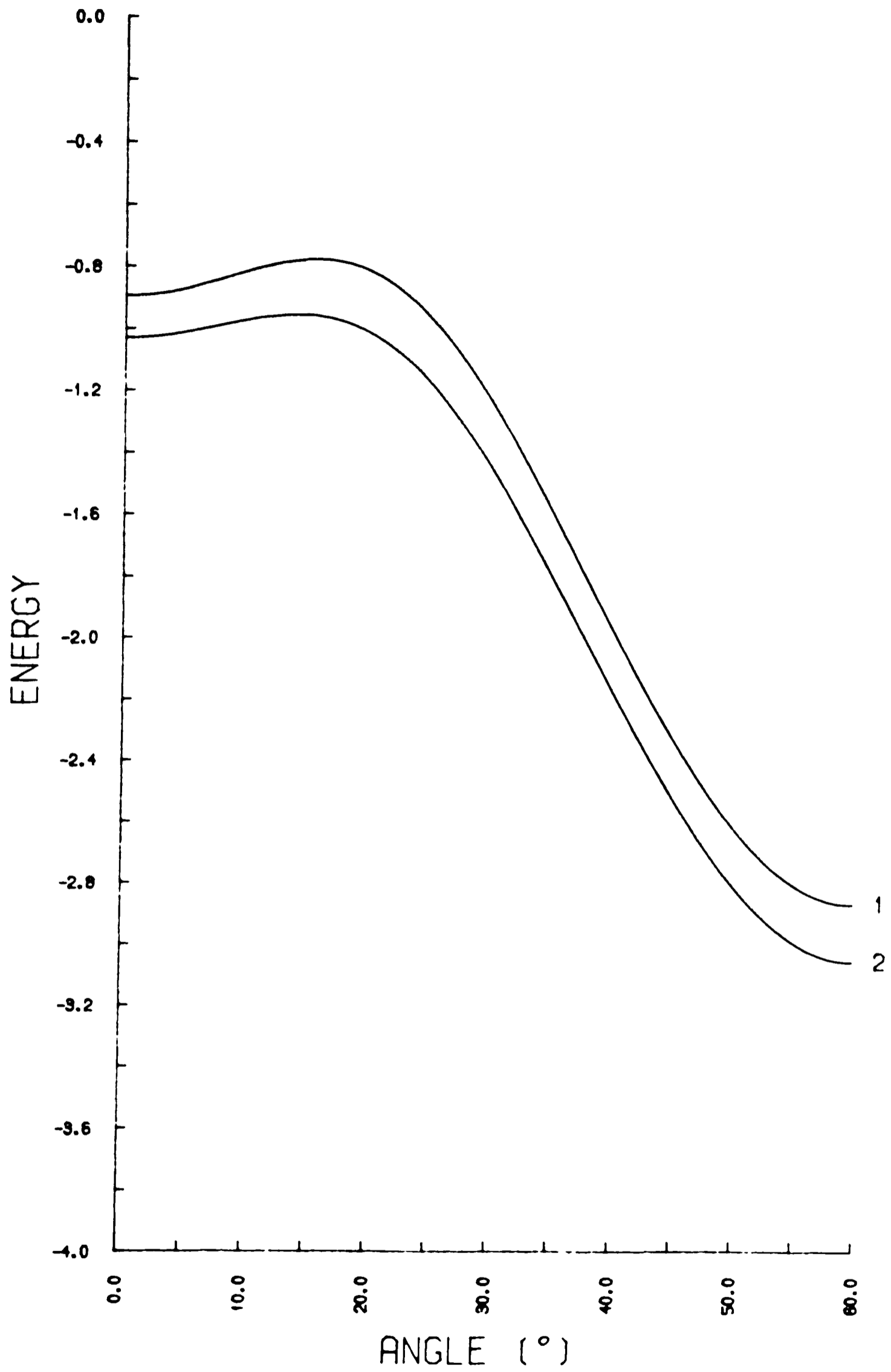
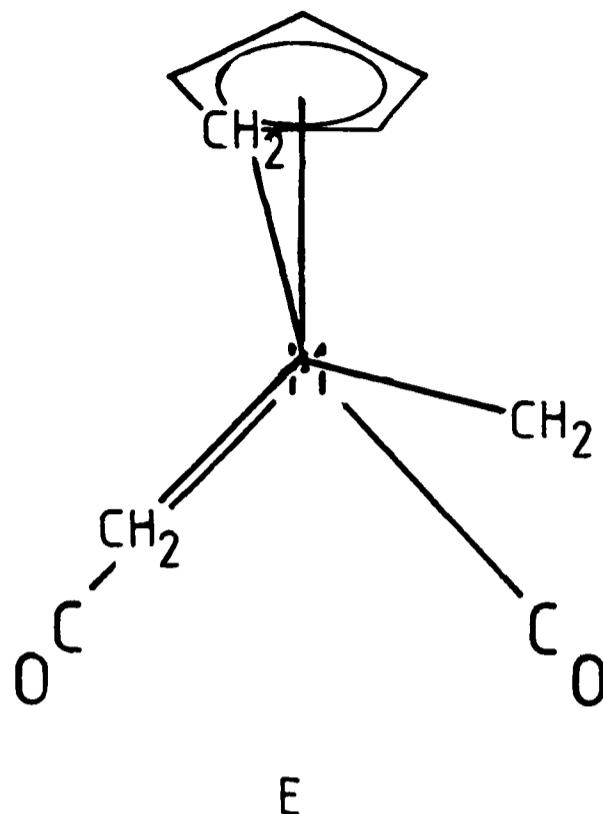


Fig. 6.4 Energy Profile for TMM Rotation.

TMM ligand eclipsing a carbonyl group, E, and occurs at  $\theta = 15.5^\circ$ .



This gives a barrier to rotation of  $202.3\text{kJmol}^{-1}$  for the flat, and  $202.7\text{kJmol}^{-1}$  for the pyramidal ligand, which must be compared with the barrier measured in solution<sup>151</sup> of  $41.4\text{kJmol}^{-1}$ . Barriers calculated by the EHMO method are usually overestimated due to the inflexibility of the process. However, the large discrepancy found here would seem to indicate an alternative type of mechanism.

The measured<sup>187</sup> and calculated<sup>148</sup> barriers to rotation for 51 are  $79\text{--}83\text{kJmol}^{-1}$  and  $98.6\text{kJmol}^{-1}$  indicating a much better modeling of the interchange mechanism. In the complex  $\text{Cp}^*\text{Ta}(\text{Me})_2\text{TMM}$ , 52, the measured<sup>153</sup> barrier to TMM interchange is  $44.3\text{kJmol}^{-1}$  whilst a "significant" barrier is calculated<sup>188</sup>.

The *syn* geometry, both found in the crystal structure of TRIMET and calculated for its Cp analogue to be the most

stable, could be considered analogous to the staggered form of 51, also the most stable, since one arm of the TMM bisects a CO-M-CO angle. Thus the high energy form, at  $\theta = 15.5^\circ$  is analogous to the eclipsed geometry of the iron species, also the high energy form.



### 6.5 CpMo(Cl)<sub>2</sub>-butadiene interaction:-

For this system overlap calculations indicate that the major metal/ligand interactions are the  $3a'/1a'$ ,  $a''/1a'$  and  $2a'/2a'$  combinations. The interaction diagram, for both *endo* and *exo* conformations, is shown in Figure 6.5.

The metal  $3a'$  orbital is localised slightly below the  $xz$  plane due to slight mixing of  $-dyz$  with the mainly  $dz^2/pz$  orbital, and since the ligand  $1a'$  orbital is localised on the inner carbon atoms, greater overlap will occur when the molecule adopts the *endo* conformation. Similarly the  $a''$  metal orbital is localised above the  $xz$  plane, due to some  $dxy$  character, whilst the ligand  $1a''$  is localised on the outer carbons, hence better overlap is again achieved in the *endo* conformation. However, in both these cases the preference is slight. The metal  $2a'$  orbital is localised mainly in the  $yz$  plane in the  $+y$  direction, thus overlap with the diene is small. However, the  $2a'/2a'$  combination does prefer the *endo* conformation whilst the  $2a'/1a'$  interaction favours the *exo*. In both cases this could be interpreted as the minor lobe of the metal  $2a'$  orbital having the greater stereochemical influence due to a large lateral separation of the major components which results in minimal overlap. This is indicated below.

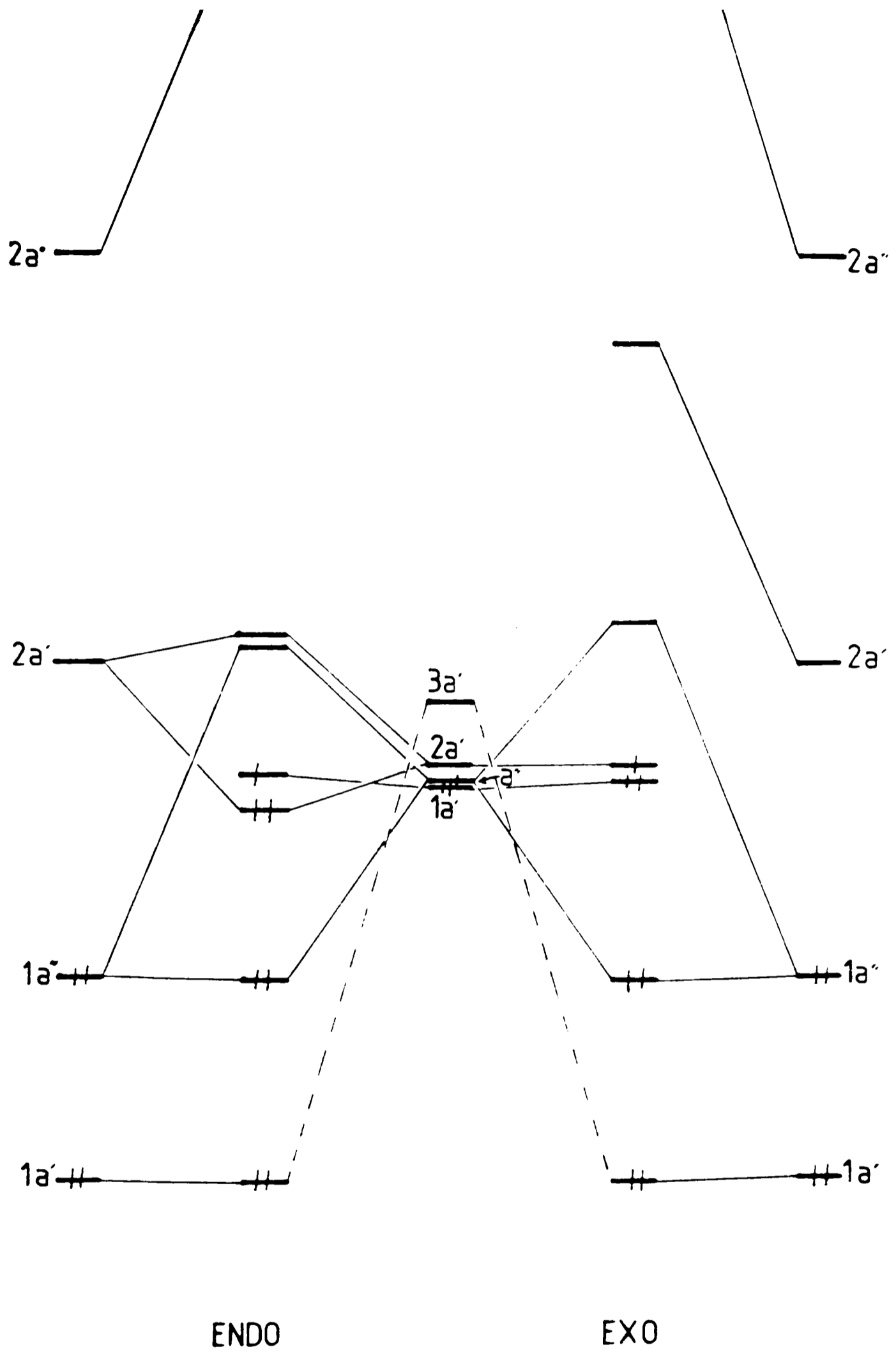
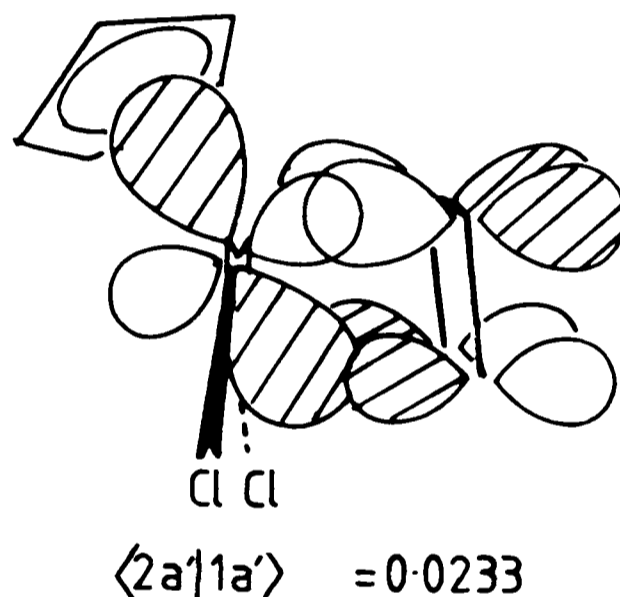
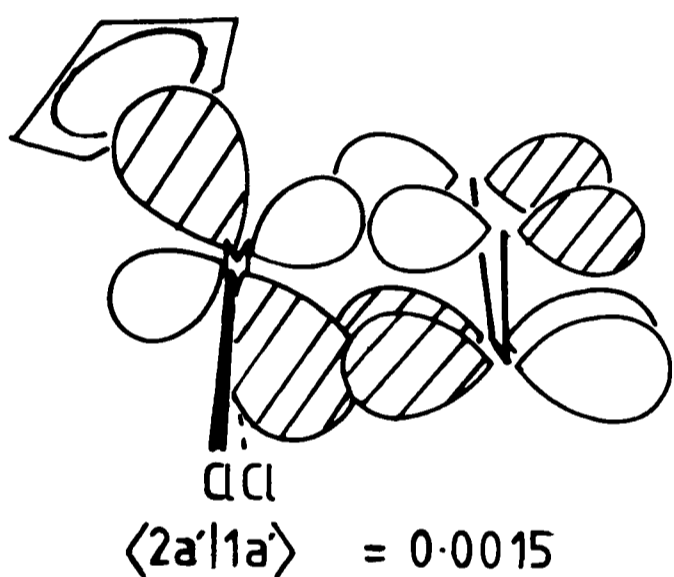
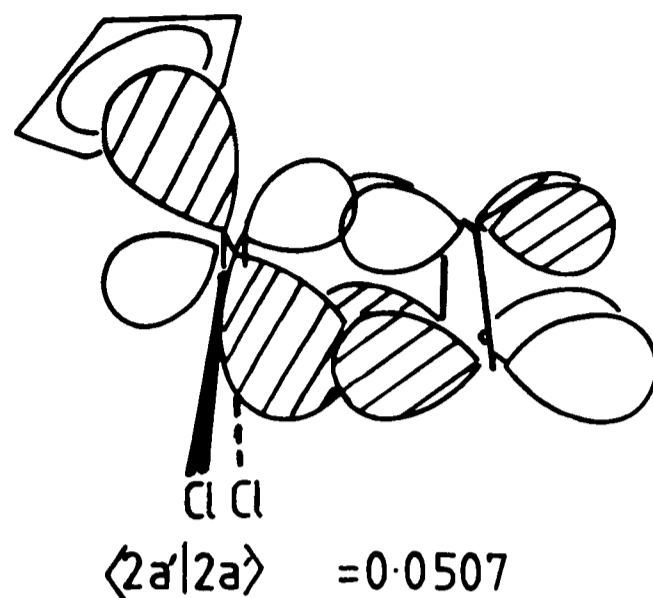
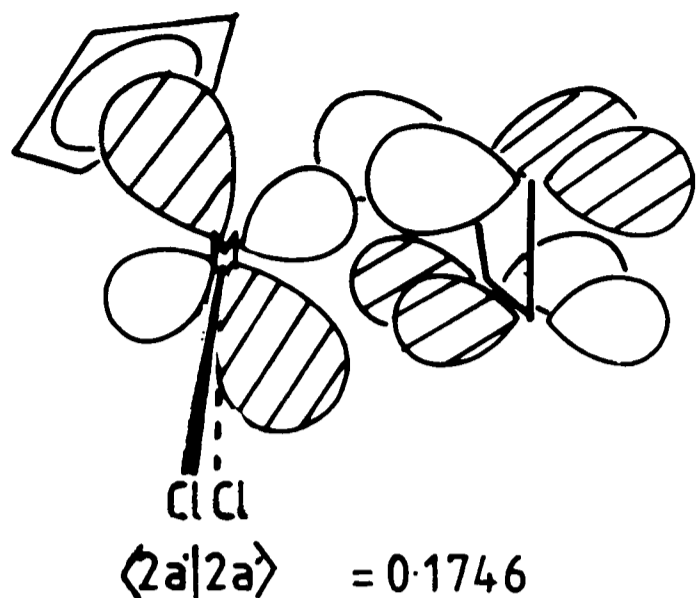


Fig 6.5  $\text{CpMo}(\text{Cl})_2$ -Butadiene Interaction diagram.



ENDO

EXO

Thus, either conformation could be preferred on the basis of these interactions. A plot of total energy versus  $\theta$  the angle of rigid rotation about the z axis is shown in Figure 6.6 (  $0^\circ = \text{endo}$ ,  $180^\circ = \text{exo}$  ). Again the energy scale ( e.V.s ) is arbitrary, demonstrating only the size of the profile. The graph clearly shows that the preferred conformation is *endo*, more stable than the *exo* by  $85.4\text{kJmol}^{-1}$ . It also reveals an intermediate conformation at  $\theta = 120^\circ$ , that is almost as

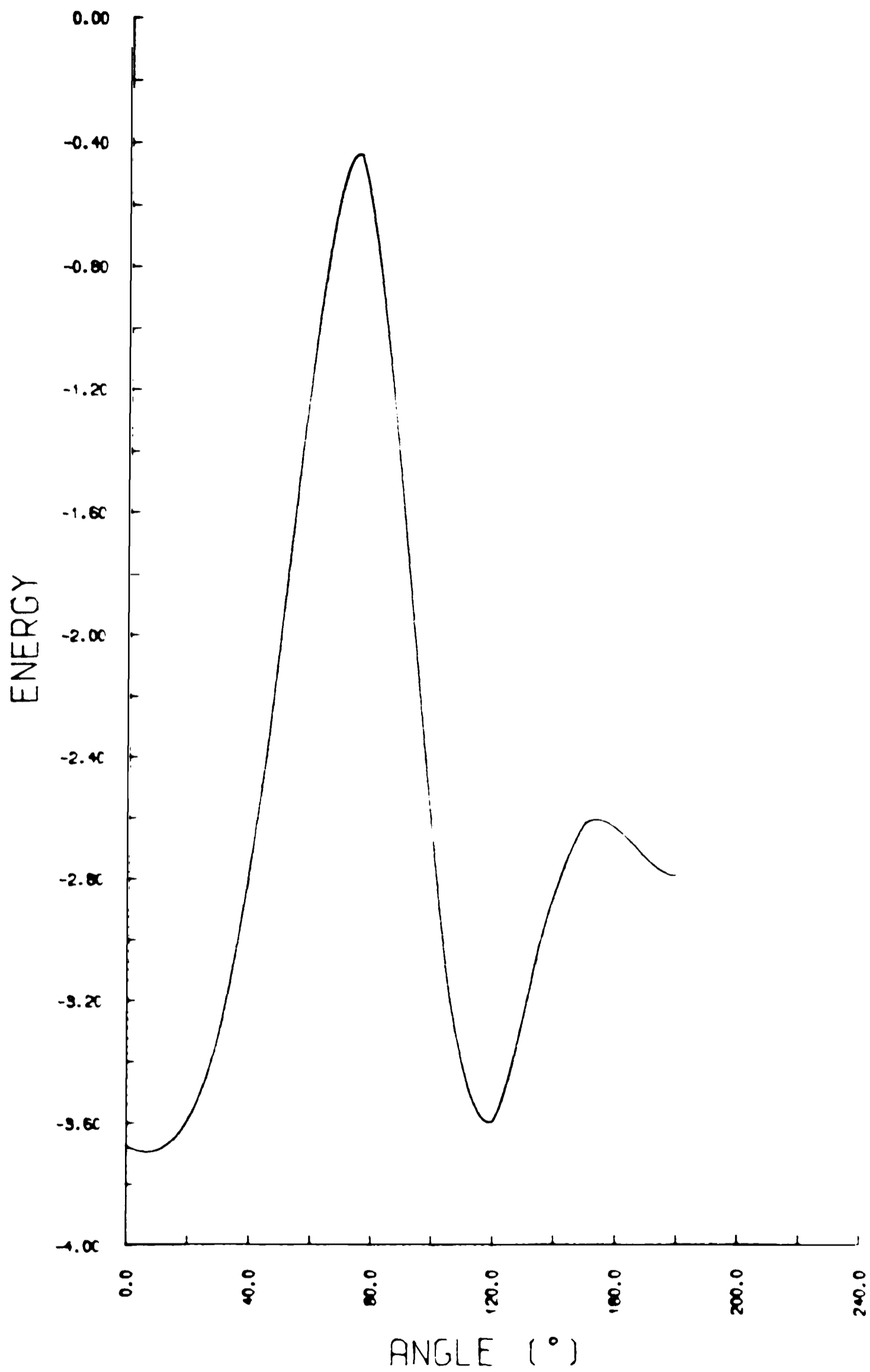
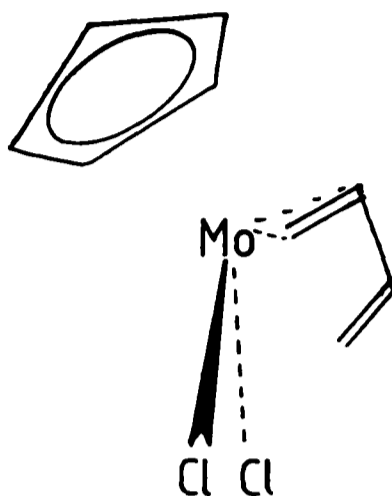


Fig 6.6 Energy Profile for Butadiene Rotation.

stable as the *endo* form. This corresponds to a fifteen electron  $\eta^2$ -ethylene species, **F**, structurally analogous to the many  $\text{CpML}_2$ -ethene complexes known<sup>189</sup>.



**F**

In **F** the coordinated  $\pi$ -ene function lies parallel to the *x* axis above the *xz* plane, and thus is bisected by the mirror plane of the metal fragment. This has been shown to be the most stable conformation, both by synthetic/structural studies<sup>189</sup> and a theoretical study on  $[\text{CpMo}(\text{CO})_2(\text{ethene})]^+$ <sup>139</sup>. Given the similarity between the orbitals of the two metal fragments a very similar bonding mode will apply here. Also apparent from the energy profile is the very large barrier to rotation, ca.  $313\text{kJmol}^{-1}$ , on both sides of the *endo* conformation. This suggests that this geometry may not only be thermodynamically but also kinetically preferred. However, as with the TMM complex studied, this may be overestimated due to the inappropriateness of the rigid rotor model. Nevertheless, it is not inconsistent with an alternative mechanism for *endo-exo* interchange, involving a metallacyclopentene intermediate, scheme 5.4. The

crystallographic results for CPMOBUT indicated some movement along this pathway as had been seen for the zirconium-diene species<sup>186</sup>. The presence of the  $\pi$ -donor halide ligands in CPMOBUT may stabilise the high oxidation state intermediate and favour this latter mechanism for interchange. The measured barrier to interchange for the the dicarbonyl analogue is only  $60\text{kJmol}^{-1}$  whilst that calculated is  $263.1\text{kJmol}^{-1}$ , with the *exo* conformation preferred, by  $6.9\text{kJmol}^{-1}$ , to the *endo*. This is also consistent with the alternative mechanism for interchange, although there will be no stabilisation of the high oxidation state intermediate.

## **APPENDIX 1**

**THERMAL PARAMETERS FOR:**

**1: PHALPD**

**2: PDETAL**

**3: CPPHAL**

**4: MOPHAL**

Thermal Vibration Parameters with Standard Deviations for PHALPD

	U11	U22	U33	U23	U13	U12
Fd	0.0272(1)	0.0242(1)	0.0286(1)	-0.0005(1)	-0.0028(1)	0.0001(1)
C(1)	0.0326(13)	0.0324(12)	0.0325(14)	-0.0097(11)	-0.0035(11)	-0.0039(11)
C(2)	0.0310(13)	0.0345(13)	0.0468(15)	-0.0058(13)	-0.0090(12)	-0.0001(12)
C(3)	0.0350(14)	0.0441(15)	0.0425(15)	-0.0025(13)	-0.0117(13)	0.0068(13)
CR(1)	0.0297(11)	0.0271(10)	0.0396(13)	-0.0130(14)	0.0023(15)	-0.0041(9)
CR(2)	0.0374(14)	0.0368(14)	0.0408(14)	-0.0070(11)	0.0059(13)	0.0039(12)
CR(3)	0.0454(15)	0.0372(13)	0.0498(18)	-0.0069(13)	-0.0027(13)	0.0094(12)
CR(4)	0.0537(16)	0.0321(14)	0.0462(16)	0.0009(13)	-0.0087(14)	-0.0043(13)
CR(5)	0.0536(16)	0.0430(15)	0.0475(15)	0.0039(14)	0.0120(15)	-0.0011(14)
CR(6)	0.0446(15)	0.0364(14)	0.0423(14)	-0.0061(13)	0.0047(13)	0.0058(13)
N(1)	0.0411(12)	0.0256(10)	0.0322(12)	-0.0014(9)	0.0030(10)	-0.0047(10)
N(2)	0.0274(11)	0.0385(12)	0.0339(12)	0.0019(12)	-0.0045(11)	-0.0021(12)
C(4)	0.0454(15)	0.0371(14)	0.0561(16)	0.0019(14)	0.0052(15)	-0.0136(14)
C(5)	0.0406(15)	0.0432(15)	0.0529(17)	-0.0039(14)	-0.0127(13)	-0.0086(13)
C(6)	0.0715(18)	0.0345(15)	0.0378(15)	0.0064(14)	0.0011(15)	0.0026(14)
C(7)	0.0498(15)	0.0350(14)	0.0405(15)	-0.0069(13)	0.0120(14)	-0.0087(13)
C(8)	0.0316(13)	0.0579(15)	0.0535(18)	-0.0011(16)	0.0028(16)	0.0097(12)
C(9)	0.0453(15)	0.0499(16)	0.0420(15)	0.0082(14)	-0.0126(14)	0.0038(14)
S	0.0361(14)	0.0342(14)	0.0367(15)	0.0004(13)	0.0050(13)	0.0052(13)
F(1)	0.0962(16)	0.1174(18)	0.0480(15)	-0.0086(16)	0.0236(16)	0.0366(16)
F(2)	0.0439(12)	0.0650(14)	0.0592(14)	-0.0067(13)	-0.0109(10)	0.0018(10)
F(3)	0.0506(11)	0.0403(11)	0.0713(14)	-0.0071(11)	-0.0137(11)	0.0145(10)
F(4)	0.0674(14)	0.0353(10)	0.0863(16)	0.0083(13)	-0.0038(14)	-0.0082(12)



Thermal Vibration Parameters with Standard Deviations for PDETAL

	U11	U22	U33	U23	U13	U12
Pd	0.0324(1)	0.0263(1)	0.0368(2)	0.0001(1)	-0.0089(1)	-0.0075(1)
C(1)	0.0534(22)	0.0329(17)	0.0516(21)	0.0129(15)	-0.0200(17)	-0.0118(15)
C(2)	0.0585(24)	0.0503(22)	0.0520(22)	0.0187(18)	-0.0169(19)	-0.0311(20)
C(3)	0.0735(31)	0.0450(22)	0.0626(26)	0.0101(19)	-0.0227(23)	-0.0338(22)
C(4)	0.0489(21)	0.0451(19)	0.0410(18)	0.0139(15)	-0.0129(15)	-0.0202(17)
C(5)	0.0489(22)	0.0614(26)	0.0450(21)	-0.0067(18)	-0.0079(17)	-0.0127(19)
C(6)	0.0537(33)	0.2042(106)	0.0969(52)	-0.0770(62)	-0.0251(34)	-0.0104(47)
D(1)	0.0462(16)	0.0566(18)	0.0599(19)	0.0065(15)	-0.0069(14)	-0.0118(14)
D(2)	0.0438(15)	0.0563(18)	0.0474(15)	-0.0032(13)	-0.0131(13)	-0.0062(13)
M(1)	0.0486(18)	0.0551(20)	0.0374(15)	-0.0056(14)	-0.0056(13)	-0.0196(16)
M(2)	0.0411(16)	0.0423(16)	0.0409(15)	-0.0026(12)	-0.0042(12)	-0.0202(13)
C(7)	0.1271(59)	0.1248(58)	0.0435(25)	0.0199(30)	-0.0178(30)	-0.0858(52)
C(8)	0.0860(39)	0.0959(43)	0.0478(24)	0.0038(25)	-0.0021(25)	-0.0621(36)
C(9)	0.0656(32)	0.0857(40)	0.0564(28)	-0.0281(27)	-0.0146(24)	0.0211(29)
C(10)	0.0647(29)	0.0654(29)	0.0467(22)	-0.0011(20)	-0.0172(21)	0.0035(23)
C(11)	0.0349(19)	0.0636(28)	0.0758(31)	-0.0087(23)	-0.0089(20)	-0.0123(19)
C(12)	0.0508(23)	0.0316(18)	0.0920(36)	-0.0080(20)	-0.0139(23)	-0.0120(17)
B	0.0751(35)	0.0500(26)	0.0478(24)	0.0025(20)	-0.0182(24)	-0.0281(25)
F(1)	0.1122(30)	0.0778(23)	0.0703(20)	0.0030(16)	-0.0334(20)	-0.0576(22)
F(2)	0.1171(36)	0.1033(33)	0.0822(26)	-0.0129(23)	-0.0406(25)	0.0303(27)
F(3)	0.4246(138)	0.3714(122)	0.0926(35)	0.0850(54)	-0.1063(58)	-0.3625(124)
F(4)	0.1909(70)	0.1618(61)	0.1385(50)	-0.0696(46)	-0.0700(49)	0.1004(55)

Thermal Vibration Parameters with Standard Deviations for CPPHAL

	U <sub>11</sub> or U <sub>11</sub>	U <sub>22</sub>	U <sub>33</sub>	U <sub>23</sub>	U <sub>13</sub>	U <sub>12</sub>
Rd	0.0234(1)	0.0263(1)	0.0158(1)	-0.0015(1)	0.0010(1)	-0.0024(1)
C(1)	0.0340(11)	0.0352(11)	0.0189(9)	0.0002(8)	0.0035(7)	-0.0022(9)
C(2)	0.0363(13)	0.0420(13)	0.0230(10)	-0.0029(8)	-0.0001(9)	-0.0065(9)
C(3)	0.0309(12)	0.0577(17)	0.0219(11)	-0.0025(9)	-0.0031(9)	0.0007(10)
CR(1)	0.0309(10)	0.0354(10)	0.0189(9)	-0.0040(8)	0.0032(7)	-0.0017(9)
CR(2)	0.0328(12)	0.0379(12)	0.0311(12)	0.0048(8)	0.0012(9)	-0.0059(9)
CR(3)	0.0326(12)	0.0573(16)	0.0410(14)	0.0064(12)	0.0085(10)	-0.0043(11)
CR(4)	0.0398(15)	0.0507(16)	0.0456(16)	-0.0047(11)	0.0002(12)	0.0139(11)
CR(5)	0.0564(18)	0.0341(13)	0.0431(14)	0.0041(11)	-0.0005(12)	0.0023(12)
CR(6)	0.0430(14)	0.0390(12)	0.0341(13)	0.0045(10)	0.0074(10)	-0.0058(12)
C(4)	0.0295(16)					
C(5)	0.0225(15)					
C(6)	0.0279(16)					
C(7)	0.0296(15)					
C(8)	0.0304(15)					
C(4')	0.0242(13)					
C(5')	0.0334(17)					
C(6')	0.0303(15)					
C(7')	0.0266(12)					
C(8')	0.0261(12)					

Thermal Vibration Parameters with Standard Deviations for MOPHAL

	U11	U22	U33	U23	U13	U12
Mo	0.0163(2)	0.0256(2)	0.0211(2)	-0.0004(2)	0.0070(1)	0.0012(2)
N	0.0190(17)	0.0316(19)	0.0261(17)	-0.0023(14)	0.0070(14)	-0.0060(15)
O	0.0210(21)	0.0454(27)	0.0231(21)	-0.0010(16)	0.0079(17)	-0.0119(19)
S	0.0372(6)	0.0318(6)	0.0567(7)	0.0037(5)	0.0163(6)	-0.0008(5)
N(1)	0.0245(17)	0.0235(16)	0.0203(16)	0.0028(12)	0.0093(14)	0.0010(13)
N(2)	0.0209(15)	0.0202(15)	0.0215(15)	0.0019(12)	0.0073(13)	0.0006(13)
C(4)	0.0224(20)	0.0228(19)	0.0221(19)	0.0019(15)	0.0097(16)	-0.0015(15)
C(5)	0.0308(22)	0.0291(20)	0.0240(20)	0.0045(16)	0.0129(17)	0.0061(17)
C(6)	0.0421(27)	0.0266(21)	0.0248(21)	0.0004(16)	0.0137(19)	-0.0002(18)
C(7)	0.0368(25)	0.0317(22)	0.0202(19)	0.0017(17)	0.0054(18)	-0.0059(18)
C(8)	0.0289(21)	0.0272(20)	0.0225(21)	0.0032(15)	0.0085(18)	-0.0087(17)
C(9)	0.0247(21)	0.0376(23)	0.0269(21)	0.0024(18)	0.0053(18)	-0.0117(18)
C(10)	0.0202(20)	0.0375(22)	0.0284(21)	0.0074(17)	0.0080(17)	-0.0038(17)
C(11)	0.0201(18)	0.0283(21)	0.0273(19)	0.0066(16)	0.0095(15)	-0.0008(16)
C(12)	0.0241(21)	0.0334(21)	0.0347(22)	0.0061(18)	0.0134(18)	0.0057(18)
C(13)	0.0317(23)	0.0297(22)	0.0402(24)	-0.0008(18)	0.0182(20)	0.0085(18)
C(14)	0.0286(21)	0.0233(20)	0.0285(21)	-0.0015(16)	0.0109(17)	0.0010(16)
C(15)	0.0181(17)	0.0219(17)	0.0220(18)	0.0045(15)	0.0061(15)	-0.0008(15)
C(1)	0.0303(23)	0.0289(22)	0.0277(22)	0.0065(17)	0.0087(19)	0.0084(18)
C(2)	0.0306(23)	0.0253(20)	0.0296(22)	0.0048(17)	0.0072(19)	0.0063(18)
C(3)	0.0369(26)	0.0364(24)	0.0307(23)	0.0008(19)	0.0096(21)	0.0148(21)
CP(1)	0.0377(24)	0.0248(20)	0.0259(21)	0.0088(16)	0.0138(18)	0.0075(17)
CP(2)	0.0439(25)	0.0267(22)	0.0343(23)	0.0034(17)	0.0179(20)	0.0061(18)
CP(3)	0.0689(34)	0.0332(23)	0.0427(26)	0.0016(20)	0.0338(25)	0.0060(23)
CP(4)	0.0677(36)	0.0381(25)	0.0560(31)	0.0074(22)	0.0466(29)	0.0069(23)
CP(5)	0.0495(29)	0.0417(26)	0.0525(29)	0.0163(22)	0.0318(25)	0.0047(22)
CP(6)	0.0394(26)	0.0327(23)	0.0380(25)	0.0104(19)	0.0164(21)	0.0013(19)
CO(1)	0.0272(22)	0.0493(26)	0.0325(22)	-0.0081(20)	0.0096(18)	-0.0043(20)
CO(2)	0.0202(20)	0.0351(21)	0.0320(21)	-0.0014(18)	0.0123(18)	0.0014(18)
O(1)	0.0330(18)	0.1050(31)	0.0736(26)	-0.0181(22)	0.0343(19)	-0.0077(20)
O(2)	0.0263(16)	0.0496(18)	0.0384(17)	-0.0132(15)	0.0066(14)	-0.0047(14)

## **APPENDIX 2**

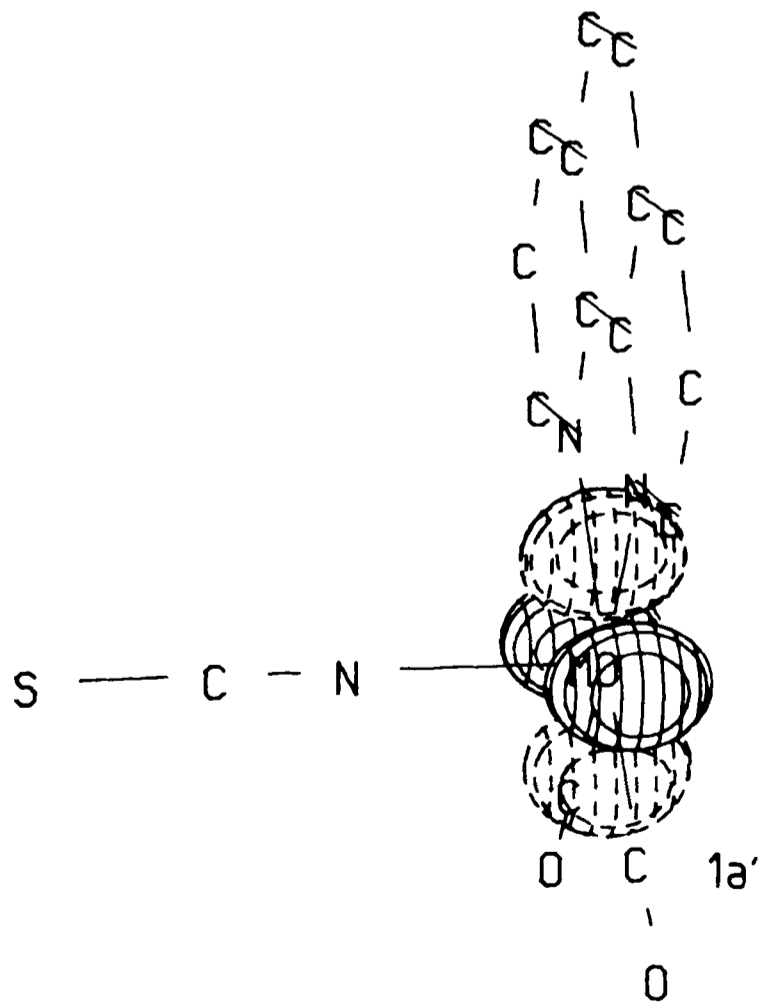
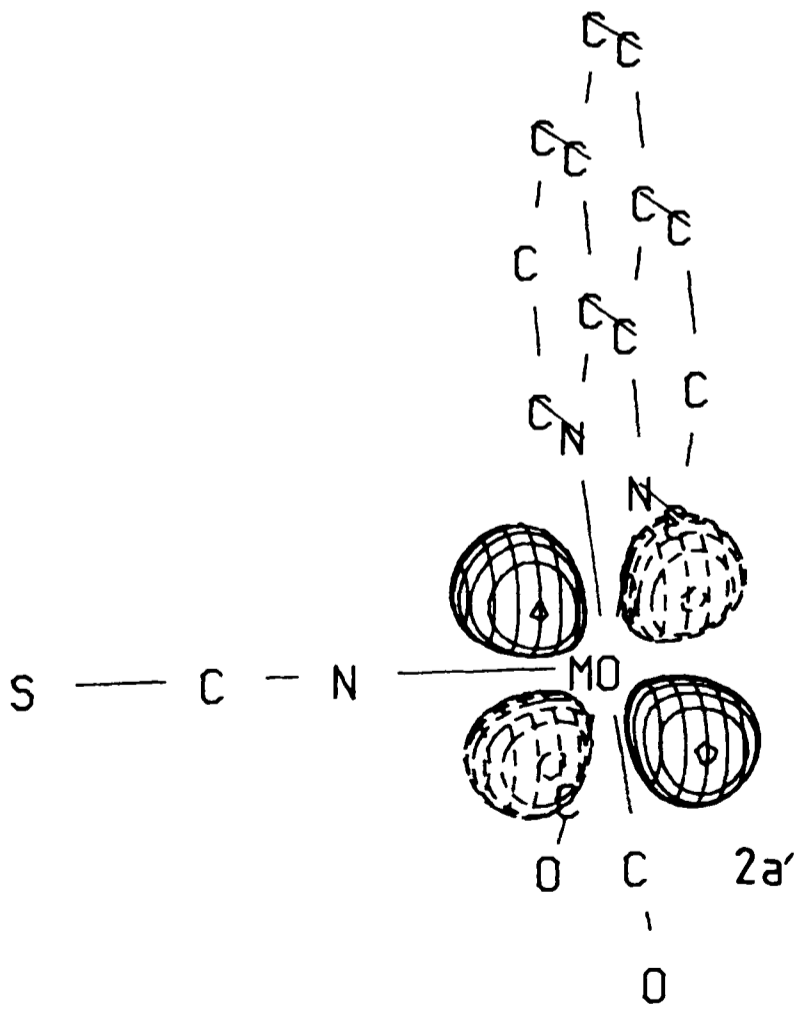
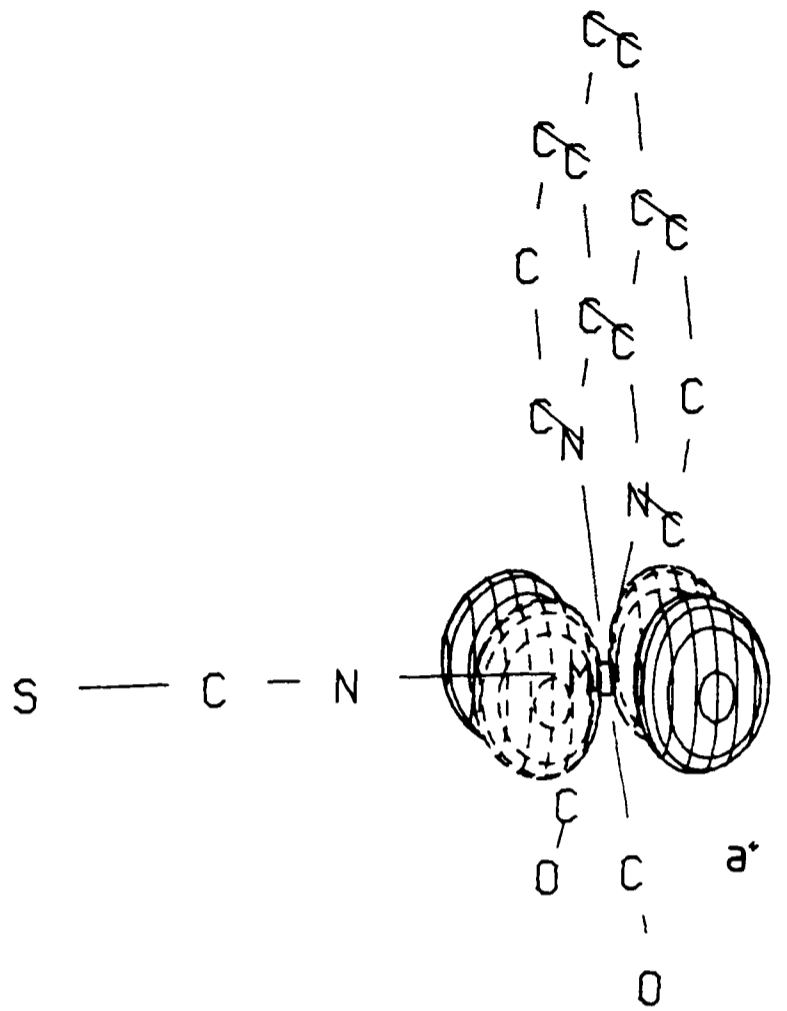
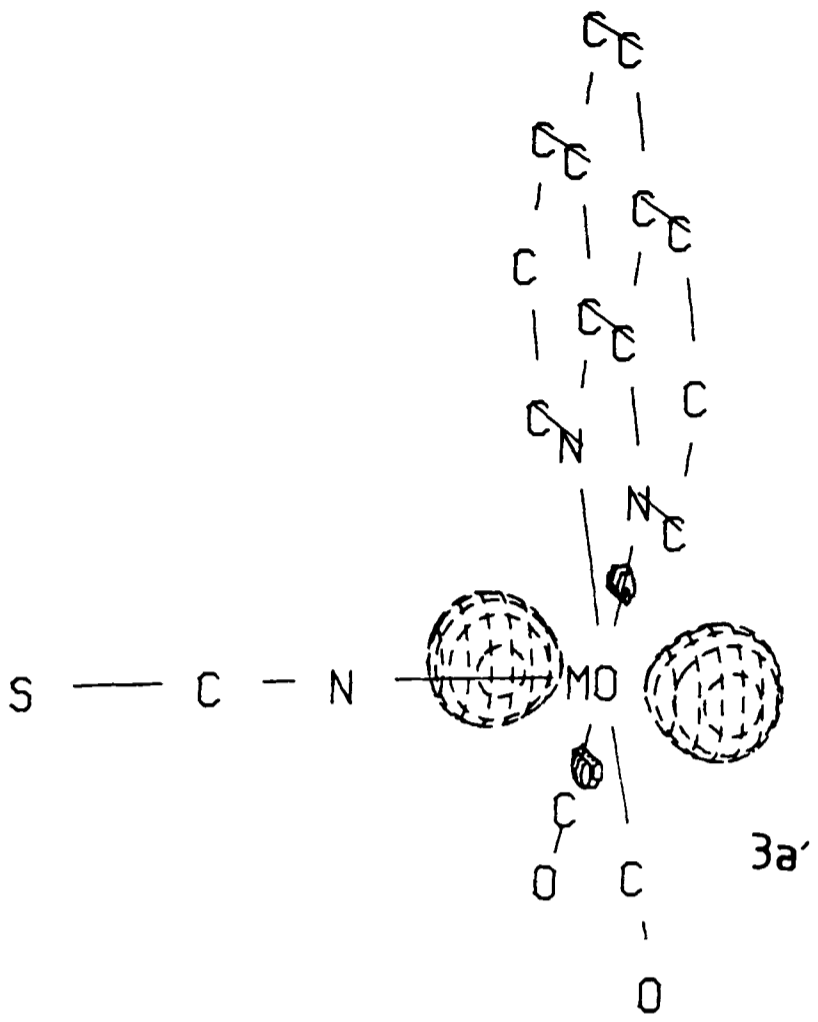
ORBITAL CONTOUR PLOTS FOR:

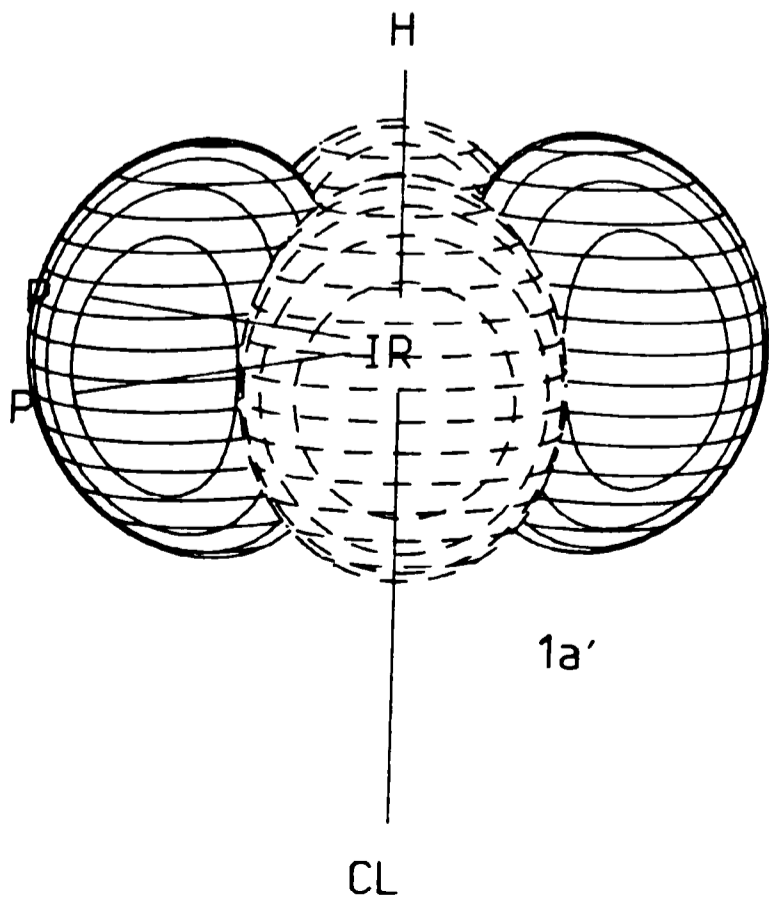
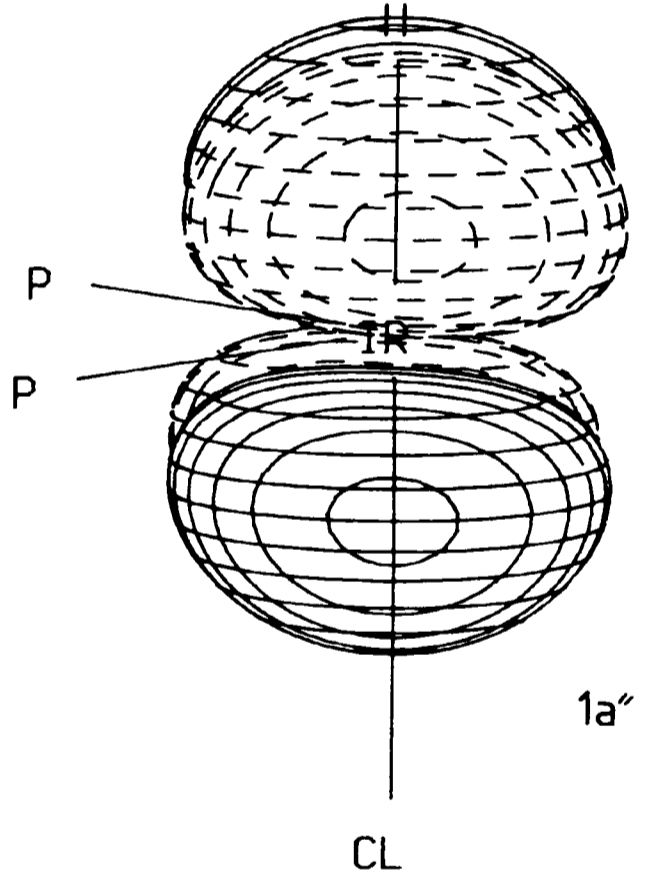
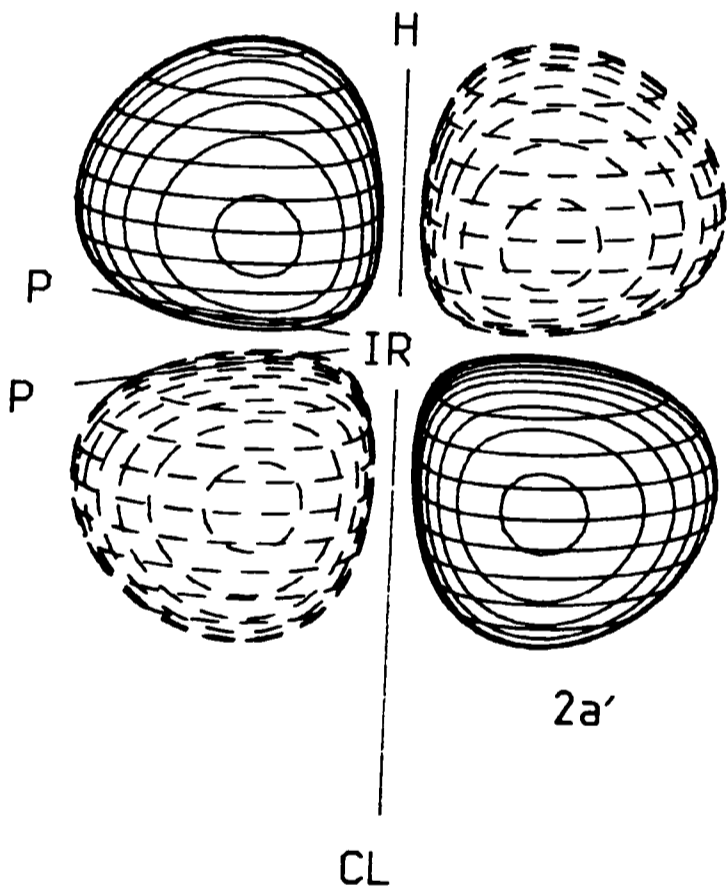
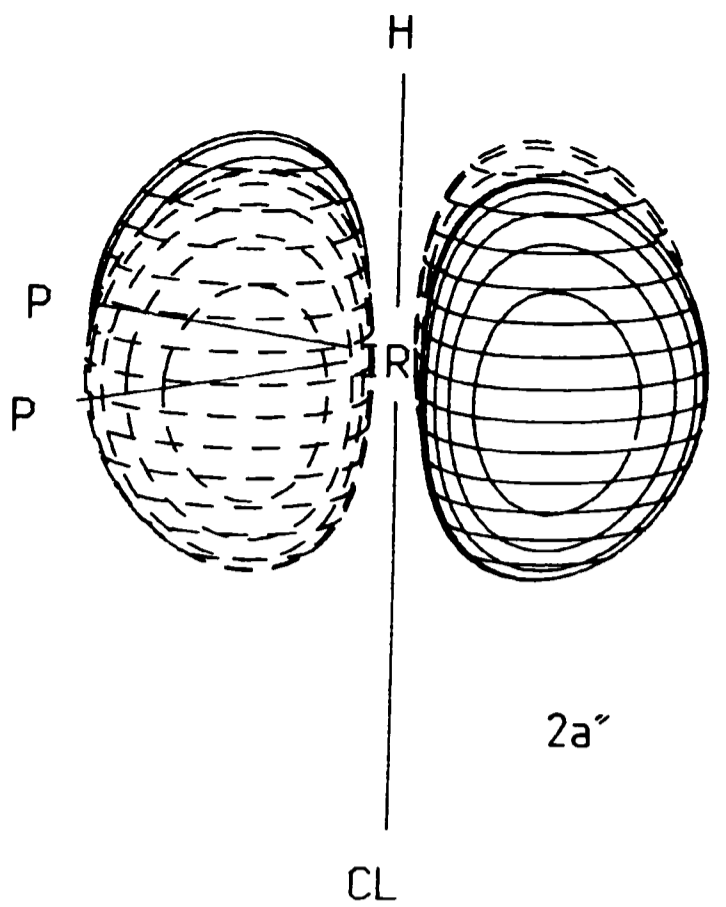
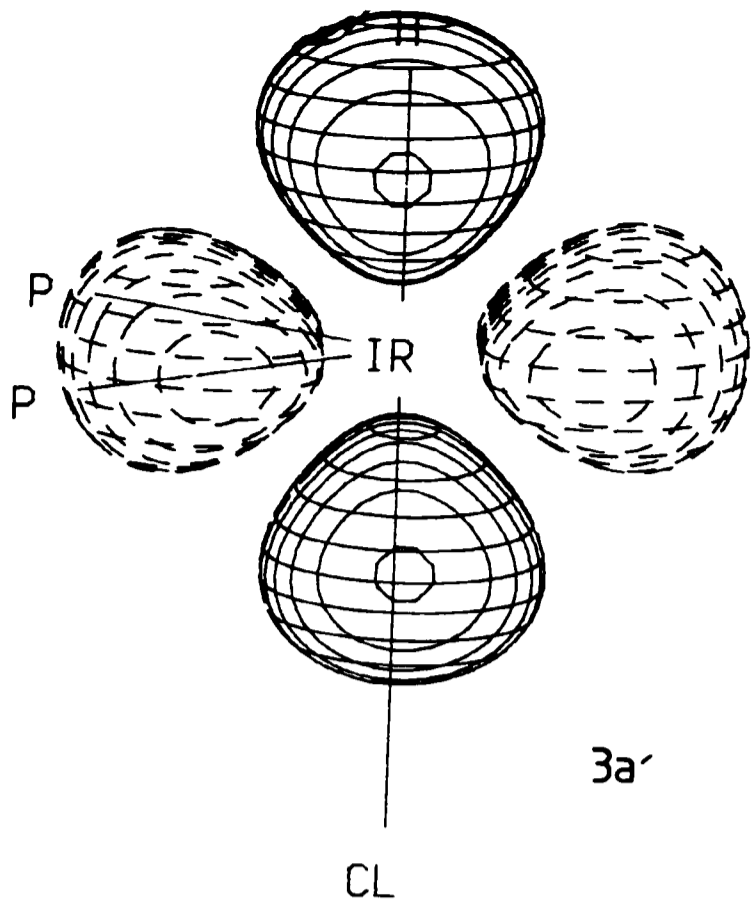
1:  $ML_2Y_2X$  FRAGMENT

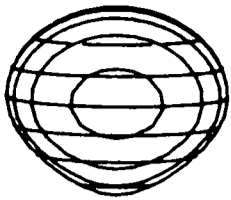
2:  $ML_2XY$  FRAGMENT

3: MCP FRAGMENT

4:  $ML_2$  FRAGMENT

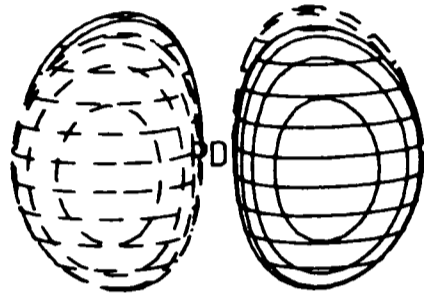
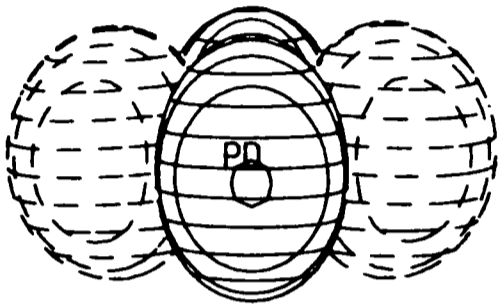
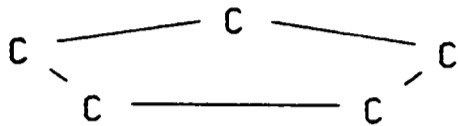
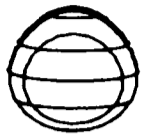




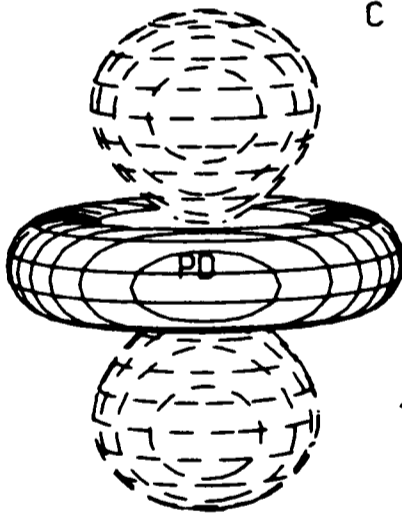
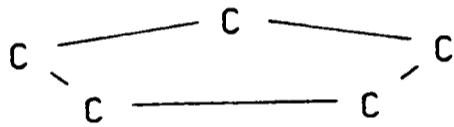
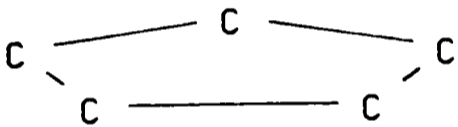


PD

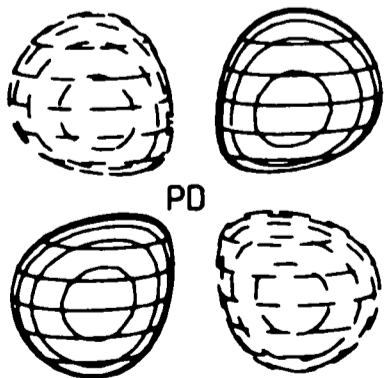
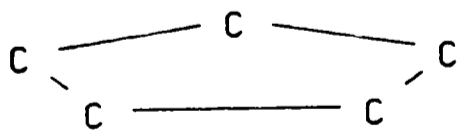
2a,



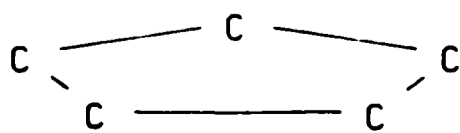
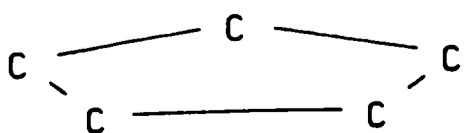
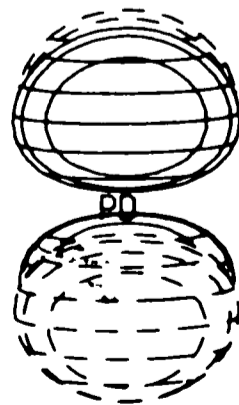
e,



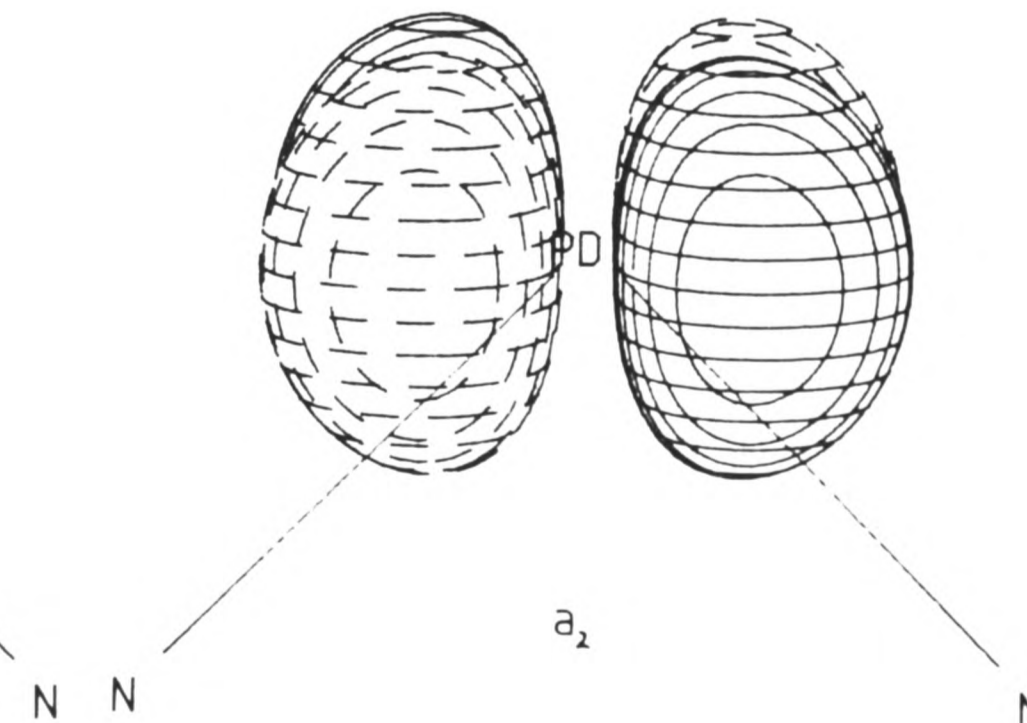
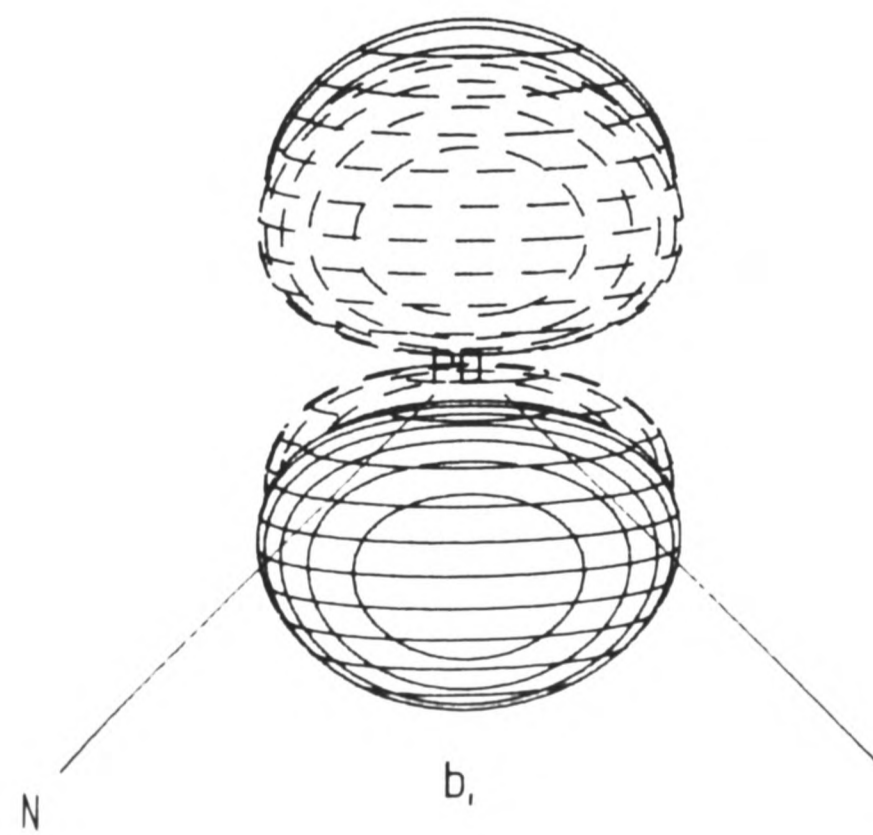
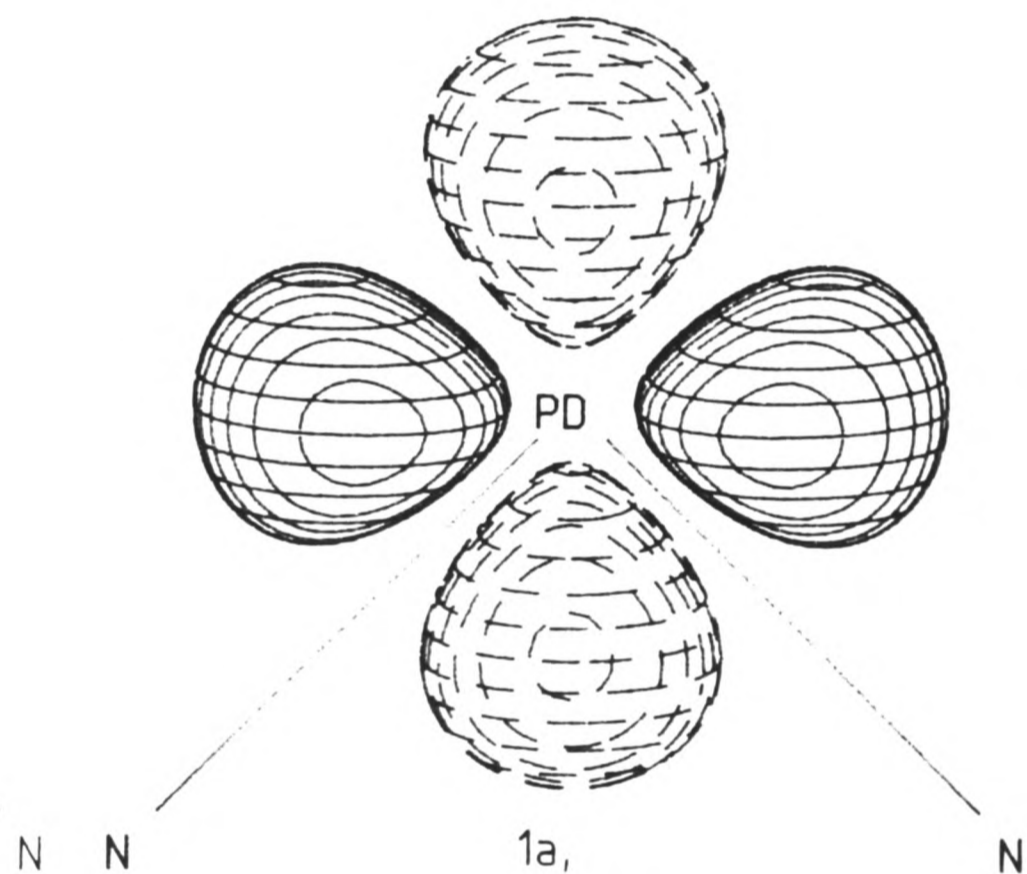
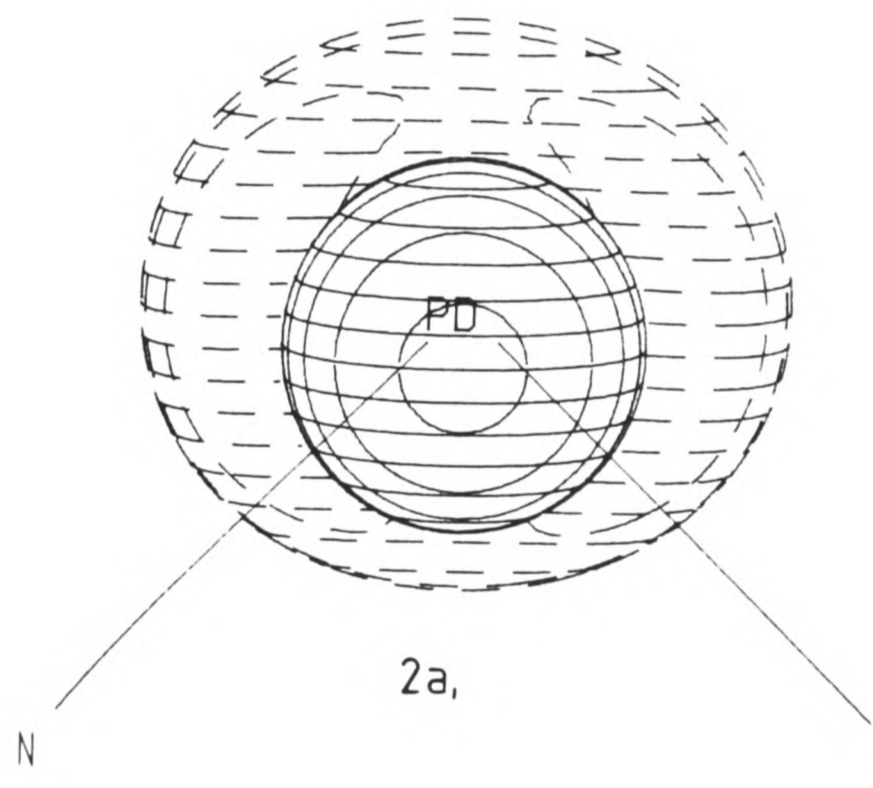
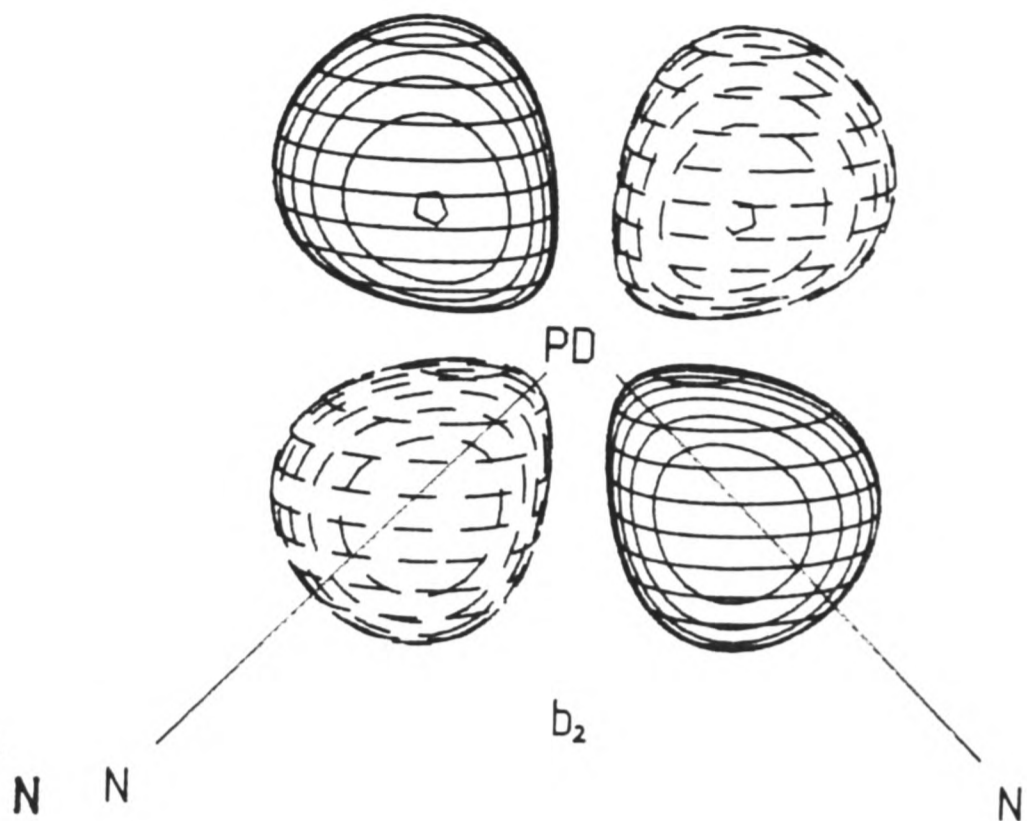
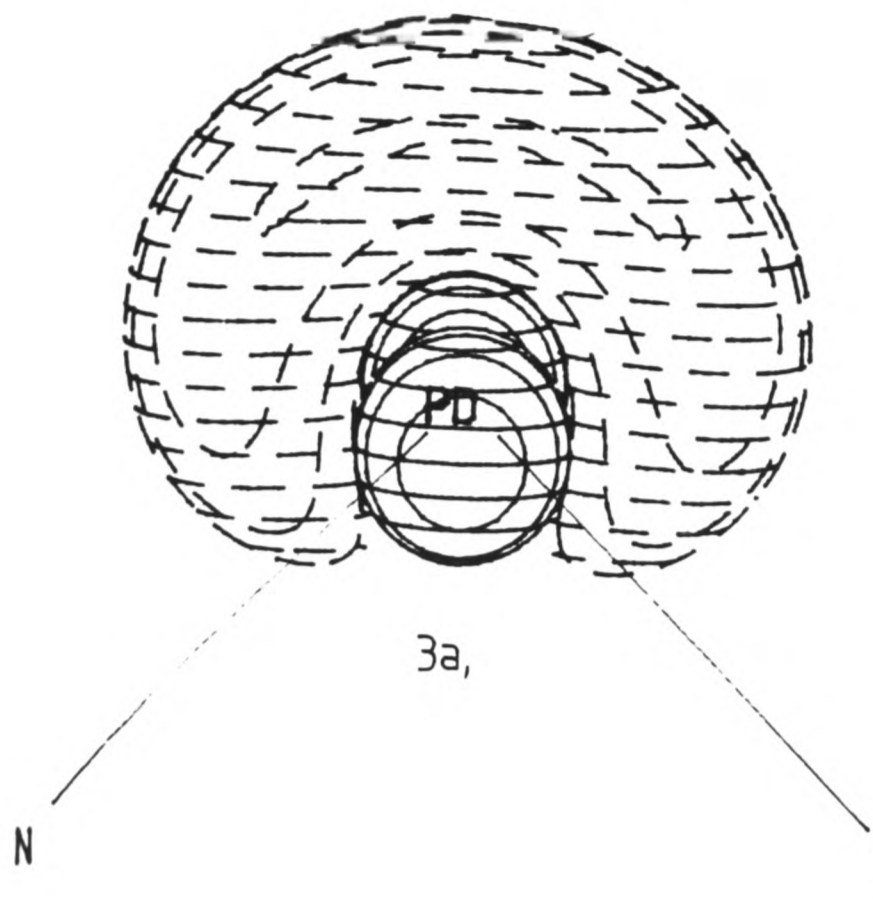
1a,



e<sub>2</sub>









### **APPENDIX 3**

**THERMAL PARAMETERS FOR:**

**1: CPMOME**

**2: CPMOBUT**

**3: TRIMET**

Thermal Vibration Parameters with Standard Deviations for CPMOME

	U11	U22	U33	U23	U13	U12
Mo	0.0231( 1)	0.0187( 1)	0.0179( 1)	0.0008( 1)	0.0033( 1)	0.0022( 1)
C(1)	0.0441(13)	0.0395(11)	0.0347(11)	-0.0026( 8)	0.0190(10)	0.0111( 8)
C(2)	0.0442(10)	0.0232( 7)	0.0283( 8)	-0.0032( 6)	0.0063( 7)	0.0108( 7)
C(3)	0.0421(10)	0.0243( 8)	0.0386(10)	-0.0036( 7)	-0.0004( 8)	-0.0024( 7)
C(4)	0.0608(14)	0.0321(10)	0.0374(11)	0.0054( 8)	0.0056(10)	0.0201(10)
C(5)	0.0456(12)	0.0635(16)	0.0672(17)	0.0381(14)	0.0213(12)	0.0310(12)
C(6)	0.0640(16)	0.0391(13)	0.0607(16)	0.0191(11)	-0.0281(14)	-0.0023(11)
C(7)	0.0923(22)	0.0508(13)	0.0260( 9)	0.0138(10)	0.0123(12)	0.0270(14)
C(8)	0.0389(11)	0.0440(13)	0.0808(20)	0.0380(14)	0.0053(12)	-0.0038(10)
C(9)	0.0888(20)	0.0263(10)	0.0388(11)	-0.0015( 8)	-0.0101(12)	0.0229(11)
C(10)	0.0301( 9)	0.0358( 9)	0.0331( 9)	-0.0067( 8)	0.0001( 7)	0.0066( 8)
C(11)	0.0321( 8)	0.0354( 9)	0.0296( 8)	0.0051( 7)	0.0090( 7)	0.0110( 7)
O(1)	0.0374( 8)	0.0776(14)	0.0567(11)	-0.0248(11)	-0.0149( 8)	0.0144(10)
O(2)	0.0581(10)	0.0685(12)	0.0412( 9)	0.0231( 9)	0.0286( 8)	0.0245(10)

Thermal Vibration Parameters with Standard Deviations for CPMOBUT

	U11	U22	U33	U23	U13	U12
Mo	0.0295(2)	0.0298(2)	0.0225(1)	0.0030(1)	0.0021(1)	0.0079(1)
C1(1)	0.0435(4)	0.0516(5)	0.0399(4)	-0.0016(3)	-0.0105(3)	-0.0068(4)
C1(2)	0.0467(4)	0.0446(4)	0.0326(4)	0.0127(3)	0.0023(3)	0.0049(3)
C(1)	0.0415(17)	0.0583(21)	0.0262(14)	0.0016(12)	0.0073(12)	0.0048(14)
C(2)	0.0496(18)	0.0566(21)	0.0282(14)	-0.0101(13)	0.0038(13)	0.0177(16)
C(3)	0.0817(27)	0.0357(16)	0.0303(15)	-0.0077(13)	-0.0045(15)	0.0071(17)
C(4)	0.0613(24)	0.0581(23)	0.0336(16)	0.0037(15)	-0.0104(16)	-0.0178(19)
C(5)	0.1000(41)	0.0502(24)	0.0770(32)	0.0231(23)	0.0300(30)	0.0347(26)
C(6)	0.1228(50)	0.1168(50)	0.0824(36)	-0.0430(33)	-0.0680(35)	0.0976(46)
C(7)	0.0399(21)	0.0652(30)	0.1308(50)	0.0009(31)	0.0306(27)	0.0219(21)
C(8)	0.0700(27)	0.0506(22)	0.0593(23)	-0.0027(18)	0.0230(21)	0.0256(21)
C(9)	0.0843(34)	0.0384(22)	0.1076(43)	-0.0037(24)	0.0264(31)	0.0193(21)

Thermal Vibration Parameters with Standard Deviations for TRIMET

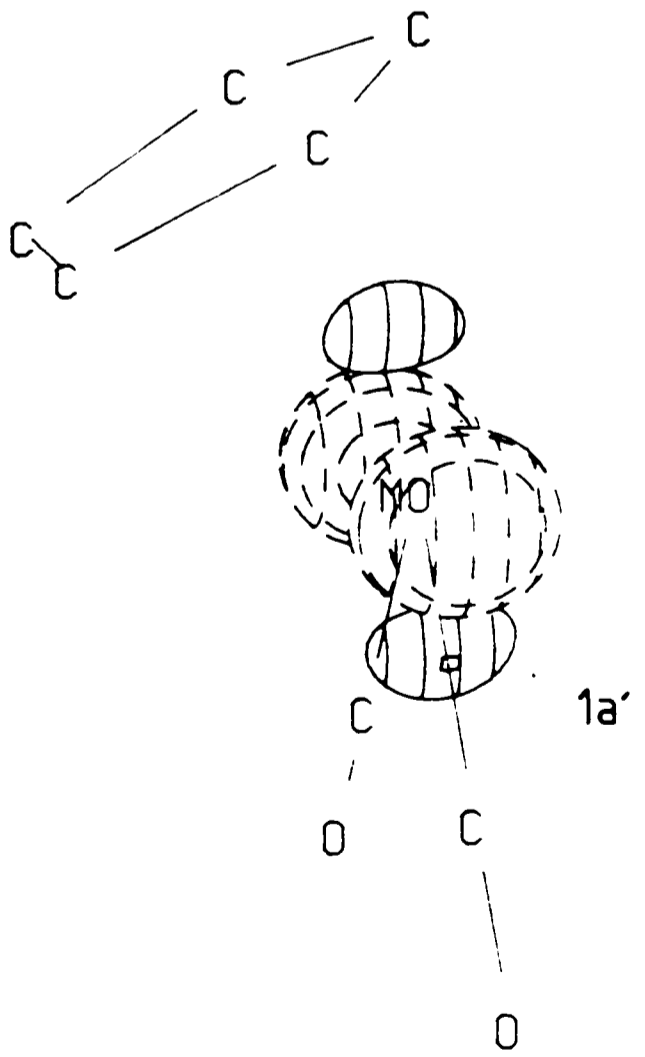
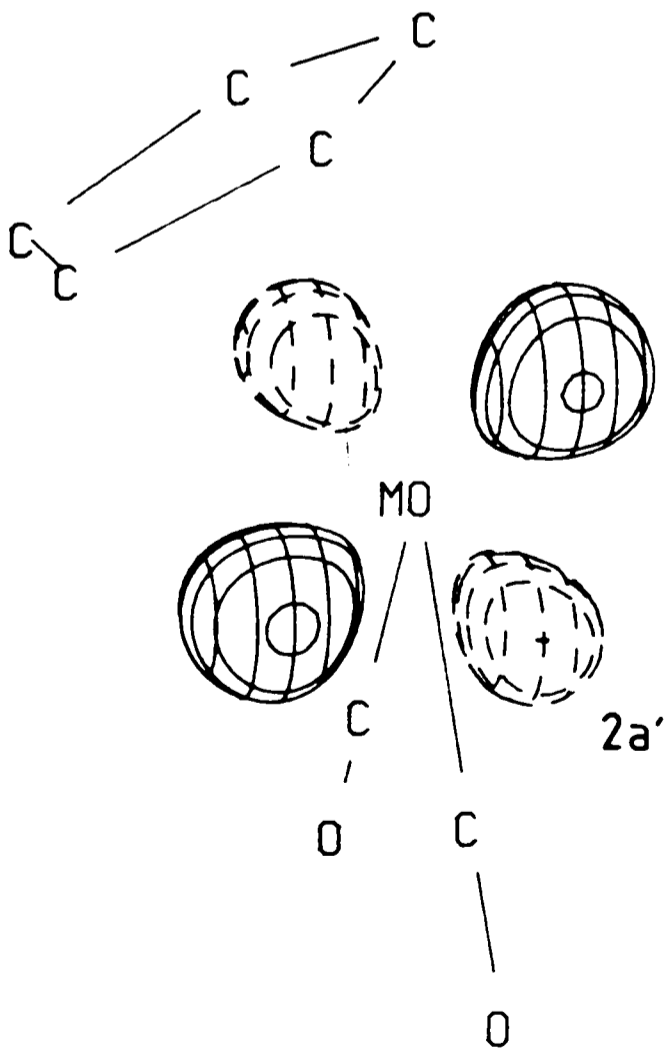
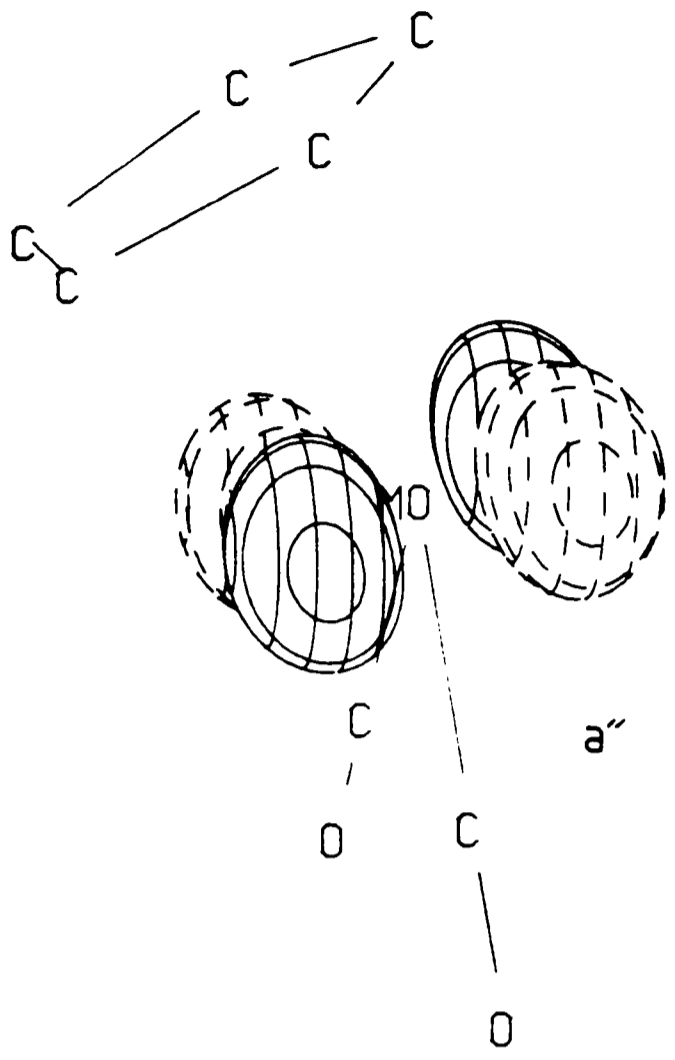
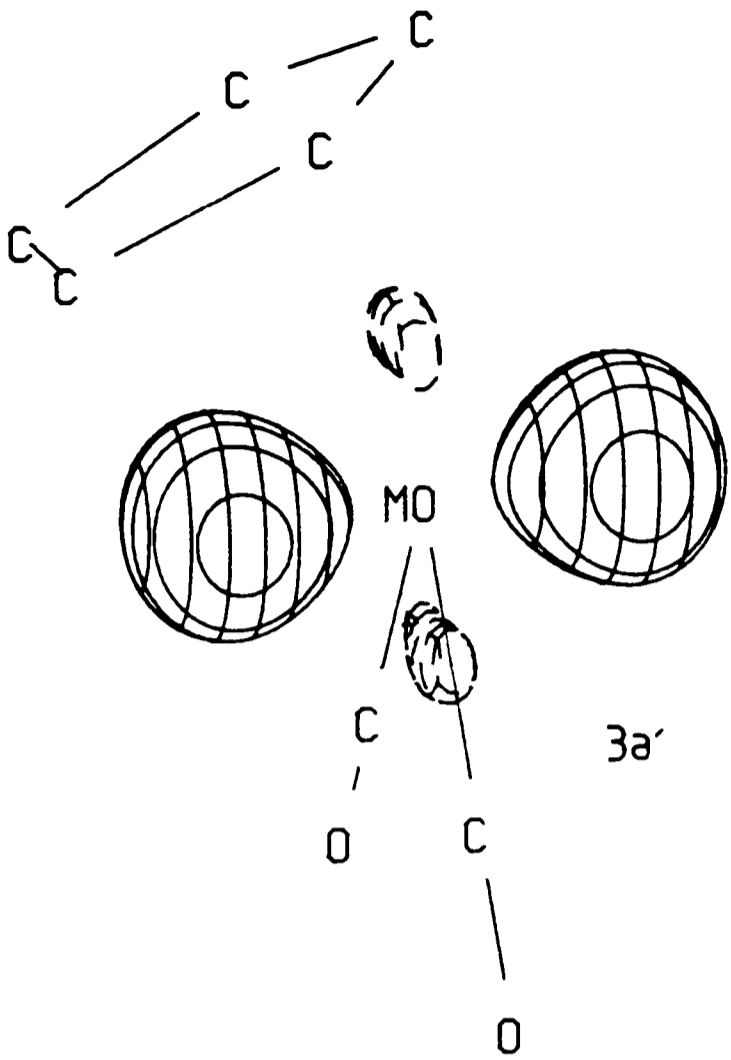
	U11	U22	U33	U23	U13	U12
Mo	0.0425(5)	0.0391(4)	0.0372(5)	0.0011(3)	0.0019(2)	-0.0023(2)
C(1)	0.0556(47)	0.0773(51)	0.0307(34)	0.0068(35)	0.0016(35)	-0.0245(35)
C(2)	0.0427(41)	0.0632(42)	0.0442(43)	-0.0081(32)	0.0048(28)	0.0101(37)
C(3)	0.0519(43)	0.0818(51)	0.0551(46)	0.0269(40)	0.0220(35)	0.0075(41)
C(4)	0.0415(36)	0.0584(41)	0.0574(47)	0.0041(36)	0.0165(33)	-0.0056(32)
C(5)	0.0580(44)	0.0594(43)	0.0604(47)	0.0018(38)	0.0164(37)	-0.0063(37)
C(9)	0.1010(57)	0.0547(45)	0.0886(59)	0.0007(44)	0.0082(52)	-0.0171(46)
C(6)	0.0780(53)	0.1246(64)	0.0511(47)	-0.0126(49)	-0.0106(42)	-0.0301(52)
C(8)	0.0283(36)	0.1162(62)	0.0815(53)	-0.0017(50)	0.0080(36)	-0.0093(41)
C(10)	0.0675(51)	0.1059(61)	0.1058(63)	0.0475(52)	-0.0063(49)	0.0136(51)
C(7)	0.0928(57)	0.0829(54)	0.1069(61)	-0.0464(51)	0.0396(52)	0.0102(49)
C(101)	0.0565(43)	0.0639(43)	0.0613(48)	-0.0019(41)	-0.0002(38)	0.0049(37)
O(101)	0.0935(43)	0.0886(44)	0.0854(47)	-0.0311(38)	-0.0311(38)	-0.0059(39)
C(102)	0.0636(46)	0.0538(43)	0.0908(57)	0.0111(42)	-0.0243(45)	0.0084(38)
O(102)	0.1126(49)	0.0698(42)	0.1731(63)	0.0221(46)	-0.0562(51)	0.0245(41)
C(11)	0.0734(51)	0.0770(50)	0.0639(49)	0.0086(44)	0.0102(43)	-0.0236(45)
C(22)	0.0443(41)	0.0985(57)	0.0880(56)	-0.0221(50)	0.0375(40)	0.0012(41)
C(33)	0.0722(49)	0.0745(49)	0.0511(44)	0.0057(41)	0.0087(40)	-0.0279(41)
C(44)	0.0822(56)	0.1222(64)	0.0513(48)	0.0128(52)	-0.0040(45)	-0.0314(54)
B	0.0161(34)	0.1229(67)	0.0796(58)	-0.0211(45)	0.0045(37)	0.0005(43)

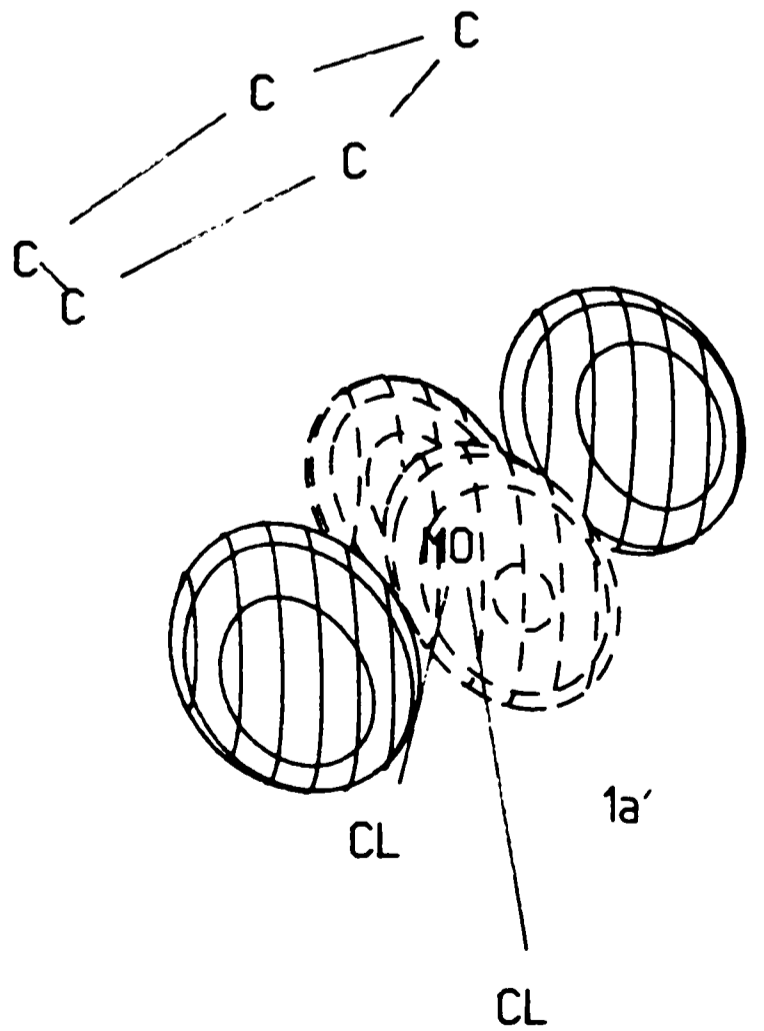
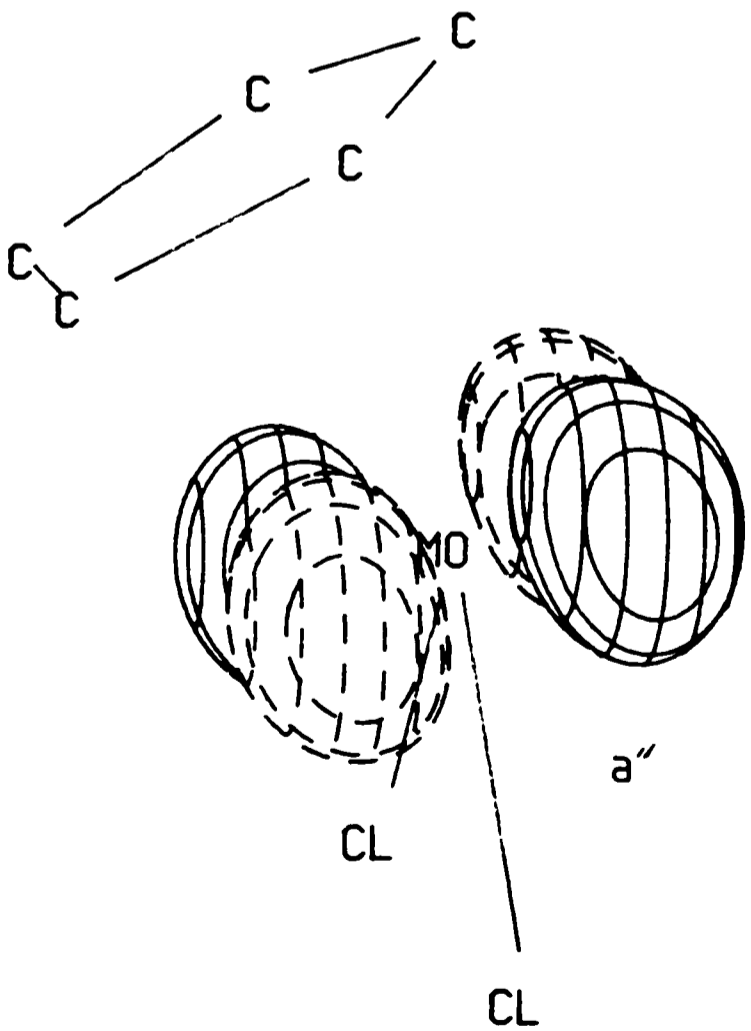
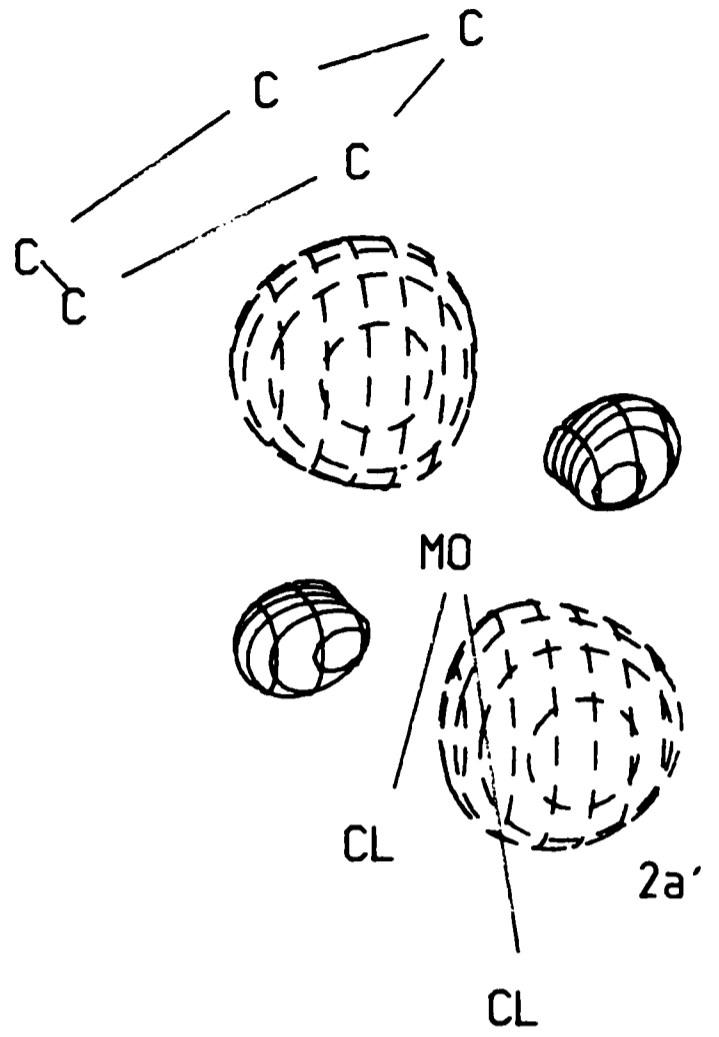
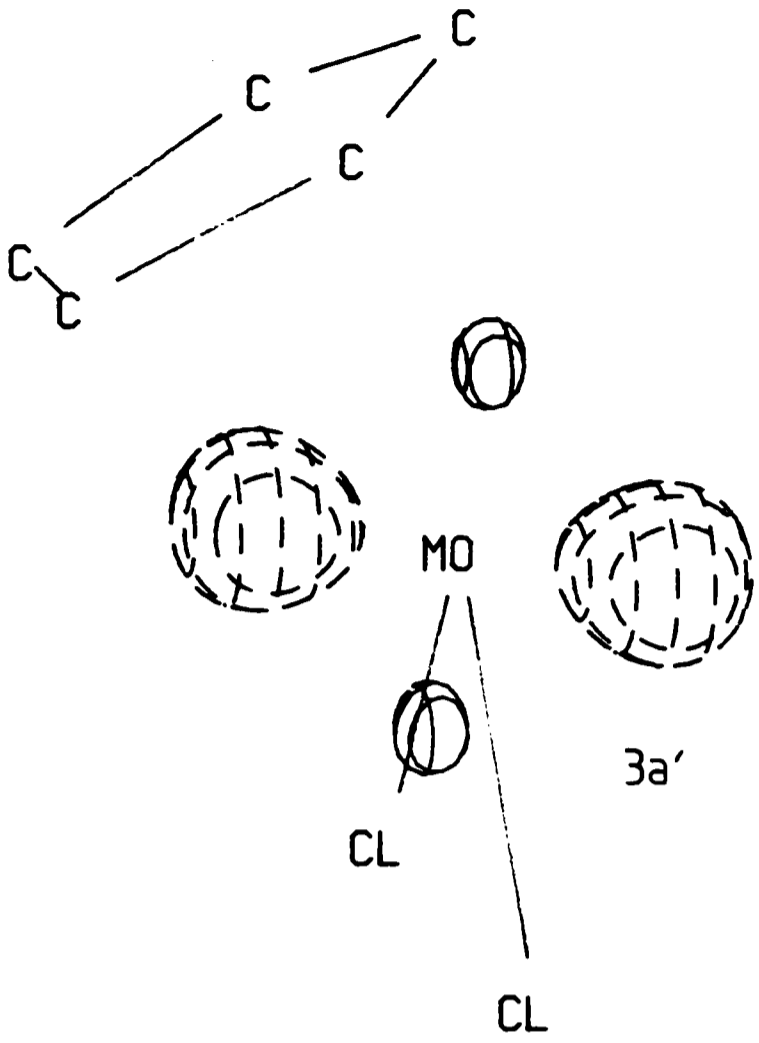
## **APPENDIX 4**

ORBITAL CONTOUR PLOTS FOR:

1:  $\text{CpMo}(\text{CO})_2^+$  FRAGMENT

2:  $\text{CpMo}(\text{Cl})_2$  FRAGMENT





***APPENDIX 5***

**REPRINTS**



## Reactions of Co-ordinated Ligands. Part 30.<sup>1</sup> The Transformation of Methylene-cyclopropanes into Cationic $\eta^4$ -Trimethylenemethanemolybdenum Complexes, Reactions with Nucleophilic Reagents, and the Molecular Structure of $[\text{Mo}\{\eta^4\text{-C}(\text{CH}_2)_3\}(\text{CO})_2(\eta\text{-C}_5\text{Me}_5)][\text{BF}_4]$ †

Stephen R. Allen, Stephen G. Barnes, Michael Green,\* Grainne Moran, and Lynda Trollope  
 Department of Inorganic Chemistry, The University, Bristol BS8 1TS

Nicholas W. Murrall and Alan J. Welch

Dewar Crystallographic Laboratory, Department of Chemistry, University of Edinburgh, Edinburgh EH9 3JJ

Dima M. Sharaiha

Department of Chemistry, The City University, London EC1V 0HB

Reaction of  $[\text{Mo}_2(\text{CO})_6(\eta\text{-C}_5\text{Me}_5)_2]$  with methylenecyclopropane and  $\text{AgBF}_4$  in  $\text{CH}_2\text{Cl}_2$  affords the cationic trimethylenemethane complex  $[\text{Mo}\{\eta^4\text{-C}(\text{CH}_2)_3\}(\text{CO})_2(\eta\text{-C}_5\text{Me}_5)][\text{BF}_4]$ . Methylene-cyclopropane and 2,2-dimethylmethylene-cyclopropane react with  $[\text{Mo}(\text{NCMe})_2(\text{CO})_2(\eta\text{-C}_5\text{H}_5)][\text{BF}_4]$  to give  $[\text{Mo}\{\eta^4\text{-C}(\text{CH}_2)_3\}(\text{CO})_2(\eta\text{-C}_5\text{H}_5)][\text{BF}_4]$  and  $[\text{Mo}\{\eta^4\text{-C}(\text{CH}_2)_2\text{CMe}_2\}(\text{CO})_2(\eta\text{-C}_5\text{H}_5)][\text{BF}_4]$  respectively. A single-crystal X-ray diffraction study of  $[\text{Mo}\{\eta^4\text{-C}(\text{CH}_2)_3\}(\text{CO})_2(\eta\text{-C}_5\text{Me}_5)][\text{BF}_4]$  confirmed that ring opening of methylenecyclopropane had occurred. The complex crystallises in the centrosymmetric orthorhombic space group *Pbca* with  $a = 12.822(2)$ ,  $b = 12.311(3)$ ,  $c = 22.660(4)$  Å, and  $Z = 8$  ion pairs. The structure has been solved by conventional methods and refined by full-matrix least squares to  $R = 0.0674$  for 2 747 observed reflections at  $268 \pm 1$  K. In the cation the trimethylenemethane ligand adopts an orientation that is *syn* with respect to the OC-Mo-CO angle. It is pyramidal with the  $\text{CH}_2$  groups bent towards the molybdenum atom by an average of  $12.4^\circ$ . There is intramolecular congestion involving the  $\text{C}_5\text{Me}_5$  and  $\text{C}(\text{CH}_2)_3$  ligands that may contribute towards the observed asymmetric bonding of the former to the metal atom. Extended Hückel molecular-orbital calculations suggest that the observed *syn* stereochemistry is electronically preferred, and that the barrier to rotation of the  $\eta^4\text{-C}(\text{CH}_2)_3$  ligand relative to a  $\text{Mo}(\text{CO})_2(\eta\text{-C}_5\text{H}_5)^+$  fragment is high. The stereochemistry of the ring-opening reaction is disrotatory-out as exemplified by the conversion of *cis*- and *trans*-2,3-dimethylmethylene-cyclopropane into *syn, syn*-dimethyl and *syn, anti*-dimethyl-trimethylenemethane complexes. The reaction of these cationic  $\eta^4$ -trimethylenemethane complexes with the nucleophiles  $\text{BH}_4^-$ ,  $\text{OH}^-$ ,  $\text{CuMe}_2^-$ , and  $\text{SPh}^-$  affords  $\eta^3$ -allylic complexes derived from attack on the peripheral carbons.

Methylene-cyclopropanes react with compounds of  $\text{Fe}^0$ ,  $\text{Rh}^1$ ,  $\text{Ir}^1$ ,  $\text{Pt}^{II}$ , and  $\text{Pt}^0$  to form simple  $\eta^2$ -bonded alkene complexes in which the three-membered ring remains intact.<sup>2,3</sup> However, these small-ring compounds are also known to undergo transition-metal-mediated reactions where carbon-carbon cleavage occurs. This is illustrated by the reaction of  $[\text{Fe}_2(\text{CO})_9]$  with methylene-2-phenylcyclopropane forming tricarbonyl( $\eta^4$ -trimethylenephénylmethane)iron, a detailed study<sup>4</sup> with deuterium-labelled methylene-2-phenylcyclopropane showing that a disrotatory-out ring-opening reaction occurs. Furthermore, a recent study<sup>5</sup> of the chloropalladation reactions of methylene-cyclopropanes carrying alkyl substituents on the three-membered ring showed that cleavage of the 2,3- $\sigma$  bond occurred in a disrotatory manner. Ring cleavage also occurs in the palladium(0)-catalysed<sup>6-10</sup> cycloaddition reactions of methylene-cyclopropanes, although the question<sup>11</sup> as to whether these reactions involve  $\eta^4$ -trimethylenemethane complexes remains to be answered. We had previously observed<sup>12</sup> that  $[\text{Mo}(\text{CO})_3(\eta\text{-C}_5\text{Me}_5)]^+$  reacts with methylene-cyclopropane to form the first cationic  $\eta^4$ -bonded trimethylenemethane complex, and this paper describes a detailed study of this reaction.

### Results and Discussion

In exploring the chemistry of cationic molybdenum complexes it was observed that room-temperature addition of  $\text{AgBF}_4$  to a methylene chloride solution of  $[\text{Mo}_2(\text{CO})_6(\eta\text{-C}_5\text{Me}_5)_2]$  and methylene-cyclopropane led to a rapid redox reaction as evidenced by the formation of a silver mirror, and the production of two molybdenum complexes  $[\text{Mo}(\text{CO})_4(\eta\text{-C}_5\text{Me}_5)][\text{BF}_4]$  and  $[\text{Mo}\{\eta^4\text{-C}(\text{CH}_2)_3\}(\text{CO})_2(\eta\text{-C}_5\text{Me}_5)][\text{BF}_4]$  (1). Examination of the  $^1\text{H}$  and  $^{13}\text{C}$  n.m.r. and i.r. spectra suggested that (1) was a trimethylenemethane complex presumably formed by 2,3- $\sigma$ -bond cleavage of an intermediate  $\eta^2$ -bonded methylene-cyclopropane species. A related reaction occurred when methylene-cyclopropane was added to *cis*-bis(acetonitrile)dicarbonyl( $\eta$ -cyclopentadienyl)molybdenum tetrafluoroborate ‡ dissolved in  $\text{CH}_2\text{Cl}_2$  affording a good yield of the cation (2), the cyclopentadienyl analogue of (1). The reaction is not limited to unsubstituted methylene-cyclopropane since 2,2-dimethylmethylene-cyclopropane also reacted smoothly with  $[\text{Mo}(\text{NCMe})_2(\text{CO})_2(\eta\text{-C}_5\text{H}_5)][\text{BF}_4]$  to give a good yield of complex (3).

In order to confirm that ring opening had in fact occurred a single-crystal X-ray diffraction study was carried out with a suitable crystal of complex (1). Figure 1 represents a perspective view of the cation of (1), and demonstrates the atomic numbering scheme adopted. Table 1 lists the internuclear distances, and Table 2 selected interbond angles. The cation has effective  $C_s$  symmetry about the plane defined by atoms

† Dicarbonyl( $\eta$ -pentamethylcyclopentadienyl)( $\eta^4$ -trimethylenemethane)molybdenum tetrafluoroborate.

Supplementary data available (No. SUP 23876, 21 pp.): thermal parameters, least-squares planes, structure factors. See Instructions for Authors, *J. Chem. Soc., Dalton Trans.*, 1984, Issue 1, pp. xvii-xix.

Non-S.I. units employed: cal = 4.184 J; eV  $\approx$   $1.60 \times 10^{-19}$  J.

‡ Prepared by protonation ( $\text{HBF}_4 \cdot \text{Et}_2\text{O}$ ) of  $[\text{MoMe}(\text{CO})_3(\eta\text{-C}_5\text{H}_5)]$  dissolved in  $\text{CH}_2\text{Cl}_2$  followed by reaction with MeCN.<sup>13</sup>

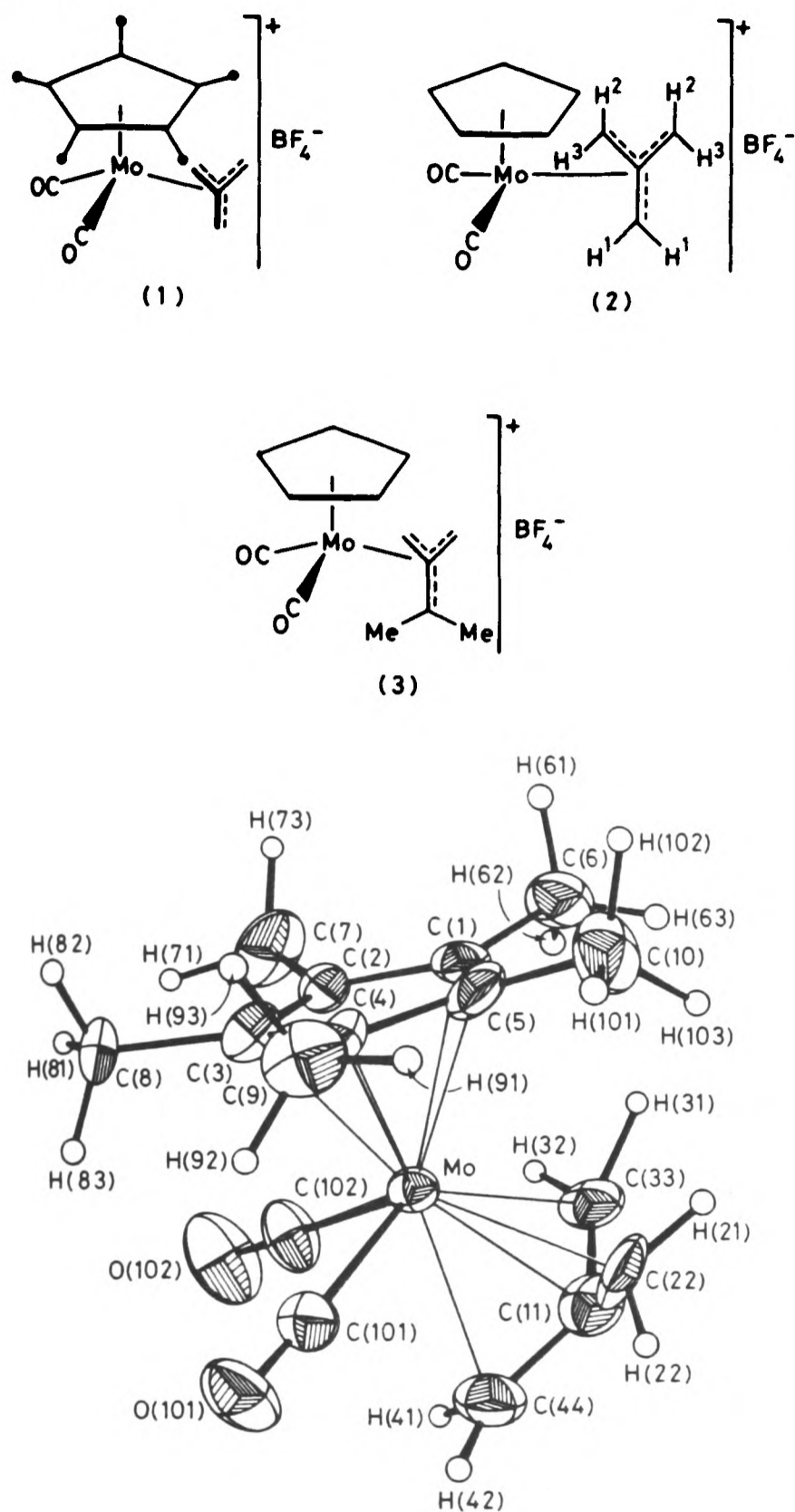


Figure 1. View of the cation  $[\text{Mo}(\eta^4\text{-C}(\text{CH}_2)_3)(\text{CO})_2(\eta\text{-C}_5\text{Me}_5)]^+$ . Thermal ellipsoids are drawn at the 30% probability level, except for H atoms which have an artificial radius of 0.1 Å for clarity. H(72) is obscured by C(7)

Mo, C(11), C(44), C(3), and C(8), and Tables 1 and 2 are organised so that parameters related across this approximate mirror are easily compared.

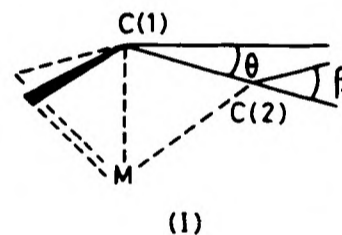
The complexed  $\eta^4$ -trimethylenemethane present in (1) is pyramidal, not flat. The reasons for pyramidalisation have been well documented<sup>14</sup> and they may be quantified by the two angular parameters  $\theta$  and  $\beta$  shown in (I), where  $\beta$  is the angle between the line C(1)-C(2) and the plane C(2)H<sub>2</sub>. For the complex  $[\text{Fe}(\eta^4\text{-C}(\text{CH}_2)_3)(\text{CO})_3]$ <sup>15</sup>  $\theta = 13.6^\circ$  and  $\beta = 14.4^\circ$ , and in the case of  $[\text{Fe}(\eta^4\text{-C}(\text{CH}_2)_2\text{CHPh})(\text{CO})_3]$   $\theta$  values of 13.9, 13.0, and  $11.7^\circ$  are recorded.<sup>16</sup> Tricarbonyl( $\eta^4$ -7-methylenecyclohepta-1,3,5-triene)iron also contains an iron-trimethylenemethane linkage, with  $\theta = 11.0, 10.1,$  and  $10.1^\circ$  and  $\beta = 14.8, 15.9,$  and  $23.4^\circ$ .<sup>17</sup>

In complex (1),  $\theta$  values are 14.6(5), 12.0(6), and  $10.6(6)^\circ$  to

Table 1. Internuclear distances (Å) \* in complex (1)

Mo-C(1)	2.374(9)	Mo-C(5)	2.349(9)
Mo-C(2)	2.314(8)	Mo-C(4)	2.318(9)
	Mo-C(3)	2.296(9)	
	Mo-C(11)	2.213(10)	
Mo-C(22)	2.324(9)	Mo-C(33)	2.358(9)
	Mo-C(44)	2.392(11)	
Mo-C(101)	2.022(10)	Mo-C(102)	2.032(10)
C(1)-C(2)	1.429(14)	C(5)-C(4)	1.464(14)
C(2)-C(3)	1.433(14)	C(4)-C(3)	1.400(12)
	C(5)-C(1)	1.396(14)	
C(1)-C(6)	1.471(13)	C(5)-C(10)	1.518(14)
C(2)-C(7)	1.477(13)	C(4)-C(9)	1.476(13)
	C(3)-C(8)	1.504(12)	
C(11)-C(22)	1.460(16)	C(11)-C(33)	1.394(14)
	C(11)-C(44)	1.402(17)	
C(101)-O(101)	1.122(11)	C(102)-O(102)	1.114(11)
C(22)-H(21)	1.06(8)	C(33)-H(31)	1.17(8)
C(22)-H(22)	0.91(9)	C(33)-H(32)	1.01(8)
C(44)-H(41)	1.06(8)	C(44)-H(42)	0.90(10)
B-F(1)	1.29(3)	B-F(8)	1.52(7)
B-F(2)	1.40(2)	B-F(9)	1.38(4)
B-F(3)	1.41(5)	B-F(10)	1.43(4)
B-F(4)	1.38(3)	B-F(11)	1.34(2)
B-F(5)	1.44(3)	B-F(12)	1.37(5)
B-F(6)	1.46(3)	B-F(13)	1.39(5)
B-F(7)	1.39(5)	B-F(14)	1.46(7)

\* Estimated standard deviations are given in parentheses throughout this paper.



C(22), C(33), and C(44) respectively. The bend-back angles at C(22) and C(44) are calculated as 55.1 and  $6.1^\circ$  respectively, whilst the C(33)H<sub>2</sub> plane appears to be tipped towards the metal atom, with  $\beta = -15.7^\circ$ . However, the positions of the hydrogen atoms are subject to relatively large errors, and we are less confident about the molecular parameters derived from them.

In all the above species the pyramidalisation of the trimethylenemethane fragment is, although significant, insufficiently severe to cause the distal carbon atoms to approach closer to the metal than does the central one; thus, for the iron complexes<sup>15-17</sup> Fe-C(central) distances lie within the narrow range 1.932-1.946 Å, whilst Fe-C(outer) values span 2.098-2.175 Å. In cation (1) the Mo-C(CH<sub>2</sub>)<sub>3</sub> distances are longer, but this difference is essentially maintained, Mo-C(11) being 2.213(10) Å whilst Mo-C(22,33,44) lie within 2.324(9)-2.392(11) Å. Some asymmetry in the C-C bonds of the trimethylenemethane ligand of (1) may be evident, the difference between C(11)-C(22) and C(11)-C(33) just lying on the verge of significance. These bond lengths extend in both directions the previous<sup>15-17</sup> range of such distances, 1.405(4)-1.45(2) Å.

Parameters within the Mo(CO)<sub>2</sub> moiety are unexceptional, but the  $\eta\text{-C}_5\text{Me}_5$  ligand shows some asymmetry that indicates intramolecular steric congestion between it and the trimethylenemethane ligand. Thus, Mo-C(1,5) > Mo-C(2,4) > Mo-C(3), demonstrating that the ligand is slightly tilted away from C(22) and C(33), and H...H contacts of 2.03, 2.05, and 2.07 Å exist between H(31) and H(63) and H(62), and H(21) and H(103), respectively. Although, consistent with this,

Table 2. Selected interbond angles (°) \*

C(1)-Mo-C(2)	35.5(3)	C(4)-Mo-C(5)	36.6(3)
C(2)-Mo-C(3)	36.2(4)	C(3)-Mo-C(4)	35.3(3)
	C(1)-Mo-C(5)	34.4(3)	
C(11)-Mo-C(22)	37.5(4)	C(11)-Mo-C(33)	35.3(4)
	C(11)-Mo-C(44)	35.2(4)	
C(22)-Mo-C(44)	60.3(5)	C(33)-Mo-C(44)	61.1(4)
	C(22)-Mo-C(33)	62.1(4)	
	C(11)-Mo-Z	137.5(6)	
	C(101)-Mo-C(102)	88.9(4)	
C(101)-Mo-Z	108.5(7)	C(102)-Mo-Z	107.5(6)
C(101)-Mo-C(11)	102.5(4)	C(102)-Mo-C(11)	101.3(5)
Mo-C(1)-C(2)	70.0(5)	Mo-C(5)-C(4)	70.6(5)
Mo-C(1)-C(5)	71.8(5)	Mo-C(5)-C(1)	73.8(5)
Mo-C(1)-C(6)	128.9(7)	Mo-C(5)-C(10)	131.1(7)
C(5)-C(1)-C(2)	106.7(8)	C(1)-C(5)-C(4)	110.2(8)
C(5)-C(1)-C(6)	125.1(11)	C(1)-C(5)-C(10)	125.5(11)
C(2)-C(1)-C(6)	127.2(9)	C(4)-C(5)-C(10)	123.4(10)
Mo-C(2)-C(3)	71.2(5)	Mo-C(4)-C(3)	71.5(5)
Mo-C(2)-C(1)	74.6(5)	Mo-C(4)-C(5)	72.9(5)
Mo-C(2)-C(7)	130.4(8)	Mo-C(4)-C(9)	131.0(7)
C(1)-C(2)-C(3)	108.4(8)	C(5)-C(4)-C(3)	105.5(8)
C(1)-C(2)-C(7)	123.7(9)	C(5)-C(4)-C(9)	124.8(9)
C(3)-C(2)-C(7)	126.6(6)	C(3)-C(4)-C(9)	128.2(8)
Mo-C(3)-C(2)	72.5(5)	Mo-C(3)-C(4)	73.2(5)
	Mo-C(3)-C(8)	127.9(7)	
C(2)-C(3)-C(8)	125.0(9)	C(4)-C(3)-C(8)	125.2(9)
	C(2)-C(3)-C(4)	109.2(2)	
Mo-C(101)-O(101)	177.3(9)	Mo-C(102)-O(102)	177.0(10)
Mo-C(11)-C(22)	75.4(5)	Mo-C(11)-C(33)	78.0(6)
	Mo-C(11)-C(44)	79.4(6)	
Mo-C(22)-C(11)	67.2(5)	Mo-C(33)-C(11)	66.7(5)
	Mo-C(44)-C(11)	65.4(6)	
C(22)-C(11)-C(44)	111.8(11)	C(33)-C(11)-C(44)	119.4(12)
	C(22)-C(11)-C(33)	115.4(10)	
Mo-C(22)-H(21)	114(4)	Mo-C(33)-H(31)	99(4)
Mo-C(22)-H(22)	126(5)	Mo-C(33)-H(32)	92(4)
H(21)-C(22)-C(11)	105(4)	H(31)-C(33)-C(11)	126(4)
H(22)-C(22)-C(11)	109(5)	H(32)-C(33)-C(11)	138(5)
H(21)-C(22)-H(22)	118(6)	H(31)-C(33)-H(32)	92(6)
Mo-C(44)-H(41)	105(5)	Mo-C(44)-H(42)	114(6)
H(41)-C(44)-C(11)	125(5)	H(42)-C(44)-C(11)	137(6)
	H(41)-C(44)-H(42)	97(7)	

\* Z is the centroid of the cyclopentadienyl ring and has fractional co-ordinates -0.015 76(16), 0.198 18(18), 0.161 71(9).

C(1)-C(5) is the shortest pentagonal distance, C-C bonds around the ring are arranged C(1)-C(5), C(3)-C(4) < C(1)-C(2), C(2)-C(3) < C(4)-C(5). The C<sub>5</sub> ring is reasonably planar (root mean square deviation 0.006 Å, see SUP 23876), but shows a small distortion towards an envelope fold across C(2)···C(4) of 1.4°, away from the metal atom. It appears that the intramolecular crowding between η-C<sub>5</sub>Me<sub>5</sub> and trimethylenemethane ligands does not cause increased out-of-plane bending of the methyl groups pendant to C(1) and C(5) since, referred to the five-atom ring, these are depressed (away from Mo) by 5.9 and 9.2° respectively, cf. 9.4, 8.4, and 9.8° for corresponding angles at C(2), C(3), and C(4).

The fluorine atoms of the tetrafluoroborate anion are disordered over 14 positions whose population parameters (p.p.) range from 10 to 55%; B-F distances span 1.29(3)-1.52(7) Å. All F atoms were given the same (fixed) thermal parameter in refinement, but in Figure 2 the anion is drawn such that U<sub>F</sub> values are in the ratio of their p.p. Although possible discrete tetrahedra can be picked out [e.g. BF-(1,2,4,11), F-B-F angles between 88 and 115°], the disorder is by no means 'clean.'

Figure 3 presents a view of the crystal packing. There are no unusual features.

There are clearly two limiting conformations of the [Mo{η<sup>4</sup>-

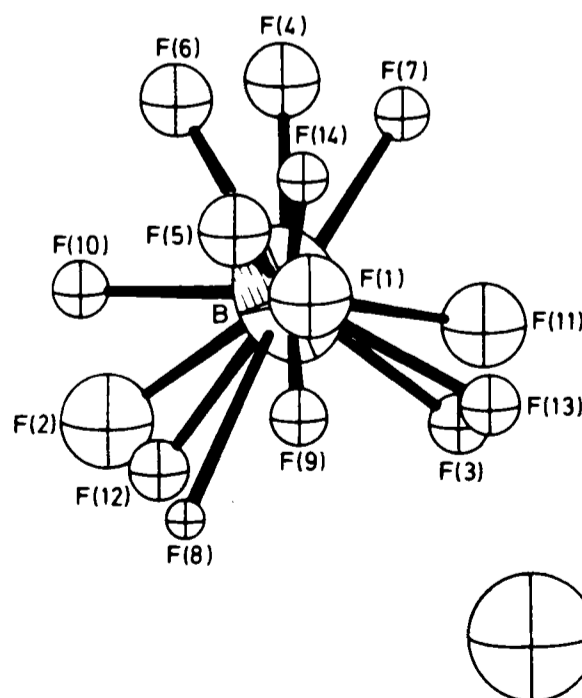


Figure 2. The disordered BF<sub>4</sub><sup>-</sup> anion. The thermal parameter of each fluorine sphere represents its fractional occupation. For scaling purposes the lower right-hand sphere corresponds to 100% occupation

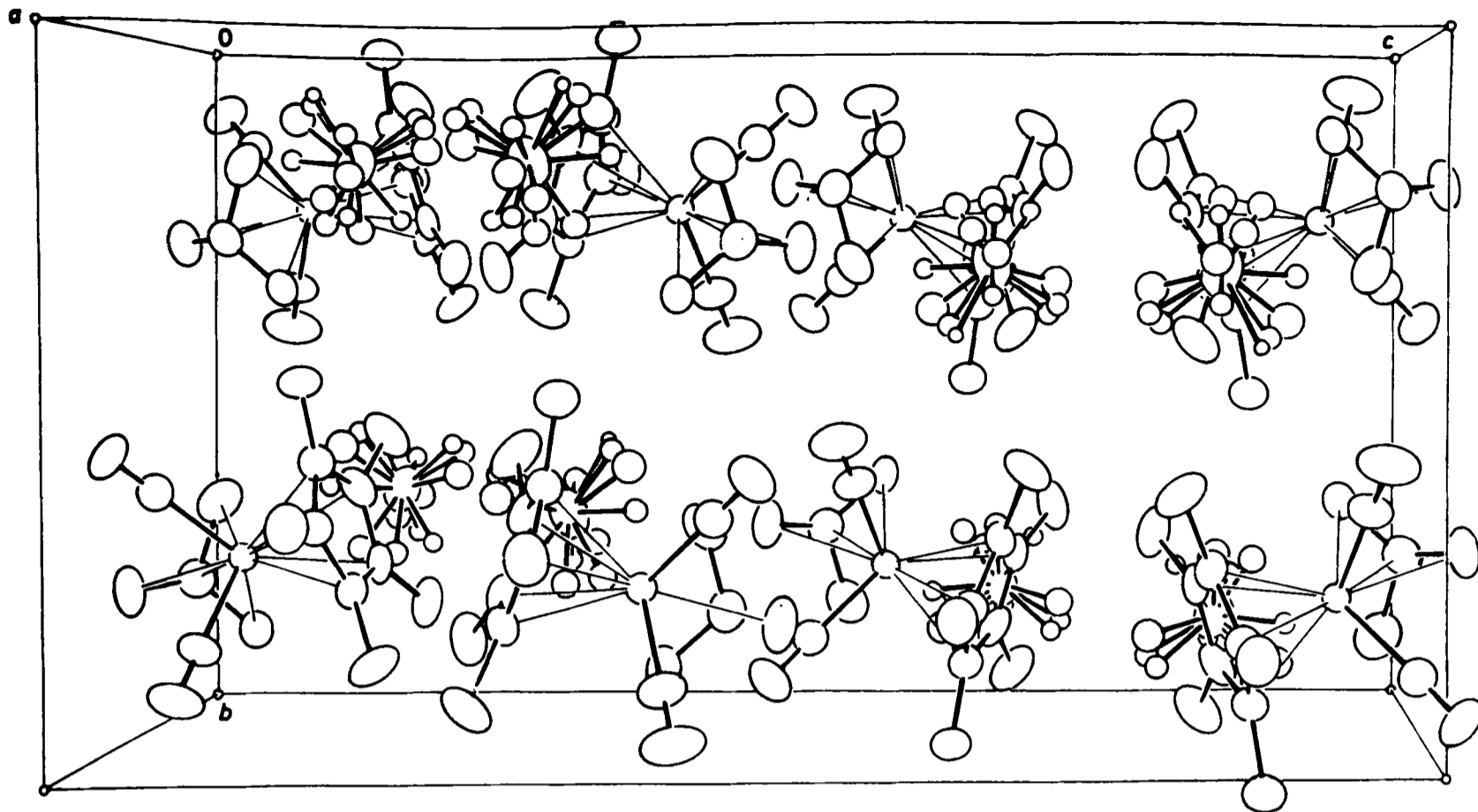
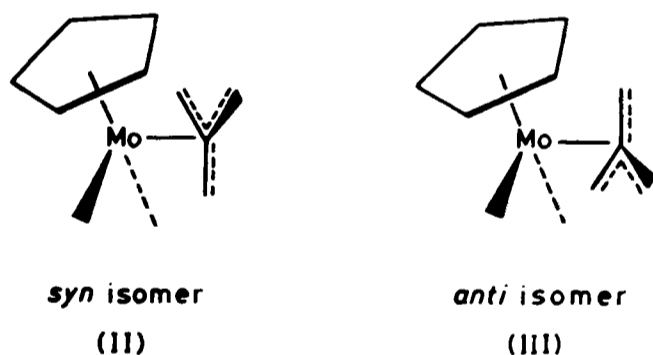


Figure 3. The crystal packing of complex (1) projected nearly onto the (011) plane. Hydrogen atoms are omitted for the sake of clarity

$C(CH_2)_3\{CO\}_2(\eta^5-C_5Me_5)^+$  cation, the *syn* isomer (II) and the *anti* isomer (III), that maintain the mirror symmetry common to both component parts. The crystallographically determined stereochemistry is *syn*. In an attempt to explore



if this stereochemistry is that which is electronically preferred it is convenient to regard the cation as a combination of  $Mo(CO)_2(\eta^5-C_5Me_5)^+$  and  $C(CH_2)_3$  fragments. Frontier orbitals of both fragments (in the case of the metal fragment, the  $\eta^5-C_5H_5$  analogue) have been reported by Albright.<sup>18</sup> The valence orbitals<sup>19</sup> of  $Mo(CO)_2(\eta^5-C_5H_5)^+$  ( $C_s$  symmetry) are drawn on the left-hand side of Figure 4. The important  $\pi$  orbitals of  $C(CH_2)_3$  (refs. 5 and 14) are also shown in Figure 4, in the centre for the *syn* molecular conformation and on the right for the *anti*. Note that the  $C_4$  fragment here is planar, and has  $D_{3h}$  symmetry. Our  $C(CH_2)_3$  ligand orbitals are labelled in only  $C_s$  symmetry (for consistency with those of the metal fragment), with the representations in parentheses denoting their origin.

Inspection of Figure 4 readily leads to an appreciation that the crystallographically observed *syn* stereochemistry is electronically derived, since in this conformation the  $1a'-2a'(e'')$  and  $a''-a''(e'')$  interactions (metal-ligand), both of which are two-electron stabilising interactions, are maximised. In both conformations the  $2a'-1a'(a_2'')$  interactions are four-electron destabilising, and will have different overlap integrals

whose relative magnitude it is difficult to assess by simple inspection. In both cases, however, the destabilisation will be mitigated somewhat by the presence of the higher-lying  $3a'$  (metal) orbital, and thus the overall destabilisation could be small in either extreme.

An important difference between the  $Mo(CO)_2(\eta^5-C_5H_5)^+$  and  $Fe(CO)_3$  fragments is that whilst the  $a''$  orbital of the former corresponds to one component of the  $2e$ <sup>18,20</sup> set of the latter there is no equivalent of the second  $2e$  component, which is noded orthogonally to the first. In the complex  $[Fe\{\eta^4-C(CH_2)_3\}(CO)_3]$  this second  $2e$  component interacts in bonding fashion with  $a''(e'')$  of  $C(CH_2)_3$  in the eclipsed conformation, albeit less effectively than does the first component in the staggered form. The absence of an equivalent stabilising interaction in the *anti* conformer of (1) might reasonably be expected to result in a larger difference in total energy between the two conformers, and indeed it does. For  $[Fe\{\eta^4-C(CH_2)_3\}(CO)_3]$  the staggered-minus-eclipsed energy difference, with flat  $C(CH_2)_3$ , is calculated<sup>14,18</sup> to be 20.8 kcal mol<sup>-1</sup>. From extended-Hückel molecular-orbital (EHMO) calculations on idealised models of  $[Mo\{\eta^4-C(CH_2)_3\}(CO)_2(\eta^5-C_5H_5)]^+$  using parameters specified in Table 3, we calculate the *syn*-minus-*anti* energy difference in the molybdenum trimethylenemethane complex [flat  $C(CH_2)_3$ ] to be 45.5 kcal mol<sup>-1</sup>, pyramidalisation ( $\theta = 12^\circ$ ,  $\beta = 12^\circ$ ) affording a slightly greater (46.7 kcal mol<sup>-1</sup>) difference between the *syn* and *anti* conformers.

This difference is nearly, but not quite, the same as the barrier of rigid rotation of the flat  $C(CH_2)_3$  ligand about the metal-ligand axis. In Figure 5 are drawn two nearly parallel curves. They represent the change in the sum of one-electron energies with rotation of the  $\eta^4-C(CH_2)_3$  ligand from the *anti* conformation (angle =  $0^\circ$ ) to the *syn* (angle =  $60^\circ$ ). The energy scale is in eV, but absolute values are arbitrary, and the upper (less stable) curve is for a flat  $C(CH_2)_3$  ligand. Clearly, the *anti* conformer is metastable and resides in a shallow, high-lying potential well. The least stable rotamer occurs when the angle is *ca.*  $15.5^\circ$ , and corresponds to eclipsing (in *z*-axis projection) of a carbonyl ligand by one arm of

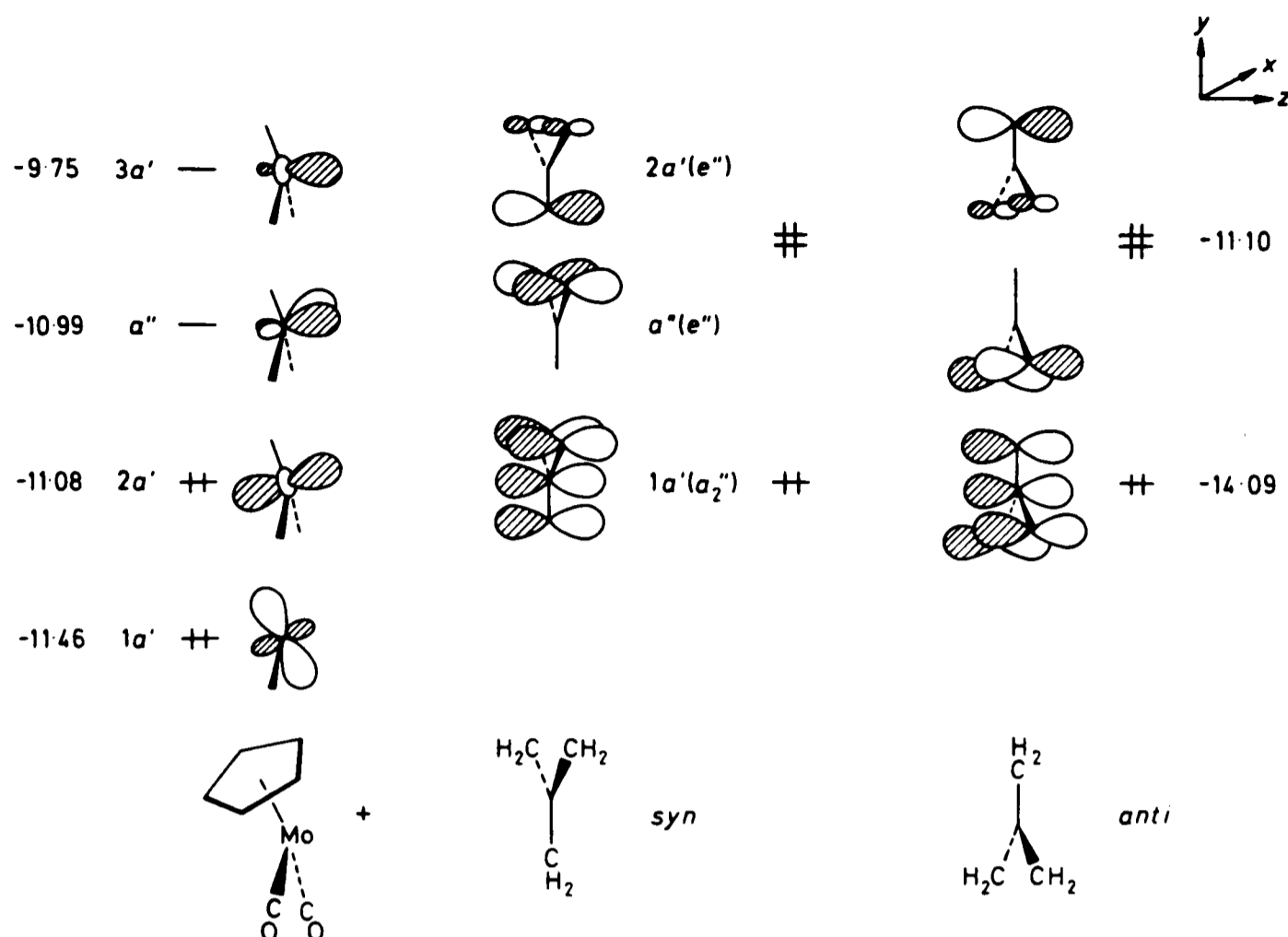


Figure 4. The frontier orbitals of  $\text{Mo}(\text{CO})_2(\eta\text{-C}_5\text{H}_5)^+$  and of  $\text{C}(\text{CH}_2)_3$ . The Figure is not to scale but the orbital energies (eV) are specified

Table 3. Parameters used in EHMO calculations <sup>a</sup>

Orbital	$H_{ii}/\text{eV}$	$\xi_i$	Distances (Å) and angles (°) <sup>c</sup>	
			Distance	Angle
Mo $4d^b$	-10.50	4.54	Mo-Z 2.02	OC-Mo-CO 90.0
Mo $5s$	-8.34	1.96	Mo-C(O) 1.97	Z-Mo-CO 126.7
Mo $5p$	-5.24	1.92	C-H 1.09	OC-Mo-L 90.0
			C-O 1.15	
C $2s$	-21.40	1.625	C-Z 1.21	
C $2p$	-11.40	1.625	C-C(tmm) 1.40	
			Mo-CH <sub>2</sub> (tmm) 2.36 (flat and bent tmm)	
O $2s$	-32.30	2.275	Mo-C(CH <sub>2</sub> ) <sub>3</sub> 1.90 (flat)	
O $2p$	-14.80	2.275	Mo-C(CH <sub>2</sub> ) <sub>3</sub> 2.2132 (bent)	
H $1s$	-13.60	1.30	Mo-C(CH <sub>2</sub> =CCH <sub>2</sub> CH <sub>2</sub> ) 2.36	
			C=C 1.40	
			C-C(CH <sub>2</sub> CH <sub>2</sub> CH <sub>2</sub> ) 1.48	

<sup>a</sup>All calculations were performed using the modified Wolfsberg-Helmholtz formula (J. H. Ammeter, H-B. Burgi, J. C. Thibeault, and R. Hoffmann, *J. Am. Chem. Soc.*, 1928, **100**, 3686). <sup>b</sup> $\xi_2 = 1.90$ ;  $c_1$  and  $c_2$  (contraction coefficients used in the double  $\xi$  expansion) = 0.589 88. <sup>c</sup>Z = Centroid of cyclopentadienyl ring; tmm = trimethylenemethane; L = tmm or methylenecyclopropane.

the  $\eta^4\text{-C}(\text{CH}_2)_3$  ligand. The barrier to rigid rotation of flat  $\eta^4\text{-C}(\text{CH}_2)_3$  in  $[\text{Mo}\{\eta^4\text{-C}(\text{CH}_2)_3\}(\text{CO})_2(\eta\text{-C}_5\text{H}_5)]^+$  is 48.4 kcal mol<sup>-1</sup>, and for bent  $\eta^4$ -trimethylenemethane 48.5 kcal mol<sup>-1</sup>. Although it is well established that the absolute values of such barriers, as given by the EHMO method, are subject to some uncertainty, since a rigid-rotor model does not allow for any subtlety or complexity in the rotation process, the important point is established that there is a substantial difference in rotational barriers for  $\eta^4$ -trimethylenemethane complexed onto  $\text{Fe}(\text{CO})_3$  and  $\text{Mo}(\text{CO})_2(\eta\text{-C}_5\text{H}_5)^+$  fragments.

In apparent contradiction of this analysis the room-temperature <sup>1</sup>H n.m.r. spectrum of complex (2) shows a singlet at  $\delta$  3.36 p.p.m. due to the six methylene protons of the coordinated trimethylenemethane. On cooling to  $-60^\circ\text{C}$  this

resonance collapses, and at  $-90^\circ\text{C}$  is replaced by three signals, two doublets at  $\delta$  3.23 (H<sup>1</sup>) and 3.49 p.p.m. (H<sup>2</sup>) [ $J(\text{H}^1\text{H}^2)$  5 Hz] and a singlet at 3.64 p.p.m. (H<sup>3</sup>) for the three inequivalent methylene sites. Estimation<sup>21</sup> of the barrier to apparent rotation by approximation to a simple two-site exchange mechanism afforded a value for  $\Delta G_{Tc}^\ddagger$  of  $9.9 \pm 1$  kcal mol<sup>-1</sup>. The coalescence temperature for the corresponding pentamethylcyclopentadienyl cation (1) was lower ( $-70^\circ\text{C}$ ) than that observed for (2), and the process was not frozen out at  $-90^\circ\text{C}$ .

This suggests that some dynamic process other than rotation is responsible for the room-temperature <sup>1</sup>H equivalence of the  $\eta^4$ -trimethylenemethane hydrogens. In fact what is required is an averaging process which does not interconvert



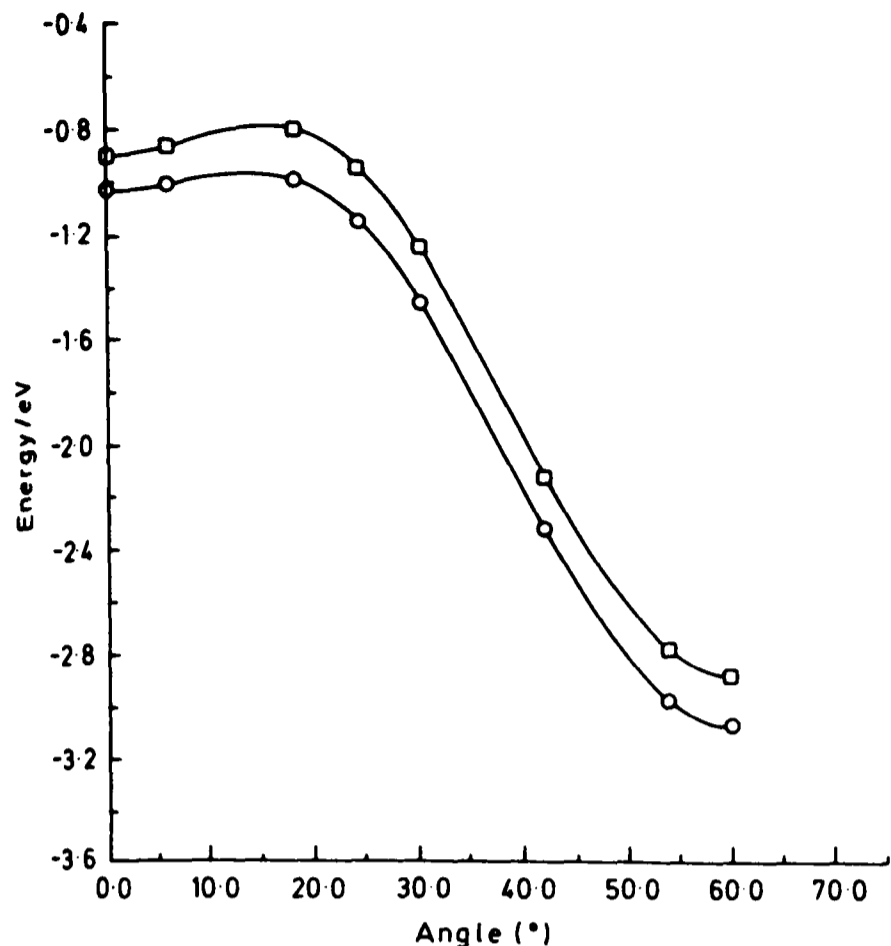
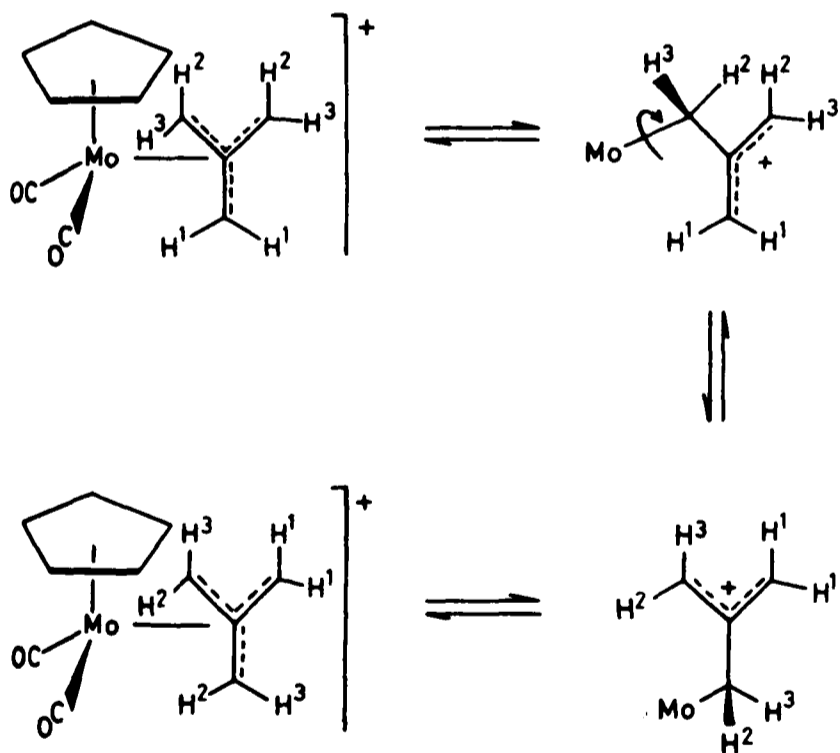


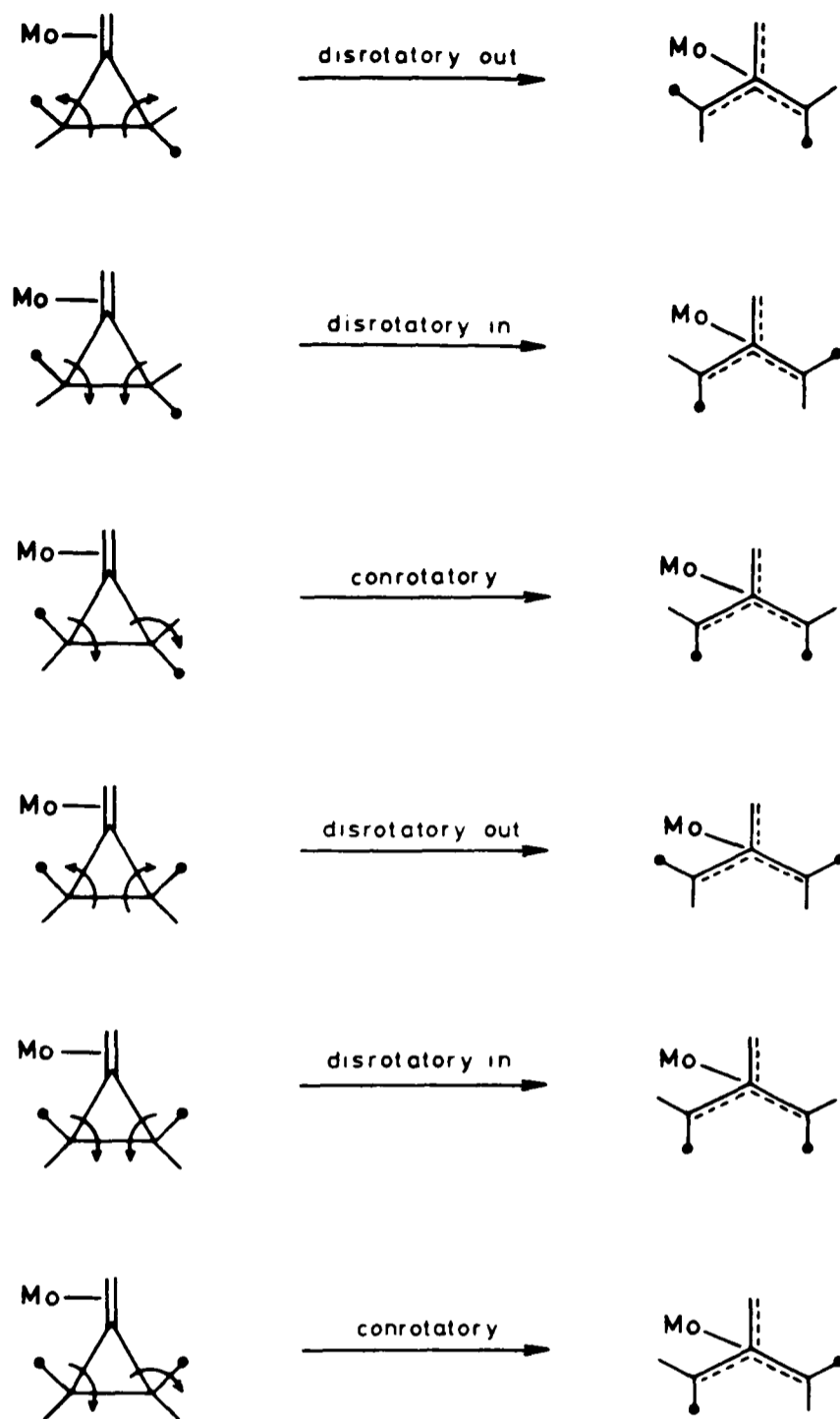
Figure 5. Potential curves for rotation of the trimethylenemethane ligand about the metal-ligand axis in  $\text{Mo}(\text{CO})_2(\eta\text{-C}_5\text{H}_5)^+$ . Zero degrees corresponds to a *anti* conformation,  $60^\circ$  corresponds to *syn*. □, Ligand has  $D_{3h}$  symmetry; ○, ligand has  $C_{3v}$  symmetry ( $\theta = \beta = 12^\circ$ )



Scheme 1. Ligands omitted for clarity

the *syn* and *anti* conformers. This can be accomplished by the reaction path shown in Scheme 1, where slippage ( $\eta^4 \rightarrow \sigma$ )<sup>\*</sup> of the molybdenum fragment occurs so as to form a delocalised allylic carbenium ion, in which rotation about a Mo-C bond is possible. Such a process interconverts  $\text{H}^2$  and  $\text{H}^3$  with  $\text{H}^1$ , and because of the presence of a molecular plane

\* It is probably not necessary for complete slippage to occur. What is required is that the metal moves towards one of the peripheral carbons reducing the Mo-C bond order sufficiently to allow rotation.

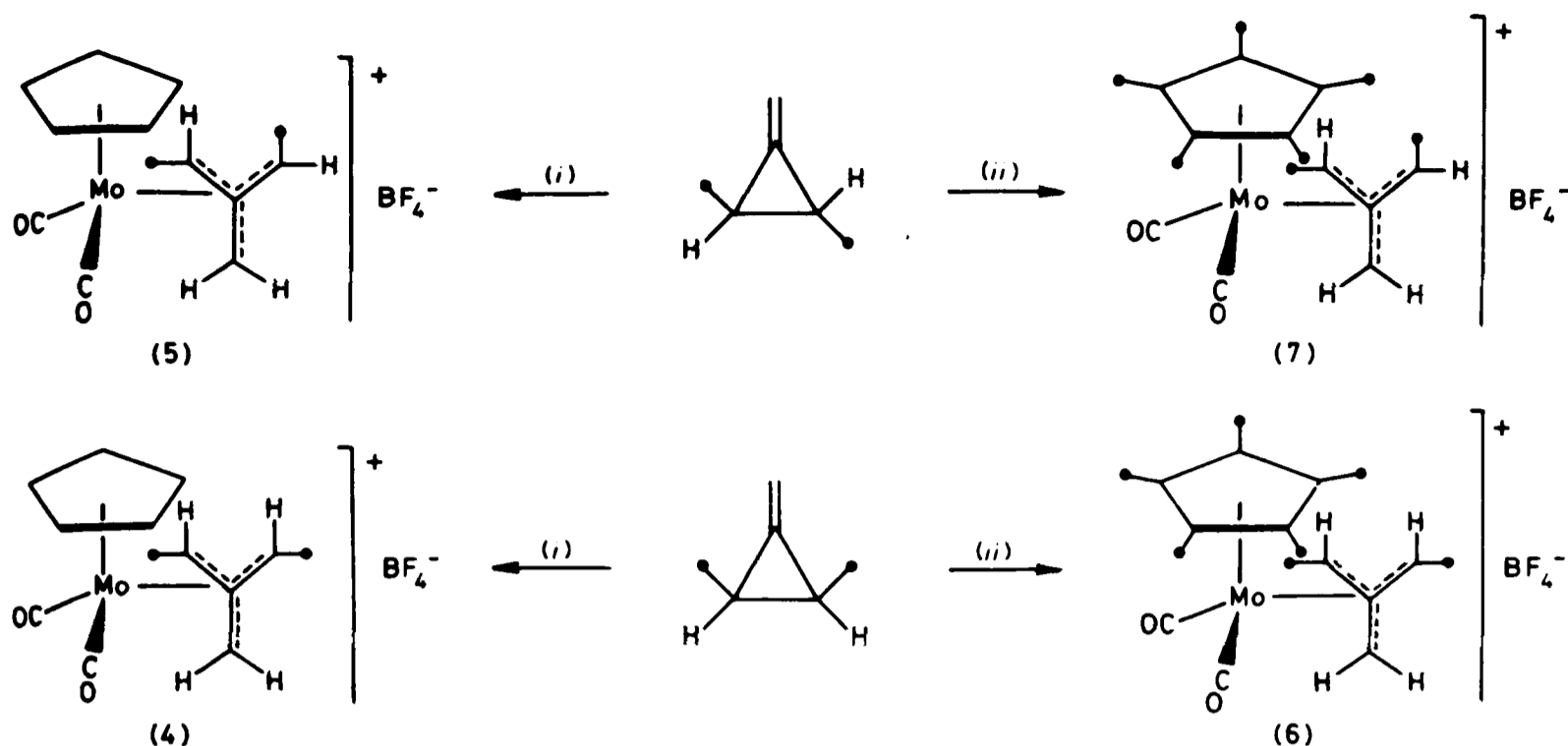


Scheme 2. ● = Me

of symmetry,  $\text{H}^2$  and  $\text{H}^3$ . This reaction has in a sense a parallel with the  $\sigma$ - $\pi$ -promoted *syn-anti* exchange process observed with  $\eta^3$ -allyl complexes.

Thus, the crystallographic study confirmed that 2,3-C-C bond cleavage does in fact occur. If it is assumed that this reaction involves initial  $\eta^2$ -co-ordination of methylenecyclopropane, then from a stereochemical standpoint there are three possible ring-opening pathways. These are disrotating out, disrotating in, and conrotatory, which can in principle be distinguished (see Scheme 2) by examining the corresponding reactions of *cis*- and *trans*-2,3-dimethylmethylenecyclopropane.

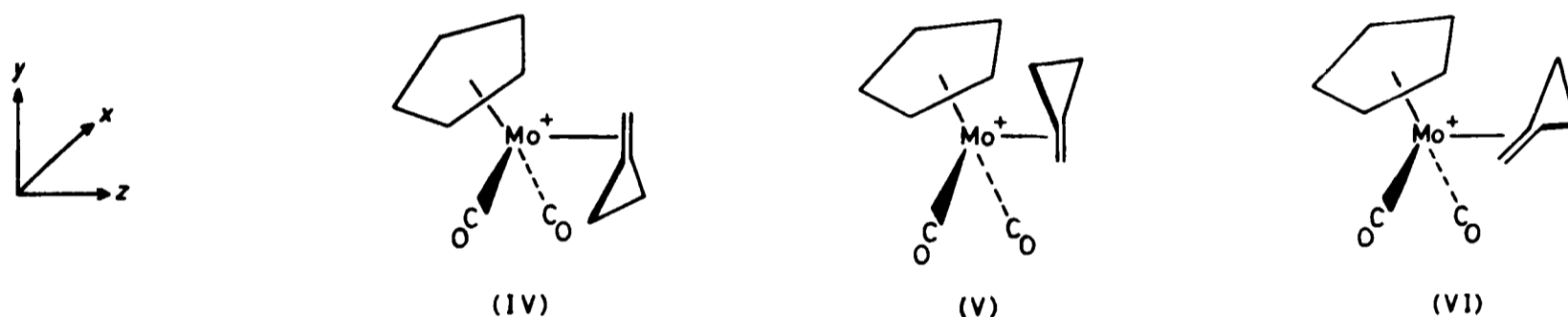
Accordingly,  $[\text{Mo}(\text{NCMe})_2(\text{CO})_2(\eta\text{-C}_5\text{H}_5)][\text{BF}_4]$  was treated with *cis*- and *trans*-2,3-dimethylmethylenecyclopropane in  $\text{CH}_2\text{Cl}_2$  as solvent affording respectively the *syn,syn*-dimethyl- and the *syn,anti*-dimethyl-trimethylenemethane complexes (4) and (5), characterised by elemental analysis and i.r. and n.m.r.<sup>4</sup> spectroscopy. Similarly, reaction of the *cis*- and *trans*-2,3-dimethylmethylenecyclopropanes with  $[\text{Mo}_2(\text{CO})_6(\eta\text{-C}_5\text{Me}_5)_2]$  and  $\text{AgBF}_4$  in  $\text{CH}_2\text{Cl}_2$  gave respectively the *syn,syn* (6) and *syn,anti* complex (7). The pentamethylcyclopentadienyl cations (6) and (7) obtained in these reactions were found to be contaminated with variable amounts of  $[\text{Mo}(\text{CO})_4(\eta\text{-C}_5\text{Me}_5)][\text{BF}_4]$  presumably formed by competitive capture



Scheme 3. ● = Me; (i)  $[\text{Mo}(\text{NCMe})_2(\text{CO})_2(\eta\text{-C}_5\text{H}_5)]\text{BF}_4^-$ ; (ii)  $[\text{Mo}_2(\text{CO})_6(\eta\text{-C}_5\text{Me}_5)_2]\text{-AgBF}_4$

of  $[\text{Mo}(\text{CO})_3(\eta\text{-C}_5\text{Me}_5)]\text{BF}_4^-$  by displaced carbon monoxide. Analytical samples of these cations were obtained by conversion (see later) into the neutral alcohols followed by re-

cleavage affords a trimethylenemethane cation. Limiting conformations for such species have the alkene function parallel to [two possible conformations, (IV) and (V)] or



generation of the trimethylenemethane cations with tetrafluoroboric acid-propionic anhydride.

These isomeric dimethyl-substituted  $\eta^4$ -trimethylenemethane cations do not interconvert in refluxing nitromethane, and therefore, the observations summarised in Scheme 3 are consistent with a disrotatory-out ring-opening reaction where the breaking 2,3- $\sigma$  bond bends away from the metal.\* The same stereochemistry, *i.e.* disrotatory out, was also observed experimentally and shown to be electronically favoured in the iron-carbonyl-promoted ring opening of methylene-2-phenylcyclopropane.<sup>4</sup> Disrotatory-out stereospecificity is also observed in the reaction of methylenecyclopropanes with  $[\text{PdCl}_2(\text{NCPH})_2]$ , where calculations suggest that the activation energy for conrotatory ring opening is substantially higher than that for either disrotatory-in or disrotatory-out opening, and further, whilst all three modes are, strictly speaking, symmetry-allowed transformations, the latter two modes are strongly so.<sup>5</sup>

If similar calculations were to be attempted with the molybdenum system then a necessary first step was to consider the nature of the intermediate just prior to ring opening. A likely candidate is the  $\eta^2$ -bonded alkene complex  $[\text{Mo}(\eta^2\text{-CH}_2=\text{CCH}_2\text{CH}_2)(\text{CO})_2(\eta\text{-C}_5\text{Me}_5 \text{ or } \eta\text{-C}_5\text{H}_5)]^+$ , which on C-C bond

perpendicular to [(VI)] the mirror plane of the metal fragment. Although it is well established<sup>19,22</sup> that the last conformation is preferred, by *ca.* 20–25 kcal mol<sup>-1</sup>, in  $d^6$  alkene complexes of the general type  $[\text{Mn}(\eta^2\text{-alkene})(\text{CO})_2(\eta\text{-C}_5\text{H}_5)]$ , we anticipated that a more facile rotation about the metal-alkene bond

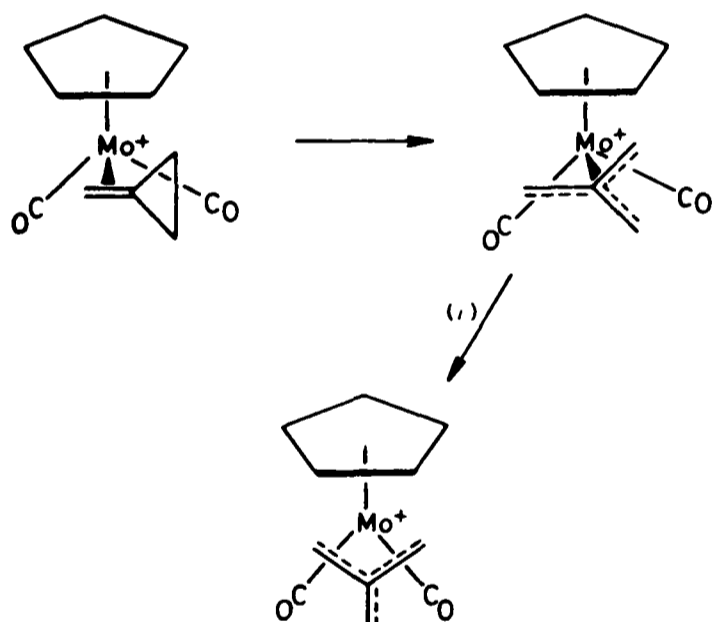
would be afforded in the  $d^4$  cation  $[\text{Mo}(\eta^2\text{-CH}_2=\text{CCH}_2\text{CH}_2)(\text{CO})_2(\eta\text{-C}_5\text{H}_5)]^+$ ; removal of two electrons from the orbitals of Figure 5 of ref. 19 readily leads to this prediction. We were surprised, therefore, to discover that EHMO calculations on  $\eta\text{-C}_5\text{H}_5$  analogues of the three conformations suggested stability decreases of 40.9 kcal mol<sup>-1</sup> in going from (VI) to (IV) and a further 46.4 kcal mol<sup>-1</sup> in going from (IV) to (V), *i.e.* a total barrier to rigid rotation of the  $\eta^2$ -methylenecyclopropane ligand about the axis from the molybdenum atom to the midpoint of C=C of >85 kcal mol<sup>-1</sup>. (Note that here we have not actually explored the barrier to rotation, only the differences between the energies of three obvious points on the rotation cycle, but barrier  $\ll$  total difference.)

Detailed examination shows that the origins of these differences largely derive from intramolecular ligand-ligand interactions rather than from substantial changes in the metal-alkene bond strength. In the least stable conformer (V) there are two very short symmetry-related contacts (1.344 Å) between a cyclopentadienyl hydrogen atom and the two nearest methylene hydrogens; the computed overlap population is -0.055. For the other parallel geometry, (IV), the same methylene hydrogens are this time *cis* to the carbonyl groups, C...H 1.510 and O...H 1.666 Å, and interact in an attrac-

\* It should be noted that if the exchange process shown in Scheme 1 also applied to these methyl-substituted  $\eta^4$ -trimethylenemethanes then a substantial substituent effect is implied.

tive sense with the carbonyl carbons (carbon-hydrogen overlap population 0.049) and in a repulsive sense with the carbonyl oxygens (oxygen-hydrogen overlap population  $-0.043$ ). The most stable conformation, (VI), is characterised by a very weakly repulsive (cyclopentadienyl)-H $\cdots$ H-(methylene) contact, 1.933 Å (overlap population  $-0.001$ ), and by a strong interaction between the methylene hydrogen and the carbonyl  $\pi_z$  system. Although the (single) C $\cdots$ H and O $\cdots$ H distances here are the same as those in (V) the carbon-hydrogen overlap population is now 0.0835 and the oxygen-hydrogen is  $-0.049$ . Further, since a greater proportion of the carbon  $2p_z$  atomic orbital is localised in the  $\pi_z^*$ , rather than in the  $\pi_z$ , bond of the CO ligand, the formation of a partial C $\cdots$ H bond in the  $z$  direction preferentially depletes  $\pi^*$  rather than  $\pi$ , resulting in enhanced C-O bonding; the carbon-oxygen overlap population for the carbonyl ligand adjacent to the cyclopropane ring is 1.165, whereas that for the other CO is proportionally reduced to 1.082. The carbon-oxygen overlap populations in (V) and (IV) are 1.145 and 1.133 respectively.

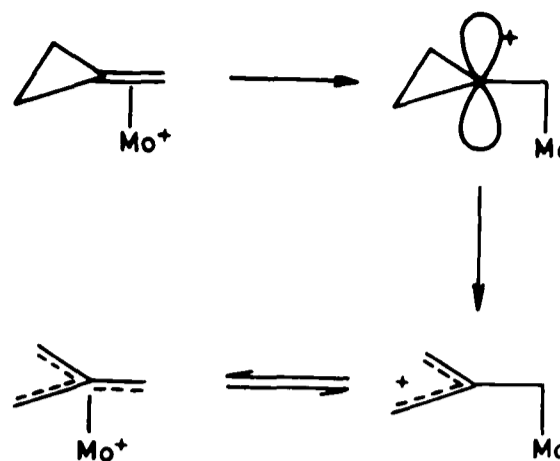
Thus, the strong conformational preference of the alkene precursor  $[\text{Mo}(\eta^2\text{-CH}_2=\text{CCH}_2\text{CH}_2)(\text{CO})_2(\eta\text{-C}_5\text{H}_5)]^+$  does not map to that of the  $\eta^4$ -trimethylenemethane complex  $[\text{Mo}\{\eta^4\text{-C}(\text{CH}_2)_3\}(\text{CO})_2(\eta\text{-C}_5\text{H}_5)]^+$  in such a manner that readily allows calculation of the activation energy required for the three ring-opening modes, and therefore, we cannot probe further the reasons why the disrotatory-out mode of ring opening is preferred. Nevertheless, a likely reaction path is



Scheme 4. (i)  $30^\circ$  rotation

that illustrated in Scheme 4, where ring opening of the preferred conformer generates a trimethylenemethane cation, which needs only a  $30^\circ$  rotation in order to descend the potential curve of Figure 5 forming the *syn*-orientated trimethylenemethane complex. A simplified view of the ring-opening step is that the  $\text{Mo}(\text{CO})_2(\eta\text{-C}_5\text{H}_5)^+$  fragment slips from  $\eta^2$  to  $\sigma$  thus generating a species not unlike a cyclopropylcarbenium ion (Scheme 5), which opens in the predicted<sup>23</sup> allowed disrotatory manner to form a metalla-substituted allylic carbenium ion, which then reversibly transforms into an  $\eta^4$ -trimethylenemethane cation.

As mentioned in the introduction these molecules are the first examples of cationic  $\eta^4$ -trimethylenemethane species, and it was therefore important to examine their reactions with nucleophilic reagents. The  $\eta^4$ -trimethylenemethane cations (1)–(7) present five possible sites for nucleophilic attack: the



Scheme 5. Ligands omitted for clarity

molybdenum centre, co-ordinated carbon monoxide, and the cyclopentadienyl and  $\eta^4$ -trimethylenemethane ligands. In the case of the latter, attack could in principle occur either at one of the three peripheral carbons or on the central carbon atom. In the event, as is shown in Scheme 6, the nucleophiles  $\text{OH}^-$ ,  $\text{BH}_4^-$ ,  $\text{CuMe}_2^-$ , and  $\text{SPh}^-$  all selectively attacked the  $\eta^4$ -trimethylenemethane ligand of (1) to form respectively the  $\eta^3$ -allylic complexes (8), (9), (10), and (11), which were isolated by column chromatography and characterised by elemental analysis and i.r. and mass spectroscopy. The reaction with hydroxide anion to afford complex (8) was first observed on attempting to chromatograph (1) on alumina, and proved useful as a way of obtaining pure (1) uncontaminated with  $[\text{Mo}(\text{CO})_4(\eta\text{-C}_5\text{Me}_5)][\text{BF}_4]$ , since addition of tetrafluoroboric acid-propionic anhydride to (8) regenerated (1) in quantitative yield.

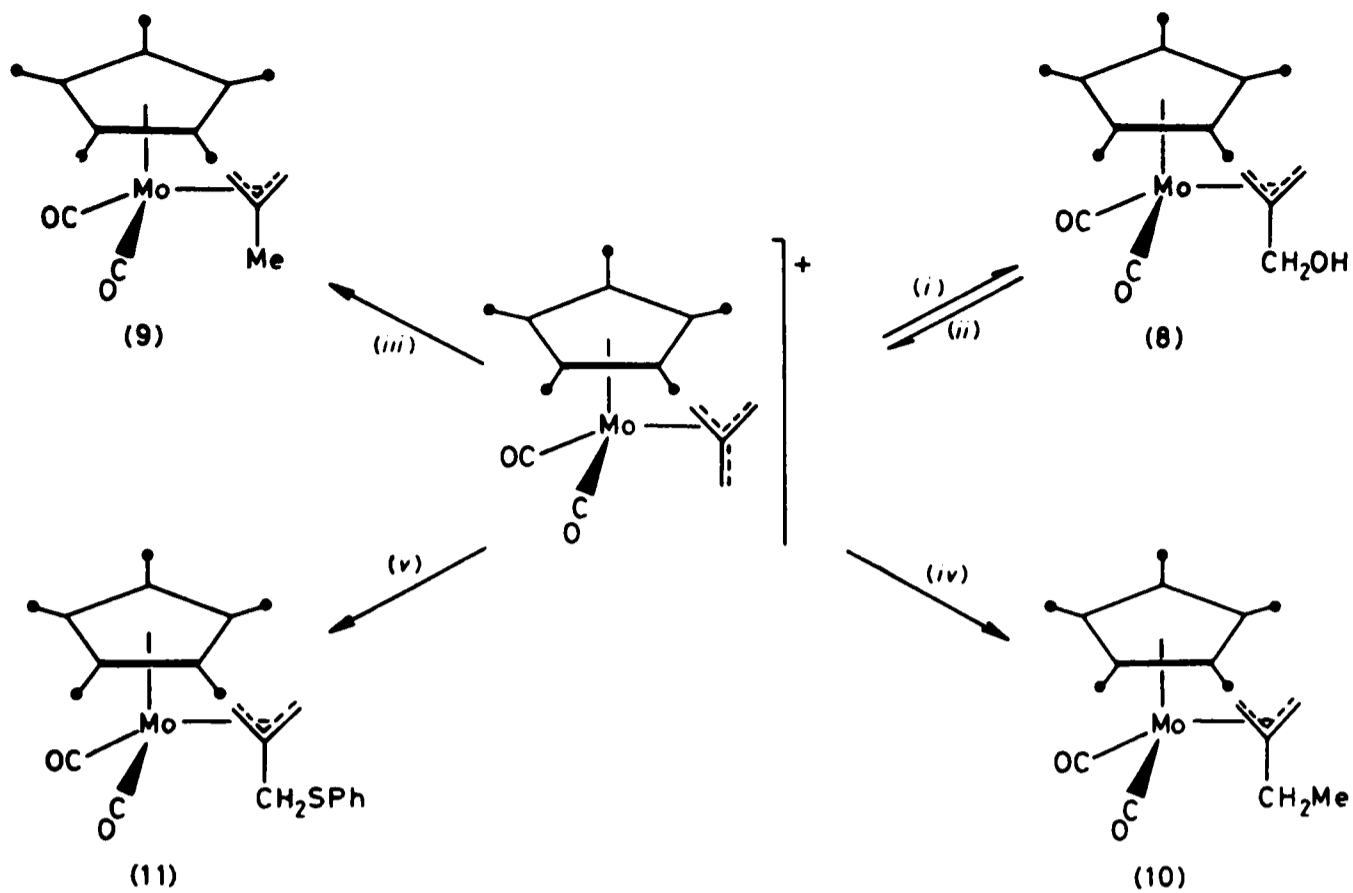
The corresponding reactions of the methyl-substituted cations (3), (6), and (7) were also examined, the results being summarised in Scheme 7. Reaction of (3) with  $\text{BH}_4^-$  in tetrahydrofuran afforded only the 2-isopropyl-substituted  $\eta^3$ -allylic complex (12). In contrast,  $\text{BH}_4^-$  with (6) led to attack on both unsubstituted and substituted carbons giving respectively the  $\eta^3$ -allyl species (13) and (14), whereas (7) reacted to give only the one product (14) arising from regioselective attack on a methyl-substituted carbon. This latter result suggests that there is an interplay of electronic and steric effects, which conclusion is reinforced by the reactions with  $\text{OH}^-$ . The cation (6) reacts regioselectively at the unsubstituted carbon to give the alcohol (15), whereas the reaction of (7) with  $\text{OH}^-$  is directed selectively to a substituted carbon atom to form (16).

### Experimental

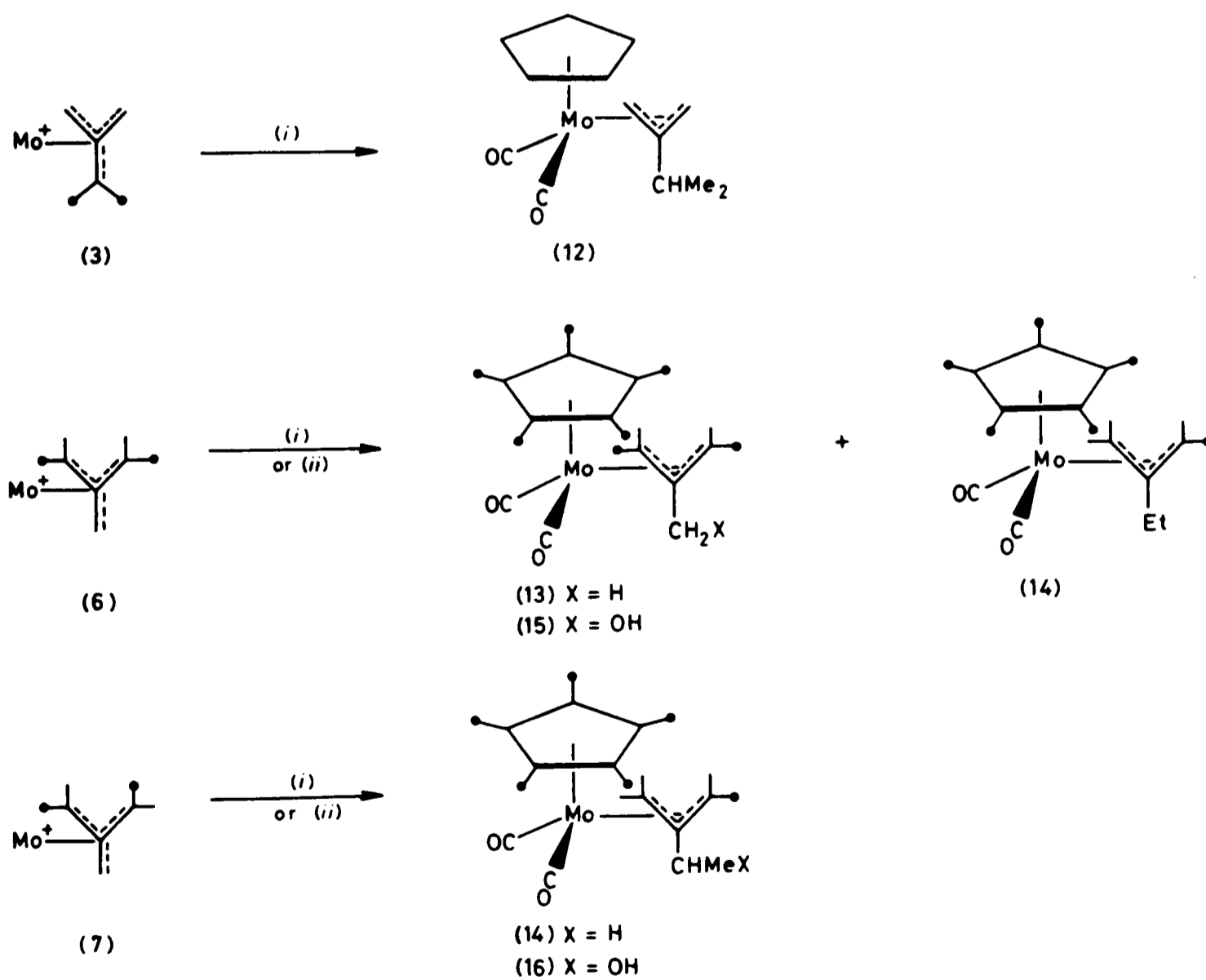
The  $^1\text{H}$  and  $^{13}\text{C}\{^1\text{H}\}$  n.m.r. spectra were recorded on JEOL FX 90 Q and FX 200 spectrometers, as appropriate. Data given are for room-temperature measurements and coupling constants are in Hz. Carbon-13 chemical shifts are relative to  $\text{SiMe}_4$  with positive values to high frequency of the reference. Tris(acetylacetonato)chromium(III) was added to reduce  $^{13}\text{C}$  relaxation times. Infrared spectra were recorded on a Perkin-Elmer 257 spectrophotometer. All reactions were carried out in Schlenk tubes under an atmosphere of dry oxygen-free nitrogen, using freshly distilled solvents. Methylene-cyclopropanes were prepared by the method of Arora and Binger.<sup>24</sup>

*Preparation of Dicarboxyl( $\eta$ -pentamethylcyclopentadienyl)-( $\eta^4$ -trimethylenemethane)molybdenum Tetrafluoroborate (1).*—An excess of methylenecyclopropane (0.5 g, 10 mmol) was added to a stirred solution of  $[\text{Mo}_2(\text{CO})_6(\eta\text{-C}_5\text{Me}_5)_2]$  (0.5 g,





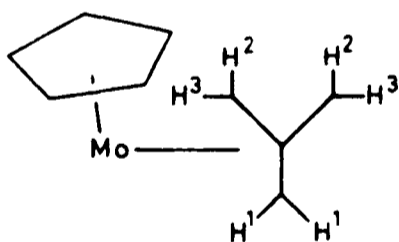
Scheme 6. (i)  $\text{OH}^-$ ; (ii) tetrafluoroboric acid-propionic anhydride; (iii)  $\text{BH}_4^-$ ; (iv)  $\text{CuMe}_2^-$ ; (v)  $\text{SPh}^-$



Scheme 7. Ligands omitted for clarity. (i)  $\text{BH}_4^-$ ; (ii)  $\text{OH}^-$

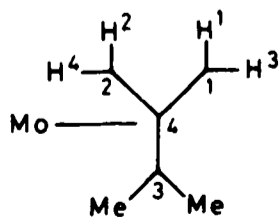
0.8 mmol) in  $\text{CH}_2\text{Cl}_2$  (30  $\text{cm}^3$ ) contained in a flask covered in metal foil. Silver tetrafluoroborate (0.31 g, 1.6 mmol) was added, and the reaction mixture stirred at room temperature for 4 h. The resultant reaction mixture was filtered through Kieselguhr, and the volume of the solvent reduced *in vacuo* to 10  $\text{cm}^3$ . The resultant solution was chromatographed on an alumina-packed column. Elution with  $\text{CH}_2\text{Cl}_2$  gave first an orange band containing  $[\text{Mo}(\text{CO})_2(\eta\text{-C}_5\text{Me}_5)]\text{[BF}_4\text{]}$ . Further elution gave a yellow band containing alcohol (8) (see later). The solution containing (8) was evaporated to dryness *in vacuo*, and the residue dissolved in propionic anhydride (5  $\text{cm}^3$ ) and cooled to 0 °C. Tetrafluoroboric acid (0.15  $\text{cm}^3$ , 30% aqueous solution) in propionic anhydride (5  $\text{cm}^3$ ) was added. After 1 h diethyl ether was slowly added to give cream crystals of (1) (0.42 g, 58%) (Found: C, 45.2; H, 5.0.  $\text{C}_{16}\text{H}_{21}\text{BF}_4\text{MoO}_2$  requires C, 44.9; H, 5.0%),  $\nu_{\text{CO}}$  (Nujol) 2 056s and 2 004s  $\text{cm}^{-1}$ . N.m.r.:  $^1\text{H}$  ( $\text{CDCl}_3$ ),  $\delta$  2.90 (s, 6 H,  $\text{CH}_2$ ) and 2.31 (s, 15 H,  $\text{C}_5\text{Me}_5$ );  $^{13}\text{C}$ - $\{^1\text{H}\}$  ( $\text{CDCl}_3$ ),  $\delta$  218.0 (CO), 117.0 [ $\text{C}(\text{CH}_2)_3$ ], 105.0 ( $\text{C}_5\text{Me}_5$ ), 68.0 [ $\text{C}(\text{CH}_2)_3$ ], and 12.0 p.p.m. ( $\text{C}_5\text{Me}_5$ ).

**Preparation of Dicarboxyl( $\eta$ -cyclopentadienyl)( $\eta^4$ -trimethylenemethane)molybdenum Tetrafluoroborate (2).**—An excess of methylenecyclopropane (0.5 g, 10 mmol) was added to a stirred suspension of the red complex *cis*- $[\text{Mo}(\text{NCMe})_2(\text{CO})_2(\eta\text{-C}_5\text{H}_5)]\text{[BF}_4\text{}]$  (0.4 g, 1 mmol) in  $\text{CH}_2\text{Cl}_2$  (10  $\text{cm}^3$ ). After 16 h at room temperature diethyl ether (20  $\text{cm}^3$ ) was added to the yellow solution. The resultant precipitate was collected and recrystallised (0 °C) from  $\text{CH}_2\text{Cl}_2$ -Et<sub>2</sub>O to give cream crystals of (2) (0.25 g, 70%) (Found: C, 36.7; H, 3.1.  $\text{C}_{11}\text{H}_{11}\text{BF}_4\text{MoO}_2$  requires C, 36.9; H, 3.1%),  $\nu_{\text{CO}}$  (Nujol) 2 065s and 2 020s  $\text{cm}^{-1}$ . N.m.r.:  $^1\text{H}$  ( $\text{CD}_3\text{NO}_2$ ),  $\delta$  5.88 (s, 5 H,  $\text{C}_5\text{H}_5$ ) and 3.36 (s, 6 H,  $\text{CH}_2$ );  $^{13}\text{C}$ - $\{^1\text{H}\}$  ( $\text{CD}_3\text{NO}_2$ ),  $\delta$  215.8 (CO), 115.3 [ $\text{C}(\text{CH}_2)_3$ ], 91.7 ( $\text{C}_5\text{H}_5$ ), and 65.3 p.p.m. [ $\text{C}(\text{CH}_2)_3$ ];  $^1\text{H}$  ( $\text{CD}_3\text{NO}_2$ , -90 °C),  $\delta$  5.88 (s, 5 H,  $\text{C}_5\text{H}_5$ ), 3.64 (s, 2 H,  $\text{H}^3$ ), 3.49 [d, 2 H,  $\text{H}^2$ ,  $J(\text{H}^1\text{H}^2)$  5.0], and 3.23 [d, 2 H,  $\text{H}^1$ ,  $J(\text{H}^1\text{H}^2)$  5.0].



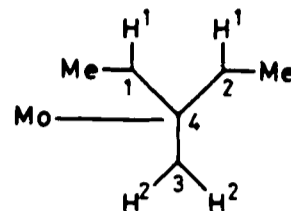
The following cations were synthesised in a similar manner.

**Dicarboxyl( $\eta$ -cyclopentadienyl)( $\eta^4$ -dimethylmethylene(dimethylmethylene)methane)molybdenum tetrafluoroborate (3).** Yield 70% (Found: C, 39.9; H, 3.9.  $\text{C}_{13}\text{H}_{15}\text{BF}_4\text{MoO}_2$  requires C, 40.4; H, 3.9%),  $\nu_{\text{CO}}$  ( $\text{CH}_2\text{Cl}_2$ ) 2 054s and 2 005s  $\text{cm}^{-1}$ . N.m.r.:  $^1\text{H}$  ( $[\text{C}_6\text{H}_6]$ acetone),  $\delta$  5.94 (s, 5 H,  $\text{C}_5\text{H}_5$ ), 3.42 (br s, 2 H,  $\text{H}^1 + \text{H}^2$ ), 3.09 (br s, 2 H,  $\text{H}^3 + \text{H}^4$ ), and 2.12 (s, 6 H,  $\text{CMe}_2$ );  $^{13}\text{C}$ - $\{^1\text{H}\}$  ( $[\text{C}_6\text{H}_6]$ acetone),  $\delta$  218.0 (CO), 125.3 ( $\text{C}^3$ ), 109.1 ( $\text{C}^4$ ), 92.5 ( $\text{C}_5\text{H}_5$ ), 54.8 ( $\text{C}^1, \text{C}^2$ ), and 24.5 p.p.m.

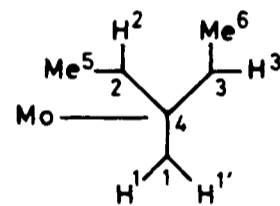


**Dicarboxyl( $\eta$ -cyclopentadienyl)( $\eta^4$ -cis-methylenebis(methylmethylene)methane)molybdenum tetrafluoroborate (4).** Yield

70% (Found: C, 40.5; H, 3.9.  $\text{C}_{13}\text{H}_{15}\text{BF}_4\text{MoO}_2$  requires C, 40.4; H, 3.9%),  $\nu_{\text{CO}}$  ( $\text{CH}_2\text{Cl}_2$ ) 2 055s and 2 006s  $\text{cm}^{-1}$ . N.m.r.:  $^1\text{H}$  ( $\text{CD}_3\text{NO}_2$ ),  $\delta$  5.8 (s, 5 H,  $\text{C}_5\text{H}_5$ ), 4.0 (m, 2 H,  $\text{H}^1$ ), 3.95 [d, 2 H,  $\text{H}^2$ ,  $J(\text{H}^1\text{H}^2)$  3.0], and 1.88 [d, 6 H,  $\text{CHMe}$ ,  $J(\text{HMe})$  3.0];  $^{13}\text{C}$ - $\{^1\text{H}\}$  ( $\text{CD}_3\text{NO}_2$ ),  $\delta$  217.3 (CO), 112.0 ( $\text{C}^4$ ), 92.1 ( $\text{C}_5\text{H}_5$ ), 83.5 ( $\text{C}^1, \text{C}^2$ ), 61.7 ( $\text{C}^3$ ), and 16.3 p.p.m. ( $\text{CHMe}$ ).



**Dicarboxyl( $\eta$ -cyclopentadienyl)( $\eta^4$ -trans-methylenebis(methylmethylene)methane)molybdenum tetrafluoroborate (5).** Yield 70% (Found: C, 39.6; H, 4.0.  $\text{C}_{13}\text{H}_{15}\text{BF}_4\text{MoO}_2$  requires C, 40.4; H, 3.9%),  $\nu_{\text{CO}}$  ( $\text{CH}_2\text{Cl}_2$ ) 2 049s and 1 997  $\text{cm}^{-1}$ . N.m.r.:  $^1\text{H}$  ( $[\text{C}_6\text{H}_6]$ acetone),  $\delta$  5.96 (s, 5 H,  $\text{C}_5\text{H}_5$ ), 5.13 [dq, 1 H,  $\text{H}^2$ ,  $J(\text{H}^2\text{Me}^5)$  7.4,  $J(\text{H}^2\text{H}^1)$  3.5], 4.26 [q, 1 H,  $\text{H}^3$ ,  $J(\text{H}^3\text{Me}^6)$  6.6], 3.58 [d, 1 H,  $\text{H}^1$ ,  $J(\text{H}^1\text{H}^1')$  1.6], 2.97 [dd, 1 H,  $\text{H}^1'$ ,  $J(\text{H}^1\text{H}^1')$  1.6], 2.01 [d, 3 H,  $\text{Me}^6$ ,  $J(\text{Me}^6\text{H}^3)$  6.56], and 1.85 [d, 3 H,  $\text{Me}^5$ ,  $J(\text{Me}^5\text{H}^2)$  7.44];  $^{13}\text{C}$ - $\{^1\text{H}\}$  ( $\text{CD}_3\text{NO}_2$ ),  $\delta$  218.6 (CO), 112.0 ( $\text{C}^4$ ), 92.5 ( $\text{C}_5\text{H}_5$ ), 90.0 ( $\text{C}^3$ ), 82.9 ( $\text{C}^2$ ), 55.5 ( $\text{C}^1$ ), 16.7 ( $\text{C}^6\text{H}_3$ ), and 16.0 p.p.m. ( $\text{C}^5\text{H}_3$ ).

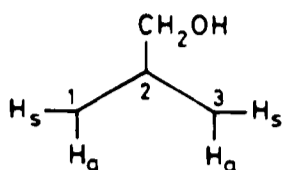


**Dicarboxyl( $\eta^4$ -cis-methylenebis(methylmethylene)methane)( $\eta$ -pentamethylcyclopentadienyl)molybdenum tetrafluoroborate (6).** Yield 60% (Found: C, 47.6; H, 5.7.  $\text{C}_{18}\text{H}_{25}\text{BF}_4\text{MoO}_2$  requires C, 47.4; H, 5.5%),  $\nu_{\text{CO}}$  ( $\text{CH}_2\text{Cl}_2$ ) 2 045s and 2 000s  $\text{cm}^{-1}$ . N.m.r.:  $^1\text{H}$  ( $\text{CD}_3\text{NO}_2$ ),  $\delta$  3.75 [d, 2 H,  $\text{H}^1$ ,  $J(\text{H}^1\text{H}^2)$  3.0], 2.80–2.55 (m, 2 H,  $\text{H}^2$ ), 2.1 (s, 15 H,  $\text{C}_5\text{Me}_5$ ), and 1.8 [d, 6 H,  $\text{Me}$ ,  $J(\text{MeH}^1)$  9.0];  $^{13}\text{C}$ - $\{^1\text{H}\}$  ( $\text{CD}_2\text{Cl}_2$ ),  $\delta$  219.4 (CO), 114.4 ( $\text{C}^4$ ), 104.6 ( $\text{C}_5\text{Me}_5$ ), 87.8 ( $\text{C}^1, \text{C}^2$ ), 61.3 ( $\text{C}^3$ ), 14.9 (Me), and 11.0 p.p.m. ( $\text{C}_5\text{Me}_5$ ).

**Dicarboxyl( $\eta^4$ -trans-methylenebis(methylmethylene)methane)( $\eta$ -pentamethylcyclopentadienyl)molybdenum tetrafluoroborate (7).** Yield 58% (Found: C, 46.9; H, 5.6.  $\text{C}_{18}\text{H}_{25}\text{BF}_4\text{MoO}_2$  requires C, 47.4; H, 5.5%),  $\nu_{\text{CO}}$  ( $\text{CH}_2\text{Cl}_2$ ) 2 040s and 1 996s  $\text{cm}^{-1}$ . N.m.r.:  $^1\text{H}$  ( $\text{CD}_2\text{Cl}_2$ ),  $\delta$  4.53 [dq, 1 H,  $\text{H}^2$ ,  $J(\text{H}^2\text{Me}^5)$  7.0,  $J(\text{H}^2\text{H}^1)$  7.0], 3.6 [d, 1 H,  $\text{H}^1$ ,  $J(\text{H}^1\text{H}^1')$  1.1], 2.72 [q, 1 H,  $\text{H}^3$ ,  $J(\text{Me}^6\text{H}^3)$  7.0], 2.0 (s, 15 H,  $\text{C}_5\text{Me}_5$ ), 1.91 [d, 3 H,  $\text{Me}^6$ ,  $J(\text{Me}^6\text{H}^3)$  7.0], 1.61 [dd, 1 H,  $\text{H}^1'$ ,  $J(\text{H}^1\text{H}^1')$  1.1];  $^{13}\text{C}$ - $\{^1\text{H}\}$  ( $\text{CD}_2\text{Cl}_2$ ),  $\delta$  221.7 (CO), 115.8 ( $\text{C}^4$ ), 106 ( $\text{C}_5\text{Me}_5$ ), 89.0 ( $\text{C}^3$ ), 87.3 ( $\text{C}^2$ ), 62.1 ( $\text{C}^1$ ), 16.7 ( $\text{Me}^6$ ), 15.1 ( $\text{Me}^5$ ), and 12.5 p.p.m. ( $\text{C}_5\text{Me}_5$ ).

**Reactions of Complex (1).**—(a) *With hydroxide anion.* A solution of complex (1) (0.5 g 1.17 mmol) in  $\text{CH}_2\text{Cl}_2$  (15  $\text{cm}^3$ ) was placed on an alumina (Brockman, activity II) packed column. Elution with  $\text{CH}_2\text{Cl}_2$  afforded a yellow band which was collected. Removal of the solvent and recrystallisation (-78 °C) from  $\text{CH}_2\text{Cl}_2$  afforded yellow crystals of (8) (0.27 g, 75%) (Found: C, 53.5; H, 5.9%;  $M$  358.  $\text{C}_{16}\text{H}_{22}\text{MoO}_3$  requires C, 53.6; H, 6.2%;  $M$  358),  $\nu_{\text{CO}}$  ( $\text{CH}_2\text{Cl}_2$ ) 1 939s and 1 863s  $\text{cm}^{-1}$ . N.m.r.:  $^1\text{H}$  ( $\text{C}_6\text{D}_6$ ),  $\delta$  3.75 (s, 2 H,  $\text{CH}_2\text{OH}$ ), 3.20 (s, 2 H,  $\text{H}_s$ ), 1.51 (s, 15 H,  $\text{C}_5\text{Me}_5$ ), and 0.67 (s, 2 H,  $\text{H}_a$ ) (*exo* isomer); 3.67 (s, 2 H,  $\text{CH}_2\text{OH}$ ), 3.06 (s, 2 H,  $\text{H}_s$ ), 1.51 (s, 15 H,  $\text{C}_5\text{Me}_5$ ),

and 0.54 (s, 2 H, H<sub>a</sub>) (*endo* isomer) (*exo/endo* = 1/2); <sup>13</sup>C-<sup>1</sup>H, δ 240.0 (CO), 102.0 (C<sup>2</sup>), 101.0 (C<sub>5</sub>Me<sub>5</sub>), 75.0 (CH<sub>2</sub>OH), 47.0 (C<sup>1</sup>, C<sup>3</sup>), and 10.0 p.p.m. (C<sub>5</sub>Me<sub>5</sub>).



(b) *With sodium tetrahydroborate.* An excess of NaBH<sub>4</sub> (0.1 g, 2.6 mmol) was added to a stirred suspension of complex (1) (0.5 g, 1.17 mmol) in tetrahydrofuran (20 cm<sup>3</sup>). After 3 h at room temperature, the solvent was removed *in vacuo* and the residue extracted with hexane. Chromatography on alumina and elution with hexane gave a pale yellow band. Recrystallisation (-78 °C) from hexane gave yellow crystals of (9) (0.3 g, 75%) (Found: C, 55.6; H, 6.7%; M 342. C<sub>16</sub>H<sub>22</sub>MoO<sub>2</sub> requires C, 56.1; H, 6.4%; M 342), ν<sub>CO</sub> (hexane) 2 047s and 1 877s cm<sup>-1</sup>. N.m.r.: <sup>1</sup>H (C<sub>6</sub>D<sub>6</sub>), δ 3.0 (s, 2 H, H<sub>a</sub>), 1.8 (s, 3 H, Me), 1.6 (s, 15 H, C<sub>5</sub>Me<sub>5</sub>), and 0.6 (s, 2 H, H<sub>a</sub>) (*endo* isomer); <sup>13</sup>C-<sup>1</sup>H (C<sub>6</sub>D<sub>6</sub>), δ 106.5 (C<sup>2</sup>), 102.1 (C<sub>5</sub>Me<sub>5</sub>), 47.7 (C<sup>1</sup>, C<sup>3</sup>), and 10.9 p.p.m. (C<sub>5</sub>Me<sub>5</sub>).

(c) *With lithium dimethylcuprate.* Addition of lithium dimethylcuprate [CuI (0.15 g, 7.8 mmol), LiMe·LiBr (0.8 cm<sup>3</sup>, 1.4 mmol)] in diethyl ether (4 cm<sup>3</sup>) to a stirred suspension (-78 °C) of complex (1) (0.3 g, 0.7 mmol) resulted in the rapid development of a bright yellow colour. After 1 h at room temperature the solvent was removed *in vacuo* and the residue extracted with pentane. Chromatography on alumina and elution with pentane gave a yellow band which was collected. Recrystallisation (-78 °C) from pentane gave yellow crystals of (10) (0.22 g, 88%) (Found: C, 57.2; H, 7.0%; M 356. C<sub>17</sub>H<sub>24</sub>MoO<sub>2</sub> requires C, 57.3; H, 6.8%; M 356), ν<sub>CO</sub> (pentane) 1 950s and 1 880s cm<sup>-1</sup>. N.m.r.: <sup>1</sup>H (C<sub>6</sub>D<sub>6</sub>), δ 3.0 (s, 2 H, H<sub>a</sub>), 1.83 [q, 2 H, CH<sub>2</sub>CH<sub>3</sub>, J(HH) 5.0], 1.61 (s, 15 H, C<sub>5</sub>Me<sub>5</sub>), 1.10 [t, 3 H, CH<sub>2</sub>CH<sub>3</sub>, J(HH) 5.0], and 0.58 (s, 2 H, H<sub>a</sub>) (*endo* isomer).

(d) *With sodium thiophenoxide.* A solution of NaSPh (0.13 g, 0.98 mmol) in tetrahydrofuran (10 cm<sup>3</sup>) was added dropwise to a stirred (-30 °C) suspension of complex (1) (0.4 g, 0.94 mmol) in tetrahydrofuran (10 cm<sup>3</sup>). The reaction mixture was allowed to warm to room temperature and the solvent removed *in vacuo*. Extraction with diethyl ether followed by chromatography on alumina and recrystallisation (-78 °C) from hexane gave yellow crystals of (11) (0.33 g, 78%) (Found: C, 58.4; H, 5.8%; M 450. C<sub>22</sub>H<sub>26</sub>MoO<sub>2</sub>S requires C, 58.7; H, 5.8%; M 450); ν<sub>CO</sub> (hexane) 1 950s and 1 880s cm<sup>-1</sup>. N.m.r.: <sup>1</sup>H (CDCl<sub>3</sub>), δ 7.2–7.5 (m, 5 H, Ph), 3.08 (s, 2 H, H<sub>a</sub>), 1.87 (s, 2 H, CH<sub>2</sub>SPh), 1.82 (s, 15 H, C<sub>5</sub>Me<sub>5</sub>), and 0.64 (s, 2 H, H<sub>a</sub>) (*endo* isomer); <sup>13</sup>C-<sup>1</sup>H (C<sub>6</sub>D<sub>6</sub>), δ 242.0 (CO), 137–127 (Ph), 105.6 (C<sup>2</sup>), 102.3 (C<sub>5</sub>Me<sub>5</sub>), 47.4 (C<sup>1</sup>, C<sup>3</sup>), 45.4 (CH<sub>2</sub>SPh), and 10.6 p.p.m. (C<sub>5</sub>Me<sub>5</sub>).

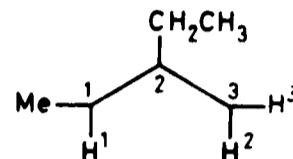
The following η<sup>3</sup>-allyl complexes were synthesised in a similar manner.

*Dicarbonyl(η-cyclopentadienyl)(η<sup>3</sup>-2-isopropylallyl)molybdenum* (12). Yield 65% (Found: C, 57.2; H, 5.3%; M 300. C<sub>15</sub>H<sub>16</sub>MoO<sub>2</sub> requires C, 57.2; H, 5.3%; M 300), ν<sub>CO</sub> (hexane) 1 959s and 1 887s cm<sup>-1</sup>. N.m.r.: <sup>1</sup>H (C<sub>6</sub>D<sub>6</sub>), δ 4.61 (s, 5 H, H<sub>a</sub>), 2.75 (br s, 2 H, H<sub>a</sub>), 2.05 [septet, 1 H, CHMe<sub>2</sub>, J(MeH) 8.1], 1.56 [br s, 2 H, H<sub>a</sub>], and 1.05 [d, 6 H, CHMe<sub>2</sub>, J(MeH) 8.1]; <sup>13</sup>C-<sup>1</sup>H (C<sub>6</sub>D<sub>6</sub>), δ 241.8 (CO), 92.6 (C<sup>2</sup>), 90.6 (C<sub>5</sub>H<sub>5</sub>), 37.7 (CHMe<sub>2</sub>), 34.3 (C<sup>1</sup>, C<sup>3</sup>), and 24.1 p.p.m. (CHMe<sub>2</sub>).

*Dicarbonyl(η-pentamethylcyclopentadienyl)(η<sup>3</sup>-syn,syn-1,3-trimethylallyl)molybdenum* (13). Yield 65% (Found: C, 58.4; H, 7.4%; M 370. C<sub>18</sub>H<sub>26</sub>MoO<sub>2</sub> requires C, 58.4; H,

7.0%; M 370), ν<sub>CO</sub> (hexane) 1 939s and 1 865s cm<sup>-1</sup>. N.m.r.: <sup>1</sup>H (C<sub>6</sub>D<sub>6</sub>), δ 1.88 [d, 6 H, CHMe, J(MeH) 6.3], 1.74 (s, 3 H, 2-Me), 1.60 (s, 15 H, C<sub>5</sub>Me<sub>5</sub>), 0.88 [q, 2 H, CHMe, J(MeH) 6.3] (*endo* isomer); <sup>13</sup>C-<sup>1</sup>H (C<sub>6</sub>D<sub>6</sub>), δ 244.6 (CO), 119.4 (C<sup>2</sup>), 101.9 (C<sub>5</sub>Me<sub>5</sub>), 60.6 (CHMe), 28.3 (Me), 16.0 (CHMe), and 10.5 p.p.m. (C<sub>5</sub>Me<sub>5</sub>).

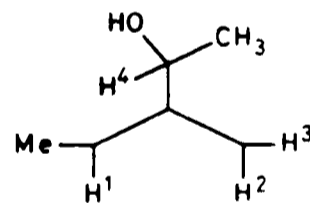
*Dicarbonyl(η<sup>3</sup>-2-ethyl-syn-1-methylallyl)(η-pentamethylcyclopentadienyl)molybdenum* (14). Yield 35% (Found: C, 57.5; H, 7.3%; M 370. C<sub>18</sub>H<sub>26</sub>MoO<sub>2</sub> requires C, 58.4; H, 7.0%; M 370), ν<sub>CO</sub> (hexane) 1 940s and 1 850s cm<sup>-1</sup>. N.m.r.: <sup>1</sup>H (C<sub>6</sub>D<sub>6</sub>), δ 2.88 (s, 1 H, H<sup>3</sup>), 2.23 (m, 1 H, CH<sub>2</sub>CH<sub>3</sub>), 1.82 [d, 3 H, Me, J(MeH) 6.1], 1.69 (m, 1 H, CH<sub>2</sub>CH<sub>3</sub>), 1.60 (s,



15 H, C<sub>5</sub>Me<sub>5</sub>), 1.21 [q, 1 H, H<sup>1</sup>, J(H<sup>1</sup>Me) 6.1], 1.04 [t, 3 H, CH<sub>2</sub>CH<sub>3</sub>, J(HMe) 6.0], and 0.22 (s, 1 H, H<sup>2</sup>); <sup>13</sup>C-<sup>1</sup>H (C<sub>6</sub>D<sub>6</sub>), δ 244.3 (CO), 244.0 (CO), 118.0 (C<sup>2</sup>), 102.0 (C<sub>5</sub>Me<sub>5</sub>), 62.3 (C<sup>1</sup>), 44.1 (C<sup>3</sup>), 28.3 (CH<sub>2</sub>CH<sub>3</sub>), 16.6 (Me), 15.3 (CH<sub>2</sub>CH<sub>3</sub>), and 10.66 p.p.m. (C<sub>5</sub>Me<sub>5</sub>).

*Dicarbonyl(η<sup>3</sup>-2-hydroxymethyl-syn,syn-1,3-dimethylallyl)(η-pentamethylcyclopentadienyl)molybdenum* (15). Yield 72% (Found: C, 56.7; H, 7.5%; M 386. C<sub>18</sub>H<sub>26</sub>MoO<sub>3</sub> requires C, 56.0; H, 6.8%; M 386), ν<sub>CO</sub> (hexane) 1 934s and 1 850s cm<sup>-1</sup>. N.m.r.: <sup>1</sup>H (C<sub>6</sub>D<sub>6</sub>), δ 3.90 (s, 2 H, CH<sub>2</sub>OH), 1.90 [d, 6 H, CHMe, J(HMe) 6.2], 1.55 (s, 15 H, C<sub>5</sub>Me<sub>5</sub>), and 0.86 [q, 2 H, CHMe, J(HMe) 6.2]; <sup>13</sup>C-<sup>1</sup>H (CDCl<sub>3</sub>), δ 243.0 (CO), 128.9 (C<sup>2</sup>), 101.9 (C<sub>5</sub>Me<sub>5</sub>), 66.4 (CH<sub>2</sub>OH), 61.7 (C<sup>1</sup>, C<sup>3</sup>), 15.4 (CHMe), and 10.5 p.p.m. (C<sub>5</sub>Me<sub>5</sub>).

*Dicarbonyl[η<sup>3</sup>-2-(1'-hydroxyethyl)-syn-1-methylallyl](η-pentamethylcyclopentadienyl)molybdenum* (16). Yield 70% (Found: C, 55.4; H, 7.1%; M 386. C<sub>18</sub>H<sub>26</sub>MoO<sub>3</sub> requires C, 56.0; H, 6.8%; M 386), ν<sub>CO</sub> (hexane) 1 944s and 1 872s



cm<sup>-1</sup>. N.m.r.: <sup>1</sup>H (C<sub>6</sub>D<sub>6</sub>), δ 4.16 [q, 1 H, H<sup>4</sup>, J(MeH) 6.6], 2.88 (s, 1 H, H<sup>3</sup>), 2.0 [d, 3 H, CHMe, J(MeH<sup>1</sup>) 6.2], 1.55 (s, 15 H, C<sub>5</sub>Me<sub>5</sub>), 1.35 [d, 3 H, CH(OH)CH<sub>3</sub>, J(MeH<sup>4</sup>) 6.6], and 1.15 [q, 1 H, H<sup>1</sup>, J(H<sup>1</sup>Me) 6.2]; <sup>13</sup>C-<sup>1</sup>H (C<sub>6</sub>D<sub>6</sub>), δ 243.9 (CO), 243.3 (CO), 112.5 (C<sup>2</sup>), 101.9 (C<sub>5</sub>Me<sub>5</sub>), 69.5 (CHOH), 62.3 (C<sup>1</sup>), 40.3 (C<sup>3</sup>), 21.1 (CHMe), 15.4 (CHOHMe), and 10.4 p.p.m. (C<sub>5</sub>Me<sub>5</sub>).

*Molecular Structure Determination of Complex (1).*—A single crystal of uniform dimensions (ca. 0.2 mm) was sealed (epoxy-resin) inside a Lindemann capillary under an atmosphere of dry nitrogen. Unit-cell dimensions and the space group were established by oscillation and zero- and first-level (equi-inclination) Weissenberg photography (Cu-Kα X-radiation).

Data collection was carried out, using the same crystal, on an Enraf-Nonius CAD4 diffractometer at Queen Mary College, London. The crystal was slowly cooled to 268 ± 1 K in a cold air stream. When steady state had been achieved 25 relatively low-angle reflections were centred (program

Table 4. Fractional co-ordinates of atoms, with standard deviations

Atom	x	y	z	p.p.	Atom	x	y	z	p.p.
Mo	0.01524(6)	0.24354(6)	0.07924(3)	1.0000	F(8)	0.010(5)	-0.425(6)	0.134(4)	0.1009
C(1)	0.0534(8)	0.2567(8)	0.1815(4)	1.0000	F(9)	-0.042(3)	-0.366(4)	0.1646(18)	0.2077
C(2)	-0.0527(7)	0.2863(9)	0.1709(4)	1.0000	F(10)	0.111(3)	-0.331(3)	0.1070(18)	0.2075
C(3)	-0.1066(7)	0.1932(7)	0.1483(4)	1.0000	F(11)	0.1042(17)	-0.3482(16)	0.2133(9)	0.4542
C(4)	-0.0364(6)	0.1066(7)	0.1431(4)	1.0000	F(12)	0.074(4)	-0.413(3)	0.1274(21)	0.2326
C(5)	0.0635(7)	0.1481(9)	0.1647(4)	1.0000	F(13)	0.065(3)	-0.380(4)	0.2146(22)	0.2313
C(6)	0.1339(9)	0.3221(11)	0.2112(5)	1.0000	F(14)	-0.032(5)	-0.249(5)	0.166(3)	0.1644
C(7)	-0.1004(10)	0.3879(10)	0.1926(7)	1.0000	H(21)	0.233(6)	0.177(6)	0.074(4)	1.0000
C(8)	-0.2228(6)	0.1850(10)	0.1407(5)	1.0000	H(22)	0.179(6)	0.134(6)	0.010(4)	1.0000
C(9)	-0.0598(10)	-0.0091(8)	0.1322(5)	1.0000	H(31)	0.195(6)	0.348(6)	0.119(4)	1.0000
C(10)	0.1569(9)	0.0761(11)	0.1775(6)	1.0000	H(32)	0.116(6)	0.427(6)	0.087(4)	1.0000
C(101)	-0.0644(7)	0.1455(8)	0.0236(4)	1.0000	H(41)	0.034(6)	0.370(6)	-0.026(6)	1.0000
O(101)	-0.1120(6)	0.0916(7)	-0.0059(4)	1.0000	H(42)	0.050(7)	0.257(6)	-0.046(5)	1.0000
C(102)	-0.0844(8)	0.3660(8)	0.0584(5)	1.0000	H(61)	0.1200	0.3203	0.2582	1.0000
O(102)	-0.1425(7)	0.4303(7)	0.0475(5)	1.0000	H(62)	0.1317	0.4051	0.1958	1.0000
C(11)	0.1540(8)	0.2879(9)	0.0264(5)	1.0000	H(63)	0.2096	0.2875	0.2018	1.0000
C(22)	0.1715(8)	0.1748(10)	0.0432(5)	1.0000	H(71)	-0.1810	0.3909	0.1789	1.0000
C(33)	0.1587(8)	0.3628(9)	0.0725(4)	1.0000	H(72)	-0.0590	0.4566	0.1744	1.0000
C(44)	0.0755(10)	0.2976(13)	-0.0163(5)	1.0000	H(73)	-0.0963	0.3906	0.2402	1.0000
B	0.0572(7)	-0.3231(13)	0.1621(6)	1.0000	H(81)	-0.2582	0.2639	0.1463	1.0000
F(1)	-0.0416(20)	-0.3063(22)	0.1675(11)	0.4314	H(82)	-0.2536	0.1298	0.1734	1.0000
F(2)	0.0827(15)	-0.3899(15)	0.1142(9)	0.5538	H(83)	-0.2401	0.1545	0.0971	1.0000
F(3)	0.092(4)	-0.394(4)	0.2067(22)	0.2238	H(91)	0.0122	-0.0543	0.1295	1.0000
F(4)	0.115(3)	-0.2284(23)	0.1609(12)	0.3358	H(92)	-0.1024	-0.0173	0.0913	1.0000
F(5)	-0.041(3)	-0.273(3)	0.1481(15)	0.3320	H(93)	-0.1065	-0.0403	0.1681	1.0000
F(6)	0.1160(24)	-0.2378(21)	0.1325(12)	0.3323	H(101)	0.1444	-0.0041	0.1595	1.0000
F(7)	0.114(4)	-0.245(3)	0.1923(24)	0.1779	H(102)	0.1675	0.0705	0.2247	1.0000
					H(103)	0.2257	0.1114	0.1578	1.0000

SEARCH) and their angles used to generate the first cell and orientation matrix. After rapid collection of data within the range  $\theta = 14-15^\circ$  (Mo- $K_\alpha$  X-radiation;  $\lambda_{\alpha_1} = 0.70926$ ,  $\lambda_{\alpha_2} = 0.71354$  Å) 25 reflections selected from this shell were carefully centred (SETANG) to furnish, by least-squares refinement, accurate cell parameters and the orientation matrix used in data collection.

**Crystal data.**  $C_{16}H_{21}BF_4MoO_2$ ,  $M = 427.75$ , orthorhombic,  $a = 12.822(2)$ ,  $b = 12.311(3)$ ,  $c = 22.660(4)$  Å,  $U = 3576.9$  Å<sup>3</sup>,  $D_m = 1.5$  g cm<sup>-3</sup> (floatation),  $Z = 8$  ion pairs,  $D_c = 1.58$  g cm<sup>-3</sup>,  $F(000) = 1728$  electrons,  $\mu(\text{Mo-}K_\alpha) = 6.9$  cm<sup>-1</sup>, space group  $Pbca$  ( $D_{2h}^{15}$ , no. 61) from systematic absences.

Intensity data were collected ( $+h +k +l$ ) between  $1.5 < \theta < 27.0^\circ$  by  $\theta-2\theta$  scans in which scan widths (s.w.) were calculated from the equation  $s.w. = 0.85 + 0.35 \tan \theta$ . The intensities of two standard reflections ( $\bar{4} \bar{6} 6$  and  $\bar{2} \bar{2} 14$ ) were remeasured once every hour, but subsequent analysis of their net counts as individual functions of time revealed no significant crystal decomposition or movement, or source variation, over the ca. 45 h of data collection. 3893 Reflections were corrected for Lorentz and polarisation effects (but not for X-ray absorption). Of these, 2747 had  $F_o > 2.0\sigma(F_o)$  and were used for structure solution and refinement.

The metal atom was sought by analysis of the Patterson function. Two feasible solutions (0.00, 0.25, 0.17 and 0.00, 0.25, 0.08 and their respective symmetry equivalents) allowed all prominent peaks to be assigned, but only adoption of the second ultimately gave a molecular model that refined well. With unit weights assigned to all reflections, remaining non-hydrogen atoms were located from a difference Fourier, and refined by full-matrix least squares, first isotropically and then (except for F atoms) anisotropically. After convergence of this model ( $R$  ca. 0.08)  $F_o$  moduli were weighted according to  $w^{-1} = \sigma^2(F_o) + 0.035 F_o^2$ . The  $BF_4^-$  anion showed spherical

partial disorder that has been modelled by the use of 14 fractional fluorine atoms with population parameters (p.p.) of 0.101–0.554 ( $\Sigma p.p. = 3.99$ ), these being optimised by least squares after assignment of  $U_F^* = 0.10$  Å<sup>2</sup>.

Methyl functions were treated as rigid groups with C–H 1.08 Å, but hydrogen atoms of the trimethylenemethane ligand were located (from a difference Fourier to which the contributions from low-angle reflections were artificially enhanced) and subsequently allowed positionally to refine. For all H atoms  $U$  was fixed at 0.08 Å<sup>2</sup>.

Refinement (2747 data, 256 variables) converged at  $R = 0.0674$ ,  $R' = 0.0983$ . A final difference Fourier showed no peak  $> 0.7 e \text{ \AA}^{-3}$ , nor trough  $< -0.7 e \text{ \AA}^{-3}$ , and there was no unusual systematic variation of the root-mean-square deviation of a reflection of unit weight versus parity group,  $(\sin \theta)/\lambda$ ,  $F_o$ ,  $h$ ,  $k$ , or  $l$ . Table 4 lists the derived atomic coordinates. Structure solution and refinement employed the SHELX 76 programs<sup>25</sup> implemented on the University of London Computer Centre CDC 7600 and University of Edinburgh ICL 2972 computers. Least-squares planes (SUP 23876) were analysed using XANADU<sup>26</sup> and Figures constructed using Johnson's ORTEP-II.<sup>27</sup>

#### Acknowledgements

We thank the S.E.R.C. for support and Dr. M. B. Hursthouse (Q.M.C., London) for diffractometer facilities. N. W. M. thanks the University of Edinburgh for a postgraduate demonstratorship.

#### References

- 1 Part 29, S. R. Allen, M. Green, G. Moran, A. G. Orpen, and G. E. Taylor, *J. Chem. Soc., Dalton Trans.*, 1984, 441.
- 2 M. Green, J. A. K. Howard, R. P. Hughes, S. C. Kellett, and P. Woodward, *J. Chem. Soc., Dalton Trans.*, 1975, 2007.

\* The isotropic thermal factor is defined as  $\exp[-8\pi^2 U(\sin^2 \theta)/\lambda^2]$ .

- 3 T. H. Whitesides and R. W. Slaven, *J. Organomet. Chem.*, 1974, **67**, 99; R. W. Slaven and J. C. Calabrese, *Inorg. Chem.*, 1974, **13**, 1895.
- 4 A. R. Pinhas, A. G. Samuelson, R. Risemberg, E. V. Arnold, J. Clardy, and B. K. Carpenter, *J. Am. Chem. Soc.*, 1981, **103**, 1668; A. G. Samuelson and B. K. Carpenter, *J. Chem. Soc., Chem. Commun.*, 1981, 354.
- 5 T. A. Albright, P. R. Clemens, R. P. Hughes, D. E. Hunton, and L. D. Margerum, *J. Am. Chem. Soc.*, 1982, **104**, 5369.
- 6 P. Binger and U. Schuchardt, *Angew. Chem., Int. Ed. Engl.*, 1977, **16**, 249.
- 7 P. Binger and U. Schuchardt, *Chem. Ber.*, 1980, **113**, 3334.
- 8 P. Binger and U. Schuchardt, *Chem. Ber.*, 1981, **114**, 3313.
- 9 P. Binger and A. Germer, *Chem. Ber.*, 1981, **114**, 3325.
- 10 P. Binger and P. Bentz, *J. Organomet. Chem.*, 1981, **221**, C33.
- 11 B. M. Trost and D. M. T. Chan., *J. Am. Chem. Soc.*, 1983, **105**, 2326.
- 12 S. G. Barnes and M. Green, *J. Chem. Soc., Chem. Commun.*, 1980, 267.
- 13 S. R. Allen, Ph.D. Thesis, University of Bristol, 1982.
- 14 T. A. Albright, P. Hofmann, and R. Hoffmann, *J. Am. Chem. Soc.*, 1977, **99**, 7546.
- 15 A. Almennigen, A. Haaland, and K. Wahl, *Acta Chem. Scand.*, 1969, **23**, 1145.
- 16 M. R. Churchill and K. Gold, *Inorg. Chem.*, 1969, **8**, 401.
- 17 M. R. Churchill and B. G. De Boer, *Inorg. Chem.*, 1973, **12**, 525.
- 18 T. A. Albright, *Acc. Chem. Res.*, 1982, **15**, 149.
- 19 B. E. R. Schilling, R. Hoffmann, and D. L. Lichtenberger, *J. Am. Chem. Soc.*, 1979, **101**, 585.
- 20 M. Elia, M. M. L. Chen, D. M. P. Mingos, and R. Hoffmann, *Inorg. Chem.*, 1976, **15**, 1148.
- 21 H. S. Gutowsky and C. H. Holm, *J. Chem. Phys.*, 1956, **25**, 1228; A. Allerhand, H. S. Gutowsky, J. Jones, and R. A. Meinzer, *J. Am. Chem. Soc.*, 1966, **88**, 3185.
- 22 B. E. R. Schilling, R. Hoffmann, and J. W. Faller, *J. Am. Chem. Soc.*, 1979, **101**, 592.
- 23 R. B. Woodward and R. Hoffmann, 'The Conservation of Orbital Symmetry,' Verlag-Chemie, Weinheim, 1970, pp. 46, 55.
- 24 S. Arora and P. Binger, *Synthesis*, 1974, 801.
- 25 G. M. Sheldrick, University Chemical Laboratory, Cambridge, 1976.
- 26 P. R. Roberts and G. M. Sheldrick, University Chemical Laboratory, Cambridge, 1976.
- 27 C. K. Johnson, Report ORNL-5138, Oak Ridge National Laboratory, Tennessee, 1976.

Received 27th July 1983; Paper 3/1300

- International Tables for X-ray Crystallography* (1974). Vol. IV. Birmingham: Kynoch Press.
- ISAGO, T., OKAMOTO, K., OHMASA, M. & HIDAKA, J. (1980). *Chem. Lett.* pp. 319–322.
- JOHNSON, C. K. (1965). *ORTEP*. Report ORNL-3794. Oak Ridge National Laboratory, Tennessee.
- KOJIMA, M. & FUJITA, J. (1983). *Bull. Chem. Soc. Jpn.* **56**, 2958–2964.
- MITSUI, Y., WATANABE, J., HARADA, Y., SAKAMAKI, T. & IITAKA, Y. (1976). *J Chem. Soc. Dalton Trans.* pp. 2095–2102.
- SAKURAI, T. & KOBAYASHI, K. (1979). *Rikagaku Kenkyusho Hokoku*, **55**, 69–77.

*Acta Cryst.* (1984). **C40**, 401–403

## The Structure of Dicarboxyl( $\eta^5$ -cyclopentadienyl) ( $\eta^3$ -2-methylallyl)molybdenum(II), [Mo(C<sub>4</sub>H<sub>7</sub>)(C<sub>5</sub>H<sub>5</sub>)(CO)<sub>2</sub>]

BY NICHOLAS W. MURRALL AND ALAN J. WELCH

*Dewar Crystallographic Laboratory, Department of Chemistry, University of Edinburgh, Edinburgh EH9 3JJ, Scotland*

(Received 27 September 1983; accepted 16 November 1983)

**Abstract.**  $M_r = 272.2$ , monoclinic,  $P2_1/n$ ,  $a = 6.1105$  (9),  $b = 12.7885$  (22),  $c = 13.7247$  (24) Å,  $\beta = 98.787$  (13)°,  $U = 1059.91$  Å<sup>3</sup>,  $D_x = 1.705$  Mg m<sup>-3</sup>,  $Z = 4$ ,  $F(000) = 544$  e,  $\lambda(\text{Mo } K\alpha) = 0.71069$  Å,  $\mu = 1.083$  mm<sup>-1</sup>,  $T = 188$  K.  $R = 0.025$  for 2867 unique reflections. The molecule crystallizes with the  $\eta^3$ -2-methylallyl ligand in the *endo* conformation, and the three Mo–C(allyl) distances are equal within experimental error, average 2.3163 (13) Å.

**Introduction.** There is currently considerable theoretical and experimental interest in the structural preferences of complexes containing the  $\eta^3$ -allyl or a substituted  $\eta^3$ -allyl ligand. Detailed NMR studies (Faller, Chen, Mattina & Jakubowski, 1973) had previously established that whilst both *exo* and *endo* (Schilling, Hoffmann & Faller, 1979) conformations of [( $\eta^5$ -C<sub>5</sub>H<sub>5</sub>)(2-*R*- $\eta^3$ -C<sub>3</sub>H<sub>5</sub>)(CO)<sub>2</sub>Mo] ( $R = \text{H, Me}$ ) are present (and rapidly interconvert) in solution, the major isomer is *exo* for  $R = \text{H}$  and *endo* for  $R = \text{Me}$ . It is, furthermore, *exo*-[( $\eta^5$ -C<sub>5</sub>H<sub>5</sub>)( $\eta^3$ -C<sub>3</sub>H<sub>5</sub>)(CO)<sub>2</sub>Mo] (I) that crystallizes (Faller, Chodosh & Katahira, 1980). To establish if a similar correspondence exists between major solution isomer and that observed in the solid state when  $R = \text{Me}$ , we have determined the crystal structure of [( $\eta^5$ -C<sub>5</sub>H<sub>5</sub>)(2-Me- $\eta^3$ -C<sub>3</sub>H<sub>5</sub>)(CO)<sub>2</sub>Mo] (II).

**Experimental.** Yellow crystals, prepared according to the literature (Faller, Chen, Mattina & Jakubowski, 1973), 0.05 × 0.04 × 0.03 cm, from diethyl ether/*n*-heptane (1:1) by slow evaporation, mounted in Lindemann tube under N<sub>2</sub>; preliminary unit cell and space group from oscillation and Weissenberg photography [ $\lambda(\text{Cu } K\alpha) = 1.54178$  Å],  $h0l$   $h+l = 2n+1$  and  $0k0$

$k = 2n+1$  absent; CAD-4 diffractometer, 188 K (ULT-1 apparatus), 25 reflections ( $17^\circ < \theta < 18^\circ$ ) centred, graphite-monochromated Mo  $K\alpha$  radiation; for data collection  $\theta_{\text{max}} = 30^\circ$ ,  $\omega$ - $2\theta$  scans in 96 steps,  $\omega$  scan width  $0.8^\circ + 0.35^\circ \tan \theta$ , rapid prescan after which reflections with  $I \geq 0.5\sigma(I)$  remeasured such that final net intensity had  $I > 33\sigma(I)$  subject to a maximum measuring time of 90 s; two quadrants measured ( $hk\pm l$  and  $-h-k\pm l$ ) over 115 X-ray hours with no detectable decay or movement; data not corrected for absorption, observed structure factors determined and merged to give 3083 unique reflections,  $R_{\text{merge}} = 0.0218$ ; for structure solution and refinement 2867 amplitudes for which  $F \geq 2\sigma(F)$ , Patterson synthesis (Mo), full-matrix least squares (on  $F$ ) (Sheldrick, 1976),  $w = [\sigma^2(F) + 0.004524(F)^2]^{-1}$ , anisotropic thermal parameters for all non-H atoms,  $U_{\text{H}}^*$  set at 0.04 Å<sup>2</sup>,  $R = 0.0250$ ,  $wR = 0.0469$ , data: variable ratio 17:1,  $(\Delta/\sigma)_{\text{max}}$  in final cycle <0.3, max. peak and min. trough in final  $\Delta F$  synthesis 0.41 and  $-1.08$  e Å<sup>-3</sup> respectively, neutral scattering factors for C, O, Mo (Cromer & Liberman, 1970) and H (Stewart, Davidson & Simpson, 1965), computer programs *SHELX76* (Sheldrick, 1976), *XANADU* (Roberts & Sheldrick, 1976), *XRAY76* (Stewart, Machin, Dickinson, Ammon, Heck & Flack, 1976), and *ORTEPII* (Johnson, 1976).†

\* The isotropic temperature factor is defined as  $\exp[-8\pi^2 U \times (\sin^2 \theta) / \lambda^2]$ .

† Lists of structure factors, H-atom coordinates, Tables 3 and 4, and anisotropic thermal parameters have been deposited with the British Library Lending Division as Supplementary Publication No. SUP 39027 (22 pp.). Copies may be obtained through The Executive Secretary, International Union of Crystallography, 5 Abbey Square, Chester CH1 2HU, England.

**Discussion.** The derived fractional coordinates are given in Table 1. Table 2 lists important molecular dimensions. Coordinates and bond lengths and angles involving H atoms have been deposited as Table 3 and full details of molecular planes are deposited as Table 4.\* Fig. 1 is a perspective view of a single molecule.

In [( $\eta^5$ -C<sub>5</sub>H<sub>5</sub>)( $\eta^3$ -allyl)LL'Mo] complexes there are two limiting molecular conformations, *exo* (A) and *endo* (B) (Schilling, Hoffmann & Faller, 1979). For (I) and for a number of its substituted-allyl analogues both conformers have been shown to co-exist in solution at ambient temperatures, and barriers to interconversion have been estimated at *ca* 63 kJ mol<sup>-1</sup> for (I) and (II) (Faller, Chen, Mattina & Jakubowski, 1973). For (I) the *exo* conformer predominates in solution, and is, moreover, the conformation characterized in the solid state. It is of interest that this conformational preference is not supported by the result of molecular-orbital calculations.



In contrast, the major solution isomer of (II) has an *endo* conformation, and the present study clearly demonstrates that this, too, is retained upon crystallization. Clearly, an important influence upon the preferred stereochemistry of (II) is the steric requirement of the 2-methyl substituent, and we have calculated that in the alternative *exo* conformation a repulsive H(Me)⋯H( $\eta^5$ -C<sub>5</sub>H<sub>5</sub>) contact would result, whereas there is no intramolecular congestion in the observed, *endo* conformation.

Unusually the Mo—C(allyl) distances in (II) are equal; this contrasts with the great majority of seven-coordinate molybdenum(II) allyls that have been

\* See deposition footnote.

Table 1. Fractional atomic coordinates with standard deviations

$$U_{eq} = \frac{1}{3} \sum_i \sum_j U_{ij} a_i^* a_j^* a_i \cdot a_j$$

	x	y	z	$U_{eq}(\text{\AA}^2)$
Mo	0.46349 (2)	0.19301 (1)	0.12509 (1)	0.0201
C(1)	0.2065 (4)	0.29750 (17)	0.18619 (19)	0.0390
C(2)	0.3405 (4)	0.36310 (14)	0.13794 (14)	0.0321
C(3)	0.5683 (4)	0.36159 (16)	0.17359 (17)	0.0357
C(4)	0.2461 (5)	0.42399 (19)	0.04816 (18)	0.0440
C(5)	0.7513 (4)	0.07415 (24)	0.16929 (24)	0.0585
C(6)	0.7330 (5)	0.12972 (20)	0.25498 (24)	0.0571
C(7)	0.5294 (6)	0.11132 (22)	0.28080 (17)	0.0567
C(8)	0.4165 (4)	0.04157 (21)	0.21231 (25)	0.0552
C(9)	0.5559 (6)	0.01847 (18)	0.14263 (19)	0.0528
C(10)	0.2145 (3)	0.16906 (18)	0.01913 (16)	0.0335
C(11)	0.5812 (3)	0.24101 (15)	0.00806 (14)	0.0324
O(1)	0.0755 (3)	0.15168 (19)	-0.04488 (17)	0.0588
O(2)	0.6451 (3)	0.27005 (18)	-0.06222 (14)	0.0552

structurally studied (Faller, Chodosh & Katahira, 1980; Allen, Baker, Barnes, Bottrill, Green, Orpen & Welch, 1983; Graham, Akrigg & Sheldrick, 1976, and references therein) in which the Mo—C(central) bond is found to be significantly the shortest.

Table 4 (deposited) presents the results of least-squares-planes' calculations. With respect to the (precise) plane through the allyl atoms C(1), C(2) and C(3), the methyl carbon C(4) and the 1,3-*syn* H atoms [H(12) and H(32)] are all displaced *towards* the metal whereas H(11) and H(31) bend away. This kind of distortion has previously been observed in other

Table 2. Interatomic distances (Å) and angles (°) and deviations of atoms from planes (Å)

Mo—C(1)	2.3146 (25)	C(1)—C(2)	1.407 (3)
Mo—C(2)	2.3169 (20)	C(2)—C(3)	1.403 (3)
Mo—C(3)	2.3175 (22)	C(2)—C(4)	1.497 (3)
Mo—C(5)	2.333 (3)	C(5)—C(6)	1.393 (4)
Mo—C(6)	2.377 (3)	C(5)—C(9)	1.390 (4)
Mo—C(7)	2.358 (3)	C(6)—C(7)	1.365 (4)
Mo—C(8)	2.318 (3)	C(7)—C(8)	1.399 (4)
Mo—C(9)	2.306 (3)	C(8)—C(9)	1.406 (4)
Mo—C(10)	1.9615 (22)	C(10)—O(1)	1.147 (3)
Mo—C(11)	1.9563 (19)	C(11)—O(2)	1.156 (3)
C(1)—Mo—C(2)	35.36 (8)	C(7)—Mo—C(8)	34.81 (10)
C(1)—Mo—C(3)	62.09 (8)	C(7)—Mo—C(9)	58.08 (10)
C(1)—Mo—C(5)	143.90 (10)	C(7)—Mo—C(10)	127.50 (10)
C(1)—Mo—C(6)	110.83 (10)	C(7)—Mo—C(11)	148.21 (9)
C(1)—Mo—C(7)	87.64 (10)	C(8)—Mo—C(9)	35.40 (10)
C(1)—Mo—C(8)	98.68 (10)	C(8)—Mo—C(10)	96.27 (10)
C(1)—Mo—C(9)	133.62 (10)	C(8)—Mo—C(11)	140.93 (9)
C(1)—Mo—C(10)	82.32 (9)	C(9)—Mo—C(10)	94.37 (10)
C(1)—Mo—C(11)	118.11 (8)	C(9)—Mo—C(11)	105.93 (9)
C(2)—Mo—C(3)	35.25 (7)	C(10)—Mo—C(11)	77.36 (8)
C(2)—Mo—C(5)	146.32 (9)	Mo—C(1)—C(2)	72.41 (13)
C(2)—Mo—C(6)	117.28 (9)	Mo—C(2)—C(1)	72.23 (13)
C(2)—Mo—C(7)	111.07 (9)	Mo—C(2)—C(3)	72.40 (12)
C(2)—Mo—C(8)	132.69 (9)	Mo—C(2)—C(4)	120.96 (15)
C(2)—Mo—C(9)	167.94 (9)	C(1)—C(2)—C(3)	116.45 (19)
C(2)—Mo—C(10)	88.81 (8)	C(1)—C(2)—C(4)	121.27 (20)
C(2)—Mo—C(11)	86.11 (7)	C(3)—C(2)—C(4)	122.08 (19)
C(3)—Mo—C(5)	111.54 (9)	Mo—C(3)—C(2)	72.35 (12)
C(3)—Mo—C(6)	88.40 (9)	Mo—C(5)—C(6)	74.50 (18)
C(3)—Mo—C(7)	98.65 (9)	Mo—C(5)—C(9)	71.50 (17)
C(3)—Mo—C(8)	132.81 (9)	C(6)—C(5)—C(9)	107.9 (3)
C(3)—Mo—C(9)	144.88 (9)	Mo—C(6)—C(5)	71.11 (18)
C(3)—Mo—C(10)	120.48 (8)	Mo—C(6)—C(7)	72.49 (18)
C(3)—Mo—C(11)	79.85 (8)	C(5)—C(6)—C(7)	109.0 (3)
C(5)—Mo—C(6)	34.40 (11)	Mo—C(7)—C(6)	74.01 (18)
C(5)—Mo—C(7)	57.18 (10)	Mo—C(7)—C(8)	71.03 (17)
C(5)—Mo—C(8)	57.94 (11)	C(6)—C(7)—C(8)	108.1 (3)
C(5)—Mo—C(9)	34.86 (10)	Mo—C(8)—C(7)	74.16 (17)
C(5)—Mo—C(10)	124.01 (10)	Mo—C(8)—C(9)	71.85 (17)
C(5)—Mo—C(11)	93.49 (9)	C(7)—C(8)—C(9)	107.7 (3)
C(6)—Mo—C(7)	33.50 (10)	Mo—C(9)—C(5)	73.64 (17)
C(6)—Mo—C(8)	56.92 (10)	Mo—C(9)—C(8)	72.75 (17)
C(6)—Mo—C(9)	57.41 (10)	C(5)—C(9)—C(8)	107.4 (3)
C(6)—Mo—C(10)	150.82 (10)	Mo—C(10)—O(1)	176.61 (21)
C(6)—Mo—C(11)	115.04 (9)	Mo—C(11)—O(2)	178.18 (18)

Plane 1: Mo -1.893 (1), C(4) -0.111 (3), H(11) 0.45 (3), C(1)—C(3) H(12) -0.10 (3), H(31) 0.47 (3), H(32) -0.18 (3)

Plane 2: Mo -2.016 (1), C(5) -0.005 (3), C(6) 0.007 (3), C(5)—C(9) C(7) -0.005 (3), C(8) 0.002 (3), C(9) 0.002 (3)

Dihedral angle: plane 1, plane 2 73.5°



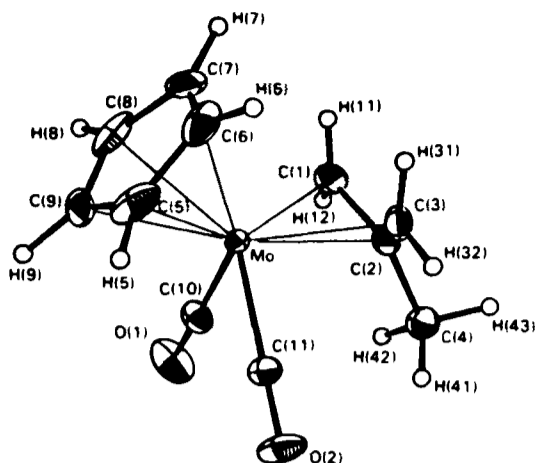


Fig. 1. Perspective view of  $[(\eta^5\text{-C}_5\text{H}_5)(2\text{-Me-}\eta^3\text{-C}_3\text{H}_5)(\text{CO})_2\text{Mo}]$  (II), with thermal ellipsoids drawn at the 30% probability level, except for H atoms which have an artificial radius of 0.1 Å for clarity.

accurately determined structures of 2-methylallyl complexes where sterically permitted (see, for example, Bandoli & Clemente, 1981), and its origin may be traced to rehybridization of the allyl  $\pi$  molecular orbitals upon complex formation (Elian, Chen, Mingos & Hoffmann, 1976).

The cyclopentadienyl ligand shows some degree of rotational disorder as evidenced by the fact that the three highest residues in the final  $\Delta F$  synthesis occur between atoms C(8) and C(9), C(9) and C(5), and C(5) and C(6). However, refinement of a model involving two independent  $C_5$  rings would not converge satisfactorily, carbon atoms tending to merge with concomitant reappearance of the residues.\* The present model was therefore adopted as more suitable.

The general orientation of the  $\eta^5\text{-C}_5\text{H}_5$  ligand does not conform to the effective  $C_5$  symmetry of the rest of the complex. Furthermore, the ligand is not bound symmetrically to the metal atom, and is not planar. Atoms C(6) and C(7) are significantly further from Mo than C(5), C(8) and C(9), and the short C(6)–C(7) bond implies some  $\pi$  localization. Thus this ligand is 'slipped' (by *ca* 0.08 Å) towards a cyclic  $\eta^3$ -allyl function (Green, Nyathi, Scott, Stone, Welch & Woodward, 1978, and references therein). The non-planarity of the  $C_5$  ring, however, does not readily correlate with this slippage, being of envelope conformation folded away from Mo about the C(5)–C(7) vector.

\* In all refinements the  $C_5$  rings were *not* idealized to regular pentagons as there is clear asymmetry in C–C distances, reflecting asymmetric Mo–( $\eta^5\text{-C}_5\text{H}_5$ ) bonding, that we did not wish to override.

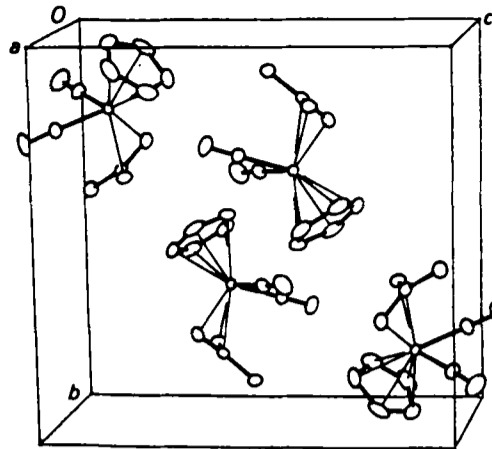


Fig. 2. Crystal-packing diagram for (II), with H atoms omitted for clarity.

Molecular parameters within the  $\text{Mo}(\text{CO})_2$  fragment are quite normal for a complex of this class. Fig. 2 is a perspective view of the contents of one unit cell. There are no significant intermolecular interactions.

We thank the Department of Chemistry, University of Edinburgh, for support (NWM).

#### References

- ALLEN, S. R., BAKER, P. K., BARNES, S. G., BOTTRILL, M., GREEN, M., ORPEN, A. G. & WELCH, A. J. (1983). *J. Chem. Soc. Dalton Trans.* pp. 927–939.
- BANDOLI, G. & CLEMENTE, D. A. (1981). *Acta Cryst.* B37, 490–491.
- CROMER, D. T. & LIBERMAN, D. (1970). *J. Chem. Phys.* 53, 1891–1898.
- ELIAN, M., CHEN, M. M. L., MINGOS, D. M. P. & HOFFMANN, R. (1976). *Inorg. Chem.* 15, 1148–1155.
- FALLER, J. W., CHEN, C.-C., MATTINA, M. J. & JAKUBOWSKI, A. (1973). *J. Organomet. Chem.* 52, 361–387.
- FALLER, J. W., CHODOSH, D. F. & KATAHIRA, D. (1980). *J. Organomet. Chem.* 187, 227–231.
- GRAHAM, A. J., AKRIGG, D. & SHELDRIK, B. (1976). *Cryst. Struct. Commun.* 5, 891–898.
- GREEN, M., NYATHI, J. Z., SCOTT, C., STONE, F. G. A., WELCH, A. J. & WOODWARD, P. (1978). *J. Chem. Soc. Dalton Trans.* pp. 1067–1080.
- JOHNSON, C. K. (1976). ORTEPII. Report ORNL-5138. Oak Ridge National Laboratory, Tennessee, USA.
- ROBERTS, P. & SHELDRIK, G. M. (1976). XANADU. Univ. of Cambridge, England.
- SCHILLING, B. E. R., HOFFMANN, R. & FALLER, J. W. (1979). *J. Am. Chem. Soc.* 101, 592–598.
- SHELDRIK, G. M. (1976). SHELX76. Program for crystal structure determination. Univ. of Cambridge, England.
- STEWART, J. M., MACHIN, P. A., DICKINSON, C. W., AMMON, H. L., HECK, H. & FLACK, H. (1976). The XRAY76 system. Tech. Rep. TR446. Computer Science Centre, Univ. Maryland, College Park, Maryland, USA.
- STEWART, R. F., DAVIDSON, E. R. & SIMPSON, W. T. (1965). *J. Chem. Phys.* 42, 3175–3187.



**APPENDIX 6**

**COURSES ATTENDED**

## **LECTURE COURSES ATTENDED**

"The Chemistry of Cluster Compounds",  
Dr. A.J. Welch, 5 lectures.

"The uses of X-ray Crystallography",  
Drs. R.O. Gould, M.D. Walkinshaw & A.J. Welch,  
10 lectures.

"Pulse Sequences and Application to n.m.r.  
Spectroscopy", Dr. G.A. Morris, 5 lectures.

"The Chemistry of the Photographic Process",  
Dr. C.A. Williams, 5 lectures.

"The History of the Department of Chemistry",  
Dr. W.P. Doyle, 5 lectures.

"Recent Advances in Electrochemistry",  
Dr. G.A. Heath, 5 lectures.

"Aspects of Structural Chemistry",  
Dr. C. Glidewell, 5 lectures.

"Modern Organometallic Chemistry",  
Dr. M. Schroder, 5 lectures.

European Crystallographic Meeting, No 8,  
Liege, Belgium, 1983.

Departmental Seminars, 1981-1984.

## ***REFERENCES***

## REFERENCES

1. (a) J. Tsuji in "Organic Synthesis by means of Transition Metal Complexes", Springer-Verlag, Berlin, 1975.  
(b) H. Alper (Ed) "Transition Metal Organometallics in Organic Synthesis", Academic Press, London, 1976.
2. B.M. Trost & T.R. Verhoeven in "Comprehensive Organometallic Chemistry", Eds. G. Wilkinson, F.G.A. Stone & E.W. Abel, Vol. 8, Pergamon Press, Oxford, 1982.
3. (a) B.M. Trost, Acc. Chem. Res., 1980, 13, 385.  
(b) J. Tsuji, "Organic Synthesis with Palladium Compounds", Springer-Verlag, Berlin, 1980.
4. P.W. Jolly in "Comprehensive Organometallic Chemistry", Vol 8, Eds. G. Wilkinson, F.G.A. Stone & E.W. Abel, Pergamon Press, Oxford, 1982.
5. P.S. Manchand, H.S. Wong & J.F. Blount, J. Org. Chem., 1978, 43, 4769.
6. B.M. Trost & T.R. Verhoeven, J. Org. Chem., 1976, 41, 3215.
7. B.M. Trost & T.R. Verhoeven, J. Am. Chem. Soc., 1978, 100, 3435.
8. J.S. Temple, M. Riediker & J. Schwartz, J. Am. Chem. Soc., 1982, 104, 1310.
9. E. Keinan & M Sahai, J. Chem. Soc., Chem. Commun., 1984, 648.

10. Y. Castanet & F. Petit, Tetrahedron Lett., 1979, 3221.
11. B.M. Trost, J. Yoshida & M. Lautens, J. Am. Chem. Soc., 1983, 105, 4494.
12. H. Matsushita & E. Negishi, J. Chem. Soc., Chem. Commun., 1982, 160.
13. R.D. Adams, D.F. Chodosh, J.W. Faller & A.M. Rosan, J. Am. Chem. Soc. 1979, 101, 2570.
14. B.E.R. Schilling, R. Hoffmann & J.W. Faller, J. Am. Chem. Soc., 1979, 101, 592.
15. B.M. Trost & C.R. Self, J. Org. Chem. 1984, 49, 468.
16. R. Mason & D.R. Russell, J. Chem. Soc., Chem. Commun., 1966, 26.
17. S.J. Lippard & S.M. Morehouse, J. Am. Chem. Soc., 1969, 91, 2504.
18. K.F. Purcell & J.C. Kotz, "Inorganic Chemistry", p705, Holt Saunders, London, 1977.
19. (a) F.A. Cotton, J.W. Faller & A. Musco, Inorg. Chem., 1967, 6, 179.  
(b) S.J. Lippard & S.M. Morehouse, J. Am. Chem. Soc., 1972, 94, 6949.  
(c) G.L. Statton & K.C. Ramey, J. Am. Chem. Soc., 1966, 88, 1327.
20. S.J. Lippard & S.M. Morehouse, J. Am. Chem. Soc. 1972, 94, 6956.
21. J.W. Faller & Y. Shvo, J. Am. Chem. Soc., 1980, 102, 5396.

22. J.W. Faller, D.F. Chodosh & D. Katahira, J. Organometal. Chem., 1980, 187, 227.
23. J.W. Faller, Y. Shvo, K. Chao & H.H. Murray, J. Organometal. Chem., 1982, 226, 251.
24. T.J. Greenhough, P. Legzdins, D.T. Martin & J. Trotter, Inorg. Chem., 1979, 18, 3268.
25. A.S. Batsanov & Yu.T. Struchkov, J. Organometal. Chem., 1983, 248, 101.
26. G. Dettlaf, U. Behrens & E. Weiss, Chem. Ber., 1978, 111, 3019.
27. R. Aumann, H. Ring, C. Kruger & R. Goddard, Chem. Ber., 1979, 112, 3644.
28. M.R. Churchill & K-N. Chen, Inorg. Chem., 1976, 15, 788.
29. Y. Becker, A. Eisenstadt & Y. Shvo, Tetrahedron, 1978, 34, 799.
30. K. Oda, N. Yasuoka, T. Ueki, N. Kasai & M. Kakudo, Bull. Chem. Soc. Jap., 1970, 43, 362.
31. J. Lukas, J.E. Ramakers-blom, T.G. Hewitt & J.J. DeBoer, J. Organometal. Chem., 1972, 46, 167.
32. T.H. Tulip & J.A. Ibers, J. Am. Chem. Soc., 1979, 101, 4201.
33. M. Green, N.C. Norman, A.G. Orpen, J. Organometal. Chem., 1981, 221, C11.
34. W.W. Prichard, U.S. Pat 2 600 571, 1952, Chem. Abstr. 46 P10188f, 1952.
35. W.R. McClellan, H.H. Hoehn, A.N. Cripps, E.L. Muetterties & B.W. Howk, J. Am. Chem. Soc., 1961, 83, 1601.

36. (a) A.E. Smith, Acta. Cryst., 1965, 18, 331.  
(b) W.E. Oberhansli & L.F. Dahl, J. Organometal. Chem., 1965, 3, 43.
37. R. Huttel & H. Christ, Chem. Ber., 1963, 96, 3101.
38. B.L. Shaw, Chem. Ind., 1962, 1190.
39. R. Huttel & J. Kratzer, Angew. Chem. 1959, 71, 456.
40. J. Smidt & W. Hafner, Angew. Chem. 1959, 71, 284.
41. W.T. Dent, R. Long & A.J. Wilkinson, J. Chem. Soc., 1964, 1585
42. J.K. Nicholson, J. Powell & B.L. Shaw, J. Chem. Soc., Chem. Commun., 1966, 174.
43. M. Sakakibara, Y. Takahashi, S. Sakai & Y. Ishii, J. Chem. Soc., Chem. Commun., 1969, 396.
44. S.D. Robinson & B.L. Shaw, J. Chem. Soc., 1963, 4806.
45. J. Tsuji & S. Imamura, Bull. Chem. Soc. Jap., 1967, 40, 197.
46. R.R. Shrock & J.A. Osborn, J. Am. Chem. Soc., 1971, 93, 3089.
47. J. Powell & B.L. Shaw, J. Chem. Soc. A, 1968, 774.
48. (a) D.J. Mabbott, B.E. Mann & P.M. Maitlis, J. Chem. Soc. Dalton, 1977, 294.  
(b) D.A. White, Synth. Inorg. Metal-Org. Chem. 1971, 1, 133.
49. L.S. Hegedus, B. Akermark, D.J. Olsen, O.P. Anderson & K. Zetterberg, J. Am. Chem. Soc., 1982, 104, 697.
50. J. Powell & A.W.-L. Chan, J. Organometal. Chem., 1972, 35, 203.

51. S.D. Robinson & B.L. Shaw, J. Chem. Soc., 1963, 4806.
52. Y. Takahashi, T. Inagaki, H. Mori, S. Sakai & Y. Ishii, Kogyo. Kagaku. Zasshi. 1970, 73, 760.
53. A.N. Nesmeyanov, A.Z. Rubezhov, L.A. Leites & S.P. Gubin, J. Organometal. Chem., 1968, 12, 187.
54. A.N. Nesmeyanov & A.Z. Rubezhov, J. Organometal. Chem., 1979, 164, 259.
55. R.G. Hayter, J. Organometal. Chem., 1968, 13, P1.
56. J.W. Faller, C.-C. Chen, M.J. Mattina & A. Jakubowski, J. Organometal. Chem., 1973, 52, 361.
57. B.J. Brisdon, D.A. Edwards, K.E. Paddick & M.G.B. Drew, J. Chem. Soc., 1980, 1317.
58. J.W. Faller, D.A. Haitko, R.D. Adams & D.F. Chodosh, J. Am. Chem. Soc., 1979, 101, 865.
59. B.J. Brisdon & A.A. Woolf, J. Chem. Soc. Dalton, 1978, 291.
60. A.J. Graham, D.A. Akrigg & B. Sheldrick, Cryst. Struct. Comm., 1976, 5, 891.
61. A.J. Graham, D. Akrigg & B. Sheldrick, Acta. Cryst., 1983, C39, 192.
62. A.J. Graham & R.H. Fenn, J. Organometal. Chem., 1969, 17, 405.
63. A.J. Graham & R.H. Fenn, J. Organometal. Chem., 1970, 25, 173.
64. F. Dawans, J. Dewailly, J. Meunier-Piret & P. Piret, J. Organometal. Chem., 1974, 76, 53.



65. A.T.T. Hsieh & B.O. West, J. Organometal. Chem.,  
1976, 112, 285.
66. M.H.B. Stiddard, J. Chem. Soc., 1962, 4712.
67. (a) C.G. Hull & M.H.B. Stiddard, J. Organometal. Chem.,  
1967, 9, 519.  
(b) H. tom Dieck & H. Friedel, J. Organometal. Chem.,  
1968, 14, 375.
68. A.J. Graham & R.H. Fenn, J. Organometal. Chem.,  
1972, 37, 137.
69. (a) A. Davidson & W.C. Rode, Inorg. Chem., 1967,  
6, 2124.  
(b) J.W. Faller & M.J. Incorvia, Inorg. Chem.,  
1968, 7, 840.
70. H.L. Clarke, J. Organometal. Chem., 1974, 80, 155.
71. K. Nakamoto, "Infrared Spectra of Inorganic and  
Coordination Compounds", p188, Wiley-Interscience,  
New York, 1963.
72. M. Karplus, J. Chem. Phys., 1959, 30, 11.
73. N.M. Boag, M. Green, J.L. Spencer & F.G.A. Stone,  
J. Chem. Soc. Dalton, 1980, 1200.
74. Y. Takahashi, H. Akahori, S. Sakai & Y. Ishii,  
Bull. Chem. Soc. Jap., 1971, 44, 2703.
75. N.M. Boag, M. Green, J.L. Spencer & F.G.A. Stone,  
J. Chem. Soc. Dalton, 1980, 1220.
76. R.W. Taft in "Steric Effects in Organic Chemistry",  
Ed. M.S. Newman Wiley, New York, 1956.

77. G.A. Heath & J.H. Leslie, J. Chem. Soc. Dalton, 1983, 1587.
78. H.S. Gutowsky, M. Karplus & D.M. Grant, J. Chem. Phys., 1959, 31, 1278.
79. A.J. Blake, S. Cradock, E.A.V. Ebsworth, D.W.H. Rankin & A.J. Welch, J. Chem. Soc., Dalton, 1984, 2029.
80. G.H. Stout & L.H. Jensen, "X-ray structure Determination", MacMillan, New York, 1968.
81. "International Tables for X-ray Crystallography", Vol 1, Kynoch Press, Birmingham, 1975.
82. D.F. Shriver, "The Manipulation of Air-sensitive Compounds", McGraw Hill, New York, 1969.
83. D.D. Perrin, W.L.F. Armanego & D.R. Perrin, "Purification of Laboratory Chemicals", 2<sup>nd</sup> Ed., Pergamon Press, Oxford, 1980.
84. R.B. King & F.G.A. Stone, Inorg. Synth., 1963, 7, 99.
85. R.A. Zelonka & M.C. Baird, Can. J. Chem., 1972, 50, 3063.
86. J.K. Beattie, Acc. Chem. Res., 1971, 4, 253.
87. J.D. Dunitz, Tetrahedron, 1972, 28, 5459.
88. A. Tiripicchio, M. Tiripicchio-Camellini, L. Maresca, G. Natile & G. Rizzardi, Cryst. Struct. Comm., 1979, 8, 689.
89. M. Lanfranchi, A. Tiripicchio, L. Maresca & G. Natile, Cryst. Struct. Comm., 1982, 11, 343.
90. A.A. Grinberg in "An Introduction to the Chemistry of Complex Compounds", 2<sup>nd</sup> Ed., Eds. J.R. Leach, D.H. Busch & R.F. Trimble, Pergamon Press, New York, 1962.

91. J.E. Huheey, "Inorganic Chemistry", p427,  
Harper & Row, New York, 1975.
92. G. Annibale, L. Maresca, G. Natile, A. Tiripicchio &  
M. Tiripicchio-Camellini, J. Chem. Soc., Dalton,  
1982, 1587.
93. M. Kh. Minasyants & Yu.T. Struchkov, Zh. Strukt. Khim.,  
1968, 9, 481.
94. J.K. Becconsall, B.E. Job & S. O'Brien, J. Chem. Soc. A,  
1967, 423.
95. M.B. Honan, J.L. Atwood, I. Bernal & W.A. Herrmann,  
J. Organometal. Chem., 1979, 179, 403.
96. S.R. Allen, P.K. Baker, S.G. Barnes, M. Bottrill,  
M. Green, A.G. Orpen, I.D.W. Williams & A.J. Welch,  
J. Chem. Soc., Dalton, 1983, 927.
97. (a) A.C. Villa, A.G. Manfredotti & C. Guastini, Cryst.  
Struct. Comm., 1973, 2, 181.  
(b) A. Kuhn, Ch. Burschka & H. Werner, Organometallics,  
1982, 1, 496.  
(c) K. Miki, M. Yama, Y. Kai & N. Kasai,  
J. Organometal. Chem., 1982, 239, 417.  
(d) K. Miki, O. Shiotani, Y. Kai, N. Kasai, H. Kanatani &  
H. Kurosawa, Organometallics, 1983, 2, 585.  
(e) H. Werner, H.-J. Kraus, U. Schubert, K. Ackermann &  
P. Hofmann, J. Organometal. Chem., 1983, 250, 517.
98. M. Green, J.Z. Nyathi, C. Scott, F.G.A. Stone,  
A.J. Welch & P. Woodward, J. Chem. Soc., Dalton,  
1978, 1067.

99. C.A. Kosky, P. Ganis & G. Avitabile, Acta. Cryst., 1971, B27, 1859.
100. E.M. Holt, S.L. Holt & K.J. Watson, J. Chem. Soc., Dalton, 1973, 2444.
101. F.A. Cotton, B.A. Frenz & C.A. Murillo, J. Am. Chem. Soc., 1975, 97, 2118.
102. K.R. Breakell, S.J. Rettig, D.L. Singbeil, A. Storr & J. Trotter, Can. J. Chem., 1978, 56, 2099.
103. M.G.B. Drew & G.F. Griffin, Acta. Cryst., 1979, B35, 3036.
104. B.A. Frenz & J.A. Ibers, Inorg. Chem., 1972, 11, 1109.
105. S. Nishigaki, H. Yoshioka & K. Nakatsu, Acta. Cryst., 1978, B34, 875.
106. J.A. Kaduk, A.T. Poulos & J.A. Ibers, J. Organometal. Chem., 1977, 127, 245.
107. C.F. Putnik, J.J. Welter, G.D. Stucky, M.J. D'Aniello Jr., B.A. Sosinsky, J.F. Kirner & E.L. Muetterties, J. Am. Chem. Soc., 1978, 100, 4107.
108. M.R. Churchill, Inorg. Chem., 1973, 12, 1213.
109. K.R. Breakell, S.J. Rettig, A. Storr & J. Trotter, Can. J. Chem., 1979, 57, 139.
110. (a) R. Mason & A.G. Wheeler, J. Chem. Soc. A, 1968, 2549.  
(b) G. Bandoli & D.A. Clemente, Acta. Cryst., 1981, B37, 490.
111. F.A. Cotton & M.D. LaPrade, J. Am. Chem. Soc., 1968, 90, 5418.

112. U. Franke & E. Weiss, J. Organometal. Chem.,  
1977, 139, 305.
113. K.S. Chong, S.J. Rettig, A. Storr & J. Trotter,  
Can. J. Chem., 1979, 57, 1335.
114. M. Elian, M.M.L. Chen, D.M.P. Mingos & R. Hoffmann,  
Inorg. Chem., 1976, 15, 1148.
115. A.J. Welch, unpublished results.
116. D.S. Gill, P.K. Baker, M. Green, K.E. Paddick,  
M. Murray & A.J. Welch, J. Chem. Soc., Chem. Commun.,  
1981, 986.
117. A.J. Welch, PhD. Thesis, Univ. of London, 1974.
118. P.B. Viossat & N. Rodier, Acta. Cryst., 1979, B35, 2715.
119. A.C.T. North, D.C. Phillips & F.S. Matthews,  
Acta. Cryst., 1968, A24, 351.
120. R.O. Gould, Univ. of Edinburgh, 1984.
121. G.M. Sheldrick, Univ. of Cambridge, 1976.
122. R.F. Stewart, E.R. Davidson & W.T. Simpson,  
J. Chem. Phys., 1965, 42, 3175.
123. D.T. Cromer & D. Liberman, J. Chem. Phys.,  
1970, 53, 1891.
124. P. Roberts & G.M. Sheldrick, Univ. of Cambridge, 1976.
125. R.O. Gould & P.T. Taylor, Univ. of Edinburgh, 1984.
126. J.M. Stewart, P.A. Machin, C.W. Dickinson, H.L. Ammon,  
H. Heck & H. Flack, Tech. Rep. TR446, Computer Science  
Centre, Univ. of Maryland, 1976.
127. C.K. Johnson, Rep. ORNL-5138, Oak Ridge National  
Laboratory, Tennessee, 1976.

128. E. Keller, Univ. of Freiburg, 1980.
129. (a) R. Hoffmann, J. Chem. Phys., 1963, 39, 1397.  
(b) R. Hoffmann & W.N. Lipscomb, J. Chem. Phys., 1962, 36, 2179, 3489; 37, 2872.
130. J. Howell, A. Rossi, D. Wallace, K. Haraki & R. Hoffmann, Quantum Chemistry Program Exchange, 1977, 10, 344.
131. (a) R. Hoffmann, H. Fujimoto, J.R. Swenson & C.-C. Wan, J. Am. Chem. Soc., 1973, 95, 7644.  
(b) H. Fujimoto & R. Hoffmann, J. Phys. Chem., 1974, 78, 1167.
132. F.A. Cotton, "Chemical Applications of Group Theory", 2<sup>nd</sup> Ed. Wiley, New York, 1971.
133. D.M.P. Mingos & M.I. Forsyth, J. Chem. Soc., Dalton, 1977, 610.
134. T.A. Albright, P.R. Clemens, R.P. Hughes, D.E. Hunton & L.D. Margerum, J. Am. Chem. Soc., 1982, 104, 5369.
135. J.H. Ammeter, H.-B. Burgi, J.C. Thibeault & R. Hoffmann, J. Am. Chem. Soc., 1978, 100, 3686.
136. (a) T.A. Albright, R. Hoffmann, J.C. Thibeault & D.L. Thorn, J. Am. Chem. Soc., 1979, 101, 3812.  
(b) T.A. Albright & R. Hoffmann, Chem. Ber., 1978, 111, 1578.
137. T.A. Albright, P. Hofmann, R. Hoffmann, C.P. Lillya & P.A. Dobosh, J. Am. Chem. Soc., 1983, 105, 3396.
138. M. Eliañ & R. Hoffmann, Inorg. Chem., 1975, 14, 1058.

139. B.E.R. Schilling, R. Hoffmann & D.L. Lichtenberger, J. Am. Chem. Soc., 1979, 101, 585.
140. W.L. Jorgensen, Quantum Chemistry Program Exchange, 1977, 340.
141. (a) R. Hoffmann, Angew Chem. Int. Ed., 1982, 21, 711.  
(b) T.A. Albright, Tetrahedron, 1982, 38, 1339.
142. S.F.A. Kettle & R. Mason, J. Organometal. Chem., 1966, 5, 573.
143. A.N. Nesmeyanov, G.G. Aleksandrov, N.G. Bokii & I.B. Zlotina, J. Organometal. Chem., 1976, 111, C9.
144. K. Nakatsu, Y. Inai, T. Mitsudo, Y. Watanabe, N. Nakanishi & Y. Takegami, J. Organometal. Chem., 1978, 159, 111.
145. (a) P. Dowd, Acc. Chem. Res., 1972, 5, 242.  
(b) J. Berson, Acc. Chem. Res., 1978, 11, 446.
146. (a) A.C. Day & J.T. Powell, J. Chem. Soc., Chem. Commun., 1968, 1241.  
(b) J.A. Mondo & J.A. Berson, J. Am. Chem. Soc., 1983, 105, 3340.
147. (a) B.M. Trost & D.M.T. Chan, J. Am. Chem. Soc., 1980, 102, 6359.  
(b) B.M. Trost & D.M.T. Chan, J. Am. Chem. Soc., 1983, 105, 2315, 2326.
148. T.A. Albright, P. Hofmann & R. Hoffmann, J. Am. Chem. Soc., 1977, 99, 7546.
149. T.A. Albright, Acc. Chem. Res., 1982, 15, 149.
150. T.A. Albright, J. Organometal. Chem., 1980, 198, 159.

151. S.R. Allen, S.G. Barnes, M. Green, G. Moran, L. Trollope, N.W. Murrall, A.J. Welch & D.M. Sharaiha, J. Chem. Soc., Dalton, 1984, 1157.
152. W. Henslee & R.E. Davis, J. Organometal. Chem., 1974, 81, 389.
153. J.M. Mayer, C.J. Curtis & J.E. Bercaw, J. Am. Chem. Soc., 1983, 105, 2651.
154. M.D. Jones, R.D.W. Kemmitt, A.W.G. Platt, D.R. Russell & L.J.S. Sherry, J. Chem. Soc., Chem. Commun., 1984, 673.
155. A. Almenningen, A. Haaland & K. Wahl, Acta. Chem. Scand., 1969, 23, 1145.
156. M.R. Churchill & K. Gold, Inorg. Chem., 1969, 8, 401.
157. M.R. Churchill & B.G. DeBoer, Inorg. Chem., 1973, 12, 525.
158. N. Yasuda, Y. Kai, N. Yasuoka, N. Kasai & M. Kakudo, J. Chem. Soc., Chem. Commun., 1972, 157.
159. A.N. Nesmeyanov, I.S. Astakhova, G.P. Zol'nikova, I.I. Kritskaya & Yu.T. Struchkov, J. Chem. Soc., Chem. Commun., 1970, 85.
160. E. Meier, O. Cherpillod, T. Boschi, R. Roulet, P. Vogel, C. Mahaim, J. Organometal. Chem., 1980, 186, 247.
161. D.M. Sharaiha, Undergraduate project, The City University, 1981.
162. A.J. Pearson, Acc. Chem. Res., 1980, 13, 463.
163. J.W. Faller, H.H. Murray, D.L. White & K.H. Chao, Organometallics 1983, 2, 400.



164. (a) J. Takats & L. Kruczynski, J. Am. Chem. Soc.,  
1974, 96, 932.  
(b) J. Takats & L. Kruczynski, Inorg. Chem.,  
1976, 15, 3140.
165. J.W. Faller & A.M. Rosan, J. Am. Chem. Soc.,  
1977, 99, 4858.
166. J.L. Davidson, K. Davidson & W.E. Lindsell,  
J. Chem. Soc., Chem. Commun., 1983, 452.
167. P. Kubacek, R. Hoffmann & Z. Havlas, Organometallics,  
1982, 1, 180.
168. M.R. Churchill & J.P. Fennessey, Inorg. Chem.,  
1967, 6, 1213.
169. F.C. Wilson & D.P. Shoemaker, J. Chem. Phys.,  
1957, 27, 809.
170. M.J. Bennett & R. Mason, Proc. Chem. Soc., 1963, 273.
171. R.J. Doedens & L.F. Dahl, J. Am. Chem. Soc.,  
1965, 87, 2576.
172. H.W. Baird & L.F. Dahl, Unpublished, see ref. 171.
173. G. Huttner, H. Brintzinger, L.G. Bell, P. Freidrich,  
V. Bejenke & D. Neugebauer, J. Organometal. Chem.,  
1978, 145, 329.
174. M.R. Churchill & J. Wormald, Inorg. Chem.,  
1971, 10, 572.
175. J.A. Ibers, J. Organometal. Chem., 1974, 73, 389.
176. M.R. Churchill & T.A. O'Brien, J. Chem. Soc. A,  
1970, 206.
177. R. Uttech & H. Diettrich, Z. Krist., 1965, 122, 60.

178. M.J. Bunker, M.L.H. Green, C. Couldwell & K. Prout, J. Organometal. Chem., 1980, 192, C6.
179. J.A. Segal, M.L.H. Green, J.-C. Daran & K. Prout, J. Chem. Soc., Chem. Commun., 1976, 766.
180. (a) D.J. Marais, N. Sheppard & B.P. Stoicheff, Tetrahedron, 1962, 17, 163.  
(b) A. Almenningen, O. Bastiansen & M. Traetteberg, Acta. Chem. Scand., 1958, 12, 1221.
181. F.A. Cotton, V.W. Day, B.A. Frenz, K.I. Hardcastle & J.M. Troup, J. Am. Chem. Soc., 1973, 95, 4522.
182. F.H. Herbststein & M.G. Reisner, Acta. Cryst., 1977, B33, 3304.
183. Y. Wakatsuki, K. Aoki & H. Yamazaki, J. Chem. Soc., Dalton, 1982, 89.
184. A. Immirzi, J. Organometal. Chem., 1974, 76, 65.
185. T.V. Ashworth, E. Singleton & M. Laing, J. Organometal. Chem., 1976, 117, C113.
186. G. Erker, K. Engel, C. Kruger & G. Muller, Organometallics, 1984, 3, 128.
187. E.S. Magyar & C.P. Lillya, J. Organometal. Chem., 1976, 116, 99.
188. R. Goddard & R. Hoffmann, unpublished, see ref. 153.
189. (a) N.A. Bailey, W.G. Kita, J.A. McCleverty, A.J. Murray, B.E. Mann & N.W.J. Walker, J. Chem. Soc., Chem. Commun., 1974, 592.  
(b) I.B. Benson, S.A.R. Knox, R.F.D. Stansfield & P. Woodward, J. Chem. Soc., Chem. Commun., 1977, 404.

(c) B. Granoff & R.A. Jacobson, Inorg. Chem.,  
1968, 7, 2328.

(d) P.G. LeBorgne, E. Gentric & D. Grandjean,  
Acta. Cryst., 1975, B31, 2824.